Serafim Paulo Melo de Oliveira

PhD Thesis

Injectable system and scaffolds to promote endochondral mechanism for bone regeneration

Tese submetida à Faculdade de Engenharia da Universidade do Porto para obtenção do grau de Doutor em Engenharia Biomédica

Faculdade de Engenharia da Universidade do Porto

2008

This thesis was supervised by:

Professor Mário A. Barbosa
FEUP – Faculdade de Engenharia, Universidade do Porto;
INEB – Instituto de Engenharia Biomédica, Laboratório de Biomateriais.

Professor Cristina Teixeira
NYUCD – New York University College of Dentistry;
Department of Basic Sciences and Craniofacial Biology;
Department of Biomaterials and Biomimetics.

The research described in this thesis was conducted at:

INEB – Instituto de Engenharia Biomédica, Laboratório de Biomateriais;
FFUP – Faculdade de Farmácia, Universidade do Porto;
NYUCD – New York University College of Dentistry, Department of Basic Sciences and Craniofacial Biology and Department of Biomaterials and Biomimetics.

The research described in this thesis was financially supported by:

PRODEP III – Programa para o Desenvolvimento Educativo para Portugal III;

Project Gaucher II – "An injectable enzyme delivery system based on apatite nanoparticles and natural hydrogel microspheres for bone regeneration", financed by FCT, ref: POCTI/FCB/41523/2001;

FLAD – Fundação Luso-Americana para o Desenvolvimento: "Engineering growing bone using three dimensional porous chitosan scaffolds – *in vitro* studies";

Fundação Calouste Gulbenkian – "Engineering growing bone using three dimensional porous chitosan scaffolds – *in vivo* studies";

American Association of Orthodontics Foundation.

To my parents and Ana

and

To my brother, Isabel and Leonor

Acknowledgements

I would like to express my sincere gratitude to all the ones who have contributed to this long term project, and made this thesis possible.

I will start acknowledging my supervisors Professor Mário Barbosa and Professor Cristina Teixeira, for all the opportunities that they gave me, and for many hours of discussion that they spend with me. THANK YOU.

My acknowledge goes also to the collaboration of the following persons who made this work possible:

At FFUP: Professor Fernanda Bahia, Professor Paulo Costa, Professor Isabel Almeida and Dr. Rosa Ferreira for helping in all studies concerning to polymeric solutions and for their availability and friendship whenever needed.

At Hospital de São João: Professor Abel Trigo Cabral and Dr. Rui Pinto for having supplied orthopaedic devices and explained the vertebroplasty procedure.

At CEMUP: to Daniela Silva for her availability in SEM analyses.

At ESTV: to Susana Ferreira for her very useful help when I was out of ESTV; to Angela Neves and Octávio Cardoso, my partners in the office, for always encouraged me; to all my other colleagues – Adelino Trindade, Admésio cabrita, Alexandre Aibéo, António Mário Rodrigues, António Martins, António Teixeira Almeida, Carlos Pereira, Cristina Romão, Daniel Gaspar, Francisco Lopes, Gabriel Ferreira, Henrique Silva, Hugo Ferreira, João Luís Paiva, João Vinhas, José Fiuza, José Salgueiro, José Luís Silva, Luís Paiva, Odete Lopes, Olga Contente and Paulo Vaz.

At NYUCD: to Louis Terracio for having always time to discuss and to suggest new approaches to solve problems regardless his very busy days as Dean of the research; to Deepak Saxena, John Ricci, Racquel LeGeros and Tim Bromage for helping me at any moment when I needed. I want also to thank all the other faculties of the Department of Biomaterials and Biomimetics and the Department of Basic Sciences and Craniofacial Biology for their guidance and help in this research project and for providing me the opportunity to use all the departmental facilities and resources (without any restriction): Casey Kinnally, Dianne Rekow, Joan Phelan, John Legeros, Peter Sacks,

Laurent DeJean, Nelson Silva, Page Caufield, Paulo Coelho, Van Thompson, Yihong Li. Thanks also: to Rushali Ringshia and Yelena Nemelivsky for helping me in the laboratory; to Dindo Mijares for his helping in all equipments in Biomaterials Department, and in FTIR assays; to Gloria Turner for her availability to do so many histological sections; to Zhiming He (James) for helping me in surgeries and to all other my friends who made my life easier at NY: Alejandro, Carlos, Elizabeth, Honza, João, Zhou Chen (Joyce), Katya, Natalyia, Paul, Seth, Shiela, Sonia, Upi, and Xuming.

Now, I would like to express my gratitude to all of my friends at INEB who always helped me and tried to make me smile even during hard moments – thanks to all of you. I will start by Cristina Barrias and Pedro Granja for always helped me, guided me, corrected me, and encouraging me in every moment of this work; to Cristina Ribeira for also guided me at the beginning of my project; to Isabel Amaral for helping in the preparation of chitosan solutions and sponges and always suggesting new approaches; to Carlos Fonseca, Hugo Oliveira, Inês Gonçalves and Sandra Teixeira – my great partners in the same room of the laboratory; to Ana Paula Filipe for always has been there helping me – Thanks; to all my other colleagues and friends at the INEB laboratory: Alis Mateus, Ana Cordeiro, Ana Queirós, Ana Paula Pêgo, Ana Rosa Carvalho, Anabela Dias, Andreia Cabral, Carla Monteiro, Cristina Martins, Dulce Carqueijó, Helder Machado, Eliana Vale, Fátima Pina, Prof. Fernando Jorge Monteiro, Judite Barbosa, Manuela Brás, Lino Ferreira, Maria Ascenção Lopes, Maria Pia Ferraz, Marta Evangelista, Meriem Lamghari, Patrícia Cardoso, Rui Azevedo, Sílvia Vidarra, Sofia Rodrigues, Susana Carrilho, Susana Sousa, and Virgínia Alves.

I would like to thank Nuno Pontes for his very important collaboration in the design of some images presented in this thesis and to Onélia Duarte for helping in the translating of the abstract into French.

Finally, I would like to express my sincere gratitude to my wonderful parents and brother for encouraging me and supporting me in any single need and moment. At last, to Ana for her patience and support especially when I was not present.

Abstract

Bone presents high mechanical properties and is the main support of the musculoskeletal system. Additionally, bone structure is able to remodel and readapt under external mechanical solicitations, and the remodeling mechanism is the result of the activity of osteocytes, osteoblasts and osteoclasts. Despite its ability to remodel, bone loss occurs as result of aging, disease, or injury. Therefore, medical intervention (conventional surgery or minimal invasion surgery) is required to maintain skeletal functionality. Conventional surgery is associated with higher risk of infection, while minimal invasion surgery has the advantage of lowering the risk of infection and allowing faster recovery of patients, leading to gain in terms of patient comfort as well as decreased hospital stay. Hence, many studies have been focused on the development of injectable materials in order to improve minimal invasion surgeries. In this project a novel injectable and osteoinductor material is described.

The injectable system was prepared from hydroxyapatite (HAp) microspheres and polymeric vehicles. Hydroxyapatite microspheres with diameter around 500 μm were obtained with enough strength to withstand extrusion procedures. To optimize the vehicle three polymers were tested: carboxymethylcellulose, hydroxypropylmethylcellulose and alginate. Rheological properties of the polymeric solutions were evaluated. The alginate solution 7.25% (w/w) was selected as vehicle for future studies since it presented the best rheological properties. Finally, the stability of the alginate solution was analyzed for 3 months, showing that either at 4 ºC or 25 ºC the rheological properties were maintained.

The gelation and the injectability of the mixtures (alginate solution/HAp microspheres) were further analyzed for clinical applications. The vehicle gelation conditions were optimized in order gelify in 10 to 15 minutes. To accomplish this objective, $CaCO_3$ as source of Ca^{2+} and GDL as acidifying agent were used. Additionally, the pH of the solution was maintained in the range of physiological conditions. Using ratios of $CaCO_3$/GDL=0.5 and Ca^{2+}/COO^{-}=0.288 allowed gelation in about 11 minutes. Finally, several mixtures were injected and allowed to gelify in order to evaluate their mechanical properties. Mixtures prepared using 35% (w/w) of microspheres originated the best compromise between injectability and mechanical properties. This system (vehicle/microspheres) may be adequate for future clinical application, since it allowed gelification at 37 ºC, used biocompatible

compounds, and its compression strength was closer to that of trabecular bone than most of the materials that have been used in vertebroplasty.

To overcome the osteoinduction limitations of the injectable system studied, in the second part of this work, a novel osteoinductor system with improved bone regeneration ability was developed. It explored the endochondral mechanism using a 3D structure of chitosan (sponges) as scaffold for chondrocyte culture.

Both *in vitro* and *in vivo* studies were completed to test the hypothesis that a mature cartilage scaffold carries all the signals to make new bone. During *in vitro* studies the chitosan sponges were seeded with chondrocytes harvested from caudal (CD) and cephalic (CP) regions of 14 days chick embryo sterna. Sponges seeded with CD cells worked as control whereas sponges seeded with CP cells were the experimental group. Both groups were cultured for 20 days and treated with retinoic acid (RA) over the last 10 days of culture to induce chondrocytes maturation. Chondrocytes proliferated into the sponges and after 20 days pores were completely filled with cells and matrix. However, only CP cells responded to the RA treatment, undergoing hypertrophy characterized by high amounts of type X collagen and active alkaline phosphatase enzyme. To investigate the ability of these scaffolds to induce new bone formation, *in vivo* studies using nude mice were conducted. Both control and experimental cartilage/chitosan scaffolds were implanted subcutaneously in the same animal, and the formation of ectopic bone was evaluated over time. Animals were sacrificed monthly for five months. In experimental scaffolds, mineralization was observed one month after surgery and a bone-like layer was formed after two months. Moreover, the amount of mineral and bone deposited increased during the period of study in those experimental scaffolds. After five months, bone trabeculae and bone marrow cavities were formed inside the scaffolds, and the bone deposited was similar to the bone of the mice vertebra. Interestingly, no bone formation was observed in control implants. In conclusion, an engineered transient cartilage template carries all the signals necessary to induce endochondral bone formation *in vivo.*

Resumo

O osso como o principal componente que sustenta estruturalmente o sistema músculo-esquelético apresenta elevadas propriedades mecânicas. Além disso, a estrutura óssea tem a capacidade de se regenerar e adaptar quando solicitada mecanicamente. Essa capacidade regenerativa resulta da actividade de osteócitos, osteoblastos e osteoclastos. No entanto, a perda de massa óssea ocorre ao longo do tempo devido ao envelhecimento, a doenças ou a acidentes. Assim, para manter o sistema esquelético funcional, há necessidade de intervenção médica, sendo as principais intervenções em estruturas ósseas realizadas através da cirurgia convencional ou da cirurgia minimamente invasiva. Enquanto que a cirurgia convencional está associada a um elevado risco de infecção, a cirurgia minimamente invasiva torna esse risco mais baixo e possibilita uma mais rápida recuperação dos pacientes ganhando-se em conforto para estes e em recursos hospitalares mobilizados. Por essas razões, diversos trabalhos têm sido orientados no sentido de desenvolver materiais injectáveis apropriados a cirurgias minimamente invasivas. No presente trabalho são descritos novos materiais injectáveis e osteoindutores.

O sistema injectável foi preparado a partir de hidroxiapatite (HAp) e de polímeros naturais. A HAp foi usada para a produção de microesferas, enquanto que soluções poliméricas foram usadas para optimização de um veículo. As microesferas obtidas apresentam diâmetro médio de aproximadamente 500 μm e a sua resistência à compressão é suficiente para suportar os esforços aplicados durante a extrusão. Para a optimização do veículo, foram estudados três polímeros: carboximetilcelulose, hidroxipropilmetilcelulose e alginato. As propriedades reológicas das soluções poliméricas foram avaliadas e a solução de alginato 7,25% (w/w) foi seleccionada como veículo para estudos futuros. No final foi analisada a estabilidade da solução de alginato durante 3 meses, tendo os resultados mostrado que as propriedades reológicas se mantiveram, quer a solução tenha sido armazenada a 4 ou a 25 ºC.

A injectabilidade e gelificação das misturas (solução de alginato/microesferas de HAp) bem como a caracterização mecânica dos compósitos obtidos foram estudadas posteriormente. O veículo foi optimizado de modo a gelificar num período de tempo entre 10 e 15 minutos. Para tal, foi usado $CaCO_3$ como fonte de iões Ca^{2+} e GDL como acidificante. O pH da mistura foi mantido semelhante ao pH fisiológico usando a razão $CaCO_3$/GDL=0,5. A razão Ca^{2+}/COO^{-}=0,288 permitiu gelificar a solução em aproximadamente 11 minutos. No final

foram injectadas e gelificadas várias misturas para avaliação das propriedades mecânicas dos compósitos obtidos. As misturas com 35% (em peso) de microesferas permitiram obter a melhor relação injectabilidade/propriedades mecânicas. Este sistema (veículo/microesferas) apresentou-se adequado para futuros testes, uma vez que gelifica à tempertura de 37 ºC, é composto por materiais biocompatíveis e, após gelificação, apresenta resistência à compressão mais próxima da do osso trabecular do que os materiais aplicados habitualmente em vertebroplastia.

Para ultrapassar as limitações osteoinductoras do sistema injectável estudado, na segunda parte deste trabalho foi desenvolvido e testado um novo sistema osteoinductor com capacidade regenerativa melhorada. Esse novo sistema explora o mecanismo endocondral usando estruturas 3D de quitosano (esponjas) como substrato para a cultura de condrócitos.
Para testar a hipótese de formação de osso endocondral a partir de cartilagem foram realizados estudos *in vitro* e *in vivo*. Durante os estudos *in vitro*, as esponjas de quitosano foram semeadas com condrócitos recolhidos das regiões caudal (CD) e cefálica (CP) do externo de embriões de pinto com 14 dias de gestação. As esponjas semeadas com células CD foram referenciadas como controlo, enquanto que as esponjas semeadas com células CP funcionaram como o grupo experimental. Ambos os conjuntos foram mantidos em cultura durante 20 dias. Durante os últimos 10 dias em cultura foi adicionado ácido retinoico (RA) ao meio para induzir a maturação dos condrócitos. Foi observado que quer os condrócitos CP quer os condrócitos CD, proliferaram para o interior das esponjas e que, após 20 dias em cultura, os poros das esponjas estavam completamente preenchidos com células e matriz. Apenas os condrócitos CP responderam ao tratamento com RA, produzindo elevadas quantidades de colagénio tipo X e de enzima fosfatase alcalina muito activa.
Para avaliar a capacidade destas estruturas na indução de novo osso foram realizados estudos *in vivo* usando ratos imunodeficientes. Ambos os grupos (controlo e experimental) foram implantados no mesmo animal subcutaneamente, tendo o estudo decorrido durante 5 meses com recolha de animais mensalmente. Os resultados mostraram que após um mês ocorreu mineralização no grupo experimental e que, após dois meses, houve formação de uma camada de osso na superfície das estruturas implantadas. Durante o estudo a quantidade de mineral e de osso depositado aumentaram continuamente. Após cinco meses, foi observado osso na secção transversal das amostras do grupo experimental, com características muito semelhantes às do osso trabecular. Na superfície o osso formado é semelhante a osso cortical e apresenta

espessura próxima da dos ossos das vértebras dos ratos. Curiosamente, não foi observado osso no controlo. Em conclusão, o modelo de cartilagem transiente desenvolvido possui todos os sinais necessários para induzir a formação de osso endocondral *in vivo*.

Résumé

L'os comme le principal composant qui soutient structurellement le système muscle-squelettique exige d'élevés propriétés mécaniques. En outre, la structure osseuse a la capacité de se régénérer et de s'adapter quand celle-ci sollicitée mécaniquement. Cette capacité régénératrice résulte de l'activité d'ostéocytes, d'ostéoblastes et d'ostéoclastes. Néanmoins, la perte de la masse osseuse peut se dérouler au long du temps dû au vieillissement, à des maladies ou à des accidents. Ainsi, pour maintenir le système squelettique fonctionnel, il y a la nécessité de l'intervention médicale. En étant les principales interventions dans des structures osseuses réalisées à travers de la chirurgie classique ou de la minimal invasive chirurgie. Tandis que la chirurgie classique est associée à un élevé risque d'infection, la minimal invasive chirurgie rend ce risque plus bas et rend possible une récupération plus rapide des patients en gagnant du confort pour ceux-ci et en ressource hospitaliers disponibles. Pour ces raisons, de divers travaux ont été guidés dans le but de développer des matériaux injectables qui permettent d'améliorer les minimales invasives chirurgies. Pendant le présent travail sont décrits de nouveaux matériaux injectables et osteoinducteurs.

Le système injectable a été préparé à partir de hydroxyapatite (HAp) et de polymères naturels. La HAp a été utilisé pour la production de microsphères tant dit que les solutions polymériques ont été utilisées pour optimisation d'un véhicule. Les microsphères obtenues présentent un diamètre moyen approximativement de 500 µm et sa résistance à la compression est suffisante pour supporter les efforts appliqués pendant l'extrusion. Pour l'optimisation du véhicule, ont été étudiés trois polymères: carboxyeméthylcellulose, hydroxypropylméthylcellulose et alginate. Les propriétés rhéologiques des solutions polymériques ont été évaluées et la solution d'alginate 7,25% (w/w) a été sélectionnée comme véhicule pour futures études. À la fin s'est analysée la stabilité de la solution d'alginate pendant 3 mois et les résultats ont montrés que les propriétés rhéologiques se sont maintenues que la solution ait été stockée à 4 ou 25 ºC.

L'injectabilité et gélification des mélanges, solution d'alginate/microsphères de HAp, ainsi que la caractérisation mécanique des composites obtenues se sont écoulées ultérieurement. Le véhicule a été optimisé de manière à gélifier dans une période de temps entre 10 et 15 minutes. Pour cela s'est utilisé $CaCO_3$ comme source d'ions Ca^{2+} et GDL comme acidifiante. Le pH du mélange a été maintenu semblable au pH physiologique en utilisant la raison

$CaCO_3$/GDL=0,5. La raison Ca^{2+}/COO^{-}=0,288 a permis gélifier la solution dans approximativement 11 minutes. À la fin ont été injectées et gélifiées plusieurs mélanges pour évaluation des propriétés mécaniques des composites obtenues. Les mélanges avec 35% (en poids) de microsphères ont permis d'obtenir la meilleure relation injectabilités/propriétés mécaniques. Ce système (véhicule/microsphères) s'est présenté approprié pour de futurs essais vu que permet la gélification à la température de 37 ºC, se compose de matériaux biocompatibles et, après gélification, présente résistance à la compression la plus proche de l'os trabéculaire que les matériaux appliqués habituellement en vertébroplastie.

Dans la deuxième partie de ce travail s'est développé et testé un nouveau système osteoinducteur avec la capacité régénératrice améliorée. Ce nouveau système explore le mécanisme endochondral de formation de l'os en utilisant des structures 3D de quitosan (éponges) comme substrat pour la culture de chondrocytes.

Pour se tester l'hypothèse de formation d'os endochondral à partir de cartilage, des études ont été réalisées *in vitro* et *in vivo*. Pendant les études *in vitro*, les éponges de quitosan ont été semées avec des chondrocytes rassemblées des régions caudal (CD) et céphalique (CP) de l'externe d'embryons de poussin avec 14 jours de gestation. Les éponges semées avec des cellules CD ont été référencées comme contrôle tandis que les éponges semées avec des cellules CP ont fonctionné comme le groupe expérimental. Les ensembles ont été maintenus en culture pendant 20 jours. Pendant les 10 derniers jours en culture a été ajoutée acide rétinoïque (RA) au moyen pour induire maturation des chondrocytes. S'est observé que, soit les chondrocytes CP soit les chondrocytes CD ont proliféré vers l'intérieur des éponges et que, après 20 jours en culture, les pores des éponges étaient complètement remplis avec cellules et matrice. Seulement les chondrocytes CP ont répondus au traitement avec RA en produisant des quantités élevées de collagène type X et d'enzyme phosphatase alcaline très active.

Pour évaluer la capacité de ces structures dans l'induction de nouvel os ont été réalisés des études *in vivo* en utilisant des souris immunodéficients. Les deux groupes (contrôle et expérimental) ont été implantés au même animal sous-cutanée et l'étude s'est déroulé pendant 5 mois avec collecte d'animaux mensuellement. Les résultats ont montré qu'après un mois s'est produit minéralisation dans le groupe expérimental et que, après deux mois, il y a eu formation d'une couche d'os à la surface des structures implantées. Durant l'étude la quantité de minéral et d'os déposé ont augmenté continûment. Après cinq mois, a été observé de l'os dans la section transversale des échantillons du groupe expérimental très semblable à l'os

trabéculaire enveloppé par moelle osseuse. Dans la surface l'os formé est semblable à l’os cortical et présente épaisseur proche à celle des os des vertèbres de souris.

Contents

	Acknowledgements	i
	Abstract	iii
	Resumo	v
	Résumé	ix
	Aim and structure of the thesis	1
Chapter I	Injectable system and scaffolds to promote endochondral mechanism for bone regeneration	7
	Introduction	7
	Ceramic materials	9
	Polymeric materials	10
	Cellulose derivatives	11
	Alginate	14
	Chitosan	18
	Injectable systems	28
	Types of injectable systems	28
	Pastes	29
	Gels	31
	Microspheres	33
	Preparation of injectable systems	34
	Thermoplastic pastes	35
	In situ crosslinked systems	35
	Endochondral ossification	39
	Endochondral mechanism	39
	Growth plate	40
	Mineralization	43
	Vascular invasion	44
	Apoptosis	45
	Ossification	46
	References	47

Chapter II	Morphology and mechanical properties of injectable ceramic microspheres	67
Chapter III	Optimization of polymeric solutions as vehicles for injectable hydroxyapatite microspheres	75
Chapter IV	Injectability of a bone filler system based on hydroxyapatite microspheres and a vehicle with *in situ* gel-forming ability	91
Chapter V	Engineering endochondral bone: *in vitro* studies	113
Chapter VI	Engineering endochondral bone: *in vivo* studies	135
Chapter VII	Conclusion remarks and future directions	153

Aim and structure of this thesis

AIM AND STRUCTURE

The search for materials to replace bone defects has been increasing over last decades. Besides mechanical properties, most of these materials should be biocompatible and present osteoinduction properties in order to improve bone formation. However, surgical techniques should also be investigated in order to diminish patients' pain. In this context, minimally invasive surgery is becoming increasingly used, for which injectable materials have to be developed.

Considering those aspects, the main aim of the work described in this thesis was the development of injectable materials and the preparation of osteoinductor scaffolds able to induce bone formation. Injectable materials were prepared using hydroxyapatite (HAp) microspheres and an alginate solution 7.25% (w/w) as vehicle, whereas the osteoinductor scaffolds were prepared using chondrocytes seeded in chitosan sponges.

This work is presented in VII chapters. A brief introduction is made in chapter I and the complete experimental work is presented in the five following chapters (chapter II to VI). Chapter VII presents the concluding remarks and future directions.

Chapter I

In this first chapter, an introduction to biomedical materials, namely ceramic and polymeric materials, is presented. Ceramic materials (glass-ceramics and calcium phosphates) properties and applications are discussed briefly, whereas polymeric materials (cellulose derivatives, alginate and chitosan) structure and properties are presented in more detail. Besides the pertinent discussion of the properties of these materials, a literature review about biocompatibility, biodegradation, and biomedical applications (drug delivery, wound dressing, orthopedics and cell culture) is presented. In addition, different types of injectable systems (pastes, gels, and microspheres), their applications and preparation methods (thermoplastic pastes and crosslinking techniques) are presented. Finally, an overview of transient cartilage during endochondral mechanism (growth plate, mineralization, vascular invasion, apoptosis, and ossification) is discussed.

Chapters II, III and IV - Injectability

For orthopedic applications, materials strength should be similar to bone strength. Thus, **Chapter II** covers the preparation and optimization of HAp microspheres able to function as the structural phase of an injectable material. The microspheres were produced by drop-wise of different suspensions of HAp particles ("Captal s", "Captal 20" or "Captal 30") into a $CaCl_2$ solution. After formed, microspheres were dried overnight and then sintered at 1100, 1200 or 1300 ºC. After sintering, the compression strength and diameters of the microspheres were evaluated. Microspheres produced from "Captal s" particles and sintered at 1200 ºC for 1 hour were selected for the rest of the work. They presented a diameter of 535±38 μm and their compression strength (0.35±0.08 N) was enough to withstand an injection procedure. Among microspheres prepared from other particles, only microspheres prepared from "Captal 20" and sintered at 1300 ºC for 6 hours presented strength higher than 0.35 N. However, these microspheres presented a surface rougher than microspheres prepared using "Captal s" particles.

Chapter III describes the selection and optimization of a biocompatible vehicle able to carry HAp microspheres through a device used to inject bone cement in minimally invasive surgeries. The selection of the vehicle was based on the rheological properties of different solutions of alginate, hydroxypropylmethylcellulose and sodium-carboxymethylcellulose. Viscosity was assessed using a viscometer fitted with concentric cylinders and injectability was performed using the device mentioned above. Among the three polymers, alginate solutions presented a behavior closer to a Newtonian fluid, showing a small decrease in viscosity at shear rates below 30 s^{-1}. After preliminary injection tests using HAp microspheres, sterile alginate 7.25% (w/w) was selected as the most appropriated vehicle. Finally, physical stability of this solution was studied at 40, 25 and 4 ºC over three months. It was observed that rheological properties presented minor changes when the vehicle was stored at 25 or at 4 ºC.

In **Chapter IV** the gelation process of sterile alginate 7.25% is described, as well as the injectability of mixtures prepared using this alginate solution and HAp microspheres. To promote gelation, $CaCO_3$ was used as source of Ca^{2+} and a ratio Ca^{2+}/COO^{-}=0.288 was able to induce gelation in about 11 minutes; therefore, this ratio was used to prepare the vehicle to perform injectability tests. This vehicle, ready to undergo gelation at 37 ºC, was mixed with

different concentrations of HAp microspheres (20, 30, 35, and 40%) and, each mixture, was extruded using the injectable device. After gelation at 37 ºC, mechanical properties of the ceramic/polymeric composites were evaluated. Composites prepared using 35% of microspheres presented the best compromise between injectability and compression strength. Therefore, this composition was considered the most appropriated formulation to inject in bone defects.

Chapters V and VI - Osteoinductible constructs

Chapter V describes the preparation and properties of chitosan sponges, and reports the *in vitro* studies conducted to evaluate chondrocytes proliferation and maturation in those scaffolds. Chitosan sponges were prepared by a freeze/drying process, resulting in pores of about 100 μm of diameter. Chondrocytes were harvested from caudal (CD), permanent cartilage, and cephalic (CP), transient cartilage, areas of the sterna of 14 days chick embryos. After seeded in sponges, chondrocytes were cultured for 20 days, and treated with retinoic acid to induce maturation and matrix synthesis. Results showed chondrocytes attachment, proliferation and an abundant matrix synthesis, completely obliterating the pores of the sponges. However, only CP chondrocytes underwent maturation and markedly changed the mechanical properties of the CP chondrocytes/chitosan constructs. As a result, transient cartilage scaffolds and permanent cartilage scaffolds were developed.

To investigate the ability of transient cartilage scaffolds to mimic the process of bone formation occurring at growth plates, *in vivo* studies were performed. These studies are reported in **Chapter VI**. After 20 days in culture, both transient and permanent cartilage scaffolds were implanted subcutaneously into the back of nude mice. Animals were sacrificed monthly and bone formation was evaluated over a period of five months. Mineralization was assessed by Faxitron, micro computed tomography, scanning electron microscopy and Fourier transform infrared spectroscopy analyses. Histological analysis provided further information on tissue changes in the scaffolds. In transient cartilage scaffolds, bone formation was evident as early as one month after surgery, and increased over the implantation period with bone and bone marrow cavities developing throughout the implant. Interestingly, bone deposited was similar to the bone of the mice vertebra and no bone formation was observed in permanent cartilage scaffolds.

Chapter VII - Concluding remarks

In the last chapter of the thesis a short general discussion is presented, while detailed discussions are provided in each of the preceding chapters. Possible directions for future research are also proposed.

PAPERS RESULTING FROM THIS THESIS

1. **Oliveira SM**, Barrias CC, Ribeiro CC, Almeida IF, Bahia MF and Barbosa MA. Morphology and mechanical properties of injectable ceramic microspheres. Key Engineering Materials, In Press **(Chapter II)**.

2. **Oliveira SM**, Almeida IF, Costa PC, Pena Ferreira MR, Barrias CC, Bahia MF and Barbosa MA. Optimization of polymeric solutions as vehicles for injectable hydroxyapatite microspheres. Submitted to European Journal of Pharmaceutical Sciences in July 2008 **(Chapter III)**.

3. **Oliveira SM**, Barrias CC, Almeida IF, Costa PC, Pena Ferreira MR, Bahia MF and Barbosa MA. Injectability of a bone filler system based on hydroxyapatite microspheres and a vehicle with *in situ* gel-forming ability. J Biomed Mat Res part B: Applied Biomaterials. Published Online – 24 Apr 2008 **(Chapter IV)**.

4. **Oliveira SM**, Amaral IF, Barbosa MA and Teixeira CC. Engineering endochondral bone: in vitro studies. Tissue Engineering, Part A, In Press **(Chapter V)**.

5. **Oliveira SM**, Mijares DQ, Turner G, Amaral IF, Barbosa MA and Teixeira CC. Engineering endochondral bone: in vivo studies. Tissue Engineering, Part A, In Press **(Chapter VI)**.

CONTRIBUTION OF THE AUTHORS TO THE PAPERS RESULTING FROM THIS THESIS

Oliveira SM planned and conducted all the experimental work and wrote the manuscripts. Co-authors contributed with their expertise in the following areas:

1. **Barrias CC and Ribeiro CC:** assistance in the preparation of microspheres and in planning the experimental work; **Almeida IF:** assistance in the characterization of microspheres compression strength.

2. **Almeida IF and Costa PC:** performing of viscosity and stability tests; **Pena Ferreira MR:** preparation of cellulose derivative and alginate solutions; **Barrias CC:** assistance in the preparation of microspheres.

3. **Barrias CC:** assistance in planning the injectability of mixtures; **Almeida IF:** assistance in injectability, gelation and mechanical tests; **Costa PC:** assistance in viscosity tests; **Pena Ferreira MR:** preparation of alginate derivative solutions;

4. **Amaral IF:** assistance in the deacetylation of chitosan, and preparation and characterization of chitosan sponges.

5. **Mijares DQ:** assistance in microCT and FTIR tests; **Turner G:** preparation of histological sections; **Amaral IF:** assistance in the characterization of chitosan sponges.

Chapter I

INJECTABLE SYSTEM AND SCAFFOLDS TO PROMOTE ENDOCHONDRAL MECHANISM FOR BONE REGENERATION

INTRODUCTION

Bone, a vigorous, well-vascularized tissue has an exceptional capability to heal and remodel, and to rapidly activate mineral stores on metabolic demand.[1] Its main role is to provide structural support for the body and to serve as a mineral reservoir. It also supports muscular contraction resulting in motion, withstands load bearing and protects internal organs.[1,2] Therefore any major change in its structure due to injury or disease can significantly alter one's body equilibrium and quality of life.

Every year, more than a million bone-implants procedures are performed in the world, about 500,000 only in the United States, using a wide variety of bone implants materials. However, the search for an ideal bone implant material is still going on. Although major advancements occurred in the field of bone regenerative medicine in the past years, current therapies, such as bone grafts still have several limitations. Despite the fact that materials science expertise has resulted in numerous improvements in the field of bone grafting, no adequate bone substitute has been developed. Thus, some of the severe injuries related to bone go inadequately treated. Current orthopedic replacement materials do not perfectly adjust to the defect to be treated, resulting in increased difficulties in adjacent tissue growth. In addition, these grafting materials need to be produced in advance, thus increasing the risk of contamination. The fact that the injury usually affects a large area and requires a considerable amount of time to regenerate, also contributes to infection.

The first mention of bone transplantation goes far back to 1682 in the church literature where a Russian soldier's cranial defect was successfully treated with a piece of dog skull.[3] Since then bone transplantation concept has changed and, nowadays, bone graft materials have been divided in different groups on the basis of their origin: 1) Autografts or autogenous bone grafts are considered the best grafting material in the craniofacial skeleton. They are obtained from another site of the patient's body. They can be cancellous (iliac crest) used to promote

osteogenesis, or cortical (tibia) used when stability is required. They have superior capacity to promote osteogenesis and are not associated with immunologic problems. Disadvantages include limited supply of the grafts, donor site morbidity and additional expense and trauma.[4] 2) Allografts – the grafts taken from another individual of same species. They are obtained 24 hours after the donor's death and then freeze dried and processed. Demineralized human bone matrix is also used as allogenic graft material. These grafts are easily obtainable but are expensive, and associated with risk of disease transmission and immunogenic problems.[5] 3) Xenografts – obtained from another species such as bovine (deproteinized bone mineral or sintered deproteinized bone), pig (porcine amelogenin), or coral. They are available in good supply but are associated with the risk of disease transmission such as bovine spongiform encephalopathy – "mad cow disease".[5]

Considering all the disadvantages above mentioned, a significant amount of research has been done to develop synthetic bone graft materials or alloplastic materials. They are available in powder, granules, blocks, cements and coatings. Those materials can be bioactive (capability to chemically bond with surface of surrounding bone without fibrous involvement occurs), or bioinert with no chemical bonding. Although some of alloplastic materials are osteoconductive, they have been incorporated with growth factors and progenitor cells to make them osteoinductive.[6] Alloplastic materials include ceramics (alumina, zirconia, calcium phosphate, calcium sulphate, calcium carbonate and bioglass), polymers (resorbable and non-resorbable) of natural origin (collagen, chitosan, alginate, etc.) or synthetic (polyethylene, polylactic acid, polyglycolic acid), metals (titanium and its alloy), and composites.[7,8]

An ideal bone graft should be biocompatible,[9-11] and have appropriate pore size, with interconnected pores to allow cell ingrowth and an accurate cell distribution throughout the porous structure. The porosity should facilitate the neovascularization, capillary ingrowth, accurate diffusion of nutrients and gases, and the removal of metabolic waste resulting from the activity of the cells that have grown into the scaffold.[12] Pore size is an important issue to address since small pores are unsuitable for tissue ingrowth while big pores would affect the mechanical properties of the scaffold which might be important in areas of higher strength. The scaffold should also be osteoinductive[13] and present appropriate surface properties since the chemistry and topography of surface affect both cellular adhesion and proliferation.[14,15] In addition, the scaffolds should withstand the hydrostatic pressures and maintain the spaces required for cell ingrowth and matrix production, *in vitro* and ultimately *in vivo*.[11] Because

bone is always under continuous stress, the mechanical properties of the implanted construct should ideally match those of living bone in order to enable a faster mobility of the injured site.[9-11] Furthermore, an ideal scaffold's degradation rate must be tuned appropriately with the growth rate of the new tissue, in such a way that by the time the injury site is totally regenerated the scaffold is totally degraded.[16]

Ceramic materials

Over the past decades, ceramic materials have been given a lot of attention as candidates for implant materials. Despite their low toughness, they possess certain highly desirable characteristics as hardness and compression strength. For instance ceramics have been used in dentistry for dental crowns owing to their inertness to the body fluids, high compressive strength, and good aesthetical appearance.[17,18] The two principal ceramic material groups used in orthopedics are glass-ceramics and calcium phosphates, which are described in next paragraphs.

In the early 1960s, polycrystalline ceramics (glass-ceramics) made by controlled crystallization of glass were developed.[19] The most used systems are SiO_2-CaO-Na_2O-P_2O_5 and Li_2O-ZnO-SiO_2 systems which are the base of Bioglass® and Ceravital®, respectively. Glass-ceramics have several desirable properties compared to glasses and ceramics. The thermal expansion coefficient is very low, typically 10^{-7}/ºC to 10^{-5}/ºC and in some cases, it can be made even negative. Due to the controlled grain size and improved resistance to surface damage, the tensile strength of these materials can be increased at least a factor of two, from about 100 MPa to 200 MPa. Another important aspect is the mechanical strength of bone-Bioglass® which is of the same order of magnitude of the bulk glass-ceramic strength (83.3 MPa) and about three-fourths of the host bone strength.

The main drawback of glass-ceramics is their brittleness. Hence, they cannot be used for making major load-bearing implants, such as joint implants. However, they can be used as fillers for bone cement, dental restorative composites, and coating material.[19-22]

Calcium phosphates are a type of ceramic that has been widely used as artificial bone. It has been synthesized and used for manufacturing of various forms of implants as well as for solid or porous coatings. Applications include dental implants, periodontal treatment, alveolar ridge augmentation, orthopedics, maxillofacial surgery, and otolaryngology, among others. Different phases of calcium phosphate are used, depending upon whether a resorbable or bioactive material is desired.[18,20] The applications of calcium phosphates as implants are also

strongly influenced by their mechanical behavior. Tensile and compressive strength and fatigue resistance depend on the total volume of porosity which can be in the form of micropores (<1μm diameter, due to incomplete sintering) or macropores (>100μm diameter, created to permit bone growth).[23]

The stable phase of calcium phosphate ceramics depends considerably upon temperature and the presence of water, either during processing or after implantation. At body temperature, only two calcium phosphates are stable when in contact with aqueous solution such as body fluids. At pH<4.2, the stable phase is $CaHPO_4.2H_2O$ (dicalcium phosphate, DCP), while at pH≥4.2 the stable phase is $Ca_{10}(PO_4)_6(OH)_2$ (hydroxyapatite, HAp). At higher temperatures, other phases such as $Ca_3(PO_4)_2$ (tricalcium phosphate, β-TCP) and $Ca_4P_2O_9$ (tetracalcium phosphate) are present. The unhydrated high-temperature calcium phosphate phases interact with water or body fluids at 37 ºC to form HAp which is the main mineral component of bone. Therefore, synthetic porous HAp is widely used as bone substitute due to its biocompatibility and its osteoconduction.[20,24-26]

Jarcho *et al*. described the bonding process to HAp implants. A cellular bone matrix from differentiated osteoblasts appears at the surface, producing a narrow amorphous electron dense band only 3 to 5 μm wide. Between this area and the cells, collagen bundles were seen. Bone mineral crystals have been identified in that amorphous area. As the site matures, the bonding zone shrunk to a depth of only 0.005 to 0.2 μm and the result was normal bone attached through a thin epitaxial bonding layer to the bulk implant.[27]

Polymeric materials

Polymeric materials represent an important group of the biomaterials used today in medical applications, since they exhibit properties (e.g. low density and high toughness) that cannot be achieved by the other groups of biomaterials.[28] Usually, polymeric materials for biomedical applications are divided into two groups: biodegradable and non-biodegradable.[29,30] In the present text we will focus in biodegradable polymers due to their suitability for the biomedical application.

The term biodegradable is associated with materials susceptible of decomposition by natural biological processes, such as the action of bacteria, plants, and animals[31] though other terms like absorbable, erodible, and resorbable have also been used in the literature to indicate biodegradation. The interest in biodegradable polymers for biomedical engineering use has dramatically increased during the past decade. The reason is the two major advantages when

compared with non-biodegradable materials. Firstly, they do not elicit permanent chronic foreign-body reactions due to the fact that they are gradually absorbed and do not permanently leave traces of residues in the implantation sites.[29] Secondly, some of them have recently been found to be able to regenerate tissues.[32,33] Hence, surgical implants made from biodegradable biomaterials could be used as a temporary scaffold for tissue regeneration. This approach towards the reconstruction of injured, diseased, or aged tissues is one of the most promising fields in this century.

Many biodegradable polymers have been studied however this thesis was focus only on some of based natural polymers that have been widely used for biomedical applications, such as: cellulose derivatives (hydroxypropylmethylcellulose and carboxymethylcellulose), alginate and chitosan.

Cellulose derivatives

Cellulose is the world's most abundant natural, renewable and biodegradable polymer, its main sources are wood pulp and cotton and it can present high stiffness and high crystallinitty serving well as a structural engineering material. Cellulose basic monomeric unit is D-glucose which are linked through a glycosidic linkage in the β-configuration between carbon 1 and carbon 4 of adjacent units to form long chain 1,4-glucans (Figure 1).

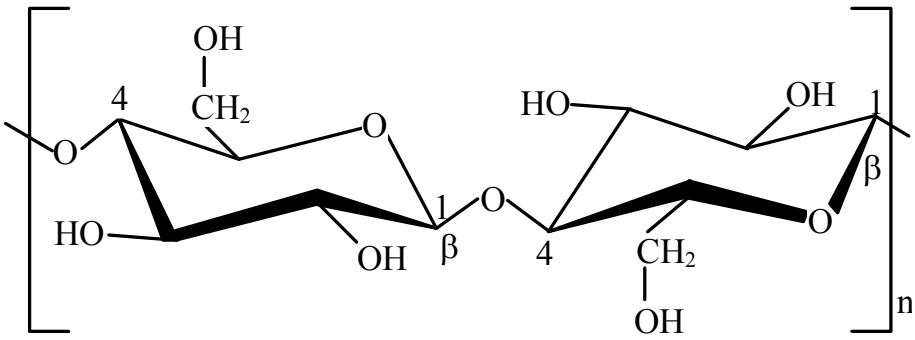

Figure 1. Cellulose structure.

Cellulose is not soluble in common solvents which make its use as pharmaceutical product more difficult.[34] To use cellulose as a pharmaceutical material it should be soluble and flexible, therefore is common to prepare cellulose derivatives to undergo those limitations. Cellulose derivatives preparation becomes an easy process since cellulose molecules contain more than 30% of hydroxyl groups. In fact, each cellulose unit possesses one primary and two

secondary hydroxyl groups and those groups can undergo addition, substitution and oxidation reactions. Although, hydroxyl groups are active, its availability to react can diverge from as little as 10 to 15% in highly crystalline cellulose to as 98 to 100% in regenerated non-crystalline cellulose.[35]

The preparation of cellulose derivatives depends on the average number of hydroxyls substituted in D-glucose unit, which is known as the degree of substitution (DS). As result, DS can vary from zero (cellulose itself) to a maximum of three (fully substituted cellulose). The substitution of hydroxyl groups using ether groups results in cellulose ethers which are the cellulose derivatives most used in medicine field and also the most widely used polysaccharides in pharmaceutical industries[36] like sodium carboxymethylcellulose and hydroxypropylmethylcellulose.

Sodium carboxymethylcellulose (NaCMC)

Sodium carboxymethylcellulose is manufactured by an industrial process. Basically, NaCMC (Figure 2) is prepared by treating cellulose with aqueous sodium hydroxide followed by reaction with sodium chloroacetate. The main applications are the food industry as a thickener or stabilizer compound and the pharmaceutical industry for personal care product. To achieve

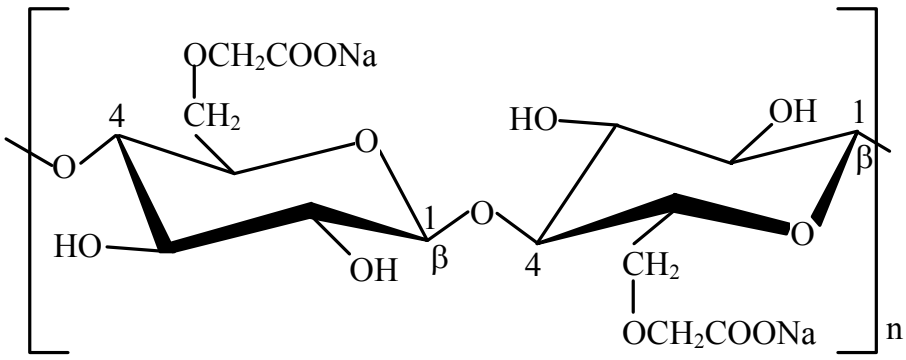

Figure 2. Sodium carboxymethylcellulose structure.

a medical grade, a more refined material has to be prepared and the excess of salt removed washing the materials with an alcohol-water solution. The DS is also an important parameter to be controlled since at low DS (below 0.4) the polymer becomes insoluble. The DS control is achieved controlling the time and the temperature of the reaction. NaCMC is non-toxic, and generally non allergenic presenting high fluid absorbance and retention for long periods

directly into its fibers which make it a good material for wound dressing applications improving the wound healing process.[37,38] When in contact with fluids, NaCMC forms a soft gel or a viscous solution which has led its use for wound care, in gel formulations and in hydrocolloid dressing.

The use of NaCMC for optical purposes has also been developed. It is common to use NaCMC in the improvement of dry eyes and to prepare ophthalmic viscosurgical devices to ensure the maintenance of the ocular space hence protecting of the corneal endothelium.[39-41]

Postoperative adhesion formation is the single greatest complication of a surgery. Fibrous adhesions form at peritoneum, central nervous system, pericardium, pleura, and synovium. The use of NaCMC as biomaterial was used in the form of films and gels reducing adhesion in a variety of animal models.[42,43] Most recently, diZerega *et al*.[44] have observed a significant reduction of adhesion formation in women undergoing pelvic surgery.

This cellulose derivative is also seen as material with antioxidant properties, as an anti-inflammatory enzyme stabilizer and it is considered as a potential matrix system for drug delivery or controlled release of bioactive agents.[45-47] Its biocompatible properties also have pushed NaCMC into bone growth research. Rodgers *et al*.[48] have described NaCMC either plain or combined with bone morphogenetic proteins as encouraging bone growth, suggesting that NaCMC influence new bone formation because it is hydrophilic.

Hydroxypropylmethylcellulose (HPMC)

Hydroxypropylmethylcellulose as a cellulose derivative like NaCMC, is also prepared using alkali cellulose, however, the reacting groups are methyl halide and propylene oxide resulting the methyl and hydroxypropyl substitutes (Figure 3). HPMC has a wide range of industrial applications particularly in food industry, pharmacy and medicine (health care, orthopaedics and opthalmics).[49,50] Specifically, HPMC is used whenever there is a need to thicken, gel, emulsity, suspend, stabilize, water retention and good workability. In food industry, HPMC uses are based more on the ability to gelify on heating while in pharmacy and biomedical fields, the drug controlled-release and the biocompatibility are very important properties. In opthalmics, the presence of extremely toxic free radicals damage the corneal endothelium inducing corneal edema, however the protection with HPMC shows effective against it, preventing those damages.[50]

In orthopaedics, HPMC (3% aqueous solution) has also been widely studied as a carrier of

ceramic particles to prepare injectable bone substitute systems (IBS). Most of these studies were performed by Daculsi and his coworkers using biphasic calcium phosphate (BCP) granules as reinforcement phase. Besides injectability, Daculsi's group also studied the

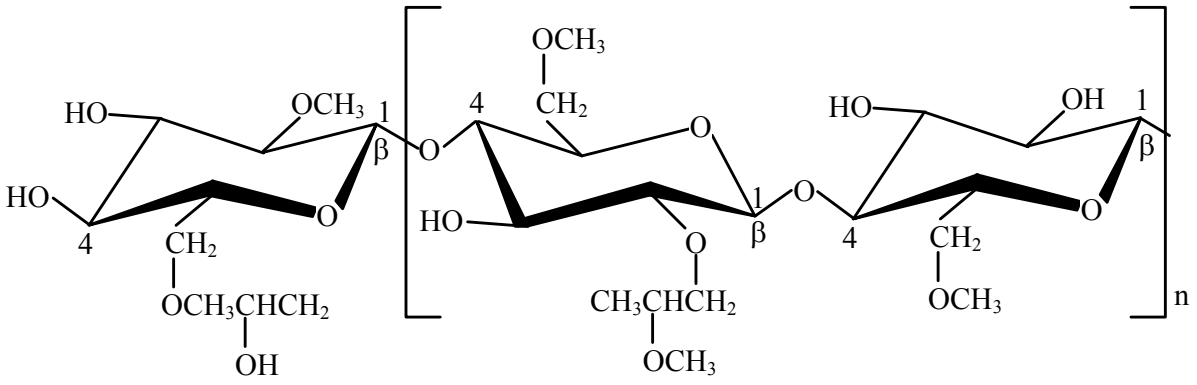

Figure 3. Hydroxypropylmethylcellulose structure.

interactions between IBS components (HPMC and BCP) as well as IBS nontoxicity, biocompatibility and osteoinduction.[51-55] In terms of HPMC/BCP interactions, it is suggested the formation of complexes between Ca and HPMC which improve its affinity to the mineral phase and the exceptional results achieved in animals studies[53] though Dorozhkin's study reports no chemical interaction between calcium phosphates and HPMC.[56]

Alginate

Alginate is a natural polymer present within the cell walls and intercellular spaces of brown algae and it is responsible for flexibility and strength of those marine plants.

Chemically, alginate is a linear unbranched copolymer of (1-4) linked α-L-guluronic (G) and β-D-mannuronic (M) acid residues. These acids are organized forming homopolymeric regions of G and M, termed G- and M-blocks, respectively, with different lengths and sequential arrangement.[57] Because of the particular shapes of the monomers and their modes of linkage in the polymer, the geometries of the G-block regions, M-block regions, and alternating regions are substantially different. Specifically, G-blocks are folded while the M-blocks have a shape referred to as an extended band (Figure 4). The G- to M-block ratio is important to control gel strength, with higher G contents resulting in higher mechanical strength.[58] However, high G content diminish the activity of cells in culture.[59,60]

In many applications, alginate gelification is required since scaffolds have to remain in site as

well as they have to enable the encapsulation of drugs and cells. To obtain a hydrogel structure, alginate crosslinking either covalently or ionically is common. The covalent crosslinking has been reached using glutaraldehyde, isopropyl alcohol and genipin.[61-65]

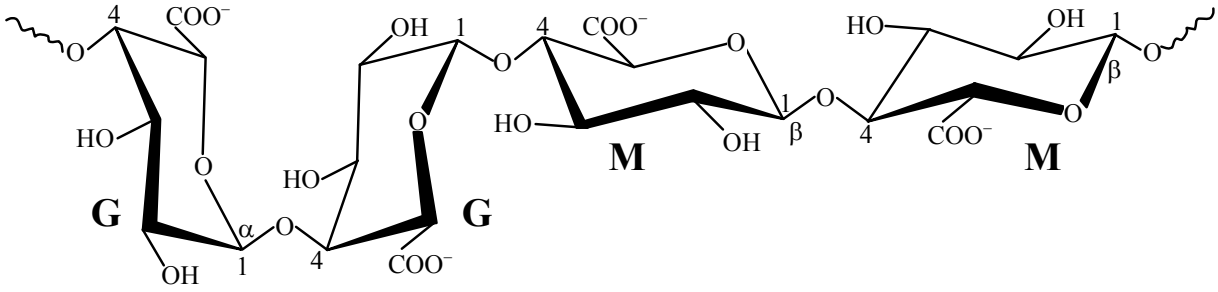

Figure 4. Chemical structure of alginate. G-blocks are folded and M-blocks extended.

Although, covalent crosslink improves the mechanical strength, the use of chemical agents may lead to toxic effects or to unwanted reactions with drugs.[66] Therefore, ionic crosslinking has been used successful in areas of pharmacy and medicine as alternative. The gelation of alginate by ionic crosslinking can be achieved by reaction with divalent ions such as Ca^{2+}, Ba^{2+}, and Sr^{2+}. Monovalent cations and Mg^{2+} ions do not induce gelation while Ba^{2+} and Sr^{2+} ions produce stronger alginate hydrogels than Ca^{2+}.[67,68] This gelation takes place when those divalent cations interact ionically with G-blocks, resulting in the formation of a three dimensional network which is usually described as "egg-box" structure (Figure 5).[69]

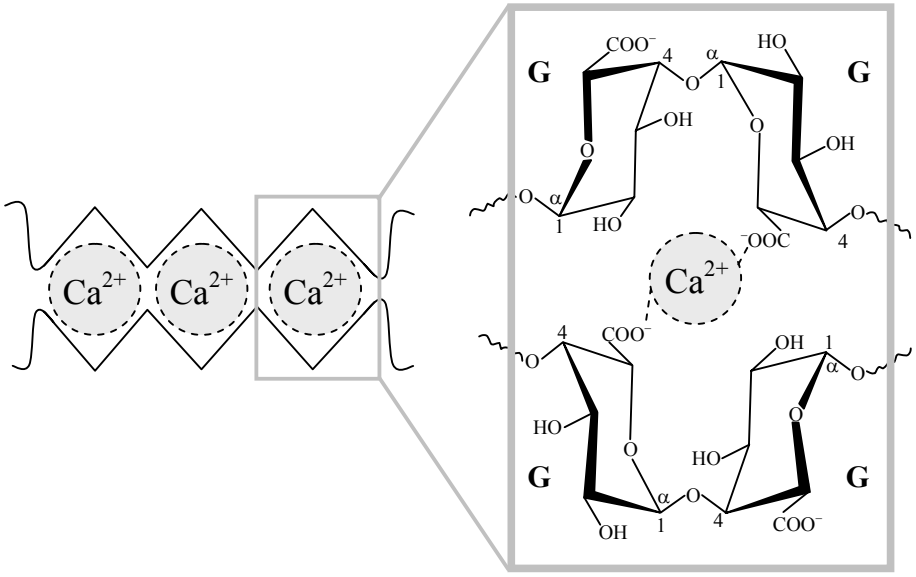

Figure 5. Egg-box juntion of Ca^{2+} ion in polyguluronate blocks.

The preparation of such gels can be almost instantaneous forming microspheres or by controlled gelation which is achieved controlling the divalent cations release into the solution. The preparation of these controlled gelation hydrogels can be based in the use of $CaCO_3$ suspensions, which are able to produce alginate gels using different gelation times since $CaCO_3$ dissociation can be controlled by the regulation of the pH solution.[70]
Alginate has been used for long time in the food industry as stabilizer and thickener. Although, that industry is very important for alginate production, its applications in pharmacy industries are also widespread. Non-toxicity and biodegradability of alginate make these products very well accepted in this industry as well in biomedical industry.

In terms of biodegradability, alginate is one of the most promising biodegradable materials and it can be resorbed in few weeks depending on the concentration of the solutions and on the composition of alginate used. The use of sodium alginate containing gentamicin sulphate for the treatment of bone infections was studied in terms of its biodegradability after has been inserted into a femur defect in rats. The physical disruption of alginate in small fragments was observed in one week and the complete removal of the implant from the body tissues happen in two weeks.[71] Comparing the behavior of three different concentrations of sodium alginate solutions in bone defects made in the tibia of rats, it was observed that a solution using 0.5% (w/w) of alginate had disappear after 4 weeks *in situ* whereas solutions using 1.0% or 1.5% (w/w) remained in the implantation site.[72] The preparation of alginate sponges using 1.0% (w/w) alginate to repair a defect in the facial nerve of cats were absorbed gradually and no alginate residue was detected remaining in the treated defect after 16 weeks post-implantation.[73] Mooney and coworkers evaluated the degradation of 3% (w/w) alginate hydrogels by measuring the tensile strength and the molecular weight changes.[74] In their study they prepared solutions using high G content alginates (MVG) and high M content alginates (LVM) and cultured them with rat bone marrow cells. The results showed that MVG hydrogels retained more strength for longer than LVM hydrogels and, after 12 days in culture, MVG still retained 27% of its initial strength. Additionally, MVG hydrogels worked as substrates for cell growth for over 4 weeks in culture. Suzuki *et al*.[75] had prepared an alginate hydrogel by dissolving ethylenediamine and water-soluble carbodiimide in 1% sodium alginate aqueous solution (AGA-100) to use in wound healing and they investigated *in vivo* degradation by implanting those dressing materials intramuscularly in rabbits. After 3 months AGA-100 disappeared without inflammation in the implanted site.

External applications of alginate as wound dressing are common since it forms hydrophilic gels providing a moist wound environment which promotes healing and epidermal regeneration.[75,76] More recently, it was developed and study a non-toxic and biodegradable gel produced from gelatin, oxidized alginate and borax able to form a hydrogel *in situ* and to mould into the shape of the wound defect which is an advantage over the preformed wound dressing. On the other hand the use of gelatin can improve the haemostasis in bleeding wounds and the borax improves the antiseptic and antiviral activity.[77]

The treatment of infections is commonly based in systemic drugs applications; however for some infections local delivery systems have also been used. Studies using alginate alone or in combination with other polymers or calcium phosphates as a carrier for products delivery has been performed. Microspheres of alginate prepared by emulsification were able to obtain a high bovine serum albumin (BSA) encapsulation efficiency as well as a slow release profile *in vitro* though this release profile was slower for alginate microspheres coated with poly(L-lysine) or prepared with high alginate molecular weight.[78] Recently, the use of poly(L-lysine)-coated alginate loaded with vancomycin was able to delivery this antibiotic locally in concentrations above the minimum inhibitory concentration of staphylococcus aureus for 21 days.[79]

In orthopedics, the regeneration and the repair of cartilage defects after trauma, cancer or metabolic disorders is still a major clinical challenge. Chondrocytes are known to dedifferentiate when cultured in monolayer. However, dedifferentiated bovine articular chondrocytes were able to redifferentiate after cultured in alginate beads subjected to a pressure of 5% of oxygen.[80] Even at atmospheric oxygen pressure, articular chondrocytes cultured in alginate gels or in alginate beads retain a chondrocytic phenotype which was showed by the synthesis of type II collagen and chondroitin-6-sulphate.[81-83]

The preparation of 3D scaffolds using alginate mixed with HAp or with chitosan also support chondrocytes, enhancing its proliferation and maintaining their phenotype and spherical shape with monoriented and sparse actin microfilaments network.[84,85]

The application of alginate and alginate derivatives scaffolds in the regeneration of bone structures has been studied using osteoblasts cells encapsulated either in alginate microspheres or just seeded in alginate solutions. Scaffolds prepared using alginate and chitosan have allowed osteoblasts attachment, proliferation and deposition of a calcium

matrix *in vitro*.[86] After *in vivo* implantation, calcium deposition occurred as earlier as the fourth week and these hybrid scaffolds have showed a high degree of tissue compatibility. To improve pre-osteoblasts attachment, proliferation and differentiation, alginate has been modified with RGD-containing peptides revealing statistically significant increases in *in vivo* bone formation compared with unmodified alginate.[87] Studies with RGD-modified alginate also improved myoblasts attachment, proliferation and differentiation.[88,89]

Alginate constructs also has been loaded with bone stromal cells and growth factors in order to induce bone regeneration either in bone defects or in ectopic areas. A scaffold prepared using 1% (w/w) alginate covalently crosslinked was loaded with morphogenetic protein-2-derived peptide and implanted into the calf muscle of rats. Three weeks post-implantation, vascular channels and an osteoblasts population followed by new bone formation were observed in the pores of alginate hydrogel and after 8 weeks calcification and bone formation increased showing that this oligopeptide possessed ectopic bone morphogenetic activity when linked to alginate hydrogel.[90] Also, an *in vitro* study was conducted with the aim of induce chondrogenesis using 1.2% (w/w) alginate beads to encapsulate human mesenchymal stem cells (HMSCs). The viability of cells was higher than 90% throughout the 4-week experiment and cells started to express type II collagen after 1 week. Besides, cells also started to express type X collagen after 2 weeks and its expression became stronger at the 4th week. Type X collagen is a well known marker for hypertrophic cartilage which suggests the beginning of endochondral ossification.[91] Cai *et al*.[92] used a 1.2% alginate solution to differentiate bone marrow mesenchymal stem cells (BMSSCs) (*in vitro*) into two different lineages (chondrogenic lineage and osteogenic lineage). After 14 days in culture, cells of chondrogenic lineage expressed chondrocytes markers and cells of osteogenic lineage became osteoblast-like in morphology. After *in vivo* implantation subcutaneously in the dorsum of nude mice, they found that osteoblasts like-cells induced new bone formation after 8 weeks whereas chondrocytes like-cells formed cartilage lacuna with a high proportion of type II collagen but no sign of endochondral ossification.

Chitosan

Chitosan is the result of partial deacetylation of chitin which is, after cellulose, the most abundant polysaccharide on earth. Chitin consists of β(1,4)-linked D-glucosamine (GlcN) with a high degree of N-acetylation forming the N-acetyl D-glucosamine (GlcNAc) units (Figure 6).

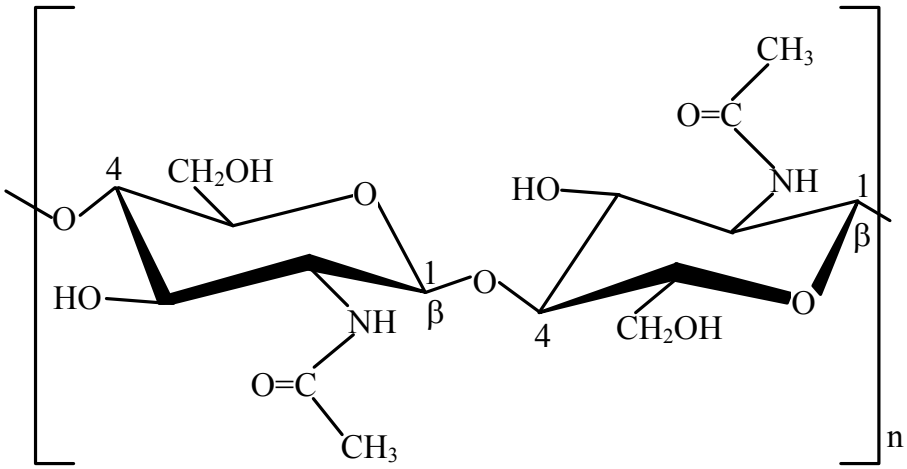

Figure 6. Chitin structure showing an N-acetyl D-glucosamine (GlcNAc).

In nature, chitin serves as a fibrous strengthening element that occurs as a structural component of exoskeleton of insects and crustaceans as well in the cell wall of yeast and fungi. The natural pathway of chitin metabolism includes enzyme-catalyzed hydrolysis by chitinases. Lysozyme enzymes which are widely distributed in plants and in animals (present in human body fluids) are also able to degrade chitin molecules.[93] In fungi, chitin turnover occurs by the action of chitin deacetylaze which deacetylate chitin to chitosan whereas, in laboratory, chitin' deacetylation is usually preformed in 50% of NaOH for 1 or 2 hours at 60 ºC under nitrogen atmosphere followed of washing in water at 70-80 ºC to neutralize. After this first treatment a degree of deacetylation of about 80% can be obtained; further deacetylation needs further treatments with alkaline solutions.

Chitin is a highly insoluble material with low chemical reactivity which is the major problem for its processing and uses. Applications of chitin and chitin-based materials are widespread and in many different areas such as environmental, food, pharmaceutical and medical industries. In the pharmaceutical and medical applications, chitin film and fiber are commonly used as wound dressing and for controlled drug release.[94,95] Also the combinations of chitin with other materials allowed the preparation of scaffolds. As example, hybrid scaffolds composed of chitin and collagen showed good affinity and proliferation in culture with fibroblasts.[96] Another interesting application is a hydroxyapatite-carboxymethyl chitin composite which was prepared and injected on the calvarial bone of rats with biocompatibility as high as that achieved with HAp materials alone.[97]

As mentioned above, chitosan is the result of chitin deacetylation. However, chitosan name is used when the deacetylated product becomes soluble in aqueous acidic solutions which usually correspond to a deacetylation degree of 50%.[98] Therefore, chitosan is a heteropolymer containing both GlcN units and GlcNAc unis (Figure 7), and their relative proportion fixes the degree of acetylation (DA) that controls many properties. The presence of the amine groups explains its unique properties among biopolymers, specially its cationic behavior in acidic solutions.

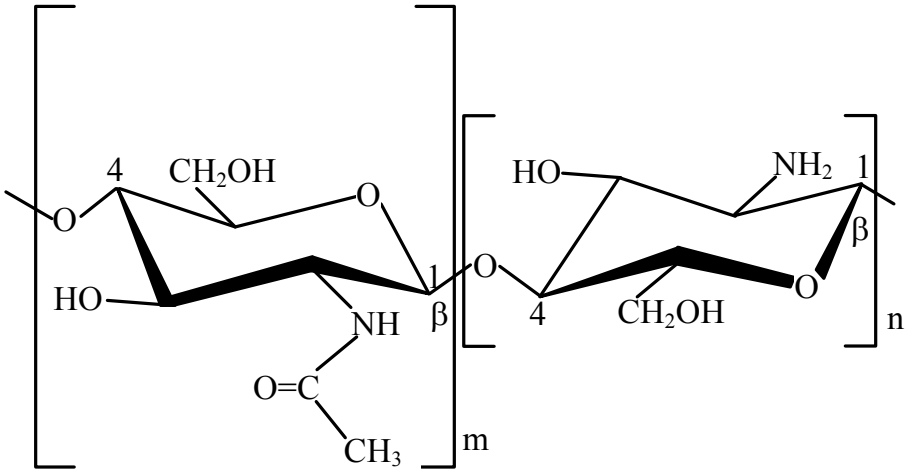

Figure 7. Chitosan structure showing an N-acetyl D-glucosamine (GlcNAc) and a D-glucosamine (GlcN) unit.

The solubilization of chitosan occurs by protonation of the $-NH_2$ group function of the C-2 position of the GlcN repeated unit, whereby the polysaccharide is converted to a polyelectrolyte in acidic media.[99,100] Solubililty is also greatly influenced by the addition of salt to solution. The higher the ionic strength the lower is the solubility.[101] This is due to the fact that chitosan in solution exists in an extended conformation due to the repelling effect of each positively charged deacetylated unit on the neighboring glucosamine unit.

The biocompatibility is an important requirement especially when chitosan is used as an implant in contact with either hard or soft tissues. If biocompatible, chitosan will be less susceptible to be rejected and more predisposed to create a good interface between host tissues and implant. Focused in this issue, many *in vitro* studies have been performed showing that chitosan and its derivatives are potentially favorable materials as substrates for the growth of different type of cells.[102-105] Other *in vitro* studies have evaluated how chitosan

compatibility depends on the degree of acetylation. Chatelet *et al.*[106] observed that higher DA's chitosan present lower cell adhesion but DA's of chitosan films did not affect the keratinocytes and fibroblasts cytocompatibility. Similar results were found by Amaral *et al.*[107,108] studying the influence of the DA in attachment, spreading and short-term proliferation of human osteoblastic MG-63 cells either in three-dimension chitosan scaffolds and on chitosan films. An *in vivo* study showed that a collagen matrix was built within pores of chitosan scaffolds implanted into mice, and angiogenic activity was observed on the external implant surface demonstrating the high degree of biocompatibility of chitosan in this animal model.[109]

Chitosan conjugated with other chemical groups in its chain have also proved to be efficient in improving the behavior of cells on its surface. The preparation of chitosan with phosphorylcholine groups presented a good biocompatibility when in culture with human umbilical vein endothelial cells[110] and the conjugation of chitosan with RGDs improved the capability for adhesion and proliferation of chondrocytes and fibroblasts.[111,112]

Besides the use of chitosan alone, its combination with other materials without chemical reaction also enabled the preparation of scaffolds. Chitosan combined with alginate, as mentioned elsewhere permitted to prepare scaffolds which have good biocompatibility in cultures with different type of cells (osteoblasts, chondrocytes, and others).[85,86,113] Using similar approaches, calcium phosphate-chitosan composites and other chitosan derivatives allowed mesenchymal stem cells and preosteoblasts viability, enhancing bone tissue formation.[114-116] On the other hand the combination of calcium phosphate cement (CPC) with chitosan produced composites stronger than CPC and composites that allow osteoblasts cells to adhere, spread and proliferate.[117] To enhance chitosan' mechanical properties is also common to crosslink it with different chemical products like glutaraldhyde, diepoxide (1,4-butanediol diglycidyl ether) and genipin which are usually more toxic compounds. However their controlled use can maintain chitosan' scaffolds biocompatibility.[118-120]

Biodegradability is another important issue in the use of a material for biomedical purposes. Usually, natural polymers have the advantage of higher biodegradability. Chitosan as a natural polymer shares that advantage, and its molecules can be broken down by lysozyme, chitosanase and chitinase enzymes.[121,122] However, chitosan's physicochemical and biological properties, such as biodegradability, are dependent on molecular weight (Mw) and DA. Zang

et al.[122] compared chitosan susceptibility to degradation by rat cecal and colonic enzymes with a commercial available almond emulsion β-glucosidase. The results show a higher degradation of chitosan molecules with lower Mw and lower DA (DA=77.8).

In human serum, chitosan is mainly depolymerized by lysozyme which biodegrades the polysaccharide by hydrolyzing the glycosidic bonds present in the chemical structure.[123] Lysozyme contains a hexameric binding site, and hexasaccharide sequences containing 3 to 4 or more acetylated units, that contribute to the initial degradation rate of N-acetylated chitosan.[124,125] This mechanism explains the slow degradation of very low DA chitosan. Freir *et al*.[126] investigating materials for nerve regeneration using concentrations of lysozyme similar to those found in the human body observed that samples with intermediated DA values were almost completely degraded in one week. However, the degradation of samples with very low or high DAs was minimal over the studied period.

In many studies, chitosan is mixed with other materials or is covalently crosslinked in order to change its mechanical properties. In those chitosan based materials, while the degradability is affected,[120,127] it still occurs by an enzymatic mechanism and depolymerization.[119,128]

Chitosan crosslinking

Despite of easy gelation and good biocompatibility, chitosan has low mechanical integrity and degrade rapidly especially in acid medium and in the presence of lysozyme.[129] On the other hand, for many applications, chitosan should be crosslinked due to its hydrophilic behavior. In this context, various crosslinking reagents, most are synthetic, have been used to prepare chitosan gels.[130,131] However, these synthetic crosslinking reagents are usually cytotoxic which may impair the biocompatibility of the crosslinked biomaterials.[132] Therefore, it is desirable to provide crosslinking reagents suitable for use in biomedical applications that are not cytotoxic and may form stable and biocompatible products. Genipin is an alternative crosslinker since it is about 5000-10000 times less cytotoxic than glutareldehyde and genipin-crosslinked chitosan microspheres have shown a superior biocompatibility and slower degradation rate than the glutaraldehyde-crosslinked chitosan microspheres.[133] Also the use of chitosan crosslinked with diepoxide-based bifunctional linkers increased its compression modulus and stiffness while supporting chondrocytes typical round shape.[119] The use of radiation is another alternative to crosslink chitosan. The UV light is a common source of energy to induce crosslinking and the use of this method enabled to successful transform azide-chitosan-lactose aqueous solution into an insoluble and flexible hydrogel. *In vivo*, this

hydrogel significantly induced wound contraction, accelerated wound closure and epithelialization of treated wounds.[134,135]

Pharmaceutical applications of chitosan

Chitosan has been widely used in the pharmaceutical industry for its potential in the development of controlled release drug delivery systems. The reason is its unique polymeric cationic character and its gel and film forming properties. Such system should allow the control of the rate of drug administration and prolong the duration of the therapeutic effect as well as the targeting of the drug to specific sites.

The potential of chitosan derivatives as vehicle for the administration of proteins was evaluated by several authors. Xu *et al.*[136] synthesized a water soluble derivative of chitosan, N-(2-hydroxyl) propyl-3-trimethylamonium chitosan chloride, and used it to incorporate bovine serum albumin (BSA), considered as a model protein drug. A preparation of Poly ethylene glycol (PEG) graft-chitosan crosslinked with genipin was able to carry BSA and poly(vinyl alcohol) (PVA), while sodium bicarbonate mixed with chitosan also worked as BSA delivery vehicle.[137,138] Chitosan microspheres were used to release transforming growth factor-β1 (TGF-β1) and its delivery profile was similar to BSA. When chitosan microspheres were loaded with TGF-β1 and seeded into porous chitosan scaffolds, chondrocyte proliferation and production of extracellular matrix were significantly increased.[139] A paste of chitosan glutamate (Protosan) and HAp was used as a delivery vehicle for bone marrow, bone morphogenetic protein-2 (BMP-2) and osteoblasts, and implanted in cranial defects of rats resulting in the formation of mineralized bone.[140] Similar tests were performed using solutions based in chitosan/polyol salt to delivery biologically active growth factors *in vivo* as well as to encapsulate living chondrocytes.[141]

Besides applications in drug delivery, chitosan and its derivatives have been widely used in the delivery of DNA, proteins and live cells. The use of DNA delivery system has the potential to overcome extracellular barriers that limit gene therapy since controlled release systems can improve gene delivery by maintaining high concentrations of DNA in the cellular environment and increasing the duration of the transgene expression. Yun *et al.*[142] prepared DNA-chitosan complexes of microspheres physically combining PEG with poly(lactic glycolic acid) (PLGA) able to sustain release for at least 9 weeks. In addition, chitosan-DNA complexes were conjugated with alpha-methoxy-omega-succinimidyl-PEG by Zhang *et al.*[143]

improving the gene expression. The preparation of chitosan microspheres incorporating adenovirus vectors for mucosal delivery was performed by Lameiro *et al.*[144] This system enabled an effective release when it was in contact with cells in monolayer while an insignificant release was observed in aqueous media. Guo *et al.*[145] combined tissue engineering with gene therapy entrapping plasmid DNA in chitosan gelation complexes, encoding TGF-β1 which has been proposed as promoter of cartilage regeneration. The transfected chondrocytes expressed TGF-β1 protein stably in 3 weeks.

Chitosan for wound dressing

On last decades the treatment of wounds was revolutionized with the use of materials on wound dressing which can replicate some of the skin's properties, like 85% water content and inherent permeability. Chitin and chitosan are known for accelerating the healing of wounds.[146,147] Chitosan stimulates the migration of cells and accelerates the regeneration of normal skin as well as it was found to promote the attachment and proliferation of fibroblasts on PVA/chitosan-blended hydrogel.[148-150] The application of cotton fiber-type chitosan for 15 days on open skin wounds of dogs demonstrated that chitosan was efficient in wound healing by increasing the formation of thick fibrin and the induction of macrophages and fibroblasts migration into the wound area.[147] Using similar materials in radiation-impaired wounds, also in dogs, was detected advanced granulation and capillary formation combined with the expressing of vascular endothelial growth factor confirming neovascularization.[151] Additionally, chitosan membranes prepared by immersion-precipitation phase-inversion method showed controlled evaporative water loss, excellent oxygen permeability and promoted fluid drainage ability.[152] In rats, wound covered with these chitosan membranes was hemostatic and healed quickly. In another study the number of living bacteria responsible to infect damaged skin was diminished using those membranes incorporating antibiotics for controlled release.[153] Using UV light, azide-chitosan-lactose hydrogels were crosslinked *in situ*. Once applied on incisions made in mice' skin, these hydrogels were enable to stop bleeding and to adhere to the skin inducing significant wound contraction, closure and healing.[134] Recently, the preparation of chitosan combined with phosphorylcholine groups through a heterogeneous reaction process showed a more hydrophilic characteristic, better anti-protein-adsorption capability, better resistance to coagulation, an improved hemocompatibility, as well as similar cell affinity and safety, compared with native chitosan.[110]

Chitosan for skeletal tissue engineering

A round cellular morphology is known to be a normal phenotypic characteristic of non-dedifferentiated chondrocytes. Since chitosan has the ability to maintain round morphology of chondrocytes and to preserve its cell specific extracellular matrix, chitosan and its derivatives have been used for studies of cartilage reconstruction. Montembault *et al.*[154] have used chitosan hydrogel substrates for culture of human and rabbit chondrocytes. Those chondrocytes were able to express mature type II collagen and aggrecan. Their phenotype was maintained for as long as 45 days, forming cartilage like nodules, while chondrocytes cultured without chitosan hydrogels dedifferentiated as indicated by the expression of immature type II collagen and type I collagen. The use of chitosan-alginate scaffolds, for culture of chondrocytes like cells (HTB-94), as well as chondroitin sulfate A combined with chitosan, for culture of bovine articular chondrocytes, allowed cells to maintain their round morphology, to produce cartilage specific type II collagen and proteoglycan, both markers of chondrocytic phenotype.[85,105] Comparing the behavior of rabbit chondrocytes on chitosan and chitosan based hyaluronic acid, Yamane *et al.*[155] suggested that hyaluronic acid improves chondrocytes proliferation while maintaining their physiological phenotype and production of a rich extracellular matrix. Additionally, scaffolds made of lactose-modified chitosan induced cell aggregation when in contact with primary culture of pig chondrocytes, leading to the formation of cartilage nodules rich in aggrecan and type II collagen.[156] Another study, using *in situ* gelling chitosan solutions (prepared by mixing chitosan disodium β-glycerol phosphate and glycosamine) loaded with primary articular chondrocytes, also supported the accumulation of cartilage matrix *in vitro.*[157] On the other hand, rabbit subchondral bone defects treated with a mixture of chitosan, glycerol phosphate and autologous blood, showed an increased inflammatory reaction, vascularization, intramembranous bone formation and subchondral bone remodeling, main factors supporting cartilage repair, when compared with untreated defects.[158]

The use of cells different from chondrocytes, but with good characteristics of proliferation and easy differentiation into chondrocytes were used also to produce cartilage using chitosan derivatives as substrate. In that study, a thermosensitive (water chitosan-poly(N-isopropylacrylamide) gel was seeded with HMSCs and injected in the submucosal layer of the bladder of rabbits inducing HMSCs differentiation into chondrocytes and the formation of cartilage in 14 weeks.[116]

The ability of chitosan and chitosan derivatives as substrate for osteoblasts and other cells related with bone regeneration has been reported in several studies. Some of those studies will be referenced in following paragraphs. The DA of chitosan plays an important role in cells morphology and proliferation as it has been showed by Amaral *et al*.[107,108]. In those studies, they demonstrated that chitosan of low DA (4%) improves cell attachment and spreading displaying long cell filopodia and numerous cell-to-cell contacts when compared with chitosan of higher DAs. Therefore low DAs chitosan as well as chitosan combined with other materials are commonly used for osteoblasts cultures. The preparation of chitosan-alginate scaffolds is one of those combinations. *In vitro* studies indicated that osteoblasts cells seeded on porous chitosan-alginate scaffolds attached and proliferated well and promoted the deposition of mineral. Additionally, *in vivo* studies, performed at same time, showed a rapid vascularization, matrix deposition and calcification.[86] It was also mentioned that all those events happened within the entire scaffolds structure though no evidences were showed. The preparation of chitosan-collagen composite sponges and CPC-chitosan scaffolds were studied *in vitro* referencing those structures as biocompatible and as good substrates for osteoblasts proliferation and differentiation.[117,159] On the other hand RGDS-modified chitosan enhanced the attachment of rat osteosarcoma cells making chitosan more biocompatible for the culture of those osteoblasts-like cells.[112]

Chitosan scaffolds were also investigated for culture of mesenchymal stem cells (MSCs), preosteoblasts and as a growth factor deliver with the purpose of bone regeneration. Chitosan scaffolds cultured *in vitro* with MSCs and preosteoblasts allowed attachment and spreading of those cells as well as their maturation into osteoblastic phenotype was successful.[114] However, comparing chitosan scaffolds with BCP embedded into chitosan scaffolds, a more uniform extracellular matrix distribution were obtained when BCP was used. Besides, cells expressed higher concentration of protein markers of osteoblastic phenotype (alkaline phosphatase and osteocalcin). The use of a paste made of chitosan glutamate and HAp cultured with osteoblasts or BMP-2 showed to be efficient in delivering these osteoinductive factors since the presence of mineralized bone spicules were observed in rat calvaria defects filled with that paste and osteoblasts or BMP-2.[140] Osteogenesis was also observed using composite porous matrix of chitosan-PLLA loaded with platelet-derived growth factor-BB (PDGF-BB) after it has been implanted in rats calvaria defects and also after porous chondroitin-4-sulfate chitosan sponges loaded with PDGF-BB has induced an increase of osteoblasts migration and

proliferation *in vitro*.[160,161] In another study performed *in vivo*, nude mice were injected subcutaneously with alginate-chitosan gels loaded with MSCs and BMP-2 as well as loaded with only one of those factors. Authors have observed that after 1 month scaffolds loaded with only one factor either MSCs or BMP-2 did not formed bone. Moreover, they started to be reabsorbed while scaffolds loaded with both factors were able to induce bone formation forming a trabecular bone like structure.[162] Another study using 3D alginate-chitosan constructs cultured with human bone marrow cells and chondrocytes also showed optimal osteocytes formation subcutaneously in immunocompromised mice. The interaction between both cells type was also studied in the creation of specific tissues.[163]

INJECTABLE SYSTEMS

Invasive surgeries are associated to high risks of infection and high levels of pain, either during or after the surgery, resulting in the need to develop alternative methods. One possible alternative consists in injectable materials, which can fill the defects up using a needle. This technique drastically decreases the affected area as well as the access to infections agents. Additionally, it enables to fill any shape defect leading to an improved grow of adjacent tissue as well as the materials can be used as delivery systems of growth factors, cells, and drugs. Thus, a new concept of surgery appears with the injectable *in situ* polymerizable and biodegradable materials, which may serve as scaffolds for guided bone regeneration and may provide an alternative for bone defect treatment. Different authors are working on the development of these new materials. Poly(propylene fumarate) (PPF) which is a unsatured linear polyester that can be crosslinked through its fumarate double bonds using a vinyl monomer is one of the materials tested. Based on this polymer, injectable composites incorporating an osteoconductive matrix β-TCP and a porogen (sodium chloride) were prepared.[164,165] These injectable products, known as injectable bone substitutes (IBS), present suitable rheological properties to ensure bonding of the mineral phase and good cell permeability. Contrary to dense materials which do not have any intrinsic porosity, this approach provides rapid and improved deep bone formation.

Other advantages of injectable formulations over conventional scaffolds are the possibility of a minimally invasive implantation, ability to fill a desirable shape, and easy incorporation of various therapeutic agents. Those advantages stimulate the search for new materials with suitable characteristics to be injected. Some of those are: Alginate, chitosan, hyaluronan, and polyethylene oxide/polypropylene oxide.[165-168] In the following pages an overview of different types of injectable systems (pastes, gels and microspheres) as well as their advantages, disadvantages, applications, and preparations methods (thermoplastic pastes and crosslinking techniques) are presented.

Types of injectable systems

The development of injectable materials were the result of different properties of the skeletal tissues (cortical and trabecular bone, and cartilage), the different places in the body where the implants are needed (femur, spinal column, pelvis, omoplate, cranial, etc.), and the different shape of defects to be repaired (spherical, lamellar, and irregular). Those differences also

require suitable mechanical properties and viscosity of the injectable materials. In terms of viscosity, an injectable material should have low viscosity before injection, but whenever injected, it should harden *in situ* (decrease viscosity) in order to provide mechanical properties similar to the bone tissue. Additionally, these materials could work as osteoinductors.

For all of the reasons described above, injectable materials are sub-divided in three systems: pastes, gels, and microspheres. Materials representing each of these categories will be presented in the following sections.

Pastes

Pastes are an example of injectable systems and a promising candidate is the above mentioned PPF. Poly(propylene fumarate) provides the orthopedic community with a new material that holds great promise for use as an injectable biodegradable composite, for filling skeletal defects.[165]

Peter *et al*.[169] used an injectable composite paste of PPF, N-vynil pyrrolinidone (N-VP), benzoyl peroxide (BP), sodium chloride (NaCl) and β-TCP to study the crosslinking temperature, heat release upon crosslinking, gel point, and the composite compressive strength and modulus. The maximum temperature reached did not vary widely among the formulations tested, with the values ranging from 38 to 48 ºC, which is below poly(methyl methacrylate) (PMMA) bone cement curing temperature, 94 ºC. Same authors also studied the degradation of these composites *in vivo*. They observed that all implants were encased in fibrous capsules within 4 days after implantation and granulation tissue was present, accompanied by remnant neutrophils and necrotic tissue debris. Newly formed capillaries, fibroblasts, and macrophages were evident at 1 week post-implantation and no multinuclear giant cells were found at any implant site. After 3 weeks, all formulations demonstrated signs of the late phase of healing, with the samples encased in a matured scar capsule of dense collagen fibers.[170]

PPF filled with calcium gluconate/hydroxyapatite (CG/HAp), which cures to a hard degradable cement by hydrolysis was investigated by Lewandrowski *et al*.[171] to evaluate the osteoconductive properties. The PPF bone cement which presented reasonable viscosity and reasonable working (6 to 7 min) and hardening (10 to 12 minutes) times for injectability, was injected into the proximal and distal portion of the intramedullary canal. The results showed that the trabecular bone volume and remodeling index were lower in the injectable cement that in the positive control but higher than in the negative control, supporting the concept of

osteoconductivity.

Self-hardening CPC are another group of pastes with interest in biomaterials research. The first published CPCs consisted of TCP and dicalcium phosphate anhydrous (DCPA). Later, additional CPCs highly biocompatible and able to set *in situ* were developed. Those properties pushed CPCs into the dental and medical applications showing good results. Xu *et al.*[172] investigated the effects of lubricants and particle sizes of the cements on the injectability of the TCP/DCPA, α-TCP/$CaCO_3$ and DCPA/$CaCO_3$ cements. The study suggested that excellent injectability can be obtained by incorporating CMC as gelling agent and by using a cement powder that contains sufficiently small (<5μm) particles.

The purpose of Grimandi *et al.*[54,173,174] was to develop an IBS for percutaneous orthopedic surgery using a multiphasic material composed of 2% (w/w) aqueous solution of HPMC and BCP (60% HAp and 40% β-TCP) where HPMC serves as the vehicle to carry BCP irregular particles (80-200 μm of diameter). The optimum ratio for BCP and polymer solution tested was 60/40 (w/w), and *in vitro* cytotoxicity assays showed that all cells survived, and there were no significant differences between the values found for control and the test materials. This system was considered nontoxic and suitable to use as IBS.[54,173,174] Weiss *et al.*[175,176] conducted *in vivo* studies also using the IBS system mentioned above and results showed high permeability to cells and biological fluids, which allowed early osteoconduction and bone substitution. Following those studies Gauthier *et al.*[177] implanted the IBS into mandibular and maxillary canine extraction sockets. After 19 days, gingival healing was achieved with no suture dehiscence or any signs of infection or inflammation of tissues and three months after implantation, extensive bone ingrowth was found.

To evaluate the importance of the particles size, Gauthier *et al.*,[178,179] in other studies, implanted two different IBS composites, each with different calcium phosphate particles granulometries, 40-80 μm (IBS 40-80) and 200-500 μm (IBS 200-500), in the femur of rabbits. Both IBS composites were prepared using BCP granules (60/40 HA/β-TCP weight ratio) and HPMC 3% (w/w), and an extensive newly formed bone was noted 2 weeks after implantation. However, earlier bone colonization occurred on IBS 40-80 than on IBS 200-500. Others have also used HPMC to improve injectability of calcium phosphate cements.[172,180,181] However, the use of HPMC in IBS produced a non-hardening material difficult to maintain within the defect during surgery so, recently, silane has been grafted to the HPMC to induce its self-hardening.[182,183] At basic pH, the silane radicals ($R–Si–O–Na^+$) grafted on cellulosic ether cycles, are ionized. Due to pH decrease, $R–Si–O–Na^+$ are

hydroxylated in R–Si–OH and covalent bridges linking hydroxyls radicals allow the formation of a 3D network of Si-HPMC. This polymerization mechanism leads to the shift of this cellulosic derivative fluid into a gel state without exothermic reaction. Besides Si-HPMC self-hardening, this new material is also biocompatible and well-adapted matrix for 3D culture and differentiation of osteoblast and chondrocytes.[180,184] The combination of Si-HPMC with BCP granules loaded with bone morphogenetic stem cells (BMSCs) showed osteoinductive properties in ectopic areas and the culture of Si-HPMC with human nasal chondrocytes revealed the formation of a cartilage like tissue with an extracellular matrix subcutaneously in nude mice.[185]

Gels

A gel is defined as a three dimensional network swollen by a solvent where, usually, the solvent is the major component of the gel system.[31]

Biocompatible polymeric formulations that exhibit sol-to-gel transition at physiological conditions are good candidates for tissue engineering applications. To select an injectable gel some factors should be considered: tissue specific cell-matrix interactions, gelation kinetics, matrix resorption rates, toxicity of degradation products and their elimination routes. In terms of gelation, it can occur by: thermal gelation (injectable polymer formulation can gel *in vivo* in response to temperature change), pH change, ionic crosslinking, or solvent exchange. Therefore, to design a tissue-supporting injectable scaffold, the correlation of the above factors is required in order to obtain injectability and both new tissue formation and scaffold reabsorption simultaneously. In the following paragraphs it will be presented some injectable gels as well as their applications.

Poly ethylene-oxide (PEO)

Poly(ethylene-oxide-b-propylene oxide-b-ethylene oxide) (PEO-PPO-PEO), or Pluronics (also known as Poloxamers), are the best known examples of thermally gelling polymers. PEO-PPO-PEO copolymers are a family of more than 30 different nonionic surfactants and it forms reversible gels at high temperatures and reverts to a liquid state upon lowering of temperature. Poloxamer 407 solutions forms gels at 37 ºC for polymer concentrations above 20% (w/w). Solutions of this Poloxamer were used in burn treatment and other wound healing applications more than 25 years ago. Cao *et al*.[186] described a novel application of PEO-PPO-PEO copolymers in the formation of a cartilage layer on the host bone. They demonstrated

cells suspended in the polymer formed higher volume of bone than cells suspended in saline.

Poly ethylene-glycol (PEG)

Recently, novel hydrogel triblock copolymers of PEG and poly(lactic glycolic acid) (PLGA), or PEG-PLGA-PEG, were developed by Jeong *et al*.[187-189] Aqueous solutions of these copolymers also exhibit sol-to-gel transitions at body temperatures. Subcutaneous injection of the copolymer formulation resulted in the formation of a transparent gel *in situ* maintaining its structural integrity as well as the mechanical strength. Similar results were obtained using poly(ethylene glycol-g-(DL-lactic acid-co-glycolic acid)) (PEG-g-PLGA) and poly((DL-lactic acid-co-glycolic acid)-g-ethylene glycol) (PLGA-g-PEG).

Hyaluronic acid

A high-viscosity, shear-thinning polymer solution or slightly crosslinked gel may be injected through a relatively small gage needle and upon removal of the injection force, a thick gel is formed *in situ*. Hyaluronan gels form *in situ* upon injection of a viscous gel formulation. Viscoelastic and shear-thinning properties of hyaluronan inspired researchers to use it as a carrier for drugs, protein, and peptide delivery, as well as tissue engineering applications such a bone fracture repair, wound healing and soft tissue augmentation procedures. Viscosity of hyaluronic acid solutions decreases with increasing temperature, which makes it suitable for infectable applications. Physicochemical properties of hyaluronan may also be improved by chemical crosslinking with divinyl sulfone. Animals studies demonstrated that hyaluronan polymers are nontoxic, nonantigenic, noninflammatory, and do not elicit a foreign body reaction.[190,191]

Radomsky *et al*.[192] evaluated sodium hyaluronate gel has a matrix to deliver basic fibroblast growth factor (b-FGF) in bone defects. A simple injection of b-FGF and hyaluronan into a freshly created fracture in the rabbit fibula resulted in increasing bone formation, and in an earlier restoration of mechanical strength at the fracture site.

Chitosan

As discussed before chitosan is a charged, water soluble polymer that may form reversible gels in response to a pH change in solution. As a specific example of pH-reversible polymeric gels, chitosan solutions exhibit a liquid-gel transition around pH=7, when pH changes from slightly acidic to neutral.

Since unmodified chitosan can be only dissolved in acidic solutions, its applications as

injectable product are limited. Therefore the use of other compounds grafted on chitosan molecules can adjust the properties of solutions in order to enable the preparation of hydrogels at neutral pH and body temperature.[116,141,193]

To overcome those difficulties, Hoemann *et al.*[157] studied the use of an *in situ* gelling chitosan-disodium β-glycerol phosphate-glucosamine solution. This solution was used to encapsulate chondrocytes supporting *in vitro* and *in vivo* accumulation of cartilage matrix. When injected in osteochondral defects hydrogels persisted at least for 1 week. Also chitosan/polyol salt solutions a liquid below room temperature, was used to encapsulate chondrocytes. These solutions were able to gelify *in situ* at body temperature after injected *in vivo.*[141]

The PEG covalently grafted to chitosan produced an injectable product able to transform into a semisolid hydrogel at body temperature.[137] This system was able to serve as carrier for BSA delivery. Furthermore, crosslinking *in situ* of this copolymer with genipin produced a new hydrogel also suitable to release BSA for 40 days with a quasi-linear profile. Another hydrogel for BSA delivery was prepared mixing chitosan with poly(vinyl alcohol) and sodium bicarbonate.[138] This new hydrogel which is liquid at low temperatures (about 4 ºC) also becomes a gel under physiological conditions and presents good mechanical properties.

Poly(N-isopropylacrylamide) (PNIPAAn), a well known thermosensitive polymer with a thermoreversible phase transition at 32 ºC, has been used to create a PNIPAAn-chitosan derivative with improved *in situ* gel formation.[194-196] These polymers also presented high potential for culturing of chondrocytes, meniscus cells, to differentiate human mesenchymal stem cells into articular chondrocytes and also for drug delivery.[116,197,198]

The synthesis of chitosan graft to methacrylic acid produced a chitosan derivative readily soluble in pure water below pH=9 but its gelation occurs by thermal treatment at body temperature.[199] Finally, the use of chitosan, citric acid and glucose solution to work as a liquid phase to carry calcium phosphate particles enabled the production of a moldable and biocompatible injectable bone substitute.[200]

Microspheres

The regular spherical shape of microspheres can be an advantage for injectability as well as in terms of package and regular porosity interparticles. Therefore many studies have focus in microspheres production for bone regeneration and other purposes. Different materials have been used to produce microspheres. Schrier *et al.*[201,202] prepared and implanted poly(lactic

glycolic acid) (PLGA) and CMC microspheres in New Zealand white rabbits observing that bone was highly enhanced when microspheres were loaded with BMP-2. Similar results were obtained in studies using PLGA sintered microspheres loaded with BMP-7. On the other hand chondrocytes cultured on PLGA microspheres and injected in athymic mice improved the production of extracellular matrix cartilage when compared with chondrocytes alone. *In vivo* studies using bioactive glass microspheres loaded with BMP-2 implanted in rat tibia bone defect highly promoted bone regeneration.[203,204]

As mentioned above HAp is widely used as bone substitute but it cannot be injected in its massive form. However, HAp powder size is compatible with injection and it can be used to mix with polymeric solutions or just to prepare HAp injectable granules. Pasquier *et al*.[205] have coated HAp granules with type I collagen, forming microspheres (HAp-COL) in order to obtain a bone substitute able to be injected and leading to better osteoconduction than HAp powders and collagen separated. The HAp-COL system shows a good pathway for the biological fluids and bone regeneration. Additionally, HAp granules released after collagen degradation sustained the new bone formation, increasing bone strength. However, the delay in collagen degradation, and its negative response in increasing new bone formation in time, lowers the efficiency of the HAp-COL microspheres.

Ferraz *et al*.[206] produced nanohydroxyapatite microspheres for antibiotics delivery observing that either microspheres load or not with antibiotics have promoted osteoblasts proliferation though in the presence of erythromycin, osteoblasts proliferation came enhanced. Barrias *et al*.[207,208] have studied HAp and calcium titanium phosphate (CTP) microspheres loaded with human osteoblasts cells and bone marrow stromal cells. After 7 days in culture, both types of cells proliferate and bone marrow stromal cells produced an abundant amount of fibrillar extracellular matrix.

Preparation of injectable systems

An injectable material should have low viscosity and keeps its shape after injection into a defect. Thus, new techniques must be developed in order to enable gelation *in situ.* To explain this concept, different strategies to prepare *in situ* setting solid biodegradable injectable implant systems will be presented. Those strategies can be divided into three categories based on the mechanism of achieving solidification *in vivo*: thermoplastic pastes; *in situ* crosslinked systems; and *in situ* precipitation.

Thermoplastic pastes

Thermoplastic pastes are characterized as having a low melting point, ranging from 25 to 65 °C, but once injected into the body as a melt, they form a semi-solid upon cooling to body temperature. They are easily injected, when heated slightly above their melting point, due to their low molecular weight and low glass transition temperature (T_g). Furtheremore, they hold their shape at room temperature and can be formed into different shapes by applying heat.[209]

Bioerodible thermoplastic pastes can be prepared from such monomers as D,L-lactide, glycolide, ε-caprolactone, trimethylene carbonate, dioxanone, etc.[210] Polymers and copolymers of these monomers have been extensively used in a number of biomedical areas, from carriers of pharmaceutical compounds to surgical sutures, ocular implants, soft tissue repair and augmentation materials.[211,212] They therefore have a demonstrated track record of biocompatibility and thus are attractive starting points for new material development.

Walter *et al.*[213] placed a Taxol-loaded poly [bis(p-carboxyphenoxy) propane-sebacic acid] implant beside brain tumors or within tumor resection sites and demonstrated the effectiveness of the method in rats after surgery. In an effort to develop a means of avoiding surgery and circumventing the invasiveness of Walter's method, Zhang *et al.*[214] developed a thermoplastic triblock polymer system composed of poly(D,L-lactide)-block-poly(ethylene glycol)-block-poly(D,L-lactide) and blends of low molecular weight poly(D,L-lactide) and poly(ε-caprolactone) (PCL) for the local delivery of Taxol. Both polymeric systems were capable of releasing Taxol for a long period of time (greater than 60 days), although at a very low rate[215,216].

In situ crosslinked systems

Crosslinked polymer networks can be formed *in situ* in a variety of ways, forming solid polymer systems or gels. Means of accomplishing this end include free radical reactions initiated by heat (thermosets) or absorption of photons, or ionic interactions between small cations and polymer anions.

Termosets

Thermoset polymers can flow and be molded when initially constituted but, after heating, they set into their final shape. This process is often called "curing" and involves the formation of covalent crosslinks between polymer chains to form a macromolecular network. Reheating a cured polymer only degrades the polymer. This curing is usually initiated chemically upon

addition of heat.

Dunn *et al.*[210] used biodegradable copolymers of D,L-lactide or L-lactide with ε-caprolactone to prepare a thermosetting system for prosthetic implants and slow release drug delivery systems. This system is liquid outside the body and is capable of being injected via a syringe and needle and, once inside the body, it cures. The multifunctional polymers in their thermosetting system were first synthesized via copolymerization of either D,L-lactide or L-lactide with ε-caprolactone using a multifunctional polyol initiator and a catalyst (e.g., peroxides) to form polyol terminated liquid pre-polymers. This pre-polymer was then converted to an acrylic ester-terminated pre-polymer. Curing of the liquid acrylic-terminated pre-polymer is initiated by the addition of either benzoyl peroxide or N,N-dimethyl-p-toluidine, prior to injection into the body. After introduction of the initiator, the polymer system is injected and polymer solidification occurs. The estimated time of reaction is between 5 to 30 min.[217] The advantage of using this system is its facile extrusion. However, there are a main disadvantages associated with this system, which have limited its application. Those disadvantages are related with the heat released upon curing due to the exothermic nature of the crosslinking reaction, which can cause necrosis to the surrounding tissues.[165] However, PMMA is still the most common system used in vertebroplasties though it is not biodegradable and it has high hardness and stiffness.

Chemically crosslinked gels

Chemically crosslinked gels can be obtained by radical polymerization of low molecular weight monomers in the presence of crosslinking agents. Poly(2-hydroxyethylmethacrylate) (pHEMA) is a well known and frequently studied hydrogel system. This hydrogel was first described by Wichterle and Lim and is obtained by polymerization of HEMA in the presence of a suitable crosslinking agent (e.g. ethylene glycol dimethacrylate).[218]

A polymerizable dextran derivative was obtained by reaction of dextran (bacterial poly-saccharide, which consists essentially of α-l,6 linked D-glucopyranose residues) with maleic anhydride.[219] These dextran derivatives can be converted into a hydrogel by UV-induced polymerization. However, the gels obtained were not degradable under physiological conditions and they did exhibit a strong pH-dependent swelling behavior due to the presence of carboxylic acid groups in the network.[220]

Water-soluble polymers with hydroxyl groups, e.g. poly(vinyl alcohol), can be crosslinked

using glutaraldehyde.[221] Crosslinking of gelatin using polyaldehydes obtained by partial oxidation of dextran has been reported. These gels were designed for application in wound treatment and epidermal growth factor was incorporated to promote wound healing.[222]
Chan *et al.*[223] prepared calcium alginate microspheres by an emulsification method and crosslinked with various aldehydes using different methods.

Water-soluble polymers can be converted into hydrogels using bis (or higher) functional crosslinking agents which react with functional groups of water-soluble polymers via addition reactions. Polysaccharides can be crosslinked with l,6-hexamethylene-di-isocyanate, divinylsulfone, or l,6-hexanedibromide and many other reagents.[224]
Recently, Hubbell and coworkers reported a degradable hydrogel in which crosslinks were introduced by reaction of PEG-dithiol with PEG-acrylates. Gel formation occurred at room temperature and physiological pH.[225]
He *et al*.[226] investigated PPF crosslinking with poly(ethylene glycol)-dimethacrylate (PEG-DMA) as a crosslinking reagent. Composites incorporating β-TCP, were also prepared. The polymerizing composite pastes showed clinically favorable temperature profiles and gel points.

Condensation reactions between hydroxyl groups or amines with carboxylic acids or derivatives thereof are frequently applied for the synthesis of polymers to yield polyesters and polyamides, respectively. These reactions can also be used for the preparation of hydrogels. A very efficient reagent to crosslink water-soluble polymers with amide bonds is N,N-(3-dimethylaminopropyl)-N-ethyl carbodiimide (EDC). Feijen and coworkers described the preparation of gelatin hydrogels using this reagent. During the reaction N-hydroxysuccinimide is added to suppress possible side-reactions and to have a better control over the crosslink density of the gels.[227] Alginate and PEG-diamines were crosslinked using EDC. The mechanical properties could be controlled through amount of PEG-diamine in the gel and the molecular weight of PEG.

Alginate is a well-known example of a polymer that can be crosslinked by ionic interactions. Alginate is a polysaccharide with manuronic and glucuronic acid residues and can be crosslinked by calcium ions. Crosslinking can be carried out at room temperature and physiological pH. Therefore, alginate gels are frequently used as matrix for the encapsulation

of living cells and for the release of proteins.[228]

A synthetic polymer that, like alginate, can also be crosslinked by ionic interactions is poly-[di(carboxylatophenoxy) phosphazene] (PCPP). Gel microbeads were prepared by spraying an aqueous solution of PCPP in an aqueous solution of calcium chloride. The ionotropic hydrogels degrade under physiological conditions and the degradation rates can be increased by incorporation of hydrolysis-sensitive glycinato groups in the polymer.[229]

Dextran also forms an hydrogel in the presence of potassium ions. The mechanism was elucidated by Watanabe *et al.*[230] who showed that the ionic radius of the potassium ion perfectly fits into the cage established by six oxygen atoms of glucose units of three polymer chains, thereby forming a microstructure.

Photocrosslinked gels

Photopolymerizable, degradable biomaterials would provide many advantages over chemically initiated thermoset systems. In this approach, pre-polymers are introduced to the desired site via injection and photocured *in situ* with fiber optic cables. These characteristics have encouraged the investigation of using this system for tissue engineering.[226,231]

Hubbell *et al.*[232] described a photopolymerizable biodegradable hydrogel (PEG-oligoglycolyl-acrylates) as a tissue contacting material and controlled release carrier using a ultraviolet or visible light.

Muggli *et al.*[233] studied anhydride monomers end-capped with methacrylate functionalities, which were photopolymerized to produce highly crosslinked polymers with mechanical properties were intermediate between those of cortical and trabecular bone.

ENDOCHONDRAL OSSIFICATION

Skeletal development occurs through two different mechanisms: intramembranous and endochondral ossification. Intramembranous bone forms by differentiation of mesenchymal cells directly into osteoblasts, while endochondral ossification involves gradual and partial replacement of a cartilage model by bone. The long bones, pelvis, vertebral column, base of the skull, and mandible are formed through the endochondral mechanism. However, until now, most of the attempts from the bone tissue engineering field have been to create bone by intramembranous bone formation not considering the alternate pathway, the endochondral mechanism. To mimic nature by creating a cartilage template *in vitro* which when implanted *in vivo* will lead to endochondral bone formation might be a very good approach to overcome the problems related to bone replacement. This alternative approach presents significant advantages including the resistance of chondrocytes to low oxygen,[234] and the fact that these cells can induce vascular invasion and osteogenesis.[4,235] We believe that the new bone formed through this mechanism will be indistinguishable from natural bone (present the same properties, respond to loading) and notably will have the potential to grow just as the patient's own bone.

This approach would simply require the production of the cartilage template, made of chondrocytes able to undergo hypertrophy, in bioactive/biodegradable materials able to support their proliferation and differentiation.

Endochondral mechanism

As mentioned above, most of bones form through a cartilage template followed by endochondral ossification, whereas few develop by intramembranous ossification. In both cases, bone formation begins when undifferentiated mesenchymal cells form condensations - clusters of cells. In intramembranous ossification, these condensations differentiate directly into bone-forming osteoblasts and producing a matrix particularly rich in type I collagen. On the other hand, if cells in the condensation become chondrocytes, primary cell type in cartilage, a process called chondrogenesis will take place. This process is regulated by Sox 9, a DNA transcription factors that is required for expression of several chondrocytes-specific proteins, including type II collagen, type IX collagen, type XI collagen, and proteoglycan aggrecan.[236,237] Type II collagen is the main collagenous protein found in cartilaginous tissue and it represents 80–95% of total cartilage collagen.[238-240] It can also be found in the

intervertebral discs and vitreous humor of the eye. In articular cartilage, type II collagen is essential for the tensile stiffness and strength of cartilage and provides the basic architecture of the tissue. Aggrecan, the largest aggregating proteoglycan, provides the osmotic properties necessary for cartilage to resist compressive loads.[241,242]

Although some cartilaginous tissues, as articular or tracheal cartilage, persist for many years (permanent cartilage), others (transient cartilage) will undergo further differentiation that lead to organized alterations in chondrocytes size, extracellular matrix components, secreted enzymes and growth factors, and receptors expression. The culmination of these events is calcification of the cartilage matrix, vascular invasion, and chondrocytes apoptosis resulting in endochondral ossification.

The alterations in transient cartilage start in the center of the cartilaginous template as early as it is formed. There, chondrocytes stop proliferating and stop producing type II collagen and aggrecan. A matrix rich in type X collagen starts to be produced and chondrocytes enlarge becoming hypertrophic. The enlargement of chondrocytes, simply through its size, is the principal engine of bone growth. Afterward, the hypertrophic cartilage is surrounded by a layer of undifferentiated cells, which during development are believed to give origin to osteoblasts; these secrete a characteristic matrix, forming a bone collar at the boundary between hypertrophic chondrocytes and the undifferentiated cells. At the chondoosseous junction hypertrophic chondrocytes undergo apoptosis, while the calcified cartilage matrix serves as a scaffold for osteoblasts and osteoclasts to remodel and form new bone.[243] Over time, this center of ossification in the middle of the cartilage template grows in both directions to the extremities, by recapitulating these events. Eventually, only two areas of cartilage will remain at the end of bones, the articular surface and the growth plates. The growth plate is a disc of cartilage responsible for postnatal bone growth, located between the primary and secondary ossification centers (Figure 8).

Growth plate

In the growth plate, chondrocytes are present in a gradient of differentiation, organized in three different zones: resting zone, proliferating zone and hypertrophic zone. In humans, growth plate is completely replaced by bone following the puberty, resulting in fusion of the epiphysis and diaphysis of long bones.

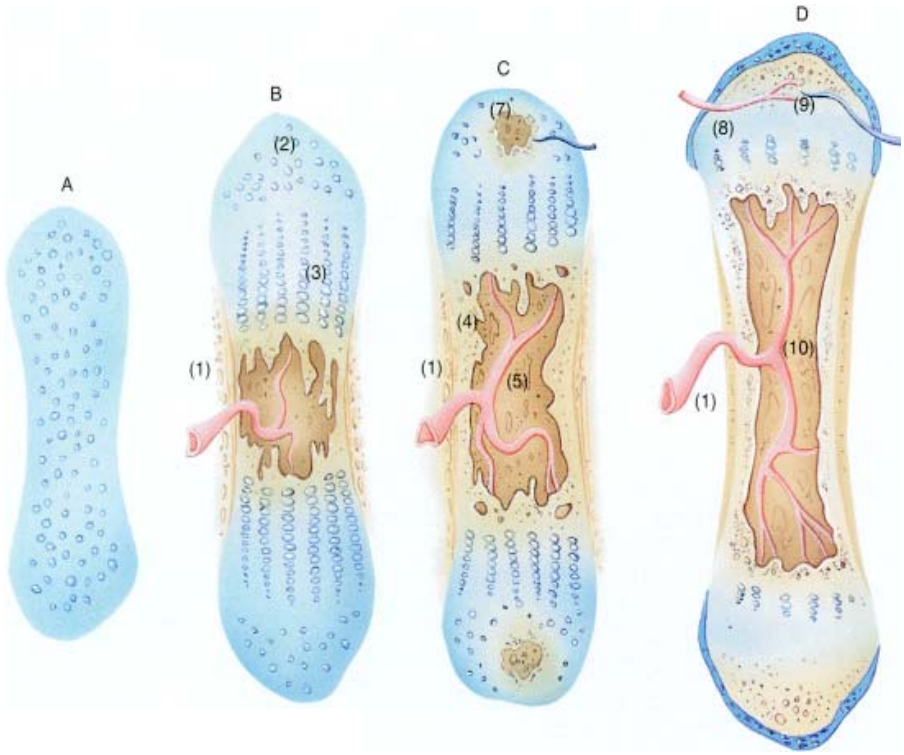

Figure 8. Endochondral bone formation during development. (A), Some of the mesenchyme in the limb area differentiates into chondrocytes to form a cartilage model of the future bone. (B), Cells in the center of the model become hypertrophic (3) inducing vascular invasion (1). (C), Blood vessels bring osteoprogenitor cells that remodel the cartilage, expand and form a marrow cavity (5), and a growth plate (8). (D), Secondary ingrowth of blood vessels (9) in the epiphysis creates a secondary ossification center (7). The growth plate between the primary (5) and secondary (7) ossification centers is formed by columns of chondrocytes that continue to proliferate, hypertrophy, secrete extracellular matrix and mineralize. This matrix is partially resorbed by osteoclasts as osteoblasts deposit new bone, resulting in bone growth. Adapted, Color Atlas of Histology, 3rd Edition, Gatner & Hiatt.

Resting Zone

The resting zone is adjacent to proliferative zone and it is considered a reserve cartilage. The chondrocytes are flat and often grouped in pairs. Chondrocytes in the resting zone are usually embedded in an extracellular matrix, presenting a high ratio of extracellular matrix to cells volume.[243]

Although, the function of resting zone is not clearly known several hypotheses have been announced. First, the resting zone might contain stem-like cells capable of generating new clones of proliferative zone chondrocytes and, after these cells divide, the daughter cell closest to the proliferative zone may proliferate to populate a column of cells in proliferative zone while the other cell may continue to serve as stem-like cell. Second, the resting zone

chondrocytes might produce a growth plate orientation factor, a morphogen that guides the spatial orientation of proliferative zone chondrocytes into columns parallel to the long axis of the bone. Third, the resting zone produces a factor that inhibits hypertrophic differentiation which can regulate one of the paracrine factors (Parathyroid hormone related protein – PTHrP, Indian hedgehog – Ihh, Bone morphogenetic proteins – BMPs, fibroblast growth factors – FGF or retinoids) that are the switch to the hypertrophic phenotype.[244-248]

Proliferative zone

The proliferative zone plays a crucial role in endochondral bone formation since it is the region of active cell replication and these chondrocytes secrete an extracellular matrix composed mostly of type II collagen and proteoglycan.[249-251] When a chondrocyte in proliferative zone divides, the two daughter cells line up along the long axis of the bone. As a result, groups of chondrocytes arrange in columns parallel to this axis directing growth in a specific direction and are thus responsible for the elongate shape assumed by many endochondral bones. The mechanism by which proliferative chondrocytes recognize and line up along this axis is unknown. However, the mechanism that keeps cells proliferation seems to be controlled by three signaling molecules synthesized by the growth plate chondrocytes (PTHrP, Ihh and transforming growth factor-β1 (TGF-β1)) through a local feedback loop.[244,246,252-255]

PTHrP is expressed in periarticular perichondrium during fetal life presumably to keep chondrocytes proliferating and it has been shown to inhibit chondrocytes differentiation. Additionally, PTHrP receptor is found in prehypertrophic cells and lower proliferating zone cells indicating that PTHrP controls the rate of hypertrophic differentiation.[256-261] Ihh was observed to be expressed by prehypertrophic chondrocytes in the developing bone of mice and it seems to send a signal back to the periarticular cells to increase production of PTHrP.[259,262] Finally, TGF-β1 acts on the perichondrial and periarticular cells to increase PTHrP synthesis and also can act directly on chondrocytes to inhibit hypertrophy, type-X collagen expression, and alkaline phosphatase activity.[255,263-266]

Hypertrophic zone

The hypertrophic zone is visually characterized by chondrocyte enlargement – chondrocytes hypertrophy.[243,267] These chondrocytes are generated by terminal differentiation of the proliferative chondrocytes farthest from the epiphysis. The phenomenon starts when cells

cease dividing and then start to enlarge and assume a more spherical shape, contributing substantially to the growth process. The mechanism of the cell enlargement seems to be associated with the synthesis of organelles though the cytoplasm and nuclear swelling also occur. It was observed an increase of 126 percent of endoplasmic reticulum and mitochondria and an increase of 779 percent of cytoplasm and nucleoplasm between the upper proliferative zone and the lower hypertrophic zone.[267] Terminal differentiation and chondrocytes hypertrophy is also associated to the marked increase in alkaline phosphatase enzyme activity and to the synthesis and secretion of type X collagen.[268,269]

Alkaline phosphatase (AP) is an inducible membrane glycoprotein known to be markedly elevated in nonproliferating and fully differentiated cells.[270] Furthermore, it is one of the most frequently used markers of osteoblasts activity and it is responsible by the initiation of mineral formation, lacking in mice suffering hypophosphatasia (a disease of defective AP formation). Indeed, the absence of AP is associated with decreased mineralization of the matrix and widening of the growth plate as well as defective mineralization of bone.[271-273]

The role of AP in the mineralization process seems to be connected with hydrolyzation of organic phosphates releasing free inorganic phosphate at sites of mineralization and, consequently, increasing the concentration of these ions which are necessary for the calcification process. However, it is still not clear which organic phosphates are hydrolyzed by AP.[274,275]

Type X collagen is a unique short chain collagen, which is only found in the hypertrophic zone of the growth plate. Although type X collagen function is not completely known, its interaction with the type II collagen and annexin V play a crucial role for Ca^{2+} loading and the formation of the first crystal phase inside matrix vesicles (MV). The disruption of these interactions has several consequences on mineralization of MV.[276] Studies using normal mice and transgenic mice to type X collagen indicate specific differences in the calcified cartilage mineral in terms of both amount present and quality of mineral.[277] Calcified cartilage mineral from transgenic mice exhibited less crystallinity and higher acid phosphate content than the corresponding mineral from normal mice. Surprisingly, transgenic mice lacking type X collagen show only subtle alterations in hematopoiesis and growth plate architecture, but no obvious skeletal changes.[278]

Mineralization

In the growth plate, MVs are extracellular microstructures that derived from chondrocytes

plasma membrane and they play an important role in the initiation of the process of mineralization since they actively accumulate calcium and are rich in alkaline phosphatase.[279,280] Mineralization occurs through the action of MV-associated phosphatases and calcium-binding phospholipids and proteins.[281] The mineral formed inside the MVs penetrates the vesicular membrane and in the presence of physiological concentrations of extravesicular Ca^{2+}, PO_4^{3-} and pyrophosphate (PPi) serves as nuclei for the formation of stellate clusters of needle-shaped biological apatite that proliferates to fill the interstices of the longitudinal septa. The mineralized matrix is eventually degraded by osteoclasts and in time is replaced with bone.[282] Numerous studies have provided important evidence on how MVs induce mineral formation. For instance, mineralization-competent MVs contain a nucleational core composed of amorphous calcium phosphate and calcium phosphate phosphatidylserine complex bound with the annexins while mineralization incompetent MVs lack these components.[283-285] Further, considerable data indicate that annexin V mediate Ca^{2+} influx into the vesicles, enabling formation of the first solid phase mineral. Inorganic phosphate (Pi) is also critical for formation of mineral within MVs and Pi is mediated, at least, by two Pi transporters.[286-288]

AP was mentioned before as a mineralization factor and it seems to be related with mineral crystal growth outward from the vesicles lumen to the extracellular matrix since in hipophosphatasia, while mineralization occurs within the vesicle lumen, it does not spread from there into extravesicular matrix. This outward growth of mineral involves the degradation of the vesicles membrane phospholipids. Rupture of the membrane also releases matrix processing enzymes present in MVs resulting in degradation of proteoglycan aggregates, which facilitates apatite mineral formation.[284,289,290]

Vascular invasion

Various findings indicate that chondrocytes are able to synthesize both angiogenesis inhibitors and stimulators, depending on their culture condition and state of differentiation. Angiogenesis inhibition and stimulation seems to be related with hypoxia inducible factor-1a (HIF-1a) which expression is stimulated in hypoxia conditions achieved during chondrogenesis.[291,292] That factor is known to be necessary for chondrocyte survival during hypoxia, it may be required for expression of chondrocyte markers such as type II collagen, and it induces expression of vascular endothelial growth factor (VEGF).[293] VEGF is a protein that targets vascular endothelial cells and stimulates their proliferation and migration and

ultimately the formation of blood vessels.[294] It is required for growth and survival during early postnatal life and it is expressed by hypertrophic chondrocytes in the growth plate, but is absent in resting and proliferating chondrocytes.[295] In animals, inhibition of the receptor for VEGF leads to loss of vascular invasion and to an increasing in the hypertrophic region and diminution of trabecular bone formation due to a disorder in the architecture of the growth plate.[296,297] VEGF, produced by hypertrophic chondrocytes, seems to recruit endothelial cells and thus induces blood vessels, which bring in nutrients, chondroclasts and osteoblasts.[297] Additionally, exposure of endothelial cells to VEGF may trigger signaling cascades that lead to production of cytokines, proteinases and other mediators that then influence chondrocytes, chondroclast and osteoblasts, and prepare these structures for endochondral ossification.

Apoptosis

Apoptosis is a physiological form of cell death, during which the dying cells disappear without any accompanying inflammatory response.[298-300] Apoptosis occurs to control cell number, as a strategy to remove infected, mutated, or damaged cells, and also as a morphogenetic step during endochondral ossification. During apoptosis, a cell activates an intrinsic suicide mechanism, which is extremely rapid (typically between few minutes and few hours), and the apoptotic fragments are also rapidly cleared up. The final stage of apoptosis, called execution, occurs through the activation and function of caspases, a highly conserved family of cysteine proteases with specificity for aspartic acid residues in their substrates.[301] All cells contain caspases in their cytoplasm in an inactive form therefore they are ready to undergo apoptosis. Another factor linked to apoptosis is the mitochondrial function, which appears to be related with the delivery of cytochrome C into the cytoplasm where it promotes the proteolytic activation of caspase 9 and thus initiate a caspase cascade.[302] In addition, a family of proteins (bcl-2 family) seems to be the major modulators of caspases activity. Bcl-2 and other members of the family are able to prevent the release of cytochrome C suggesting that this can be the mechanism by which bcl-2 prevents apoptosis.[303]

Though controversial, several studies based largely on immunochemical detection of osteoblast associated gene products, indicate that under some circumstances hypertrophic chondrocytes may not apoptose but transform into bone forming cells. However, under normal circumstances, it appears that the vast majority of hypertrophic chondrocytes in the growth plate terminate their differentiation with apoptosis.[304-306]

In concordance with this proposal Bcl-2, an apoptosis inhibitor, was shown to be distributed throughout mouse and rat growth plate with the highest levels in dividing and early hypertrophic chondrocytes, and lower levels in late hypertrophic chondrocytes adjacent to the metaphyseal vasculature.[307]

DNA fragmentation was also detected in some chondrocytes adjacent to the invading vasculature in the region which contained chondrocytes with a condensed morphology.[303]

Phosphate ions which are involved in mineralization appear to play an important role in the chondrocytes apoptosis. Phosphate ions effect was compared in embryonic sternal cephalic and caudal chondrocytes and terminally differentiated tibial cells showing that differentiated chondrocytes seem to be more sensitive to increased phosphate levels than less differentiated cells.[308] Moreover, this behavior appears to be linked to chondrocyte maturation and mineralization of the extracellular matrix.

Although several studies have suggested that chondrocytes apoptosis may play a prominent role in the nucleation of matrix calcification and chondrocyte apoptotic bodies have been suggested to be a source of calcifying matrix vesicles, recently Pourmand *et al*.[309] have demonstrated that the stimulation of apoptosis prior to the onset of calcification resulted in a decrease of total calcium uptake and the formation of abnormal mineral crystals meaning that chondrocytes apoptosis is not essential for calcification.

Ossification

As a result of all the events described above, a cartilage template and later the growth plate is invaded by blood vessels and osteoblasts, which will remove the calcified cartilage and replace it by bone, completing the endochondral ossification pathway. In this process other factors seen as essential for osteoblasts differentiation, such as runx2, come into action.[310-312] Although runx2 is involved in osteoblasts differentiation, its inactivation results in severe inhibition of chondrocyte maturation and in retardation of endochondral ossification.[313-315] Ihh which is presented as an inductor of chondrocytes proliferation is also involved in osteoblasts differentiation.[246] Ihh deficient mice present a disorganized growth plate and they also have no osteoblasts cells in bone that is formed through endochondral ossification. Although poorly understood, all these factors are engaged with only one purpose that culminates into endochondral ossification.

REFERENCES

1. Sommerfeldt DW, Rubin CT. Biology of bone and how it orchestrates the form and function of the skeleton. Eur Spine J 2001;10 Suppl 2:S86-95.
2. Rodan GA. Introduction to bone biology. Bone 1992;13 Suppl 1:S3-6.
3. Curtiss PH, Jr., Herndon CH. Immunologic factors in homogenous bone transplantation. I. Serological studies. Ann N Y Acad Sci 1955;59(3):434-42.
4. Maes C, Carmeliet P, Moermans K, Stockmans I, Smets N, Collen D, Bouillon R, Carmeliet G. Impaired angiogenesis and endochondral bone formation in mice lacking the vascular endothelial growth factor isoforms VEGF164 and VEGF188. Mech Dev 2002;111(1-2):61-73.
5. Aichelmann-Reidy ME, Yukna RA. Bone replacement grafts. The bone substitutes. Dent Clin North Am 1998;42(3):491-503.
6. Reddi AH, Muthukumaran N, Ma S, Carrington JL, Luyten FP, Paralkar VM, Cunningham NS. Initiation of bone development by osteogenin and promotion by growth factors. Connect Tissue Res 1989;20(1-4):303-12.
7. Costantino PD, Hiltzik D, Govindaraj S, Moche J. Bone healing and bone substitutes. Facial Plast Surg 2002;18(1):13-26.
8. LeGeros RZ. Properties of osteoconductive biomaterials: calcium phosphates. Clin Orthop Relat Res 2002(395):81-98.
9. Hutmacher DW. Scaffolds in tissue engineering bone and cartilage. Biomaterials 2000;21(24):2529-43.
10. Agrawal CM, Ray RB. Biodegradable polymeric scaffolds for musculoskeletal tissue engineering. J Biomed Mater Res 2001;55(2):141-50.
11. Leong KF, Cheah CM, Chua CK. Solid freeform fabrication of three-dimensional scaffolds for engineering replacement tissues and organs. Biomaterials 2003;24(13):2363-78.
12. Freed LE, Martin I, Vunjak-Novakovic G. Frontiers in tissue engineering. In vitro modulation of chondrogenesis. Clin Orthop Relat Res 1999(367 Suppl):S46-58.
13. Albrektsson T, Johansson C. Osteoinduction, osteoconduction and osseointegration. Eur Spine J 2001;10 Suppl 2:S96-101.
14. Lange R, Luthen F, Beck U, Rychly J, Baumann A, Nebe B. Cell-extracellular matrix interaction and physico-chemical characteristics of titanium surfaces depend on the roughness of the material. Biomol Eng 2002;19(2-6):255-61.
15. Cassinelli C, Morra M, Bruzzone G, Carpi A, Di Santi G, Giardino R, Fini M. Surface chemistry effects of topographic modification of titanium dental implant surfaces: 2. In vitro experiments. Int J Oral Maxillofac Implants 2003;18(1):46-52.
16. Langer R, Vacanti JP. Tissue engineering. Science 1993;260(5110):920-6.
17. Wolf WD, Vaidya KJ, Francis LF. Mechanical properties and failure analysis of alumina-glass dental composites. Journal of the American Ceramic Society 1996;79(7):1769-1776.
18. Rey A, Hina S, Amrah-Bouali X. Surface reactions of calcium phosphate bioceramics, comparison with bone mineral surface chemistry, . Bioceramics 1995;8:301-312.

19. Hench LL. La Fabbricazione dei bioceramici. Ceramurgia 1977;5:253-266.
20. Hench LL. Bioceramics - from Concept to Clinic. Journal of the American Ceramic Society 1991;74(7):1487-1510.
21. Lin FH, Hon MH. A Study on Bioglass Ceramics in the Na2O-Cao-Sio2-P2O5 System. Journal of Materials Science 1988;23(12):4295-4299.
22. Ohtsuki C, Kushitani H, Kokubo T, Kotani S, Yamamuro T. Apatite formation on the surface of Ceravital-type glass-ceramic in the body. J Biomed Mater Res 1991;25(11):1363-70.
23. Gauthier O, Goyenvalle E, Bouler JM, Guicheux J, Pilet P, Weiss P, Daculsi G. Macroporous biphasic calcium phosphate ceramics versus injectable bone substitute: a comparative study 3 and 8 weeks after implantation in rabbit bone. J Mater Sci Mater Med 2001;12(5):385-90.
24. Kotani S, Fujita Y, Kitsugi T, Nakamura T, Yamamuro T, Ohtsuki C, Kokubo T. Bone bonding mechanism of beta-tricalcium phosphate. J Biomed Mater Res 1991;25(10):1303-15.
25. Fanovich MA, Lopez JMP. Influence of temperature and additives on the microstructure and sintering behaviour of hydroxyapatites with different Ca/P ratios. Journal of Materials Science-Materials in Medicine 1998;9(1):53-60.
26. Yamada S, Heymann D, Bouler JM, Daculsi G. Osteoclastic resorption of calcium phosphate ceramics with different hydroxyapatite/beta-tricalcium phosphate ratios. Biomaterials 1997;18(15):1037-41.
27. Jarcho M. Calcium-Phosphate Ceramics as Hard Tissue Prosthetics. Clinical Orthopaedics and Related Research 1981(157):259-278.
28. Dumitriu S. Polymeric biomaterials. New York USA: Marcel Dekker; 1994.
29. Chu CC. The biomedical Engineering Handbook. New York, USA: CRC/IEEE Press; 2000.
30. Lanza RP, Langer R, Vacanti J. Principles of tissue engineering; . San Diego, USA: Academic Press 2000.
31. Morris CG. Dictionary of science and technology. Academic Press, 1992.
32. Dumitriu S. Polysaccharides in medical applications. New York, USA: Marcel Dekker. 1996.
33. Benedetti L, Cortivo R, Berti T, Berti A, Pea F, Mazzo M, Moras M, Abatangelo G. Biocompatibility and biodegradation of different hyaluronan derivatives (Hyaff) implanted in rats. Biomaterials 1993;14(15):1154-60.
34. Isogai A, Atalla RH. Dissolution of Cellulose in Aqueous NaOH Solutions. Cellulose 1998;5(4):309-319.
35. O'Sullivan A. Cellulose: the structure slowly unravels. Cellulose 1997;4(3):173-207.
36. Methacanon P, Chaikumpollert O, Thavorniti P, Suchiva K. Hemicellulosic polymer from Vetiver grass and its physicochemical properties. Carbohydrate Polymers 2003;54(3):335-342.
37. Moseley R, Walker M, Waddington RJ, Chen WY. Comparison of the antioxidant properties of wound dressing materials--carboxymethylcellulose, hyaluronan benzyl ester and hyaluronan, towards polymorphonuclear leukocyte-derived reactive oxygen species. Biomaterials 2003;24(9):1549-57.
38. Waring MJ, Parsons D. Physico-chemical characterisation of carboxymethylated spun cellulose fibres. Biomaterials 2001;22(9):903-912.
39. Lemp MA. Artificial Tear Solutions. International Ophthalmology Clinics Spring 1973;13(1):221-230.
40. Bruix A, Adan A, Casaroli-Marano RP. Efficacy of sodium carboxymethylcellulose in the treatment of dry eye syndrome. Arch Soc Esp Oftalmol 2006;81(2):85-92.

41. Andrews GP, Gorman SP, Jones DS. Rheological characterisation of primary and binary interactive bioadhesive gels composed of cellulose derivatives designed as ophthalmic viscosurgical devices. Biomaterials 2005;26(5):571-80.
42. Rodgers KE, Schwartz HE, Roda N, Thornton M, Kobak W, diZerega GS. Effect of oxiplex films (PEO/CMC) on adhesion formation and reformation in rabbit models and on peritoneal infection in a rat model. Fertility and Sterility 2000;73(4):831-838.
43. Liu LS, Berg RA. Adhesion barriers of carboxymethylcellulose and polyethylene oxide composite gels. Journal of Biomedical Materials Research 2002;63(3):326-332.
44. diZerega GS, Cortese S, Rodgers KE, Block KM, Falcone SJ, Juarez TG, Berg R. A modern biomaterial for adhesion prevention. Journal of Biomedical Materials Research Part B: Applied Biomaterials 2007;81B(1):239-250.
45. Moseley R, Leaver M, Walker M, Waddington RJ, Parsons D, Chen WYJ, Embery G. Comparison of the antioxidant properties of HYAFF(R)-11p75, AQUACEL(R) and hyaluronan towards reactive oxygen species in vitro. Biomaterials 2002;23(10):2255-2264.
46. Chiumiento A, Dominguez A, Lamponi S, Villalonga R, Barbucci R. Anti-inflammatory properties of superoxide dismutase modified with carboxymetil-cellulose polymer and hydrogel. J Mater Sci Mater Med 2006;17(5):427-35.
47. Pal K, Banthia AK, Majumdar DK. Preparation of Novel pH-Sensitive Hydrogels of Carboxymethyl Cellulose Acrylates: A Comparative Study. Materials & Manufacturing Processes 2006;21(8):877-882.
48. Rodgers JB, Vasconez HC, Wells MD, DeLuca PP, Faugere MC, Fink BF, Hamilton D. Two lyophilized polymer matrix recombinant human bone morphogenetic protein-2 carriers in rabbit calvarial defects. Journal of Craniofacial Surgery 1998;9(2):147-153.
49. Liu Z, Li J, Nie S, Liu H, Ding P, Pan W. Study of an alginate/HPMC-based in situ gelling ophthalmic delivery system for gatifloxacin. International Journal of Pharmaceutics 2006;315(1-2):12-17.
50. Artola A, Alio JL, Bellot JL, Ruiz JM. Protective Properties of Viscoelastic Substances (Sodium Hyaluronate and 2-Percent Hydroxymethylcellulose) against Experimental Free-Radical Damage to the Corneal Endothelium. Cornea 1993;12(2):109-114.
51. Iooss P, Le Ray AM, Grimandi G, Daculsi G, Merle C. A new injectable bone substitute combining poly(epsilon-caprolactone) microparticles with biphasic calcium phosphate granules. Biomaterials 2001;22(20):2785-94.
52. Gauthier O, Khairoun I, Bosco J, Obadia L, Bourges X, Rau C, Magne D, Bouler JM, Aguado E, Daculsi G and others. Noninvasive bone replacement with a new injectable calcium phosphate biomaterial. J Biomed Mater Res 2003;66A(1):47-54.
53. Bohic S, Weiss P, Roger P, Daculsi G. Light scattering experiments on aqueous solutions of selected cellulose ethers: contribution to the study of polymer-mineral interactions in a new injectable biomaterial. Journal of Materials Science-Materials in Medicine 2001;12(3):201-205.
54. Grimandi G, Weiss P, Millot F, Daculsi G. In vitro evaluation of a new injectable calcium phosphate material. Journal of Biomedical Materials Research 1998;39(4):660-666.
55. Gauthier O, Muller R, von Stechow D, Lamy B, Weiss P, Bouler JM, Aguado E, Daculsi G. In vivo bone regeneration with injectable calcium phosphate biomaterial: A three-dimensional micro-computed

tomographic, biomechanical and SEM study. Biomaterials 2005;26(27):5444-5453.

56. Sergey VD. Is there a chemical interaction between calcium phosphates and hydroxypropylmethylcellulose (HPMC) in organic/inorganic composites? Journal of Biomedical Materials Research 2001;54(2):247-255.
57. Grasdalen H, Larsen B, Smisrod O. 13C-n.m.r. studies of monomeric composition and sequence in alginate. Carbohydrate Research 1981;89(2):179-191.
58. Simpson NE, Stabler CL, Simpson CP, Sambanis A, Constantinidis I. The role of the CaCl2-guluronic acid interaction on alginate encapsulated [beta]TC3 cells. Biomaterials 2004;25(13):2603-2610.
59. Constantinidis I, Rask I, Long RC, Sambanis A. Effects of alginate composition on the metabolic, secretory, and growth characteristics of entrapped [beta]TC3 mouse insulinoma cells. Biomaterials 1999;20(21):2019-2027.
60. Stabler C, Wilks K, Sambanis A, Constantinidis I. The effects of alginate composition on encapsulated [beta]TC3 cells. Biomaterials 2001;22(11):1301-1310.
61. Kulkarni AR, Soppimath KS, Aminabhavi TM, Dave AM, Mehta MH. Glutaraldehyde crosslinked sodium alginate beads containing liquid pesticide for soil application. Journal of Controlled Release 2000;63(1-2):97-105.
62. Kulkarni A, Soppimath K, Aralaguppi M, Aminabhavi T, Rudzinski W. Preparation of Cross-Linked Sodium Alginate Microparticles Using Glutaraldehyde in Methanol. Drug Development & Industrial Pharmacy 2000;26(10):1121.
63. Wan LSC, Heng PWS, Chan LW. Drug encapsulation in alginate microspheres by emulsification. Journal of Microencapsulation 1992;9(3):309 - 316.
64. Chen S-C, Wu Y-C, Mi F-L, Lin Y-H, Yu L-C, Sung H-W. A novel pH-sensitive hydrogel composed of N,O-carboxymethyl chitosan and alginate cross-linked by genipin for protein drug delivery. Journal of Controlled Release 2004;96(2):285-300.
65. Ferreira Almeida P, Almeida AJ. Cross-linked alginate-gelatine beads: a new matrix for controlled release of pindolol. Journal of Controlled Release 2004;97(3):431-439.
66. Esposito E, Cortesi R, Nastruzzi C. Gelatin microspheres: influence of preparation parameters and thermal treatment on chemico-physical and biopharmaceutical properties. Biomaterials 1996;17(20):2009-2020.
67. Sutherland IW. Biomaterials: Novel Materials from Biological Sources. Stockton, New York; 1991. 309-331 p.
68. Ouwerx C, Velings N, Mestdagh MM, Axelos MAV. Physico-chemical properties and rheology of alginate gel beads formed with various divalent cations. Polymer Gels and Networks 1998;6(5):393-408.
69. Elcin YM. Encapsulation of urease enzyme in xanthan-alginate spheres. Biomaterials 1995;16(15):1157-1161.
70. Kuo CK, Ma PX. Ionically crosslinked alginate hydrogels as scaffolds for tissue engineering: part 1. Structure, gelation rate and mechanical properties. Biomaterials 2001;22(6):511-21.
71. Iannuccelli V, Coppi G, Bondi M, Pinelli M, Mingione A, Cameroni R. Biodegradable intraoperative system for bone infection treatment II. In vivo evaluation. International Journal of Pharmaceutics 1996;143(2):187-194.
72. Ishikawa K, Ueyama Y, Mano T, Koyama T, Suzuki K, Matsumura T. Self-setting barrier membrane for

guided tissue regeneration method: Initial evaluation of alginate membrane made with sodium alginate and calcium chloride aqueous solutions. Journal of Biomedical Materials Research 1999;47(2):111-115.

73. Wu S, Suzuki Y, Tanihara M, Ohnishi K, Endo K, Nishimura Y. Repair of facial nerve with alginate sponge without suturing: an experimental study in cats. Scandinavian Journal of Plastic and Reconstructive Surgery and Hand Surgery 2002;36(3):135-140.
74. Wang L, Shelton RM, Cooper PR, Lawson M, Triffitt JT, Barralet JE. Evaluation of sodium alginate for bone marrow cell tissue engineering. Biomaterials 2003;24(20):3475-81.
75. Suzuki Y, Tanihara M, Nishimura Y, Suzuki K, Yamawaki Y, Kudo H, Kakimaru Y, Shimizu Y. In vivo evaluation of a novel alginate dressing. J Biomed Mater Res 1999;48(4):522-7.
76. Suzuki Y, Nishimura Y, Tanihara M, Suzuki K, Nakamura T, Shimizu Y, Yamawaki Y, Kakimaru Y. Evaluation of a novel alginate gel dressing: cytotoxicity to fibroblasts in vitro and foreign-body reaction in pig skin in vivo. J Biomed Mater Res 1998;39(2):317-22.
77. Balakrishnan B, Mohanty M, Umashankar PR, Jayakrishnan A. Evaluation of an in situ forming hydrogel wound dressing based on oxidized alginate and gelatin. Biomaterials 2005;26(32):6335-6342.
78. Lemoine D, Wauters F, Bouchend'homme S, Preat V. Preparation and characterization of alginate microspheres containing a model antigen. International Journal of Pharmaceutics 1998;176(1):9-19.
79. Ueng SWN, Yuan L-J, Lee N, Lin S-S, Chan E-C, Weng J-H. In vivo study of biodegradable alginate antibiotic beads in rabbits. Journal of Orthopaedic Research 2004;22(3):592-599.
80. Domm C, Schunke M, Christesen K, Kurz B. Redifferentiation of dedifferentiated bovine articular chondrocytes in alginate culture under low oxygen tension. Osteoarthritis and Cartilage 2002;10(1):13-22.
81. Hauselmann HJ, Fernandes RJ, Mok SS, Schmid TM, Block JA, Aydelotte MB, Kuettner KE, Thonar EJ. Phenotypic stability of bovine articular chondrocytes after long-term culture in alginate beads. J Cell Sci 1994;107 (Pt 1):17-27.
82. Fragonas E, Valente M, Pozzi-Mucelli M, Toffanin R, Rizzo R, Silvestri F, Vittur F. Articular cartilage repair in rabbits by using suspensions of allogenic chondrocytes in alginate. Biomaterials 2000;21(8):795-801.
83. Lee DA, Reisler T, Bader DL. Expansion of chondrocytes for tissue engineering in alginate beads enhances chondrocytic phenotype compared to conventional monolayer techniques. Acta Orthop Scand 2003;74(1):6-15.
84. Miralles G, Baudoin R, Dumas D, Baptiste D, Hubert P, Stoltz JF, Dellacherie E, Mainard D, Netter P, Payan E. Sodium alginate sponges with or without sodium hyaluronate: *In vitro* engineering of cartilage. Journal of Biomedical Materials Research 2001;57(2):268-278.
85. Li Z, Zhang M. Chitosan-alginate as scaffolding material for cartilage tissue engineering. Journal of Biomedical Materials Research Part A 2005;75A(2):485-493.
86. Li Z, Ramay HR, Hauch KD, Xiao D, Zhang M. Chitosan-alginate hybrid scaffolds for bone tissue engineering. Biomaterials 2005;26(18):3919-3928.
87. Alsberg E, Anderson KW, Albeiruti A, Franceschi RT, Mooney DJ. Cell-interactive alginate hydrogels for bone tissue engineering. J Dent Res 2001;80(11):2025-9.
88. Rowley JA, Mooney DJ. Alginate type and RGD density control myoblast phenotype. J Biomed Mater Res 2002;60(2):217-23.

89. Rowley JA, Madlambayan G, Mooney DJ. Alginate hydrogels as synthetic extracellular matrix materials. Biomaterials 1999;20(1):45-53.
90. Suzuki Y, Tanihara M, Suzuki K, Saitou A, Sufan W, Nishimura Y. Alginate hydrogel linked with synthetic oligopeptide derived from BMP-2 allows ectopic osteoinduction *in vivo*. Journal of Biomedical Materials Research 2000;50(3):405-409.
91. Ma H, Hung S, Lin S, Chen Y, Lo W. Chondrogenesis of human mesenchymal stem cells encapsulated in alginate beads. Journal of Biomedical Materials Research 2003;64A(2):273-281.
92. Cai X, Lin Y, Ou G, Luo E, Man Y, Yuan Q, Gong P. Ectopic osteogenesis and chondrogenesis of bone marrow stromal stem cells in alginate system. Cell Biology International 2007;31(8):776-783.
93. Muzzarelli RA. Human enzymatic activities related to the therapeutic administration of chitin derivatives. Cell Mol Life Sci 1997;53(2):131-40.
94. Yusof N, Wee A, Yong L, Lim L, Khor E. Flexible chitin films as potential wound-dressing materials: Wound model studies. Journal of Biomedical Materials Research Part A 2003;66A(2):224-232.
95. Kato Y, Onishi H, Machida Y. Application of chitin and chitosan derivatives in the pharmaceutical field. Curr Pharm Biotechnol 2003;4(5):303-9.
96. Lee SB, Kim YH, Chong MS, Lee YM. Preparation and characteristics of hybrid scaffolds composed of beta-chitin and collagen. Biomaterials 2004;25(12):2309-17.
97. Uda H, Sugawara Y, Nakasu M. Experimental studies on hydroxyapatite powder-carboxymethyl chitin composite: injectable material for bone augmentation. Journal of Plastic, Reconstructive & Aesthetic Surgery 2006;59(2):188-196.
98. Rinaudo M. Chitin and chitosan: Properties and applications. Progress in Polymer Science 2006;31(7):603-632.
99. Rinaudo M, Pavlov G, Desbrieres J. Influence of acetic acid concentration on the solubilization of chitosan. Polymer 1999;40(25):7029-7032.
100. Sorlier P, Denuziere A, Viton C, Domard A. Relation between the degree of acetylation and the electrostatic properties of chitin and chitosan. Biomacromolecules 2001;2(3):765-772.
101. Filion D, Lavertu M, Buschmann MD. Ionization and Solubility of Chitosan Solutions Related to Thermosensitive Chitosan/Glycerol-Phosphate Systems. Biomacromolecules 2007;8(10):3224-3234.
102. Lahiji A, Sohrabi A, Hungerford DS, Frondoza CG. Chitosan supports the expression of extracellular matrix proteins in human osteoblasts and chondrocytes. J Biomed Mater Res 2000;51(4):586-95.
103. Mori T, Okumura M, Matsuura M, Ueno K, Tokura S, Okamoto Y, Minami S, Fujinaga T. Effects of chitin and its derivatives on the proliferation and cytokine production of fibroblasts in vitro. Biomaterials 1997;18(13):947-51.
104. Mori T, Irie Y, Nishimura SI, Tokura S, Matsuura M, Okumura M, Kadosawa T, Fujinaga T. Endothelial cell responses to chitin and its derivatives. J Biomed Mater Res 1998;43(4):469-72.
105. Sechriest VF, Miao YJ, Niyibizi C, Westerhausen-Larson A, Matthew HW, Evans CH, Fu FH, Suh JK. GAG-augmented polysaccharide hydrogel: a novel biocompatible and biodegradable material to support chondrogenesis. J Biomed Mater Res 2000;49(4):534-41.
106. Chatelet C, Damour O, Domard A. Influence of the degree of acetylation on some biological properties of chitosan films. Biomaterials 2001;22(3):261-268.

107. Amaral IF, Sampaio P, Barbosa MA. Three-dimensional culture of human osteoblastic cells in chitosan sponges: the effect of the degree of acetylation. J Biomed Mater Res A 2006;76(2):335-46.
108. Amaral IF, Cordeiro AL, Sampaio P, Barbosa MA. Attachment, spreading and short-term proliferation of human osteoblastic cells cultured on chitosan films with different degrees of acetylation. J. Biomater. Sci. Polymer Edn 2007;18(4):469-485.
109. VandeVord PJ, Matthew HW, DeSilva SP, Mayton L, Wu B, Wooley PH. Evaluation of the biocompatibility of a chitosan scaffold in mice. J Biomed Mater Res 2002;59(3):585-90.
110. Meng S, Liu Z, Zhong W, Wang Q, Du Q. Phosphorylcholine modified chitosan: Appetent and safe material for cells. Carbohydrate Polymers 2007;70(1):82-88.
111. Masuko T, Iwasaki N, Yamane S, Funakoshi T, Majima T, Minami A, Ohsuga N, Ohta T, Nishimura SI. Chitosan-RGDSGGC conjugate as a scaffold material for musculoskeletal tissue engineering. Biomaterials 2005;26(26):5339-5347.
112. Ho M, Wang D, Hsieh H, Liu HC, Hsien TY, Lai JY, Hou LT. Preparation and characterization of RGD-immobilized chitosan scaffolds. Biomaterials 2005;26(16):3197-3206.
113. Yang Y, He Q, Duan L, Cui Y, Li J. Assembled alginate/chitosan nanotubes for biological application. Biomaterials 2007;28(20):3083-3090.
114. Sendemir-Urkmez A, Jamison RD. The addition of biphasic calcium phosphate to porous chitosan scaffolds enhances bone tissue development *in vitro*. Journal of Biomedical Materials Research Part A 2007;81A(3):624-633.
115. Zhang Y, Zhang MQ. Three-dimensional macroporous calcium phosphate bioceramics with nested chitosan sponges for load-bearing bone implants. Journal of Biomedical Materials Research 2002;61(1):1-8.
116. Cho JH, Kim SH, Park KD, Jung MC, Yang WI, Han SW, Noh JY, Lee JW. Chondrogenic differentiation of human mesenchymal stem cells using a thermosensitive poly(N-isopropylacrylamide) and water-soluble chitosan copolymer. Biomaterials 2004;25(26):5743-51.
117. Xu HH, Simon CG, Jr. Fast setting calcium phosphate-chitosan scaffold: mechanical properties and biocompatibility. Biomaterials 2005;26(12):1337-48.
118. Jameela SR, Jayakrishnan A. Glutaraldehyde cross-linked chitosan microspheres as a long acting biodegradable drug delivery vehicle: studies on the in vitro release of mitoxantrone and in vivo degradation of microspheres in rat muscle. Biomaterials 1995;16(10):769-775.
119. Subramanian A, Lin HY. Crosslinked chitosan: its physical properties and the effects of matrix stiffness on chondrocyte cell morphology and proliferation. J Biomed Mater Res A 2005;75(3):742-53.
120. Mi FL, Tan YC, Liang HF, Sung HW. In vivo biocompatibility and degradability of a novel injectable-chitosan-based implant. Biomaterials 2002;23(1):181-91.
121. Hirano S, Tsuchida H, Nagao N. N-acetylation in chitosan and the rate of its enzymic hydrolysis. Biomaterials 1989;10(8):574-576.
122. Zhang H, Neau SH. In vitro degradation of chitosan by a commercial enzyme preparation: effect of molecular weight and degree of deacetylation. Biomaterials 2001;22(12):1653-8.
123. Varum KM, Myhr MM, Hjerde RJN, Smidsrod O. In vitro degradation rates of partially N-acetylated chitosans in human serum. Carbohydrate Research 1997;299(1-2):99-101.

124. Pangburn SH, Trescony PV, Heller J. Lysozyme degradation of partially deacetylated chitin, its films and hydrogels. Biomaterials 1982;3(2):105-8.
125. Nordtveit RJ, Varum KM, Smidsrod O. Degradation of partially N-acetylated chitosans with hen egg white and human lysozyme. Carbohydrate Polymers 1996;29(2):163-167.
126. Freier T, Koh HS, Kazazian K, Shoichet MS. Controlling cell adhesion and degradation of chitosan films by N-acetylation. Biomaterials 2005;26(29):5872-5878.
127. Wang X, Ma J, Wang Y, He B. Bone repair in radii and tibias of rabbits with phosphorylated chitosan reinforced calcium phosphate cements. Biomaterials 2002;23(21):4167-4176.
128. Hong Y, Song H, Gong Y, Mao Z, Gao C, Shen J. Covalently crosslinked chitosan hydrogel: Properties of in vitro degradation and chondrocyte encapsulation. Acta Biomaterialia 2007;3(1):23-31.
129. Madihally SV, Matthew HWT. Porous chitosan scaffolds for tissue engineering. Biomaterials 1999;20(12):1133-1142.
130. Kawamura Y, Mitsuhashi M, Tanibe H, Yoshida H. Adsorption of metal ions on polyaminated highly porous chitosan chelating resin. Industrial and Engineering Chemistry Research 1993;32(2):386-391.
131. Remunan-Lopez C, Bodmeier R. Mechanical, water uptake and permeability properties of crosslinked chitosan glutamate and alginate films. Journal of Controlled Release 1997;44(2-3):215-225.
132. Ballantyne B, Jordan SL. Toxicological, medical and industrial hygiene aspects of glutaraldehyde with particular reference to its biocidal use in cold sterilization procedures. Journal of Applied Toxicology 2001;21(2):131-151.
133. Sung H, Huang R, Huang L, Tsai C, Chiu C. Feasibility study of a natural crosslinking reagent for biological tissue fixation. Journal of Biomedical Materials Research 1998;42(4):560-567.
134. Ishihara M, Nakanishi K, Ono K, Sato M, Kikuchi M, Saito Y, Yura H, Matsui T, Hattori H, Uenoyama M and others. Photocrosslinkable chitosan as a dressing for wound occlusion and accelerator in healing process. Biomaterials 2002;23(3):833-840.
135. Renbutsu E, Hirose M, Omura Y, Nakatsubo F, Okamura Y, Okamoto Y, Saimoto H, Shigemasa Y, Minami S. Preparation and Biocompatibility of Novel UV-Curable Chitosan Derivatives. Biomacromolecules 2005;6(5):2385-2388.
136. Xu Y, Du Y, Huang R, Gao L. Preparation and modification of N-(2-hydroxyl) propyl-3-trimethyl ammonium chitosan chloride nanoparticle as a protein carrier. Biomaterials 2003;24(27):5015-5022.
137. Bhattarai N, Ramay HR, Gunn J, Matsen FA, Zhang MQ. PEG-grafted chitosan as an injectable thermosensitive hydrogel for sustained protein release. Journal of Controlled Release 2005;103(3):609-624.
138. Tang YF, Du YM, Hu XW, Shi XW, Kennedy JF. Rheological characterisation of a novel thermosensitive chitosan/poly(vinyl alcohol) blend hydrogel. Carbohydrate Polymers 2007;67(4):491-499.
139. Kim SE, Park JH, Cho YW, Chung H, Jeong SY, Lee EB, Kwon IC. Porous chitosan scaffold containing microspheres loaded with transforming growth factor-beta1: implications for cartilage tissue engineering. J Control Release 2003;91(3):365-74.
140. Mukherjee DP, Tunkle AS, Roberts RA, Clavenna A, Rogers S, Smith D. An animal evaluation of a paste of chitosan glutamate and hydroxyapatite as a synthetic bone graft material. Journal of Biomedical Materials Research Part B-Applied Biomaterials 2003;67B(1):603-609.

141. Chenite A, Chaput C, Wang D, Combes C, Buschmann MD, Hoemann CD, Leroux JC, Atkinson BL, Binette F, Selmani A. Novel injectable neutral solutions of chitosan form biodegradable gels in situ. Biomaterials 2000;21(21):2155-61.
142. Yun Y, Jiang H, Chan R, Chen W. Sustained release of PEG-g-chitosan complexed DNA from poly(lactide-co-glycolide). Journal of Biomaterials Science, Polymer Edition 2005;16(11):1359-1378.
143. Zhang Y, Chen J, Zhang Y, Pan Y, Zhao J, Ren L, Liao M, Hu Z, Kong L, Wang J. A novel PEGylation of chitosan nanoparticles for gene delivery. Biotechnol. Appl. Biochem. 2007;46(Pt 4):197-204.
144. Lameiro MH, Malpique R, Silva AC, Alves PM, Melo E. Encapsulation of adenoviral vectors into chitosan-bile salt microparticles for mucosal vaccination. Journal of Biotechnology 2006;126(2):152-162.
145. Guo T, Zhao J, Chang J, Ding Z, Hong H, Chen J, Zhang J. Porous chitosan-gelatin scaffold containing plasmid DNA encoding transforming growth factor-[beta]1 for chondrocytes proliferation. Biomaterials 2006;27(7):1095-1103.
146. Cho YW, Cho YN, Chung SH, Yoo G, Ko SW. Water-soluble chitin as a wound healing accelerator. Biomaterials 1999;20(22):2139-2145.
147. Ueno H, Yamada H, Tanaka I, Kaba N, Matsuura M, Okumura M, Kadosawa T, Fujinaga T. Accelerating effects of chitosan for healing at early phase of experimental open wound in dogs. Biomaterials 1999;20(15):1407-1414.
148. Kojima K, Okamoto Y, Miyatake K, Yukisato K, Minami S. Collagen typing of granulation tissue induced by chitin and chitosan. Carbohydrate Polymers 1998;37(2):109-113.
149. Koyano T, Minoura N, Nagura M, Kobayashi K. Attachment and growth of cultured fibroblast cells on PVA/chitosan-blended hydrogels. Journal of Biomedical Materials Research 1998;39(3):486-490.
150. Chuang WY, Young TH, Yao CH, Chiu WY. Properties of the poly(vinyl alcohol)/chitosan blend and its effect on the culture of fibroblast in vitro. Biomaterials 1999;20(16):1479-1487.
151. Ueno H, Ohya T, Ito H, Kobayashi Y, Yamada K, Sato M. Chitosan application to X-ray irradiated wound in dogs. Journal of Plastic, Reconstructive & Aesthetic Surgery 2007;60(3):304-310.
152. Mi FL, Wu YB, Shyu SS, Schoung JY, Huang YB, Tsai YH, Hao JY. Control of wound infections using a bilayer chitosan wound dressing with sustainable antibiotic delivery. Journal of Biomedical Materials Research 2002;59(3):438-449.
153. Mi FL, Shyu SS, Wu YB, Lee ST, Shyong JY, Huang RN. Fabrication and characterization of a sponge-like asymmetric chitosan membrane as a wound dressing. Biomaterials 2001;22(2):165-173.
154. Montembault A, Tahiri K, Korwin-Zmijowska C, Chevalier X, Corvol MT, Domard A. A material decoy of biological media based on chitosan physical hydrogels: application to cartilage tissue engineering. Biochimie 2006;88(5):551-564.
155. Yamane S, Iwasaki N, Majima T, Funakoshi T, Masuko T, Harada K, Minami A, Monde K, Nishimura S. Feasibility of chitosan-based hyaluronic acid hybrid biomaterial for a novel scaffold in cartilage tissue engineering. Biomaterials 2005;26(6):611-9.
156. Donati I, Stredanska S, Silvestrini G, Vetere A, Marcon P, Marsich E, Mozetic P, Gamini A, Paoletti S, Vittur F. The aggregation of pig articular chondrocyte and synthesis of extracellular matrix by a lactose-modified chitosan. Biomaterials 2005;26(9):987-98.
157. Hoemann CD, Sun J, Legare A, McKee MD, Buschmann MD. Tissue engineering of cartilage using an

injectable and adhesive chitosan-based cell-delivery vehicle. Osteoarthritis Cartilage 2005;13(4):318-29.

158. Chevrier A, Hoemann CD, Sun J, Buschmann MD. Chitosan-glycerol phosphate/blood implants increase cell recruitment, transient vascularization and subchondral bone remodeling in drilled cartilage defects. Osteoarthritis and Cartilage 2007;15(3):316-327.
159. Arpornmaeklong P, Suwatwirote N, Pripatnanont P, Oungbho K. Growth and differentiation of mouse osteoblasts on chitosan-collagen sponges. International Journal of Oral and Maxillofacial Surgery 2007;36(4):328-337.
160. Lee JY, Nam SH, Im SY, Park YJ, Lee YM, Seol YJ, Chung CP, Lee SJ. Enhanced bone formation by controlled growth factor delivery from chitosan-based biomaterials. J Control Release 2002;78(1-3):187-97.
161. Park YJ, Lee YM, Lee JY, Seol YJ, Chung CP, Lee SJ. Controlled release of platelet-derived growth factor-BB from chondroitin sulfate-chitosan sponge for guided bone regeneration. Journal of Controlled Release 2000;67(2-3):385-394.
162. Park DJ, Choi BH, Zhu SJ, Huh JY, Kim BY, Lee SH. Injectable bone using chitosan-alginate gel/mesenchymal stem cells/BMP-2 composites. Journal of Cranio-Maxillofacial Surgery 2005;33(1):50-54.
163. Pound JC, Green DW, Chaudhuri JB, Mann S, Roach HI, Oreffo RO. Strategies to promote chondrogenesis and osteogenesis from human bone marrow cells and articular chondrocytes encapsulated in polysaccharide templates. Tissue Eng 2006;12(10):2789-99.
164. Payne RG, Yaszemski MJ, Yasko AW, Mikos AG. Development of an injectable, in situ crosslinkable, degradable polymeric carrier for osteogenic cell populations. Part 1. Encapsulation of marrow stromal osteoblasts in surface crosslinked gelatin microparticles. Biomaterials 2002;23(22):4359-71.
165. Temenoff JS, Mikos AG. Injectable biodegradable materials for orthopedic tissue engineering. Biomaterials 2000;21(23):2405-12.
166. Molinaro G, Leroux JC, Damas J, Adam A. Biocompatibility of thermosensitive chitosan-based hydrogels: an in vivo experimental approach to injectable biomaterials. Biomaterials 2002;23(13):2717-22.
167. Bodic F, Amouriq Y, Gayet-Delacroix M, Gauthier O, Bouler J-M, Daculsi G, Hamel L. Méthode nom invasive d'evaluation d'un substitut osseux injectable / Non-invasive evaluation of an injectable bone substitute. C. R. Biologies 2002;325:1-9.
168. Halberstadt C, Austin C, Rowley J, Culberson C, Loebsack A, Wyatt S, Coleman S, Blacksten L, Burg K, Mooney D and others. A hydrogel material for plastic and reconstructive applications injected into the subcutaneous space of a sheep. Tissue Eng 2002;8(2):309-19.
169. Peter SJ, Kim P, Yasko AW, Yaszemski MJ, Mikos AG. Crosslinking characteristics of an injectable poly(propylene fumarate)/beta-tricalcium phosphate paste and mechanical properties of the crosslinked composite for use as a biodegradable bone cement. Journal of Biomedical Materials Research 1999;44(3):314-321.
170. Peter SJ, Miller ST, Zhu G, Yasko AW, Mikos AG. In vivo degradation of a poly(propylene fumarate)/beta-tricalcium phosphate injectable composite scaffold. J Biomed Mater Res 1998;41(1):1-7.
171. Lewandrowski KU, Gresser JD, Wise DL, White RL, Trantolo DJ. Osteoconductivity of an injectable and

bioresorbable poly(propylene glycol-co-fumaric acid) bone cement. Biomaterials 2000;21(3):293-8.

172. Xu HH, Weir MD, Burguera EF, Fraser AM. Injectable and macroporous calcium phosphate cement scaffold. Biomaterials 2006;27(24):4279-87.
173. Daculsi G. Biphasic calcium phosphate concept applied to artificial bone, implant coating and injectable bone substitute. Biomaterials 1998;19(16):1473-1478.
174. Schmitt M, Weiss P, Bourges X, Amador del Valle G, Daculsi G. Crystallization at the polymer/calcium-phosphate interface in a sterilized injectable bone substitute IBS. Biomaterials 2002;23(13):2789-94.
175. Weiss P, Gauthier O, Bouler JM, Grimandi G, Daculsi G. Injectable bone substitute using a hydrophilic polymer. Bone 1999;25(2 Suppl):67S-70S.
176. Daculsi G, Weiss P, Bouler JM, Gauthier O, Millot F, Aguado E. Biphasic calcium phosphate/hydrosoluble polymer composites: a new concept for bone and dental substitution biomaterials. Bone 1999;25(2 Suppl):59S-61S.
177. Gauthier O, Boix D, Grimandi G, Aguado E, Bouler JM, Weiss P, Daculsi G. A new injectable calcium phosphate biomaterial for immediate bone filling of extraction sockets: a preliminary study in dogs. J Periodontol 1999;70(4):375-83.
178. Gauthier O, Bouler JM, Weiss P, Bosco J, Daculsi G, Aguado E. Kinetic study of bone ingrowth and ceramic resorption associated with the implantation of different injectable calcium-phosphate bone substitutes. Journal of Biomedical Materials Research 1999;47(1):28-35.
179. Gauthier O, Bouler JM, Weiss P, Bosco J, Aguado E, Daculsi G. Short-term effects of mineral particle sizes on cellular degradation activity after implantation of injectable calcium phosphate biomaterials and the consequences for bone substitution. Bone 1999;25(2):71S-74S.
180. Trojani C, Weiss P, Michiels JF, Vinatier C, Guicheux J, Daculsi G, Gaudray P, Carle GF, Rochet N. Three-dimensional culture and differentiation of human osteogenic cells in an injectable hydroxypropylmethylcellulose hydrogel. Biomaterials 2005;26(27):5509-5517.
181. Dupraz A, Delecrin J, Moreau A, Pilet P, Passuti N. Long-term bone response to particulate injectable ceramic. J Biomed Mater Res 1998;42(3):368-375.
182. Bourges X, Weiss P, Daculsi G, Legeay G. Synthesis and general properties of silated-hydroxypropyl methylcellulose in prospect of biomedical use. Advances in Colloid and Interface Science 2002;99(3):215-228.
183. Trojani C, Boukhechba F, Scimeca JC, Vandenbos F, Michiels JF, Daculsi G, Boileau P, Weiss P, Carle GF, Rochet N. Ectopic bone formation using an injectable biphasic calcium phosphate/Si-HPMC hydrogel composite loaded with undifferentiated bone marrow stromal cells. Biomaterials 2006;27(17):3256-3264.
184. Vinatier C, Magne D, Weiss P, Trojani C, Rochet N, Carle GF, Vignes-Colombeix C, Chadjichristos C, Galera P, Daculsi G and others. A silanized hydroxypropyl methylcellulose hydrogel for the three-dimensional culture of chondrocytes. Biomaterials 2005;26(33):6643-6651.
185. Vinatier C, Magne D, Moreau A, Gauthier O, Malard O, Vignes-Colombeix C, Daculsi G, Weiss P, Guicheux J. Engineering cartilage with human nasal chondrocytes and a silanized hydroxypropyl methylcellulose hydrogel. Journal of Biomedical Materials Research Part A 2007;80A(1):66-74.
186. Cao YL, Ibarra C, Vacanti C. Preparation and use of thermosensitive polymers; 1999.
187. Jeong B, Bae YH, Kim SW. In situ gelation of PEG-PLGA-PEG triblock copolymer aqueous solutions

and degradation thereof. Journal of Biomedical Materials Research 2000;50(2):171-177.

188. Jeong B, Bae YH, Kim SW. Drug release from biodegradable injectable thermosensitive hydrogel of PEG-PLGA-PEG triblock copolymers. J Control Release 2000;63(1-2):155-63.
189. Jeong B, Lee KM, Gutowska A, An YH. Thermogelling biodegradable copolymer aqueous solutions for injectable protein delivery and tissue engineering. Biomacromolecules 2002;3(4):865-8.
190. Duranti F, Salti G, Bovani B, Calandra M, Rosati ML. Injectable hyaluronic acid gel for soft tissue augmentation - A clinical and histological study. Dermatologic Surgery 1998;24(12):1317-1325.
191. Kobayashi K, Amiel M, Harwood FL, Healey RM, Sonoda M, Moriya H, Amiel D. The long-term effects of hyaluronan during development of osteoarthritis following partial meniscectomy in a rabbit model. Osteoarthritis and Cartilage 2000;8(5):359-365.
192. Radomsky ML, Aufdemorte TB, Swain LD, Fox WC, Spiro RC, Poser JW. Novel formulation of fibroblast growth factor-2 in a hyaluronan gel accelerates fracture healing in nonhuman primates. Journal of Orthopaedic Research 1999;17(4):607-614.
193. Felix L, Hernandez J, Arguelles-Monal WM, Goycoolea FM. Kinetics of gelation and thermal sensitivity of N-isobutyryl chitosan hydrogels. Biomacromolecules 2005;6(5):2408-15.
194. Maeda T, Kanda T, Yonekura Y, Yamamoto K, Aoyagi T. Hydroxylated Poly(N-isopropylacrylamide) as Functional Thermoresponsive Materials. Biomacromolecules 2006;7(2):545-549.
195. Hsiue GH, Chang RW, Wang CH, Lee SH. Development of in situ thermosensitive drug vehicles for glaucoma therapy. Biomaterials 2003;24(13):2423-2430.
196. Chen J, Cheng T. Thermo-Responsive Chitosan-graft-poly(N-isopropylacrylamide) Injectable Hydrogel for Cultivation of Chondrocytes and Meniscus Cells. Macromolecular Bioscience 2006;6(12):1026-1039.
197. Seetapan N, Mai-ngam K, Plucktaveesak N, Sirivat A. Linear viscoelasticity of thermoassociative chitosan-g-poly(N-isopropylacrylamide) copolymer. Rheologica Acta 2006;45(6):1011-1018.
198. Hsiue G, Hsu S, Yang CC, Lee SH, Yang IK. Preparation of controlled release ophthalmic drops, for glaucoma therapy using thermosensitive poly-N-isopropylacrylamide. Biomaterials 2002;23(2):457-462.
199. Hong Y, Mao Z, Wang H, Gao C, Shen J. Covalently crosslinked chitosan hydrogel formed at neutral pH and body temperature. Journal of Biomedical Materials Research Part A 2006;79A(4):913-922.
200. Liu H, Li H, Cheng W, Yang Y, Zhu M, Zhou C. Novel injectable calcium phosphate/chitosan composites for bone substitute materials. Acta Biomaterialia 2006;2(5):557-565.
201. Schrier JA, Fink BF, Rodgers JB, Vasconez HC, DeLuca PP. Effect of a freeze-dried CMC/PLGA microsphere matrix of rhBMP-2 on bone healing. AAPS PharmSciTech 2001;2(3):E18.
202. Borden M, Attawia M, Khan Y, El-Amin SF, Laurencin CT. Tissue-engineered bone formation in vivo using a novel sintered polymeric microsphere matrix. J Bone Joint Surg Br 2004;86(8):1200-8.
203. Kang SW, Yoon JR, Lee JS, Kim HJ, Lim HW, Lim HC, Park JH, Kim BS. The use of poly(lactic-co-glycolic acid) microspheres as injectable cell carriers for cartilage regeneration in rabbit knees. J. Biomater. Sci. Polymer Edn 2006;17(8):925–939.
204. Valimaki VV, Yrjans JJ, Vuorio EI, Aro HT. Molecular biological evaluation of bioactive glass microspheres and adjunct bone morphogenetic protein 2 gene transfer in the enhancement of new bone formation. Tissue Eng 2005;11(3-4):387-94.
205. Pasquier G, Flautre B, Blary MC, Anselme K, Hardouin P. Injectable percutaneous bone biomaterials: An

experimental study in a rabbit model. Journal of Materials Science-Materials in Medicine 1996;7(11):683-690.

206. Ferraz MP, Mateus AY, Sousa JC, Monteiro FJ. Nanohydroxyapatite microspheres as delivery system for antibiotics: Release kinetics, antimicrobial activity, and interaction with osteoblasts. Journal of Biomedical Materials Research Part A 2007;81A(4):994-1004.
207. Barrias CC, Ribeiro CC, Lamghari M, Miranda CS, Barbosa MA. Proliferation, activity, and osteogenic differentiation of bone marrow stromal cells cultured on calcium titanium phosphate microspheres. Journal of Biomedical Materials Research 2005;72A(1):57-66.
208. Barrias CC, Ribeiro CC, Barbosa MA. Adhesion and proliferation of human osteoblastic cells seeded on injectable hydroxyapatite microspheres. Bioceramics, Vol 16 2004;254-2:877-880.
209. Bezwada RS; Liquid copolymers of epsilon-caprolactone and lactide patent US 5 442 033. 1995.
210. Dunn RL, English JP, Cowsar DR, Vanderbelt DD; Biodegradable in-situ forming implants and methods of producing the same. U.S. Pat. 5/340/849. 1994.
211. Einmahl S, Behar-Cohen F, Tabatabay C, Savoldelli M, D'Hermies F, Chauvaud D, Heller J, Gurny R. A viscous bioerodible poly(ortho ester) as a new biomaterial for intraocular application. J Biomed Mater Res 2000;50(4):566-73.
212. Scopelianos AG, Bezwada RS, Arnold SC; Injectable liquid copolymers for soft tissue repair and augmentation, U.S. Pat. 5/824/333, 20 October 1998.
213. Walter KA, Cahan MA, Gur A, Tyler B, Hilton J, Colvin OM, Burger PC, Domb A, Brem H. Interstitial taxol delivered from a biodegradable polymer implant against experimental malignant glioma. Cancer Res 1994;54(8):2207-12.
214. Zhang X, Jackson JK, Wong W, Min W, Cruz T, Hunter WL, Burt HM. Development of biodegradable polymeric paste formulations for taxol: An in vitro and in vivo study. International Journal of Pharmaceutics 1996;137(2):199-208.
215. Dordunoo SK, Oktaba AMC, Hunter W, Min W, Cruz T, Burt HM. Release of taxol from poly(epsilon-caprolactone) pastes: Effect of water-soluble additives. Journal of Controlled Release 1997;44(1):87-94.
216. Hatefi A, Amsden B. Biodegradable injectable in situ forming drug delivery systems. J Control Release 2002;80(1-3):9-28.
217. Moore LA, Norton RL, Whitman SL, Dunn RL. An injectable biodegradable drug delivery system based on acrylic terminated poly n-caprolactone. 1995; CA USA.
218. Langer RS, Peppas NA. Present and future applications of biomaterials in controlled drug delivery systems. Biomaterials 1981;2(4):201-14.
219. Brondsted H, Andersen C, Hovgaard L. Crosslinked dextran--a new capsule material for colon targeting of drugs. J Control Release 1998;53(1-3):7-13.
220. Hennink WE, van Nostrum CF. Novel crosslinking methods to design hydrogels. Adv Drug Deliv Rev 2002;54(1):13-36.
221. Peppas NA, Benner RE. Proposed Method of Intracordal Injection and Gelation of Poly (Vinyl Alcohol) Solution in Vocal Cords - Polymer Considerations. Biomaterials 1980;1(3):158-162.
222. Yamamoto M, Tabata Y, Hong L, Miyamoto S, Hashimoto N, Ikada Y. Bone regeneration by transforming growth factor beta1 released from a biodegradable hydrogel. J Control Release 2000;64(1-

3):133-42.

223. Chan LW, Heng PW. Effects of aldehydes and methods of cross-linking on properties of calcium alginate microspheres prepared by emulsification. Biomaterials 2002;23(5):1319-26.

224. Coviello T, Grassi M, Rambone G, Santucci E, Carafa M, Murtas E, Riccieri FM, Alhaique F. Novel hydrogel system from scleroglucan: synthesis and characterization. J Control Release 1999;60(2-3):367-78.

225. Elbert DL, Luthof MP, Pratt AB, Halstenberg S, Hubbel JA. Protein release from PEG hydrogels that are similar to ideal Flory-Rehner Networks. Proc. Int. Symp. Controlled Rel. Bioact. Mat. 2001;28:987-988.

226. He S, Yaszemski MJ, Yasko AW, Engel PS, Mikos AG. Injectable biodegradable polymer composites based on poly(propylene fumarate) crosslinked with poly(ethylene glycol)-dimethacrylate. Biomaterials 2000;21(23):2389-94.

227. Kuijpers AJ, van Wachem PB, van Luyn MJ, Engbers GH, Krijgsveld J, Zaat SA, Dankert J, Feijen J. In vivo and in vitro release of lysozyme from cross-linked gelatin hydrogels: a model system for the delivery of antibacterial proteins from prosthetic heart valves. J Control Release 2000;67(2-3):323-36.

228. Liu LS, Liu SQ, Ng SY, Froix M, Ohno T, Heller J. Controlled release of interleukin-2 for tumour immunotherapy using alginate/chitosan porous microspheres. Journal of Controlled Release 1997;43(1):65-74.

229. Andrianov AK, Payne LG, Visscher KB, Allcock HR, Langer R. Hydrolytic Degradation of Ionically Cross-Linked Polyphosphazene Microspheres. Journal of Applied Polymer Science 1994;53(12):1573-1578.

230. Watanabe T, Ohtsuka A, Murase N, Barth P, Gersonde K. NMR studies on water and polymer diffusion in dextran gels. Influence of potassium ions on microstructure formation and gelation mechanism. Magn Reson Med 1996;35(5):697-705.

231. Lu SX, Anseth KS. Photopolymerization of multilaminated poly(HEMA) hydrogels for controlled release. Journal of Controlled Release 1999;57(3):291-300.

232. Hubbell JA, Pathak CP, Sawhney AS, Desai NP, Hill JL; Photopolymerizable biodegradable hydrogels as tissue contacting materials and controlled-release carriers. US patent 6,306,922. 2000.

233. Muggli DS, Burkoth AK, Anseth KS. Crosslinked polyanhydrides for use in orthopedic applications: Degradation behavior and mechanics. Journal of Biomedical Materials Research 1999;46(2):271-278.

234. Rajpurohit R, Koch CJ, Tao Z, Teixeira CM, Shapiro IM. Adaptation of chondrocytes to low oxygen tension: relationship between hypoxia and cellular metabolism. J Cell Physiol 1996;168(2):424-32.

235. Petersen W, Tsokos M, Pufe T. Expression of VEGF121 and VEGF165 in hypertrophic chondrocytes of the human growth plate and epiphyseal cartilage. J Anat 2002;201(2):153-7.

236. Akiyama H, Chaboissier MC, Martin JF, Schedl A, Crombrugghe B. The transcription factor Sox9 has essential roles in successive steps of the chondrocyte differentiation for expression of pathway and is required Sox6 and Sox5

Genes & Dev. 2002;16:2813-2828.

237. Bi WM, Deng JM, Zhang ZP, Behringer RR, de Crombrugghe B. Sox9 is required for cartilage formation. Nature Genetics 1999;22(1):85-89.

238. LeBaron RG, Athanasiou KA. Ex vivo synthesis of articular cartilage. Biomaterials 2000;21(24):2575-

2587.

239. Mow VC, Wang CCB. Some bioengineering considerations for tissue engineering of articular cartilage. Clinical Orthopaedics and Related Research 1999(367):S204-S223.
240. Gemmiti CV, Guldberg RE. Fluid flow increases type II collagen deposition and tensile mechanical properties in bioreactor-grown tissue-engineered cartilage. Tissue Engineering 2006;12(3):469-479.
241. Asanbaeva A, Masuda K, Thonar EJMA, Klisch SM, Sah RL. Mechanisms of cartilage growth - Modulation of balance between proteoglycan and collagen in vitro using chondroitinase ABC. Arthritis and Rheumatism 2007;56(1):188-198.
242. Byers S, vanRooden JC, Foster BK. Structural changes in the large proteoglycan, aggrecan, in different zones of the ovine growth plate. Calcified Tissue International 1997;60(1):71-78.
243. Cancedda R, Cancedda FD, Castagnola P. Chondrocyte differentiation. Int Rev Citol 1995;159:265-358.
244. Minina E, Wenzel HM, Kreschel C, Karp S, Gaffield W, McMahon AP, Vortkamp A. BMP and Ihh/PTHrP signaling interact to coordinate chondrocyte proliferation and differentiation. Development 2001;128(22):4523-4534.
245. Grimsrud CD, Romano PR, D'Souza M, Puzas JE, Reynolds PR, Rosier RN, O'Keefe RJ. BMP-6 is an autocrine stimulator of chondrocyte differentiation. Journal of Bone and Mineral Research 1999;14(4):475-482.
246. St-Jacques B, Hammerschmidt M, McMahon AP. Indian hedgehog signaling regulates proliferation and differentiation of chondrocytes and is essential for bone formation (vol 13, pg 2072, 1999). Genes & Development 1999;13(19):2617-2617.
247. Minina E, Kreschel C, Naski MC, Ornitz DM, Vortkamp A. Interaction of FGF, lhh/Pthlh, and BMP signaling integrates chondrocyte proliferation and hypertrophic differentiation. Developmental Cell 2002;3(3):439-449.
248. Shingleton WD, Jones D, Xu X, Cawston TE, Rowan AD. Retinoic acid and oncostatin M combine to promote cartilage degradation via matrix metalloproteinase-13 expression in bovine but not human chondrocytes. Rheumatology 2006;45(8):958-965.
249. Kember NF, Walker KVR. Control of Bone Growth in Rats. Nature 1971;229(5284):428-&.
250. Anderson HC, Sajdera SW. Fine Structure of Bovine Nasal Cartilage - Extraction as a Technique to Study Proteoglycans and Collagen in Cartilage Matrix. Journal of Cell Biology 1971;49(3):650-&.
251. Miller EJ, Matukas VJ. Chick Cartilage Collagen . A New Type of Alpha1 Chain Not Present in Bone or Skin of Species. Proceedings of the National Academy of Sciences of the United States of America 1969;64(4):1264-&.
252. Lee JE, Kim KE, Kwon IC, Ahn HJ, Lee SH, Cho HC, Kim HJ, Seong SC, Lee MC. Effects of the controlled-released TGF-beta 1 from chitosan microspheres on chondrocytes cultured in a collagen/chitosan/glycosaminoglycan scaffold. Biomaterials 2004;25(18):4163-4173.
253. Tschan T, Bohme K, Conscienceegli M, Zenke G, Winterhalter KH, Bruckner P. Autocrine or Paracrine Transforming Growth-Factor-Beta Modulates the Phenotype of Chick-Embryo Sternal Chondrocytes in Serum-Free Agarose Culture. Journal of Biological Chemistry 1993;268(7):5156-5161.
254. Kato Y, Iwamoto M. Fibroblast Growth-Factor Is an Inhibitor of Chondrocyte Terminal Differentiation. Journal of Biological Chemistry 1990;265(10):5903-5909.

255. Bohme K, Winterhalter KH, Bruckner P. Terminal Differentiation of Chondrocytes in Culture Is a Spontaneous Process and Is Arrested by Transforming Growth-Factor-Beta-2 and Basic Fibroblast Growth-Factor in Synergy. Experimental Cell Research 1995;216(1):191-198.
256. Alvarez J, Sohn P, Zeng X, Doetschman T, Robbins DJ, Serra R. TGF beta 2 mediates the effects of Hedgehog on hypertrophic differentiation and PTHrP expression. Development 2002;129(8):1913-1924.
257. Medill NJ, Praul CA, Ford BC, Leach RM. Parathyroid hormone-related peptide expression in the epiphyseal growth plate of the juvenile chicken: Evidence for the origin of the parathyroid hormone-related peptide found in the epiphyseal growth plate. Journal of Cellular Biochemistry 2001;80(4):504-511.
258. Long FX, Linsenmayer TF. Regulation of growth region cartilage proliferation and differentiation by perichondrium. Development 1998;125(6):1067-1073.
259. Vortkamp A, Lee K, Lanske B, Segre GV, Kronenberg HM, Tabin CJ. Regulation of rate of cartilage differentiation by Indian hedgehog and PTH-related protein. Science 1996;273(5275):613-622.
260. Volk SW, Leboy PS. Regulating the regulators of chondrocyte hypertrophy. Journal of Bone and Mineral Research 1999;14(4):483-486.
261. Lee K, Lanske B, Karaplis AC, Deeds JD, Kohno H, Nissenson RA, Kronenberg HM, Segre GV. Parathyroid hormone-related peptide delays terminal differentiation of chondrocytes during endochondral bone development. Endocrinology 1996;137(11):5109-5118.
262. Brouwers JEM, van Donkelaar CC, Sengers BG, Huiskes R. Can the growth factors PTHrP, Ihh and VEGF, together regulate the development of a long bone? Journal of Biomechanics 2006;39(15):2774-2782.
263. Serra R, Karaplis A, Sohn P. Parathyroid hormone-related peptide (PTHrP)-dependent and -independent effects of transforming growth factor beta (TGF-beta) on endochondral bone formation. Journal of Cell Biology 1999;145(4):783-794.
264. Alvarez J, Horton J, Sohn P, Serra R. The perichondrium plays an important role in mediating the effects of TGF-beta 1 on endochondral bone formation. Developmental Dynamics 2001;221(3):311-321.
265. Ferguson CM, Schwarz EM, Reynolds PR, Puzas JE, Rosier RN, O'Keefe RJ. Smad2 and 3 mediate transforming growth factor-beta 1-induced inhibition of chondrocyte maturation. Endocrinology 2000;141(12):4728-4735.
266. Pateder DB, Ferguson CM, Ionescu AM, Schwarz EM, Rosier RN, Puzas JE, O'Keefe RJ. PTHrP expression in chick sternal chondrocytes is regulated by TGF-beta through Smad-mediated signaling. J Cell Physiol 2001;188(3):343-51.
267. Buckwalter JA, Mower D, Ungar R, Schaeffer J, Ginsberg B. Morphometric Analysis of Chondrocyte Hypertrophy. Journal of Bone and Joint Surgery-American Volume 1986;68A(2):243-255.
268. Schmid TM, Linsenmayer TF. Immunohistochemical Localization of Short Chain Cartilage Collagen (Type-X) in Avian-Tissues. Journal of Cell Biology 1985;100(2):598-605.
269. Gerstenfeld LC, Landis WJ. Gene-Expression and Extracellular-Matrix Ultrastructure of a Mineralizing Chondrocyte Cell-Culture System. Journal of Cell Biology 1991;112(3):501-513.
270. Ishikawa Y, Valhmu WB, Wuthier RE. Induction of Alkaline-Phosphatase in Primary Cultures of Epiphyseal Growth Plate Chondrocytes by a Serum-Derived Factor. Journal of Cellular Physiology

1987;133(2):344-350.

271. Magnusson P, Larsson L, Magnusson M, Davie MWJ, Sharp CA. Isoforms of bone alkaline phosphatase: Comparison between HPLC and two immunoassays in patients with severe renal insufficiency. Journal of Bone and Mineral Research 1999;14:S422-S422.
272. Whyte MP. Hypophosphatasia and the role of alkaline phosphatase in skeletal mineralization. Endocr Rev 1994;15(4):439-61.
273. Narisawa S, Frohlander N, Millan JL. Inactivation of two mouse alkaline phosphatase genes and establishment of a model of infantile hypophosphatasia. Developmental Dynamics 1997;208(3):432-446.
274. Hamade E, Azzar G, Radisson J, Buchet R, Roux B. Chick embryo anchored alkaline phosphatase and mineralization process in vitro - Influence of Ca2+ and nature of substrates. European Journal of Biochemistry 2003;270(9):2082-2090.
275. Robison R. The Possible Significance of Hexosephosphoric Esters in Ossification (Reprinted from Biochem J, Vol 17, Pg 286, 1923). Clinical Orthopaedics and Related Research 1991(267):2-7.
276. Kirsch T, Harrison G, Golub EE, Nah HD. The roles of annexins and types II and X collagen in matrix vesicle-mediated mineralization of growth plate cartilage. Journal of Biological Chemistry 2000;275(45):35577-35583.
277. Kansiz M, Heraud P, Wood B, Burden F, Beardall J, McNaughton D. Fourier Transform Infrared microspectroscopy and chemometrics as a tool for the discrimination of cyanobacterial strains. Phytochemistry 1999;52(3):407-417.
278. Gress CJ, Jacenko O. Growth plate compressions and altered hematopoiesis in collagen X null mice. Journal of Cell Biology 2000;149(4):983-993.
279. Anderson HC. Vesicles Associated with Calcification in Matrix of Epiphyseal Cartilage. Journal of Cell Biology 1969;41(1):59-&.
280. Anderson HC. Molecular-Biology of Matrix Vesicles. Clin Orthop Relat Res 1995;314:266-280.
281. Garimella R, Bi XH, Camacho N, Sipe JB, Anderson HC. Primary culture of rat growth plate chondrocytes: an in vitro model of growth plate histotype, matrix vesicle biogenesis and mineralization. Bone 2004;34(6):961-970.
282. Matsuzaw T, Anderson HC. Phosphatases of Epiphyseal Cartilage Studied by Electron Microscopic Cyctochemical Methods. Journal of Histochemistry & Cytochemistry 1971;19(12):801-&.
283. Genge BR, Sauer GR, Wu LNY, Mclean FM, Wuthier RE. Correlation between Loss of Alkaline-Phosphatase Activity and Accumulation of Calcium during Matrix Vesicle-Mediated Mineralization. Journal of Biological Chemistry 1988;263(34):18513-18519.
284. Wu LNY, Yoshimori T, Genge BR, Sauer GR, Kirsch T, Ishikawa Y, Wuthier RE. Characterization of the Nucleational Core Complex Responsible for Mineral Induction by Growth-Plate Cartilage Matrix Vesicles. Journal of Biological Chemistry 1993;268(33):25084-25094.
285. Kirsch T, Nah HD, Shapiro IM, Pacifici M. Regulated production of mineralization-competent matrix vesicles in hypertrophic chondrocytes. Journal of Cell Biology 1997;137(5):1149-1160.
286. Genge BR, Wu LNY, Wuthier RE. Identification of Phospholipid-Dependent Calcium-Binding Proteins as Constituents of Matrix Vesicles. Journal of Biological Chemistry 1989;264(18):10917-10921.
287. Arispe N, Rojas E, Genge BR, Wu LNY, Wuthier RE. Similarity in calcium channel activity of annexin V

and matrix vesicles in planar lipid bilayers. Biophysical Journal 1996;71(4):1764-1775.

288. Kirsch T, Nah HD, Demuth DR, Harrison G, Golub EE, Adams SL, Pacifici M. Annexin V-mediated calcium flux across membranes is dependent on the lipid composition: Implications for cartilage mineralization. Biochemistry 1997;36(11):3359-3367.
289. Dean DD, Schwartz ZVI, Muniz OE, Gomez R, Swain LD, Howell DS, Boyan BD. Matrix Vesicles Contain Metalloproteinases That Degrade Proteoglycans. Bone and Mineral 1992;17(2):172-176.
290. Boskey AL, Boyan BD, Schwartz Z. Matrix vesicles promote mineralization in a gelatin gel. Calcified Tissue International 1997;60(3):309-315.
291. Schipani E, Ryan HE, Didrickson S, Kobayashi T, Knight M, Johnson RS. Hypoxia in cartilage: HIF-1 alpha is essential for chondrocyte growth arrest and survival. Genes & Development 2001;15(21):2865-2876.
292. Pfander D, Cramer T, Schipani E, Johnson RS. HIF-1alpha controls extracellular matrix synthesis by epiphyseal chondrocytes. J Cell Sci 2003;116(Pt 9):1819-26.
293. Ferrara N. Role of vascular endothelial growth factor in the regulation of angiogenesis. Kidney International 1999;56(3):794-814.
294. Nakagawa M, Kaneda T, Arakawa T, Morita S, Sato T, Yomada T, Hanada K, Kumegawa M, Hakeda Y. Vascular endothelial growth factor (VEGF) directly enhances osteoclastic bone resorption and survival of mature osteoclasts. FEBS Lett 2000;473(2):161-4.
295. Gerber HP, Hillan KJ, Ryan AM, Kowalski J, Keller GA, Rangell L, Wright BD, Radtke F, Aguet M, Ferrara N. VEGF is required for growth and survival in neonatal mice. Development 1999;126(6):1149-1159.
296. Garcia-Ramirez M, Toran N, Andaluz P, Carrascosa A, Audi L. Vascular endothelial growth factor is expressed in human fetal growth cartilage. Journal of Bone and Mineral Research 2000;15(3):534-540.
297. Gerber HP, Vu TH, Ryan AM, Kowalski J, Werb Z, Ferrara N. VEGF couples hypertrophic cartilage remodeling, ossification and angiogenesis during endochondral bone formation. Nat Med 1999;5(6):623-8.
298. Green DR. Apoptotic Pathways: The Roads to Ruin. Cell 1998;94(18):695-698.
299. Vaux DL, Korsmeyer SJ. Cell Death in Development. Cell 1999;96(22):245-254.
300. Fraser A, Evan G. A License to Kill. Cell 1996;85(14):781-784.
301. Salvesen GS, Dixit VM. Caspases: Intracellular Signaling by Proteolysis. Cell 1997;91(14):443-446.
302. Cohen GM. Caspases: the executioners of apoptosis. Biochemical Journal 1997;326:1-16.
303. Gibson G. Active role of chondrocyte apoptosis in endochondral ossification. Microscopy Research and Technique 1998;43(2):191-204.
304. Gentili C, Bianco P, Neri M, Malpeli M, Campanile G, Castagnola P, Cancedda R, Cancedda FD. Cell-Proliferation, Extracellular-Matrix Mineralization, and Ovotransferrin Transient Expression during in-Vitro Differentiation of Chick Hypertrophic Chondrocytes into Osteoblast-Like Cells. Journal of Cell Biology 1993;122(3):703-712.
305. Gerstenfeld LC, Shapiro FD. Expression of bone-specific genes by hypertrophic chondrocytes: Implications of the complex functions of the hypertrophic chondrocyte during endochondral bone development. Journal of Cellular Biochemistry 1996;62(1):1-9.

306. Yamada S, Heymann D, Bouler JM, Daculsi G. Osteoclastic resorption of biphasic calcium phosphate ceramic in vitro. J Biomed Mater Res 1997;37(3):346-52.

307. Wang Y, Toury R, Hauchecorne M, Balmain N. Expression of Bcl-2 protein in the epiphyseal plate cartilage and trabecular bone of growing rats. Histochemistry and Cell Biology 1997;108(1):45-55.

308. Mansfield K, Rajpurohit R, Shapiro IM. Extracellular phosphate ions cause apoptosis of terminally differentiated epiphyseal chondrocytes. Journal of Cellular Physiology 1999;179(3):276-286.

309. Pourmand EP, Binderman I, Doty SB, Kudryashov V, Boskey AL. Chondrocyte Apoptosis Is Not Essential for Cartilage Calcification: Evidence From an In Vitro Avian Model. J Cell Biochem 2007;100:43-57

310. Iwamoto M, Kitagaki J, Tamamura Y, Gentili C, Koyama E, Enomoto H, Komori T, Pacifici M, Enomoto-Iwamoto M. Runx2 expression and action in chondrocytes are regulated by retinoid signaling and parathyroid hormone-related peptide (PTHrP). Osteoarthritis and Cartilage 2003;11(1):6-15.

311. Komori T, Kishimoto T. Cbfa1 in bone development. Current Opinion in Genetics & Development 1998;8(4):494-499.

312. Ducy P, Karsenty G. Genetic control of cell differentiation in the skeleton. Current Opinion in Cell Biology 1998;10(5):614-619.

313. Enomoto H, Enomoto-Iwamoto M, Iwamoto M, Nomura S, Himeno M, Kitamura Y, Kishimoto T, Komori T. Cbfa1 is a positive regulatory factor in chondrocyte maturation. Journal of Biological Chemistry 2000;275(12):8695-8702.

314. Ueta C, Iwamoto M, Kanatani N, Yoshida C, Liu Y, Enomoto-Iwamoto M, Ohmori T, Enomoto H, Nakata K, Takada K and others. Skeletal malformations caused by overexpression of Cbfa1 or its dominant negative form in chondrocytes. Journal of Cell Biology 2001;153(1):87-99.

315. Enomoto-Iwamoto M, Enomoto H, Komori T, Iwamoto M. Participation of Cbfa1 in regulation of chondrocyte maturation. Osteoarthritis and Cartilage 2001;9:S76-S84.

Chapter II

Morphology and mechanical properties of injectable ceramic microspheres

S. M. Oliveira[1,2,3], C. C. Barrias[2], C. C. Ribeiro[2,4], I. F. Almeida[5], M. F. Bahia[5], M.A. Barbosa[2,3]

[1]ESTV – Escola Superior de Tecnologia de Viseu, Dep. de Eng. Mecânica e Gestão Industrial, Campus Politécnico de Repeses, 3504-510 Viseu, Portugal;

[2]INEB – Instituto de Engenharia Biomédica, Divisão de Biomateriais, Rua do Campo Alegre 823, Porto, Portugal;

[3]FEUP – Faculdade de Engenharia da Universidade do Porto, Departamento de Engenharia Metalúrgica e de Materiais, Rua Roberto Frias, 4200-465 Porto, Portugal;

[4]ISEP – Instituto Politécnico do Porto, Departamento de Física, Rua Dr. António Bernardino de Almeida 431, 4200-465 Porto, Portugal;

[5]FFUP – Faculdade de Farmácia da Universidade do Porto, Departamento de Tecnologia Farmacêutica, Rua Aníbal Cunha 164, 4050-047 Porto, Portugal.

ABSTRACT

The aim of this study was to analyze the effect of starting powder granulometry and sintering conditions on the morphological structure and mechanical properties of injectable hydroxyapaptite (HAp) microspheres. The mechanical properties of the microspheres were evaluated to investigate if their integrity could be maintained during the injection process. To obtain microspheres, HAp powders were dispersed in a sodium alginate solution and spherical particles were prepared by droplet extrusion under a co-axial air stream, coupled with ionotropic gelation in the presence of Ca^{2+}. This was followed by a sintering process at various temperatures and times. The morphology of microspheres was observed under SEM, diameter measurements were performed in an optical microscope and the compression strength was evaluated using a texture analyzer. Finally, microspheres prepared using lower granulometry HAp powders and sintered at 1200 ºC for 1 hour presented the best properties and were selected as the most suitable for the envisaged application.

Keywords: Injectability, hydroxyapatite, microspheres.

INTRODUCTION

Minimal invasive surgical procedures are becoming the first choice therapy for their lower risk of infection and lower recovery time. In orthopaedics, the injectability of materials into bone cavities is common practice (vertebroplasty) but, in our perspective, many improvements can still be done. Therefore the search for new materials has to continue in order to reach the suitable requirements. Our group has been working in the development of injectable materials to be used as bone-fillers.[1-3] The preparation and characterization of ceramic microparticles of spherical-shape and uniform size have been previously described, and *in vitro* studies revealed that they can be used as supports for culturing osteoblastic-like and mesenchymal stem cells, suggesting their applicability as cell microcarriers for bone regeneration applications.[1,2,4] In this study, the granulometry of the starting ceramic powders and sintering conditions were varied to enable the preparation of microspheres with different porous sizes and surface textures, increasing the range of possible applications of the system. For example, higher and interconnected porosity may allow cell migration into the microspheres, as well as facilitate nutrient and metabolite exchange. Moreover, larger particles are also expected to result in an increased surface roughness, which may improve cell attachment and osteogenic differentiation.[5] On the other hand, an increase in porosity may negatively affect the mechanical properties of the microspheres, which is not desirable since their integrity must be maintained during the injection process. Taking all this into consideration, different HAp microspheres were prepared and characterized in terms of morphological structure (dimension, sphericity and surface texture) and mechanical properties (compression strength).

MATERIALS AND METHODS

As starting materials to prepare the microspheres, HAp and Na-alginate were used. HAp powders – Captal s (Cs), Captal 20 (C20) and Captal 30 (C30) of different granulometric size distributions and Na-alginate (Protanal LF 10/60) with a high α-L-guluronic acid content (65–75%, as specified by the manufacturer) were kindly supplied by Plasma Biotal Ltd (Buxton, UK) and Pronova BioPharma (Lysaker, Norway) respectively.

Characterization of HAp particles distribution was performed on laser diffraction particle size analyzer (Coulter Electronics, Villepinte, France) and microspheres were prepared as

previously described[2]. Briefly, HAp powder was mixed with Na-alginate solution 3% (w/v) at a ratio of 0.2 (w/w) and homogenised. The paste was extruded drop-wise into a 0.1 M $CaCl_2$ crosslinking solution, where spherical-shaped microspheres instantaneously formed and were allowed to harden for 30 min. The microspheres size was controlled by regulating the extrusion flow rate using a syringe pump (Cole-Parmer), and by applying a coaxial air flow (Encapsulation Unit Var J1–Nisco). At completion of the gelling period, microspheres were recovered and rinsed in water in order to remove the excess of solution. Finally, they were dried overnight in a vacuum-oven at 30 ºC, and then sintered at 1100 ºC, 1200 ºC, 1300 ºC for 1 hour and at 1300 ºC for 6 hours using a uniform heating rate of 5 ºC/min.

For morphological characterization, HAp particles and microspheres were sputter coated with gold using JEOL JFC-100 (Croissy-sur-Seine, France) fine coat ion sputter device and observed under a JEOL JSM-6301F scanning electron microscopy (SEM). Microspheres diameter was measured using an optical microscope Olympus equipped with an ocular micrometer with an accuracy of 10 μm. The average diameter of n=20 microspheres was calculated and the experiment was repeated at least three times. Microspheres compression strength was evaluated in a Texture Analyzer TA-XT2i (*Stable Micro Systems Ltd,* Godalming, UK). The load was applied vertically, to individual microspheres, using a cylindrical metallic probe with a diameter of 2 mm. In each experiment 10 microspheres were assayed and the average from at least three experiments was calculated. Compression strength was calculated from the maximum force reached (breaking point).

RESULTS AND DISCUSSION

In this work, HAp powders with different granulometries were used to produce injectable microspheres. Those were prepared using a previously reported methodology that has the advantage of allowing the preparation of spherical-shaped particles with an adequate and uniform size.[2] In what concerns the granulometry of the HAp powders, the Cs batch was characterized by particles with an average diameter of 5.1±0.3 μm, while for C20 and C30 the average diameter were 22.6±1.5 μm and 38.9±2.4 μm respectively. Size distribution curves and SEM pictures of the particles are presented in Figure 1.

After sintering, microspheres surface roughness and pores size were very different, depending on the particles used as can be observed in Figure 2. Microspheres prepared from Cs (Figure 2A) exhibited the smoothest surface whereas microspheres prepared using C30 (Figure 2C)

particles presented a more irregular surface and bigger pores (around 20 μm) between particles.

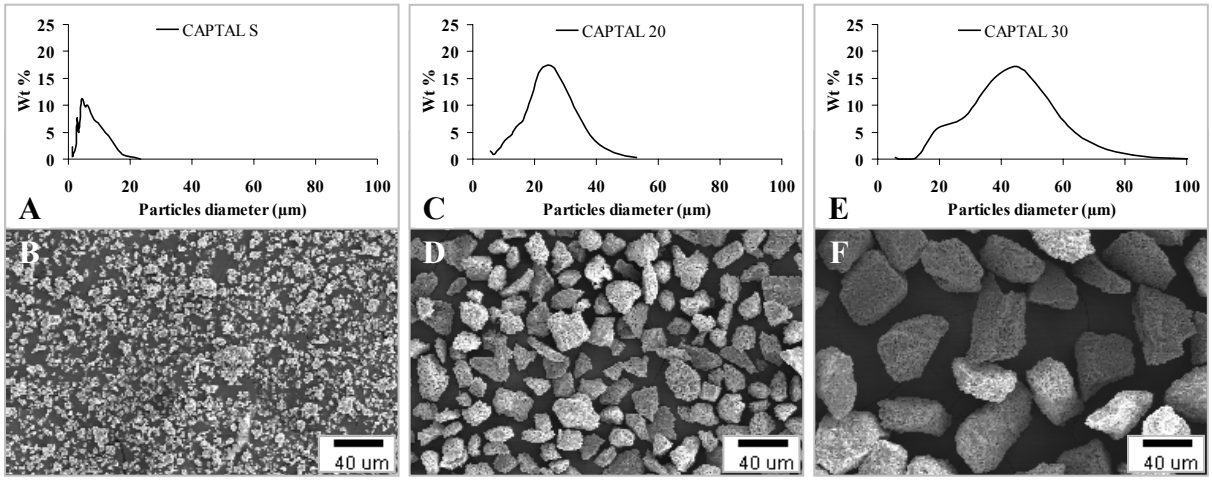

Figure 1. Size distribution of HAp particles and their SEM images. Pictures A, C and E show the granulometric size distribution of Cs, C20 and C30 particles respectively. Pictures B, D and F show the SEM photomicrographs of Cs, C20 and C30 particles, respectively.

The shape was also slightly affected by the particle size, with larger particles resulting in less spherical microspheres. However, a spherical shape is desirable in order to increase the injectability yield since that is the shape used as model for fluid transportation studies, and it is known as the easiest way to carry high concentration of solid particles using a fluid vehicle.[6]

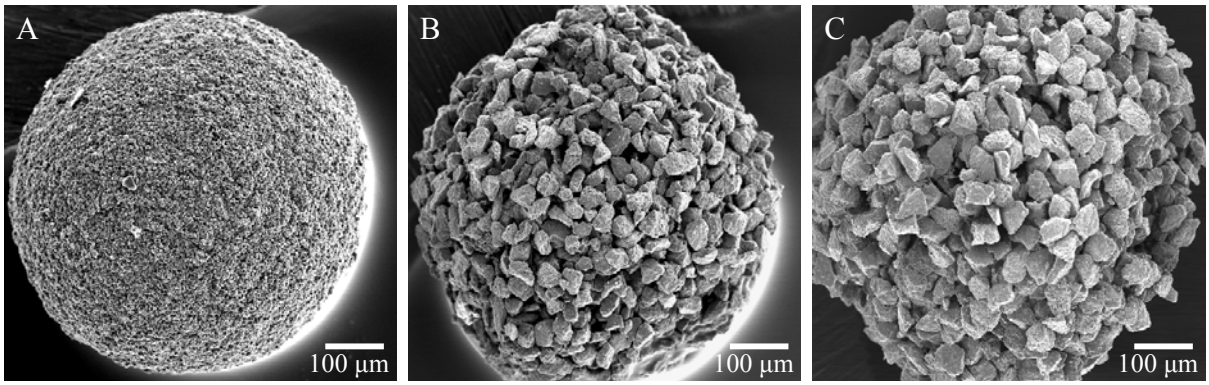

Figure 2. The SEM images of microspheres. Photomicrograph A corresponds to a microsphere prepared using Cs particles and microspheres showed in photomicrographs B and C were prepared using C20 and C30 particles respectively.

The microspheres size is also an important factor to take into consideration. The literature shows that microspheres with diameters around 500 μm are considered injectable.[7]

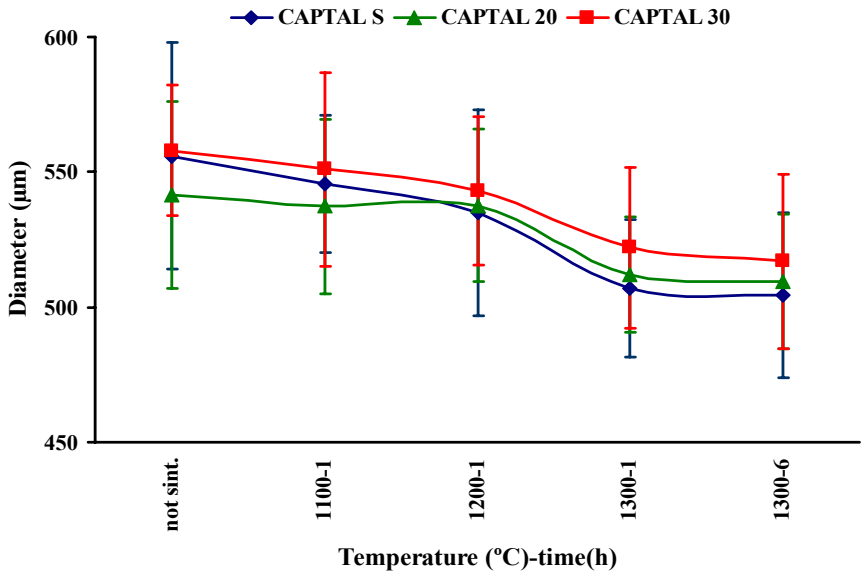

Figure 3. Microspheres' diameter change with sintering temperatures. Microspheres prepared from C30 particles show a bigger diameter than microspheres prepared using Cs or C20 particles. An increase of sintering temperature corresponds to a decrease of microspheres diameter.

Microspheres prepared with C30 particles have a diameter higher than those prepared using Cs or C20. However, all obtained microspheres during this study fall in the range 500 to 600 µm which correspond to the values found in literature. Figure 3 shows the diameters of microspheres versus sintering temperature. As expected, not sintered (not sint.) microspheres are the largest ones. After sintering, microspheres diameter decreases due to the alginate burning and to the compactation (decrease of porosity/volume) commonly associated with the sintering process. Thus, microspheres diameter is not only a function of the type of particles used, but also a function of the sintering temperature. A narrow size distribution of microspheres sizes was obtained for all the formulations. This is an important aspect since a uniform size is expected to create homogeneous spaces between microspheres when packed at the bone cavity whereas a wide size distribution or a bimodal size distribution will create smaller spaces.

During the injection process microspheres integrity must be maintained. However, if microspheres compression strength is lower than the tension used to extrude the injectable material, they will most probably break down. The rupture forces of the microspheres prepared in this study are presented in Figure 4. Those forces can be as higher as 4.30±0.31 N and as lower as 0.07±0.01 N, depending on the state of the microspheres (sintered or not) and also on the type of HAp particles used. After sintering at 1100 ºC, all microspheres presented

low rupture strength. Moreover, the strength of microspheres prepared from C20 or C30 particles could not be measured since the force necessary to break them was out of the range of the texture analyzer used. The rupture force increased along with the sintering temperature. A force as high as 3.79±0.76 N was needed to break microspheres prepared from Cs after sintered at 1300 ºC for 6 hours.

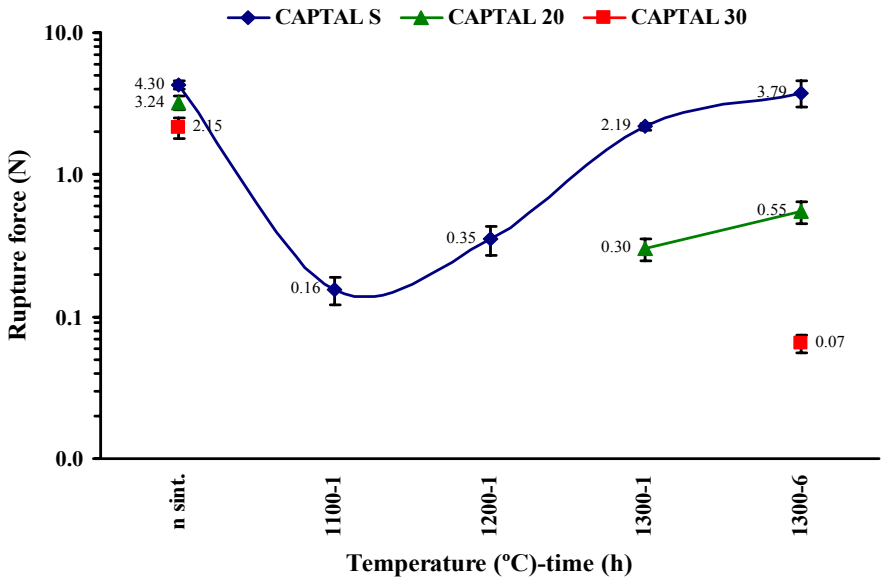

Figure 4. Rupture force of microspheres prepared using different sintering temperatures. Microspheres' strength increases with sintering temperature. Rupture force of microspheres prepared using C20 and C30 particles could not be measured for sintering temperatures below 1300 ºC.

That increase of rupture force resulted from the establishment of bridges (known as "necks") among the HAp particles during the sintering process. According to the literature, during an injectable procedure the force reached on an area similar to the equatorial area of our microspheres is below 0.30 N.[8,9] Therefore microspheres prepared using Cs particles and sintered at temperatures equal or superior to 1200 ºC as well as microspheres prepared using C20 particles and sintered at 1300ºC had enough strength to be injected. However, the injection process will probably be facilitated when using the microspheres with the smoothness surface.

CONCLUSIONS

The use of HAp powders with different granulometries enabled the preparation of

microspheres with different morphological structures and mechanical properties. Microspheres prepared using HAp powders with higher granulometry needed higher sintering temperature to achieve enough compression strength, and presented a more irregular surface. Microspheres prepared using HAp powders with the lower granulometry presented a homogeneous size distribution (around 500 μm) and its strength was 0.35 N after sintering at 1200 ºC for 1 hour which make them the most suitable microspheres to use in our approach.

ACKNOWLEDGEMENTS

SM Oliveira is grateful to the Program for Education Development in Portugal III (PRODEP III) for supporting his salary at Escola Superior de Tecnologia de Viseu, Portugal. This work was supported by Foundation for Science and Technology (FCT) under contract POCTI/FCB/41523/2001.

REFERENCES

1. Barrias CC, Ribeiro CC, Lamghari M, Miranda CS, Barbosa MA. Proliferation, activity, and osteogenic differentiation of bone marrow stromal cells cultured on calcium titanium phosphate microspheres. Journal of Biomedical Materials Research 2005;72A(1):57-66.
2. Barrias CC, Ribeiro CC, Barbosa MA. Adhesion and proliferation of human osteoblastic cells seeded on injectable hydroxyapatite microspheres. Bioceramics, Vol 16 2004;254-2:877-880.
3. Ribeiro CC, Barrias CC, Barbosa MA. Calcium phosphate-alginate microspheres as enzyme delivery matrices. Biomaterials 2004;25(18):4363-73.
4. Silva RV, Camilli JA, Bertran CA, Moreira NH. The use of hydroxyapatite and autogenous cancellous bone grafts to repair bone defects in rats. International Journal of Oral and Maxillofacial Surgery 2005;34(2):178-184.
5. Boyan BD, Lossdörfer S, Wang L, Zhao G, Lohmann CH, Cochran DL, Schwartz Z. Osteoblasts generate an osteogenic microenvironment when grown on surfaces with rough microtopographies. Eur Cell Mater 2003;6:22-27.
6. Cardoso ON, Sotto Mayor T, Pinto AMFR, Campos JBLM. Axial dispersion of particles in a slugging column--the role of the laminar wake of the bubbles. Chemical Engineering Science 2003;58(18):4159-4172.
7. Gauthier O, Bouler JM, Weiss P, Bosco J, Aguado E, Daculsi G. Short-term effects of mineral particle sizes on cellular degradation activity after implantation of injectable calcium phosphate biomaterials and the consequences for bone substitution. Bone 1999;25(2):71S-74S.
8. Xu HH, Weir MD, Burguera EF, Fraser AM. Injectable and macroporous calcium phosphate cement scaffold. Biomaterials 2006;27(24):4279-87.

9. Ginebra MP, Rilliard A, Fernandez E, Elvira C, San Roman J, Planell JA. Mechanical and rheological improvement of a calcium phosphate cement by the addition of a polymeric drug. J Biomed Mater Res 2001;57(1):113-8.

Chapter III

Optimization of polymeric solutions as vehicles for injectable hydroxyapatite microspheres

S.M. Oliveira[1,2,3], I.F. Almeida[4], P.C. Costa[4], C.C. Barrias[2], M.R. Pena Ferreira[4], M.F. Bahia[4], M.A. Barbosa[2,3]

[1]ESTV – Escola Superior de Tecnologia de Viseu, Dep. de Eng. Mecânica e Gestão Industrial, Campus Politécnico de Repeses, 3504-510 Viseu, Portugal;

[2]INEB – Instituto de Engenharia Biomédica, Divisão de biomateriais, Rua do Campo Alegre 823, 4150-180 Porto, Portugal;

[3]FEUP – Faculdade de Engenharia Universidade do Porto, Dep. de Eng. Metalúrgica e de Materiais, Rua Roberto Frias, 4200-465 Porto, Portugal;

[4]FFUP – Faculdade de Farmácia da Universidade do Porto, Departamento de Tecnologia Farmacêutica, Rua Aníbal Cunha 164, 4050-047 Porto, Portugal.

ABSTRACT

Injectable materials for bone defects fillers can be based in the combination of a vehicle and a reinforcement phase. Therefore, the properties of the vehicle should be suitable to enable the transport of that extra phase. Additionally, the use of biocompatible materials is a requirement for tissue regeneration. Thus, we intended to optimize a biocompatible vehicle able to carry hydroxyapatite microspheres into bone defects using an orthopaedic injectable device. To achieve that goal, polymers usually regarded as biocompatible were selected, namely sodium carboxymethylcellulose, hydroxypropylmethylcellulose and sodium alginate (ALG). The rheological properties of the polymeric solutions at different concentrations were assessed by viscosimetry before and after moist heat sterilization. In order to correlate rheological properties with injectability, solutions were tested using an orthopaedic device applied for minimal invasive surgeries. Among the three polymers, ALG solutions presented the most suitable properties for our goal and a non-sterile ALG 6% solution was successfully used to perform preliminary injection tests of hydroxyapatite microspheres. Sterile ALG 7.25% solution was found to closely match non-sterile ALG 6% properties and it was selected as the optimal vehicle. Finally, sterile ALG 7.25% physical stability was studied at different

temperatures over a three month period. It was observed that its rheological properties presented minor changes when stored at 25 ºC or at 4 ºC.

Keywords: Injectability, alginate, carboxymethylcellulose, hydroxypropylmethylcellulose, microspheres.

INTRODUCTION

Minimal invasive surgery has been commonly used over the past two decades since it uses smaller incisions and partial anesthesia, induces fewer complications and less post-operative pain as well as a fast patient recovery. As result, research in this particular area is being pushed forward in order to obtain further improvements.[1] Minimal invasive surgery can be used to repair some damaged areas involving the procedure itself alone (endoscopy, thorascopy and laproscopy) or the procedure associated with injection of materials to fill defects and/or to deliver drugs. When injectable materials are used, the surgical procedures will depend on factors such as the type of materials, their rheological properties, setting time, etc. If the material is a single liquid solution, the procedure becomes easier. However, when solid particles are mixed with the liquid solutions, other features should be taken into consideration, namely the shape, density, porosity, size and amount of particles to be used, since the solid phase has to be efficiently carried by the liquid solution (vehicle). Thus, rheological properties of the vehicle must be a compromise between easy manipulation (injectability) and a suitable viscosity to enable microparticles transportation. On the other hand, viscosity at different shear rates must be approximately constant since manual injection rate is difficult to control. In order to fulfill all these requirements several polymers have been tested as injectable materials. Some of them include chitosan,[2,3] Na-alginate (ALG),[4] hyaluronic acid,[5,6] hidroxypropylmethylcellulose (HPMC),[7-10] sodium carboxymethylcellulose (NaCMC),[11] poly(propylene fumarate),[12,13] poly(ethylene glycol)-dimethacrylate), poly(β-caprolactone)[14], carboxylmethyl chitin,[15] polymethylmetacrylate (PMMA) and others.[16] However, the use of specific solid particles in suspension requires an optimization of the vehicles in terms of their viscosity, injectability and stability.

In this study, we were interested in selecting a suitable vehicle for injectable hydroxyapatite (HAp) microspheres developed at our laboratory.[17] The preparation and characterization of these ceramic microparticles of spherical-shape and uniform size (diameter around 500 μm)

have been previously described, and *in vitro* studies revealed that they can be used as supports for culturing osteoblastic-like cells, suggesting their applicability as cell microcarriers for bone regeneration applications[18]. However, in order to display adequate handling properties and to enable minimally invasive implantation, the microspheres must be combined with a vehicle. To accomplish our goal, we tested three polymers (ALG, HPMC and NaCMC), in terms of viscosity and injectability. Finally, ALG was selected as the most promising solution and its stability was evaluated over a three month period storage at different temperatures.

MATERIALS AND METHODS

Materials

Sodium alginate (Protanal 10/60LS) with a high α-L-guluronic acid content (65–75%, as specified by the manufacturer) was kindly donated by Pronova Biopolymers, Norway and used without further purification. Alginate solutions were freshly prepared as needed, using deionised water. HPMC (Methocel E4M Premium) was a gift from Colorcon, USA and NaCMC was purchased from Guinama, Spain. Hydroxyapatite was purchased from Plasma Biotal, Ltd., UK. All products were of pharmaceutical grade.

Preparation of the polymer solutions

Sodium alginate was dissolved in deionised water for 24 hours in order to obtain a homogeneous dispersion. The cellulose derivatives were dispersed in deionised water under mechanical agitation.

Preparation of the microspheres

Hydroxyapatite microspheres were optimized in our laboratory in order to fill all the requirements for injectability.[19,20] Briefly, a suspension of HAp particles in an ALG 3% (w/v) solution was extruded drop-wise into $CaCl_2$ solution followed by sintering at 1200 ºC for 1 hour. After sintering, spherical-shaped microparticles with a uniform size were obtained as depicted in Figure 1. The microspheres diameter and compression strength were found to be around 500 μm and 0.35 N, respectively, as described in detail previous chapter.[17]

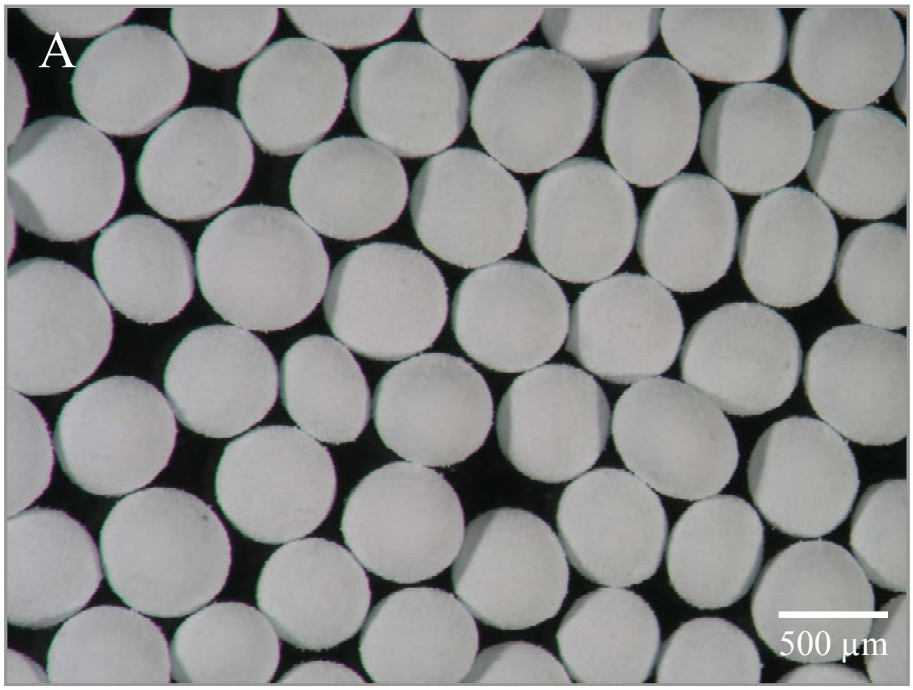

Figure 1. HAp microspheres sintered at 1200 ºC for 1 hour. The picture was obtained by optical microscope, showing the homogeneous size and sphericity of microspheres after sintering.

Evaluation of the rheological behaviour

Flow assay

The rheological behaviour was assessed by performing flow measurements at 20 ºC using a viscometer Viscotester VT550 (ThermoElectron, UK), fitted with concentric cylinder geometry (SV-DIN), between 1 and 1000 s^{-1} (unless high viscosity did not allowed it) and backwards, with a 60 s delay period between measurements. The experimental results were fitted with Power law model $\tau = k \times \dot{\gamma}^n$ and consistency, *k,* and flow index, *n,* were determined. In Power law equation τ is the shear stress and $\dot{\gamma}$ is the shear rate.[21]

Injectability (extrusion) assay

The injectability of the mixtures was evaluated using an injection device (LP2 Stainless Steel Delivery System - Biomet, Portugal) commonly used in vertebroplasty surgical procedures, which consisted of a plastic syringe (20 mm internal diameter), a cannula (2.7 mm internal diameter and 173 mm length) and a polymeric connection tube (Figure 2). The syringe was filled up with the polymeric solution and the whole device was mounted on a Texture Analyzer TA-XT2*i* (Stable Mycro Systems, UK) working in compression mode. During extrusion tests, samples were assayed in triplicate applying the force vertically and using a

plunger displacement rate of 1 mm/s. Results were expressed as the force needed to push the solution out from the cannula. Some preliminary tests using non-sterile ALG 6% (NS-ALG 6%) mixed with 20% or 40% (w/w) of microspheres were also performed.

The effects of the ALG concentration and sterilization on the mechanical properties were statistically evaluated by one-way ANOVA. Post hoc comparisons of the means of individual groups were performed using Tukey's Honestly Significant Difference test. A value of p=0.05 was taken to denote significance. Statistical analysis was performed with SPSS 15.0 for Windows software (SPSS Inc., Chicago, IL, USA).

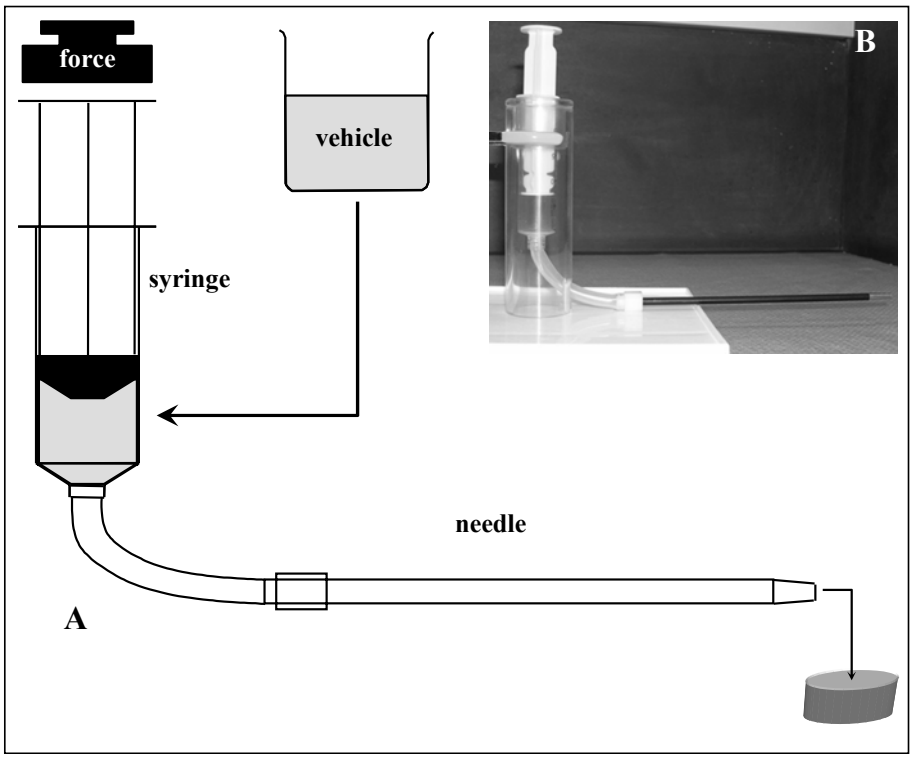

Figure 2. Injectability device. Schematic representation of the procedure and device used to evaluate the injectability of the polymers. Injectability device scheme (A) and image of the injectability device (B).

Influence of sterilization on the rheological behaviour

Sterilization was carried out in an autoclave (15 minutes at 121 ºC) and the evaluation of the mechanical properties was accessed as described previously *(injectability assay)* after a storage period of 24 hours at 20 ºC.

Influence of sterilization on alginate molecular weight

Molecular weight was characterized at room temperature by High Performance Size

Exclusion Chromatography (HP-SEC) using a modular system, composed of an isocratic pump (K-1001 Knaeur), a vacuum degasser (K-5002 Knaeur), a viscometer/right angle laser light scattering (RALLS) dual detector (T60 Viscotek), and a refractive index detector (K5002 Knaeur) operating at the same wavelength as the RALLS detector (670 nm). Separations were performed in a set of PL aquagel-OH mixed columns. The mobile phase consisted of 0.1 M $NaNO_3$ with 0.02% (w/v) NaN_3 and the flow-rate was maintained at 1.0 ml/min. Samples were dissolved in the mobile phase at 1 mg/ml, sterilised, filtered and injected through a manual injection valve equipped with a 116 μl loop.

Evaluation of the physical stability

The physical stability of the sterile ALG 7.25% (S-ALG 7.25%) solution was studied after storage for three months at 4 ºC, 25 ºC and 40 ºC. Rheological properties were assessed on three batches performing flow measurements at 20 ºC using a viscometer (Viscotester VT550, ThermoElectron, UK) fitted with concentric cylinder geometry, in the shear rate range from 1 to 500 s^{-1} and backwards, with 60 s delay period between measurements.

RESULTS AND DISCUSSION

Evaluation of the rheological behaviour

When polymeric solutions are used in injectable systems their rheological behaviour becomes one of the most important properties to be studied. In this work, the rheograms obtained showed that all polymeric solutions presented shear thinning behaviour characterized by a decrease of viscosity for an increase of shear rate (Figure 3). The parameters of the Power law model are presented in Table I. The flow index, *n*, varies from 0.140 to 0.834. The polymeric solution with higher viscosity was NaCMC 4%.

An increase in consistency, *k*, following an increase in concentration was observed in all cases. Increasing the concentration of NaCMC and HPMC solutions, the rheological behaviour showed a trend to be more shear-thinning (lower *n* values) whereas ALG solutions presented a behaviour closer to Newtonian fluid (n=1), showing a decrease in viscosity only at medium to high shear rates. This behaviour did not change with concentration as flow indexes remained approximately constant.

The polymeric solutions did not present thixotropy (represented by a hysteresis area between up and down curves) with the exception of the NaCMC solutions at higher concentrations.

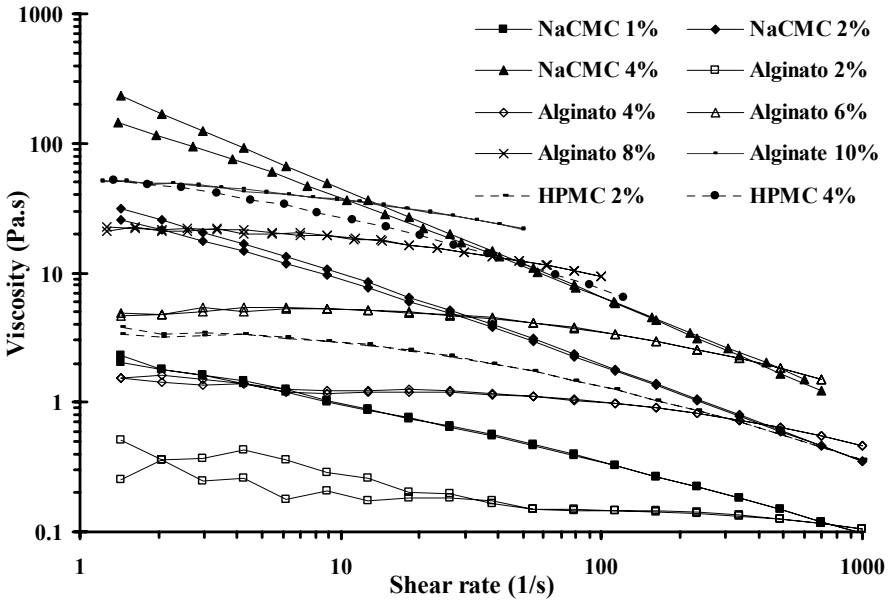

Figure 3. Rheograms of polymeric solutions at different concentrations (T=20 ºC). NaCMC solutions showed a decrease of viscosity for the whole range of shear rates tested while most of the Na-alginate solutions presented a viscosity approximately constant at shear rates below 30 s^{-1}.

Low modification of the mechanical properties after sterilization was found for cellulose derivatives solutions (Figures 4 and 5). In contrast, the ALG solutions showed a marked decrease of viscosity (Figure 6).

Table I. Parameters of the power law model.

Product	Concentration (% w/w)	K	n	R^2
NaCMC	1	1.05	0.623	0.9987
	2	51.63	0.279	0.9939
	4	337.83	0.140	0.989
HPMC	2	14.32	0.480	0.9928
	4	126.33	0.391	0.9850
ALG	2	0.34	0.834	0.999
	4	4.69	0.669	0.9964
	6	20.47	0.614	0.995
	8	37.95	0.704	0.9972
	10	74.62	0.695	0.9977

k - consistency, *n* - flow index, and R^2- R-squared value.

Injectability

In order to evaluate the injectability, polymeric solutions were extruded through a specially designed injection apparatus (Figure 2) and force versus distance values were recorded and plotted (Figure 7). The curves show the evolution of applied force during polymeric solution movement through the device.

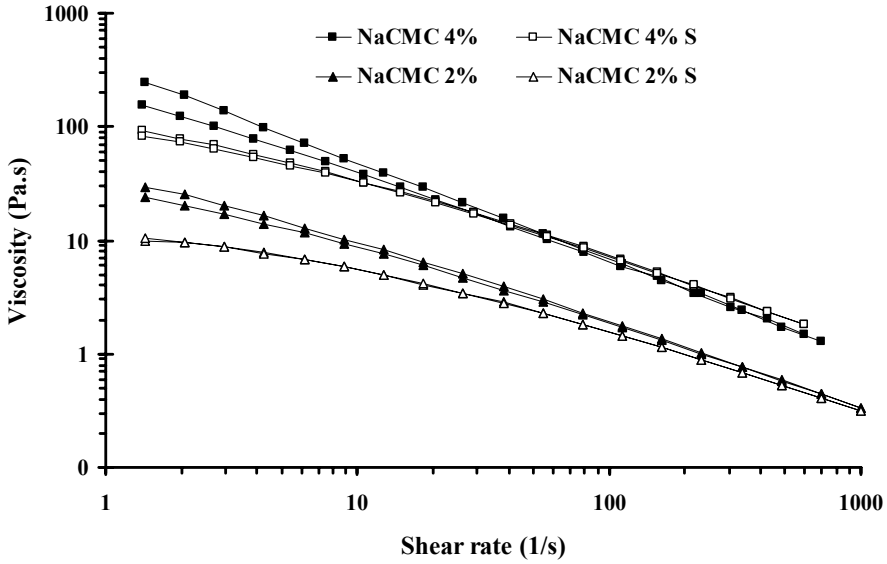

Figure 4. Effect of sterilization on NaCMC solutions viscosity. After sterilization, a decrease of 50% in NaCMC solutions viscosity was detected for low shear rates, while at high shear rates the decrease was smaller. Sterile solutions are represented by "S".

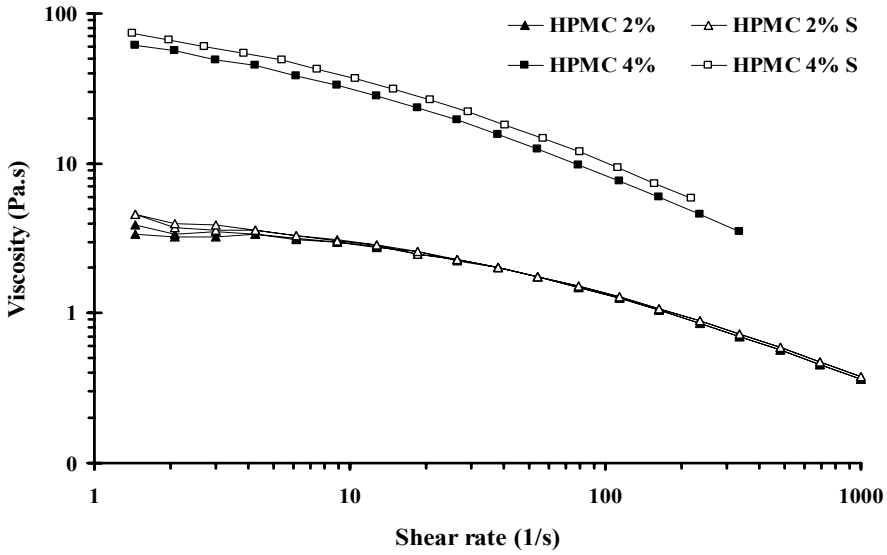

Figure 5. Effect of sterilization on HPMC solutions viscosity. HPMC solutions viscosity was almost the same before and after sterilization. Sterile solutions are represented by "S".

The evaluation of extrusion force showed that HPMC 2%, NaCMC 2% and ALG 2% solutions were able to extrude at low forces, respectively 33.3±1.4 N, 35.4±3.8 N and 16.3±0.7 N (Mean±SD). Furthermore, ALG 4% and ALG 6% solutions were not extruded at high forces (18.4±1.3 N and 34.3±0.8 N respectively) but HPMC 4% and NaCMC 4% needed around 100 N to be extruded (123.5±7.4 N and 92.7±5.6 N respectively).

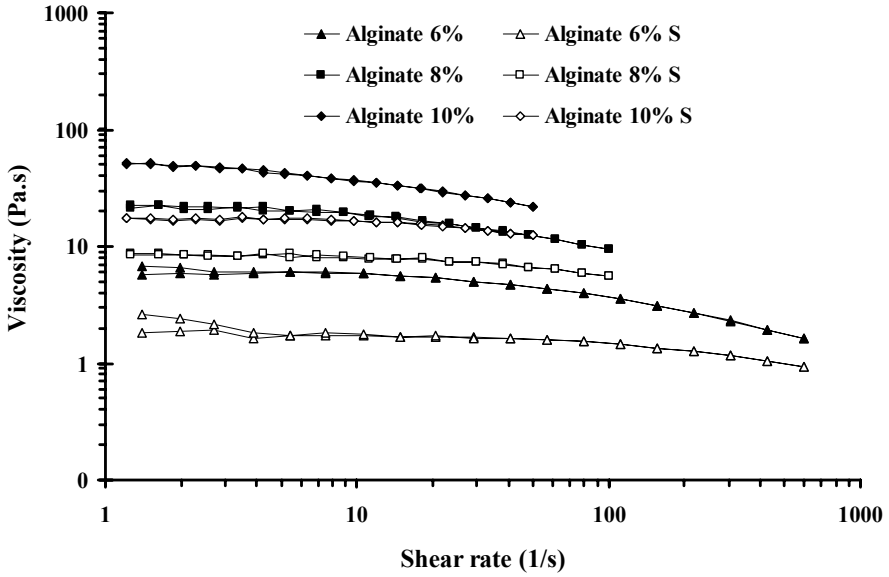

Figure 6. Effect of sterilization on Na-alginate solutions viscosity. Alginate solutions viscosity dropped sharply after sterilization. However, it is still approximately constant at low shear rates. Sterile solutions are represented by "S".

The injectability is highly dependent of viscosity as well as of the orthopedic device design as can be observed from the extrusion curves (Figure 7). Each component of the device affects the extrusion process. At the beginning, extrusion force increased in order to extrude the solution out from the syringe into the connection tube and the maximum force did not go above 20 N. As the connection tube was filled up (first plateau) the extrusion force becames approximately constant. Once solution reached the cannula, extrusion force increased again until the solution started to come out from it. Following this last slope, a second plateau was observed (constant value of extrusion force). At high viscosities (HPMC 4% and NaCMC 4%), the influence of the cannula was marked by a high increase in the extrusion force. Therefore, during a surgical procedure, the use of cannulas of smaller length and higher diameter could eventually decrease the extrusion force needed to accomplish the injection procedure.

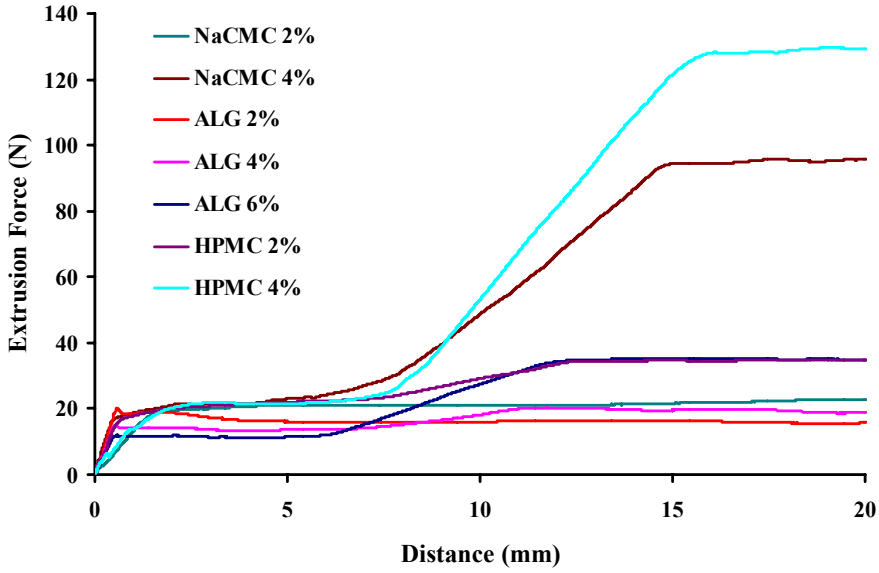

Figure 7. Curves of injectability of polymeric solutions after extrusion using the device shown in fig. 2. The curves were drawn using the values recorded during extrusion process and correspond to different polymeric solutions. The curves profile identifies the position of solutions inside of the device.

Both high and low viscosity solutions can be associated with poor injectability upon addition of a solid phase. With high viscosity a high force has to be applied to extrude a mixture, while for low viscosity solutions a phenomenon known as filtering will occur and solid particles will not be pushed through the cannula.[22] Furthermore, solutions with low viscosity may also present the disadvantage of easily leaking and potentially invading blood vessels.[23-26] On the other hand, solution's viscosity should be approximately constant at different shear rates (close to a Newtonian fluid) since injection is usually performed manually (variable injection rate). Among the studied vehicles, ALG solutions presented the closest behaviour to a Newtonian fluid (n=1) and they were easily injected using the orthopaedic device above described. Thus, NS-ALG 6% was used to perform some preliminary tests, using both 20% and 40% (w/w) of HAp microspheres (diameter of 535±35 μm). In those assays both mixtures were able to be extruded; however, the mixtures containing 40% (w/w) of microspheres were only extruded at forces of 166±40 N while mixtures prepared with 20% (w/w) of microspheres were extruded at 42±5 N. In the literature, values in the range 40 to 300 N (most accepted 100N) have been found as forces suitable to perform material injections which suggests that, in terms of rheological properties, NS-ALG 6% solution could be an appropriate solution to work as an injectable vehicle.[27-29]

Although viscosity of NS-ALG 6% proved, empirically, to be proper to keep microspheres in suspension and to accomplish several injection assays, the sterilization method decreased its viscosity and microspheres in suspension fall down. Therefore, new studies had to be performed in order to find a suitable concentration that, after sterilization, presents rheological properties similar to NS-ALG 6%.

In Figure 8 it is observed that the force to extrude sterile ALG 6% (S-ALG 6%) decrease to about 20 N (18.7±0.6) as the result of sterilization. On the other hand, both sterile ALG 8% and sterile ALG 10% needed higher force to be extruded, 47.5 ±2.6 N and 82.7±1.3 N respectively.

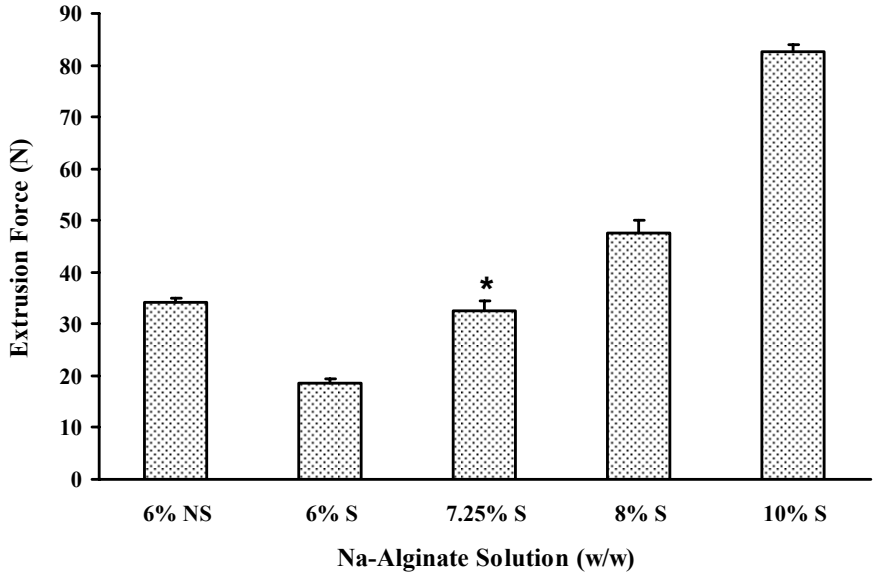

Figure 8. Extrusion force of Na-alginate solutions. Na-Alginate solutions were autoclaved at 121 ºC for 15min. "NS" represents a solution non-autoclaved and "S" represents autoclaved solutions. *Not significantly different from 6%NS.

Besides injectability, high mechanical strength of the injected mixtures was also a goal in this study. This objective can be accomplished by injecting a mixture combining the maximum possible amount of ceramic microspheres. However, the extrusion of sterile ALG 8% and sterile ALG 10% needed high extrusion forces, consequently a lower percentage of microspheres would have to be used to enable extrusion at forces below 100 N. Therefore, we focused on finding the alginate solution concentration with rheological properties similar to those of NS-ALG 6%. The approach used was based in the correspondence between extrusion forces for sterile and non-sterile ALG 6%, ALG 8% and ALG 10%. Using the regression equations (Figure 9) we calculated that S-ALG 7.25% was the appropriate solution to replace

the NS-ALG 6%. To confirm our approach, injectability tests using S-ALG 7.25% were performed and results showed that both S-ALG 7.25% and NS-ALG 6% presented similar extrusion forces (Figure 8), which was also confirmed by the rheological tests. The statistical tests showed that the ALG concentration influenced the extrusion force, and only the extrusion forces found for S-ALG 7.25% and NS-ALG 6% were not significantly different (p=0.662).

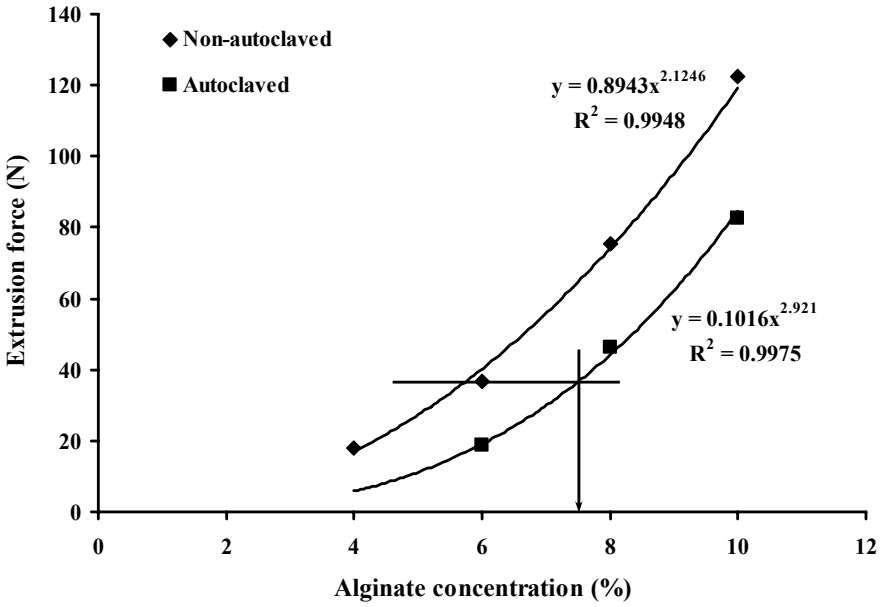

Figure 9. Extrusion forces of Na-alginate after and before sterilization. Extrusion forces were measured on both autoclaved and non-autoclaved ALG solutions. Sterile ALG concentration that matched NS-ALG 6% extrusion force was computed from the regression equations of autoclaved and non-autoclaved solutions.

Influence of sterilization on the alginate molecular weight

Upon submission to moist heat sterilization (121ºC, 15 min), a decrease in the viscosity of alginate solutions was observed, as discussed before. In order to understand this behaviour, the molecular weight of those solutions was measured and a decrease of more than 15% was observed. Before sterilization the molecular weight of alginate solutions was 85 kDa and after sterilization it has dropped to 70 kDa. This behaviour was expected since moist heat sterilization promotes polymer breakdown, resulting in the reduction of the average molecular weight and consequently altering the rheological properties of the polymer solution.[30]

Evaluation of physical stability

A marked decrease on the viscosity of polymer solutions after storage at 40 ºC was found,

while minor modifications were observed on the other test conditions (Figure 10). At this temperature, a viscosity decrease was found even 1 day after preparation (data not shown), it continued to decrease with time and after 3 months viscosity decreased more that four folds (Figure 10). In contrast, at both 4 ºC and 25 ºC only a slight decrease of viscosity was observed and no differences could be detected between 1 and 3 months.

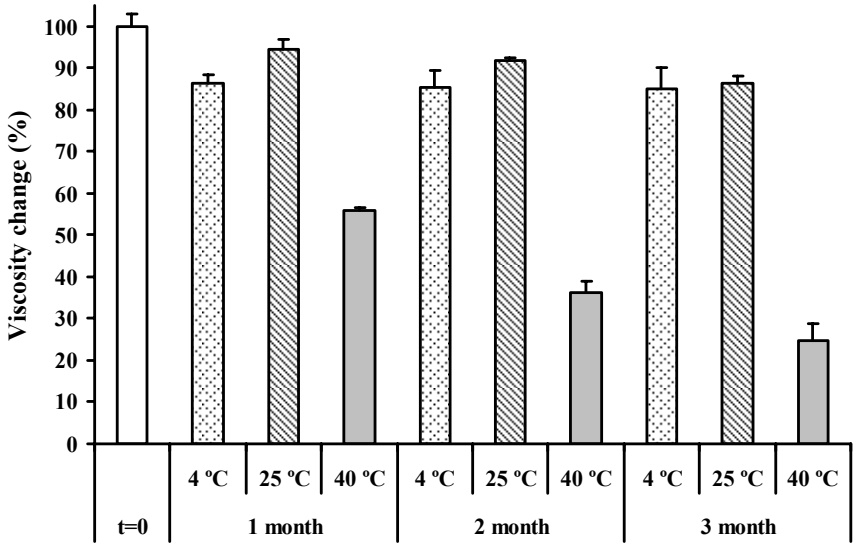

Figure 10. Influence of storage time on S-ALG 7.25% solutions viscosity. The viscosity was highly affected after stored at 40 ºC. After 1 month the viscosity decrease was notorious and continued for the 2nd and 3rd months. At both 4 ºC and 25 ºC only a slight decrease of viscosity was observed but no differences could be detected between 1 and 3 months.

Since both NS-ALG 6% and S-ALG 7.25% presented similar rheological behavior and S-ALG 7.25% was stable for a period of at least three months when stored either at 25 ºC or at 4 ºC, it was chosen as the vehicle to perform future injectability tests using different concentrations of HAp microspheres.

CONCLUSIONS

In order to use a polymeric solution as a vehicle capable of carrying solid particles, suitable rheological and chemical properties should be reached. In this investigation we were looking for a vehicle suitable to carry HAp microspheres through an orthopaedic device during an injection procedure. Among the polymeric solutions studied, sodium alginate presented the

closest behaviour to a Newtonian fluid, so it was selected as the polymer for future studies. NS-ALG 6% proved to be able to carry 40% (w/w) of HAp microspheres through an orthopaedic device. Moreover, S-ALG 7.25% presented rheological properties similar to NS-ALG 6%. For injection into a bone defect, sterility is a mandatory feature, and so S-ALG 7.25% was selected as the vehicle. Its rheological properties presented minor changes over a three months period when stored either at 25 ºC or at 4 ºC. This behaviour is considered acceptable for a pharmaceutical product of extemporaneous preparation.

ACKNOWLEDGEMENTS

SM Oliveira is grateful to the Program for Education Development in Portugal III (PRODEP III) for supporting his salary at Escola Superior de Tecnologia de Viseu, Portugal. This work was supported by Foundation for Science and Technology (FCT) under contract POCTI/FCB/41523/2001.

REFERENCES

1. Verlaan JJ, Oner FC, Dhert WJ. Anterior spinal column augmentation with injectable bone cements. Biomaterials 2006;27(3):290-301.
2. Chenite A, Chaput C, Wang D, Combes C, Buschmann MD, Hoemann CD, Leroux JC, Atkinson BL, Binette F, Selmani A. Novel injectable neutral solutions of chitosan form biodegradable gels in situ. Biomaterials 2000;21(21):2155-61.
3. Hoemann CD, Sun J, Legare A, McKee MD, Buschmann MD. Tissue engineering of cartilage using an injectable and adhesive chitosan-based cell-delivery vehicle. Osteoarthritis Cartilage 2005;13(4):318-29.
4. Balakrishnan B, Jayakrishnan A. Self-cross-linking biopolymers as injectable in situ forming biodegradable scaffolds. Biomaterials 2005;26(18):3941-3951.
5. Shu XZ, Ghosh K, Liu Y, Palumbo FS, Luo Y, Clark RA, Prestwich GD. Attachment and spreading of fibroblasts on an RGD peptide-modified injectable hyaluronan hydrogel. J Biomed Mater Res 2004;68A(2):365-75.
6. Shu XZ, Ahmad S, Liu Y, Prestwich GD. Synthesis and evaluation of injectable, in situ crosslinkable synthetic extracellular matrices for tissue engineering. J Biomed Mater Res A 2006;79(4):902-12.
7. Weiss P, Gauthier O, Bouler JM, Grimandi G, Daculsi G. Injectable bone substitute using a hydrophilic polymer. Bone 1999;25(2 Suppl):67S-70S.
8. Trojani C, Weiss P, Michiels JF, Vinatier C, Guicheux J, Daculsi G, Gaudray P, Carle GF, Rochet N. Three-dimensional culture and differentiation of human osteogenic cells in an injectable hydroxypropylmethylcellulose hydrogel. Biomaterials 2005;26(27):5509-5517.
9. Virto MR, Frutos P, Torrado S, Frutos G. Gentamicin release from modified acrylic bone cements with lactose and hydroxypropylmethylcellulose. Biomaterials 2003;24(1):79-87.

10. Bodic F, Amouriq Y, Gayet-Delacroix M, Gauthier O, Bouler J-M, Daculsi G, Hamel L. Méthode nom invasive d'evaluation d'un substitut osseux injectable / Non-invasive evaluation of an injectable bone substitute. C. R. Biologies 2002;325:1-9.
11. Andrews GP, Gorman SP, Jones DS. Rheological characterisation of primary and binary interactive bioadhesive gels composed of cellulose derivatives designed as ophthalmic viscosurgical devices. Biomaterials 2005;26(5):571-80.
12. He S, Yaszemski MJ, Yasko AW, Engel PS, Mikos AG. Injectable biodegradable polymer composites based on poly(propylene fumarate) crosslinked with poly(ethylene glycol)-dimethacrylate. Biomaterials 2000;21(23):2389-94.
13. Temenoff JS, Mikos AG. Injectable biodegradable materials for orthopedic tissue engineering. Biomaterials 2000;21(23):2405-12.
14. Iooss P, Le Ray AM, Grimandi G, Daculsi G, Merle C. A new injectable bone substitute combining poly(epsilon-caprolactone) microparticles with biphasic calcium phosphate granules. Biomaterials 2001;22(20):2785-94.
15. Uda H, Sugawara Y, Nakasu M. Experimental studies on hydroxyapatite powder-carboxymethyl chitin composite: injectable material for bone augmentation. J Plast Reconstr Aesthet Surg 2006;59(2):188-96.
16. Carrodeguas RG, Lasa BV, Del Barrio JS. Injectable acrylic bone cements for vertebroplasty with improved properties. J Biomed Mater Res B Appl Biomater 2004;68(1):94-104.
17. Oliveira SM, Barrias CC, Ribeiro CC, Almeida IF, Bahia MF, Barbosa MA. Morphology and mechanical properties of injectable ceramic microspheres. Accepted for publication in Key Engineering Materials, 2008.
18. Barrias CC, Ribeiro CC, Barbosa MA. Adhesion and proliferation of human osteoblastic cells seeded on injectable hydroxyapatite microspheres. Bioceramics, Vol 16 2004;254-2:877-880.
19. Ribeiro CC, Barrias CC, Barbosa MA. Preparation and characterisation of calcium-phosphate porous microspheres with a uniform size for biomedical applications. J Mater Sci Mater Med 2006;17(5):455-63.
20. Oliveira SM, Barrias CC, Almeida IF, Costa PC, Ferreira MP, Bahia MF, Barbosa MA. Injectability of a bone filler system based on hydroxyapatite microspheres and a vehicle with in situ gel-forming ability. J Biomed Mater Res B Appl Biomater 2008;In Press.
21. Barnes HA, Hutton JF, Walters K. An Introduction to Rheology. Amsterdam: Elsevier Science; 1998.
22. Bohner M, Baroud G. Injectability of calcium phosphate pastes. Biomaterials 2005;26(13):1553-63.
23. Hide IG, Gangi A. Percutaneous vertebroplasty: history, technique and current perspectives. Clin Radiol 2004;59(6):461-7.
24. Lewis G. Injectable bone cements for use in vertebroplasty and kyphoplasty: State-of-the-art review. Journal of Biomedical Materials Research Part B-Applied Biomaterials 2006;76B(2):456-468.
25. Baumann A, Tauss J, Baumann G, Tomka M, Hessinger M, Tiesenhausen K. Cement embolization into the vena cava and pulmonal arteries after vertebroplasty: Interdisciplinary management. European Journal of Vascular and Endovascular Surgery 2006;31(5):558-561.
26. Mathis JM, Wong W. Percutaneous vertebroplasty: Technical considerations. Journal of Vascular and Interventional Radiology 2003;14(8):953-960.
27. Xu HH, Weir MD, Burguera EF, Fraser AM. Injectable and macroporous calcium phosphate cement

scaffold. Biomaterials 2006;27(24):4279-87.

28. Gisep A, Curtis R, Hanni M, Suhm N. Augmentation of implant purchase with bone cements: an in vitro study of injectability and dough distribution. J Biomed Mater Res B Appl Biomater 2006;77(1):114-9.
29. Krebs J, Ferguson SJ, Bohner M, Baroud G, Steffen T, Heini PF. Clinical measurements of cement injection pressure during vertebroplasty. Spine 2005;30(5):E118-22.
30. Draget KI, Skjak-Braek G, Smidsrod O. Alginate based new materials. Int J Biol Macromol 1997;21(1-2):47-55.

CHAPTER IV

Injectability of a bone filler system based on hydroxyapatite microspheres and a vehicle with *in situ* gel-forming ability

S.M. Oliveira[1,2,3], C.C. Barrias[2], I.F. Almeida[4], P.C. Costa[4], M.R. Pena Ferreira[4], M.F. Bahia[4], M.A. Barbosa[2,3]

[1]ESTV – Escola Superior de Tecnologia de Viseu, Dep. de Eng. Mecânica e Gestão Industrial, Campus Politécnico de Repeses, 3504-510 Viseu, Portugal;

[2]INEB – Instituto de Engenharia Biomédica, Divisão de biomateriais, Rua do Campo Alegre 823, 4150-180 Porto, Portugal;

[3]FEUP – Faculdade de Engenharia Universidade do Porto, Dep. de Eng. Metalúrgica e de Materiais, Rua Roberto Frias, 4200-465 Porto, Portugal;

[4]FFUP – Faculdade de Farmácia da Universidade do Porto, Departamento de Tecnologia Farmacêutica, Rua Aníbal Cunha 164, 4050-047 Porto, Portugal.

ABSTRACT

The aim of this study was to test the injectability of a bone filler system based on the combination of ceramic microspheres with a gel-like vehicle, for minimal invasive surgery. Porous hydroxyapatite microspheres with a uniform size and an average diameter of 535±38 μm were prepared, and their compression strength and friability were tested. The sodium-alginate solution with a concentration of 7.25% (w/w) was used as the vehicle. To promote its *in situ* gelation, calcium carbonate and D-gluconic-δ-lactone were added to the solution. Microspheres were mixed with the vehicle at different percentages, 20% to 40% (w/w). Gelation times in the range of 8 to 20 min were obtained, depending on the formulation. Mixtures of HAp microspheres with alginate solution at 7.25% originating a gel in 11 min present an adequate handling time to perform an injection. Their injectability was evaluated using an injection device commonly employed in vertebroplasty surgical procedures, coupled to a texturometer in compression mode. Using an extrusion rate of 0.1 mm/s, the force required to extrude any of the mixtures tested was lower than 100 N. For an extrusion rate of 1 mm/s mixtures with 40% (w/w) of microspheres were very difficult to inject. Mixtures with 35% (w/w) of microspheres presented the best compromise between injectability and

compression strength of the gelled system. MicroCT analysis revealed a homogeneous distribution of the microspheres inside the vehicle, as well as full interconnection of the intra-microspheres spaces. The compression strength for the gelled systems ranged from 80 kPa (gel itself) to 600 kPa (composite with 40% of microspheres).

Keywords: Microspheres, hydroxyapatite, ceramic, hydrogel, alginate.

INTRODUCTION

Loss of bone has been a problem, especially for women after menopause since their capacity to rebuild new bone is diminished and bone absorption is high, resulting in osteoporosis. Other identical processes, like the loss of bone in Gaucher disease (type I), which is related to the absence of the enzyme glucocerebrosidase,[1,2] can occur and hence fractures and failure of some bones takes place. Usually, those losses result in the collapse of some vertebra causing pain and, in many cases, an anatomically normal posture cannot be maintained anymore.[3] In order to relieve the pain and to strengthen osteoporotic bones surgery is frequently performed. The most common procedure consists of injecting and filling up the inside of a vertebral body with a polymer, polymethylmethacrylate (PMMA), using minimum invasion surgery such as percutaneous vertebroplasty (PVP) or kyphoplasty. These are fast procedures and allow an immediate pain relief and patient's recovery in few days.[4-6] However, some problems remain unsolved: PMMA cannot be absorbed, does not allow or induce bone regeneration, has a high setting temperature[7] and its high hardness and strength after setting is associated with new cracks in surrounding bone and fracture on adjacent vertebras.[8-11] Taking into consideration all the advantages associated with the PVP, we intend to use the same procedure to inject a different material (composite) to overcome some of the difficulties related to the use of PMMA. One of the strategies is to test the injectability of an alginate solution mixed with ceramic microspheres of a uniform size that will gelify *in situ* within a few minutes at body temperature and may be loaded with drugs and/or osteoblastic or osteoprogenitor cells to customize for specific applications. In this way, drugs could be released *in situ*, allowing the treatment of some diseases, and the cells could induce new bone formation.[1,12]

As a component of seaweed, alginate is a natural and abundant polymer which has been described by several authors as a biocompatible and biodegradable material (ultra-pure grade).[13-19] When used as a solution, alginate can easily be crosslinked *in situ* using calcium

or some other divalent positive ions.[20-22] Some of the applications where it has been used are as a vehicle for drug delivery and as a scaffold for tissue engineering, either as porous structures or modified with RGD-containing peptide sequences.[1,12,23] Among others polymers that have been studied in this work, alginate was the one that had least variation in viscosity in the range of shear rates applied in this study.

In the system described in this paper a ceramic phase has been used to reinforce the calcium alginate phase. Hydroxyapatite (HAp) is one of the ceramics that can be used as reinforcement because it has good strength and an excellent biocompatibility due to its chemical similarity with the mineral phase of hard tissues.[23,24]

The injection of ceramic materials into a bone cavity is not a new concept; however, a literature search revealed that most of the works used particles with an irregular shape, a broad size distribution and too large or too small dimensions.[25-29] Since spherical particles with narrow size distribution can create more homogeneous interparticle spaces, as well as being easier to inject, we have produced porous HAp microspheres with an average diameter of 535±38 μm (mean±SD). The injectability tests were performed using a device applied in PVP, in order to increase the similarity with surgical procedures.

MATERIALS AND METHODS

Materials

Commercial hydroxyapatite (HAp) (Captal S, Plasma Biotal) was used to produce microspheres. Granulometric analysis of the powder was performed using a laser scanner particle size analyzer (Coulter Electronics Incorporation), and a particle average diameter of 5.1±0.3 μm was found. Pharmaceutical-grade sodium alginate (Na-alginate, Protanal 10/60LS) with a high α-L-guluronic acid content (65–75%, as specified by the manufacturer) was kindly donated by Pronova Biopolymers and used without further purification. Na-alginate solutions were freshly prepared as needed, using deionised water. Calcium carbonate ($CaCO_3$) powder and D-glucono-δ-lactone (GDL) were obtained from Sigma.

Preparation and characterization of HAp microspheres

Preparation

HAp microspheres were prepared as reported previously.[1] Briefly, the HAp powder was dispersed at a ratio of 0.2 (w/w) with 3% (w/v) Na-alginate aqueous solution under gentle

stirring until a homogeneous paste was obtained. The paste was extruded drop-wise into a 0.1 M $CaCl_2$ crosslinking bath, where spherical-shaped particles were instantaneously formed and allowed to harden for 30 min. The particle size was controlled by regulating the extrusion flow rate using a syringe pump (Cole-Parmer), and by applying a coaxial air flow (Encapsulation Unit Var J1–Nisco). At completion of the gelling period the microspheres were recovered and rinsed in water in order to remove the excess of $CaCl_2$. Finally, they were dried overnight in a vacuum oven at 37 ºC, and then sintered at 1200 °C for 1 h, with a uniform heating rate of 5 °C/min from room temperature.

Morphological characterization (SEM and dimensional analysis)

Morphological characterization of the microspheres was carried out using a stereomicroscope (Olympus SZX9) and a scanning electron microscopy (SEM). For SEM, samples were sputter coated with gold using a JEOL JFC-100 fine coat ion sputter device and observed using a JEOL JSM-6301F SEM. The diameter was measured using an inverted plate microscope (Olympus) equipped with an ocular micrometer with an accuracy of 10 μm. The average diameter of n=20 microspheres was calculated and the experiment was repeated at least three times.

Physicochemical characterization (XRD, FTIR)

For Fourier transform infrared spectroscopy (FTIR) microspheres were reduced to powder and analysed as KBr pellets using a Perkin Elmer System 2000 spectrometer. For X-ray diffraction (XRD), microspheres were reduced to powder and analysed with CuKα radiation using a Rigaku PMG-VH diffractometer.

Mechanical properties (friability and compression strength)

Friability tests were performed according to a procedure described in the European Pharmacopeia (5^{th} edition) with minor modifications. Briefly, 2 g of HAp-microspheres were loaded into a drum (SOTAX/F1) operating at 25 rpm. The fall height was 150 mm and the same microspheres were used for 3 cycles of 4 min each. After each cycle, the desegregated powder was blown out and the microspheres were collected and weighted again. Friability is reported as percentage of total weigh lost.

Microsphere compression strength was evaluated in a Texture Analyzer (TA-XT2i, *Stable Micro Systems Ltd*). The load was applied vertically, to individual microspheres, using a

cylindrical metallic probe with a diameter of 2 mm. In each experiment 10 microspheres were assayed and the average from at least three experiments was calculated. Compression strength was calculated from the maximum force reached (breaking point).

Preparation and characterization of the alginate vehicle

Preparation

Preliminary studies using Na-alginate, carboxymethylcellulose and hydroxypropylmethyl cellulose solutions at different concentrations, before and after sterilization, were carried out (previous chapter). From those studies, a Na-alginate solution with a concentration of 7.25% (w/w) was chosen as the most adequate vehicle. It was obtained by dissolving Na-alginate in deionised water for 24 hours in order to obtain a homogeneous solution, and then sterilizing in an autoclave according to the standard pharmacopoeia procedure (15 min at 121 ºC).

Characterization of the molecular weight and viscosity

The molecular weigh of Na-alginate, before and after sterilization, was calculated by high performance-size exclusion chromatography (HP-SEC). The analysis was performed at room temperature using a modular system, composed of an isocratic pump (K-1001 Knaeur), a vacuum degasser (K-5002 Knaeur), a viscometer/right angle laser light scattering (RALLS) dual detector (T60 Viscotek), and a refractive index detector (K-5002 Knaeur) operating at the same wavelength as the RALLS detector (670 nm). Separations were performed in a set of PL aquagel-OH mixed columns. The mobile phase consisted of 0.1 M $NaNO_3$ with 0.02% (w/v) NaN_3 and the flow-rate was maintained at 1.0 ml/min. Samples were dissolved in the mobile phase at 1 mg/ml, filtered and injected through a manual injection valve equipped with a 116 µl loop.

The viscosity of Na-alginate solutions was assessed by performing flow measurements at 20 ºC using a viscometer (Viscotester VT550, ThermoElectron, UK), fitted with concentric cylinder geometry, between 1 and 100 s^{-1} and backwards, with a 60 s delay period between measurements. All measurements were performed in triplicate.

Gel formation

Internal gelation of the 7.25% (w/w) Na-alginate solution was promoted using a method previously described by Kuo *et al*.[30] with minor modifications. Briefly, a calcium salt with limited solubility, in this case $CaCO_3$, was mixed with the alginate solution and used as a

source of calcium ions. The release of Ca^{2+} into the solution was promoted by the generation of an acidic pH with D-glucono-δ-lactone (GDL), a slowly dissociating acid, which was also incorporated in the solution. Once released, Ca^{2+} ions can participate in the interchain ionic binding between carboxyl groups (COO^-) of guluronic acids blocks in the polymer chain, giving rise to a crosslinked gel.

To obtain a sterile gel, the $CaCO_3$ powder was previously autoclaved (15 min at 121 ºC), while GDL aqueous solutions were filtered through a 0.22 μm membrane filter and used immediately after preparation. The $CaCO_3$/GDL ratio was set at 0.5 to yield a neutral pH value.[30] All components were pre-equilibrated at room temperature (set at 20 ºC) before being mixed. An aqueous $CaCO_3$ suspension was added to the Na-alginate solution, which was mixed and vortexed for 1 min and allowed to equilibrate at 20 ºC for 15 min. Several Ca^{2+}/COO^- ratios were tested (0.180, 0.216, 0.252, 0.288, 0.324 and 0.360). To initiate gel formation, a fresh GDL solution was subsequently added to each mixture and vortexed for 20 sec. Immediately after, the mixtures were poured into test tubes, incubated at 20 ºC in water bath and allowed to gelify. The gelation time was calculated according to the procedure of Oakenfull *et al*.[31] It was defined as the time required for the mixtures to form a gel just strong enough to remain held in position upon inversion of the test tubes. All samples were assayed in triplicate.

Preparation and characterization of the microspheres-vehicle system

Preparation of the system

Microspheres were added to the vehicle (Na-alginate with $CaCO_3$ and GDL) and the mixture was carefully homogenised. Different percentages of microspheres – 20, 30, 35 and 40% (w/w) – were tested. In this study, a Ca^{2+}/COO^- ratio of 0.288 was used, since preliminary results showed that it promotes gelation in approximately 11 min. This was considered an adequate handling period, giving the surgeon enough time to prepare, manipulate and inject the system.

Osmolality

The osmolality (mOsm/kg) of extemporaneously prepared microspheres-vehicle mixtures was measured in an osmometer (Semi-Micro Osmometer, Knauer).

Injectability (extrusion) assay

The injectability of the mixtures was evaluated according to the scheme of Figure 1A. In the procedure, an injection device commonly used in vertebroplasty surgical procedures was used, which was coupled to a Texture Analyzer (Figure 1B). The device consisted of a plastic syringe (20 mm internal diameter), a cannula (2.7 mm internal diameter, 173 mm length) and a polymeric connection tube. The syringe was filled with extemporaneously prepared microspheres-vehicle mixtures and the whole device was mounted on the Texture Analyzer operating in the compression mode. For extrusion, the load was applied vertically using two different plunger displacement rates (1 mm/s or 0.1 mm/s). Results are expressed as the force needed to extrude the mixture out from the syringe. The percentage of injectability, defined as the ratio between the mass of mixture expelled from the syringe and the total mass loaded, was also calculated. All samples were assayed in triplicate.

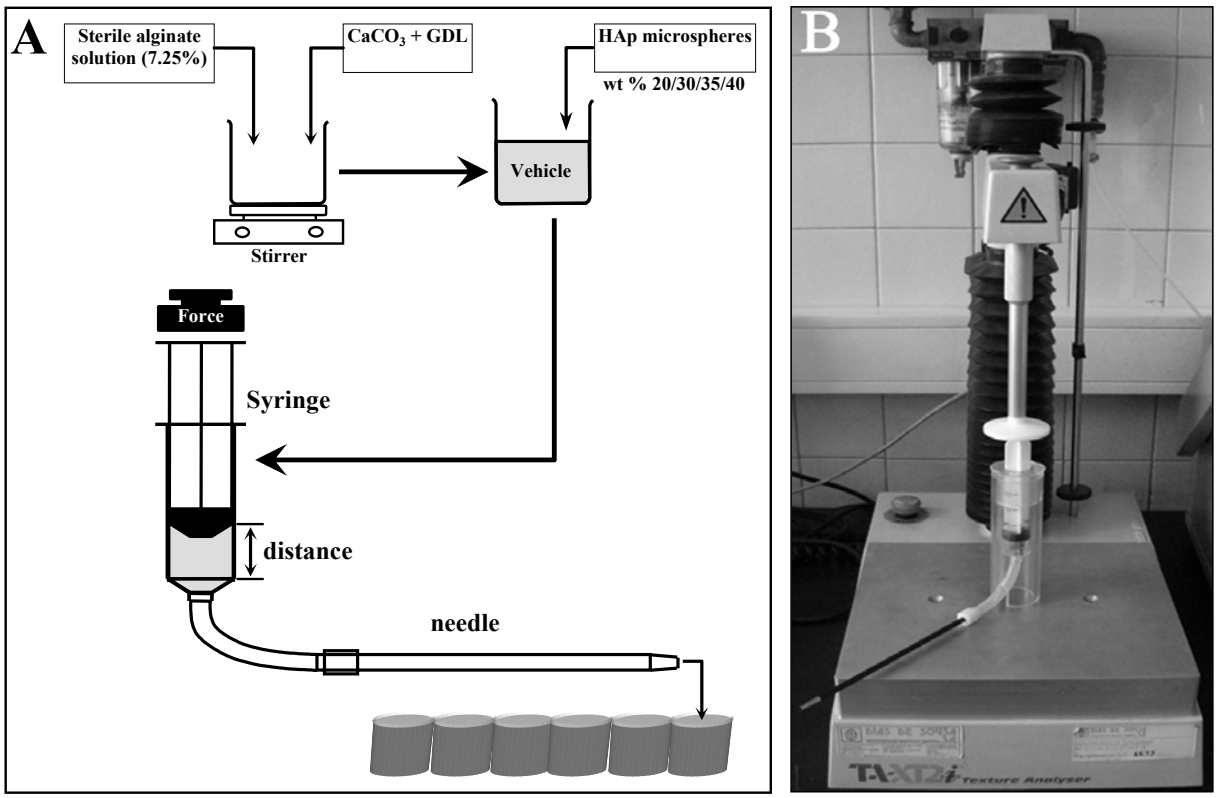

Figure 1. Schematic representation of the procedure and device used to evaluate the injectability of the microspheres-vehicle system. Global procedure (A), injectability device and texture analyzer TA-XT2i (B).

Gel formation

The microspheres-vehicle mixtures were extruded into cylindrical shape moulds, transferred to an oven at 37 ºC under controlled humidity (to prevent dehydration) and incubated for 24 h.

At the end, crosslinked systems with a cylindrical shape were obtained.

Characterization of the gelled systems (Compression strength and MicroCT)

The compression strength of the systems obtained after 24 hours of gelation was calculated with a Texture Analyzer, with the load applied vertically using a cylindrical probe with a diameter of 4 mm. In each cylindrical composite, three compression tests were performed and the force profile curves were used to estimate the rupture force and the associated compression strength.

The spatial distribution of the microspheres in the gelled systems was analysed by micro computed tomography (MicroCT, Scanco Med), using a resolution of 10 μm scans and a thresholding range of 260 to 1000 to yield three-dimension (3D) reconstruction. Only crosslinked systems prepared with 35% (w/w) microspheres and extruded at 0.1 mm/s were used in this test.

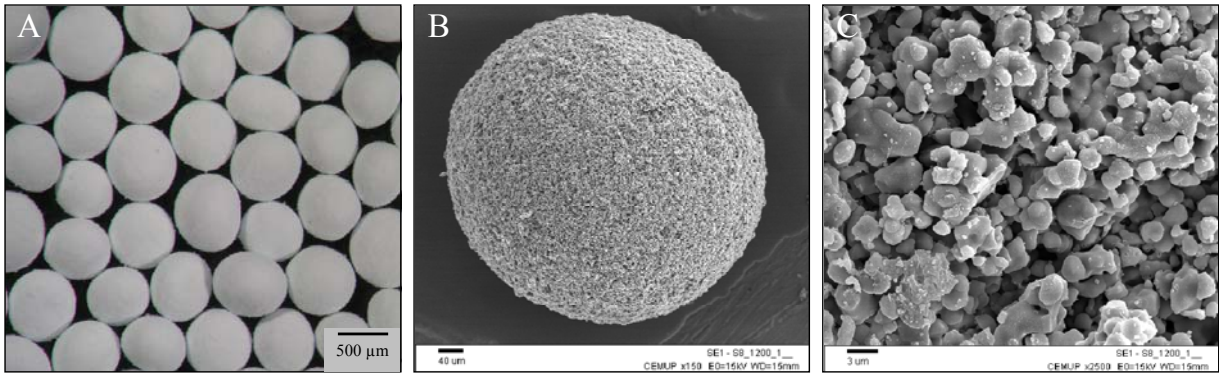

Figure 2. Photomicrographs of HA-microspheres. Image A was obtained with a stereomicroscope and illustrates the spherical-shape of the microspheres and their uniform size. Images B and C were obtained by SEM at different magnifications (150× and 2500× respectively).

RESULTS

Preparation and characterization of HAp-microspheres

HAp-microspheres were obtained from a HAp-alginate slurry by droplet extrusion into a crosslinking bath containing Ca^{2+}, where composite hydrogel beads instantaneously formed. This was followed by a sintering stage (1 hour at 1200 ºC). During this process the polymer was burned-off and the ceramic particles became associated yielding HAp-microspheres with an average diameter of 535±38 μm (mean±SD, n=20), as assessed by optical microscopy.

Figure 2A illustrates the spherical-shape of the microspheres as well as their uniform size. At

higher magnification it can be seen from Figure 2B and 2C that HAp-microspheres are porous and present a rough surface.

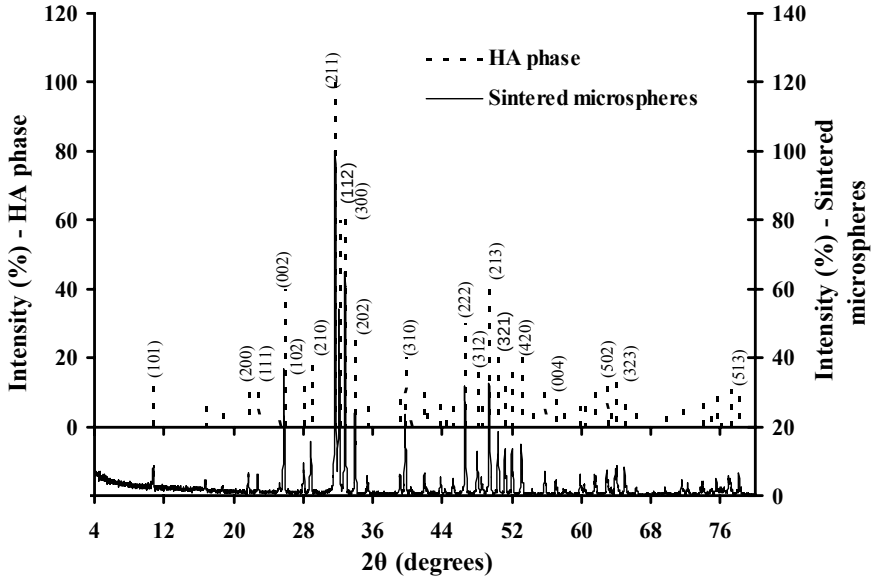

Figure 3. XRD spectra of the sintered HA-microspheres and peaks of the HA phase.

Physical-chemical characterization was carried out by XRD and FTIR. In terms of phase constitution, the HAp-microspheres do not present other crystalline phases than those observed in the original HAp powder, as observed by XRD (Figure 3). Moreover, the FTIR characteristics bands present in the microspheres match the ones of the HAp powders (Figure 4), confirming that the ceramic kept its integrity.

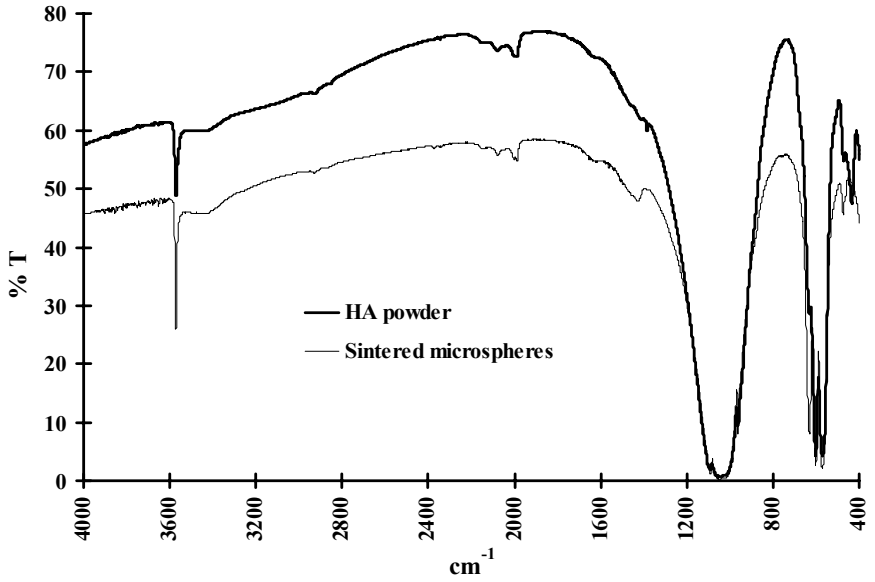

Figure 4. FTIR spectra of the sintered HA-microspheres and of the original HA powder.

In order to characterize the mechanical properties of microspheres, both friability tests and compression strength tests were performed. Friability was determined as the difference between the weight before and after the test, and a value of 0.9±0.1% (mean±SD) was obtained. In terms of compression strength, microspheres have only fractured when 0.35±0.08 N (mean±SD) were reached.

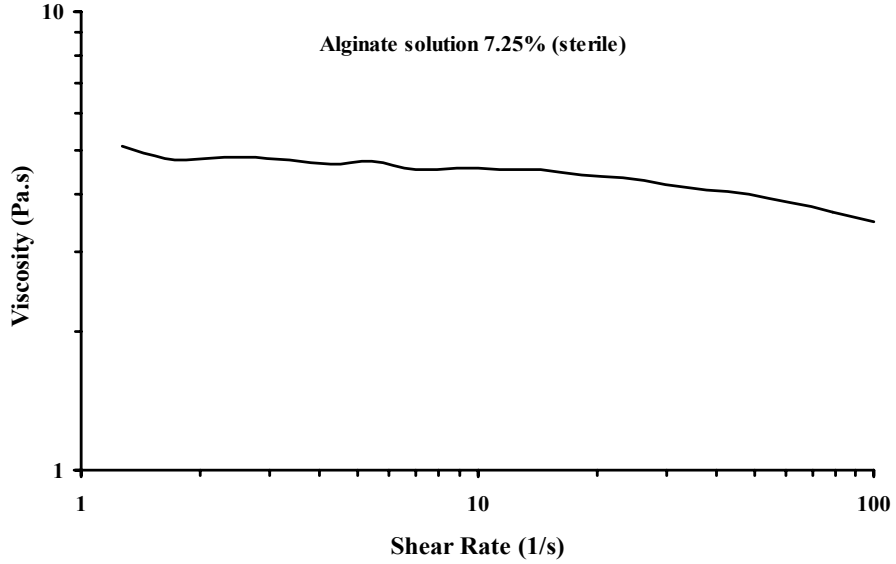

Figure 5. Viscosity versus shear rate for sterile alginate solution at 7.25%. The variation of viscosity with shear rate is approximately constant.

Preparation and characterization of the alginate vehicle

Characterization of the molecular weight and viscosity

Since we wanted to obtain a sterile system, the alginate solution used to prepare the vehicle was submitted to moist heat sterilization (121 ºC, 15 min), and the influence of this sterilization method on its rheological properties was assessed.

Molecular weight (Mw) determinations before and after sterilization showed that the Mw of Na-alginate decreases from 85 to 70 kDa.

The viscosity also decreases with autoclaving, but its values are approximately constant in a range of shear rates below 30 s^{-1} and only starts to decrease for higher shear rates, as depicted in Figure 5. In the range studied (1-100 s^{-1}), the viscosity decreases from 4.8 to 3.5 Pa.s.

Gel formation

The gelation time for an alginate solution (Figure 6) is related to the Ca^{2+}/COO^{-} ratio, being

dependent on the amount of Ca^{2+} in solution. For Ca^{2+}/COO^{-} ratios below 0.288 the decrease of gelation time is approximately linear while for higher ratios this behaviour is not observed. At concentration ratios of 0.324 and 0.360 the gelation times are 9±2 min and 8±1 min respectively.

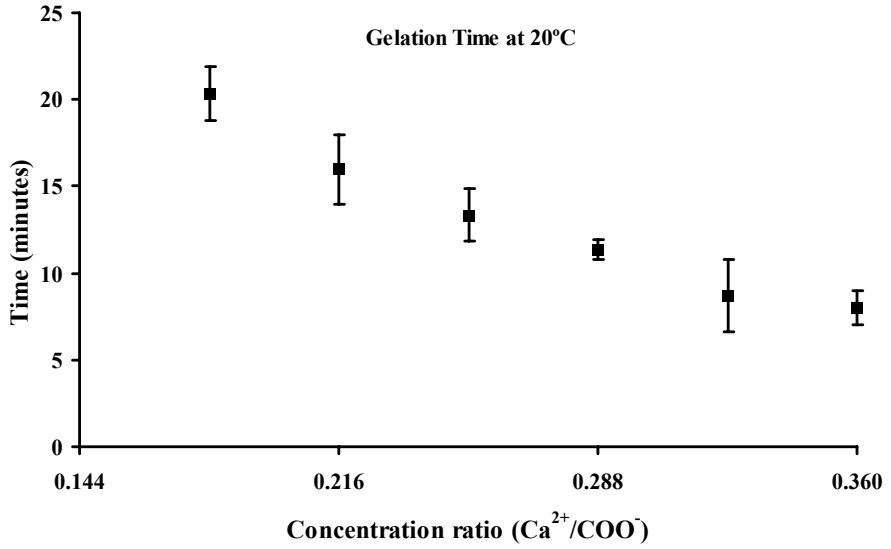

Figure 6. Gelation time of sterile alginate solution. At ratios below 0.288 the gelation time decreases rapidly as concentration of Ca^{2+} decreases.

Preparation and characterization of the microspheres-vehicle system

Osmolality

After injection, an osmotic equilibrium between the system and the surrounding tissues should be easily attained. The osmolality (Figure 7) of our system has an average value of 330±9 mOsm/kg (mean±SD) which seems adequate since it is close to that of blood and human fluids, which is around 285 mOsm/kg.[32]

Injectability (extrusion) assay

To simulate the injection/extrusion of the microspheres-vehicle system, a device commonly used in PVP procedures (Figure 1B), and well known among orthopaedic surgeons, was used. When evaluating the injectability of bone-filing materials, two main parameters should be taken into consideration, namely the force needed to perform the injection and the yield of the procedure itself. In this procedure, the force versus distance during extrusion of the mixtures through the connection tube and the cannula were recorded, and at the end the extruded product was collected. The results are presented in Figure 8, where each curve represents the

evolution of the force during extrusion for a particular formulation. At the end, a plateau is observed, corresponding to the point at which the mixtures start being expelled from the cannula. Since pressure does not subside immediately, the mixtures still continued to flow out from the cannula, even after the force had been stopped.

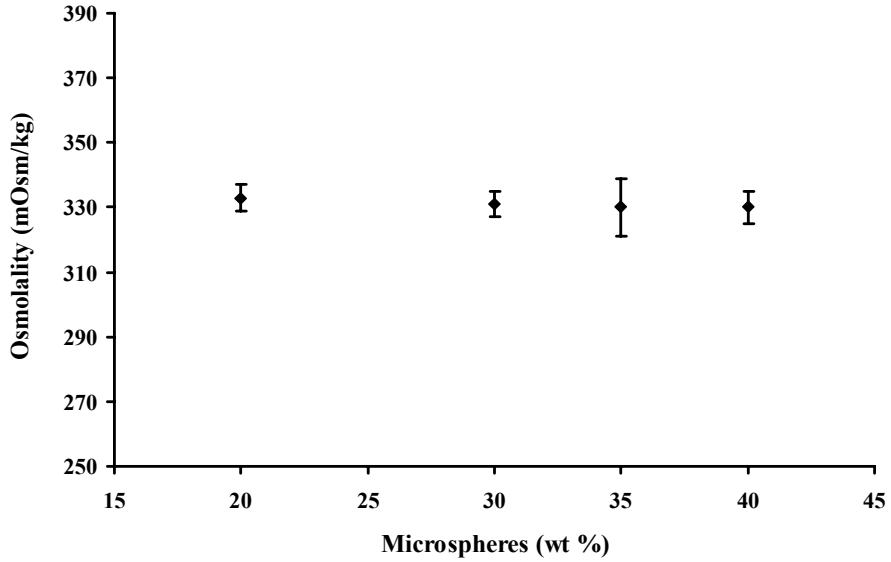

Figure 7. Osmolality of mixtures. Osmolality was measured by comparing the freezing points of pure water and the sample using 1 g of each mixture prepared just before measurement. The values among the samples are approximately 330 mOsm/kg.

Figure 8 shows that only mixtures with 40% and 35% (w/w) of microspheres extruded at 1 mm/s needed the application of forces higher than 100 N (reference line), but even for those mixtures the extrusion force does not go above 200 N. On the other hand, if such mixtures are extruded at 0.1 mm/s the extrusion pressure falls below the reference line, to 233 and 153 kPa respectively (Figure 9).

The yields of injection (% of injectability) found for each of the mixtures and rates of extrusion respectively, are depicted in Table I. As can be observed, the percentage of injectability presents a large range of values among the mixtures studied in this work. The highest percentage of injectability (83.3%) was found for a mixture with 20% (w/w) of microspheres, whereas the lowest (18.1%) was found for mixtures with 40% (w/w), both extruded at 1 mm/s.

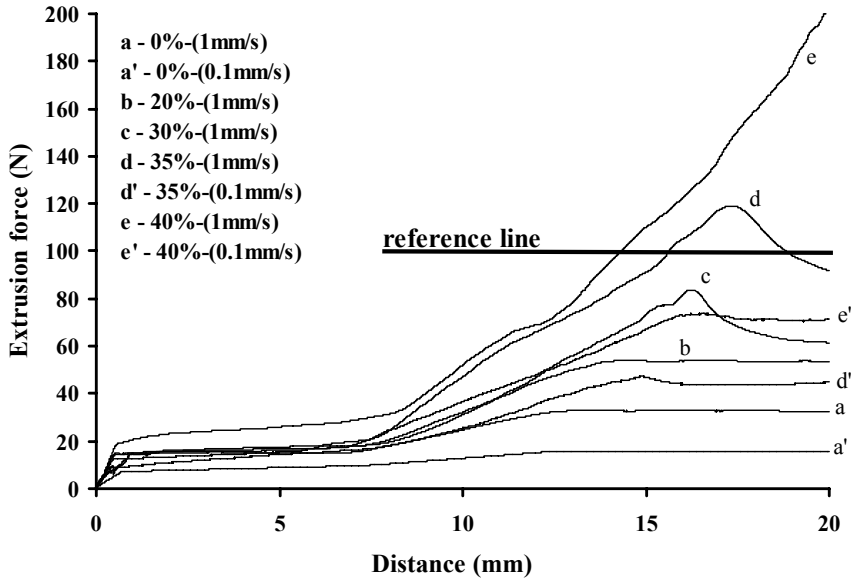

Figure 8. Extrusion force of different microspheres/alginate composites. During extrusion, the profile of curves identifies the position where the mixture is in each moment. The first slope is the beginning of extrusion and corresponds to the force need to extrude the mixture out from the syringe into the connection tube which will be filled up at extrusion force approximately constant. Once mixture reached the cannula, extrusion force increases again until mixture starts to come out from it. Following the slope is observed a decrease or constant extrusion force.

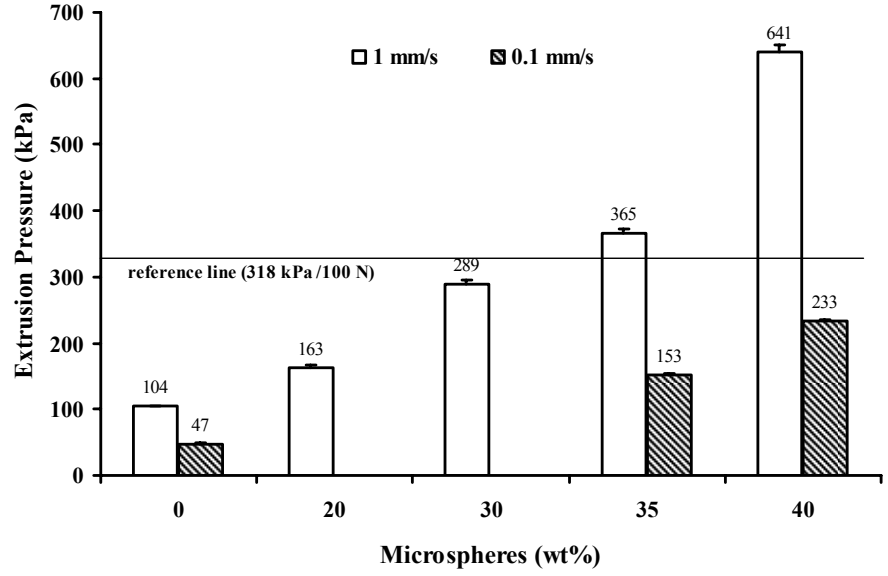

Figure 9. Extrusion pressure of different microspheres/alginate composites. According to the syringe used, a force of 100 N corresponds to a pressure of 318 N, our reference line. Mixtures extruded at 0.1 mm/s experienced a pressure decrease of more than 50%.

Mixtures with 35% (w/w) of microspheres presented an injectability of 76.4 % at an extrusion rate of 0.1 mm/s, while mixtures with 40% (w/w) of microspheres extruded at 0.1 mm/s present an injectability similar to that of mixtures with 30% (w/w) of microspheres extruded at 1 mm/s.

Table I. Injectability obtained for different formulations and extrusion rates.

Microspheres (%)	Extrusion rate (mm/s)	Injectability (%)
20	1	83.3
30	1	56.9
35	1	40.3
	0.1	76.4
40	1	18.1
	0.1	55.6

Characterization of the gelled systems (Compression strength and MicroCT)

MicroCT scans performed on composites with 35% (w/w) of microspheres extruded at 0.1 mm/s show a homogeneous distribution of the microspheres across the gel (Figure 10). Figure 10A is the result of a three dimensional (3D) reconstruction of the microCT scans and shows

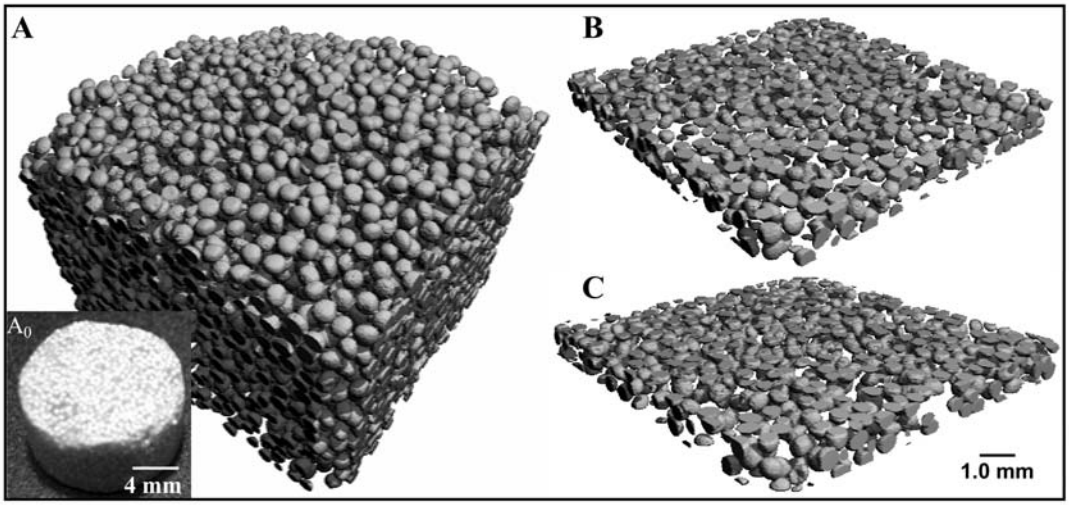

Figure 10. MicroCT analysis of composites prepared with 35% of microspheres. Composites obtained after mixtures (matrix – alginate and reinforcement phase – HAp microspheres) gelification; picture A_0 represent a composite prepared using 35% of microspheres. Scanning under microCT and three dimensional (3D) reconstructions were performed using a threshold in the range of 255 to 1000. Picture A shows microspheres distribution on composite. Picture B and C correspond to layers took at different depths inside the composite.

microspheres distribution on the composite. Figures 10B and 10C correspond to layers taken at different depths inside the composite using the same parameters.

The compression strength of the gelled systems was measured and the results are presented in Figure 11. For an extrusion rate of 0.1 mm/s, the compression strength increased from ≅90 kPa to ≅600 kPa, as the percentage of microspheres increased from 0 to 40% (w/w). For an extrusion rate of 1 mm/s, the compression strength is somewhat lower since lower extrusion rates allow better accommodation of microspheres and at same time generate less residual stress on alginate chains during gelification.

DISCUSSION

In this study the injectability of a bone filler system based on hydroxyapatite microspheres and a vehicle with *in situ* gel-forming ability was evaluated.

Particles diameter and spherical shape are important parameters to take in consideration during injection procedures. Therefore we have produced microspheres with diameters around 500 μm, which is the value considered acceptable according to Gauthier *et al*.[33] Moreover, mechanical properties of the microspheres are relevant for their functional behavior since during the process of transportation, packing and handling, pharmaceutical and biomedical products such as tablets, granules and other particulate materials generally erode to some

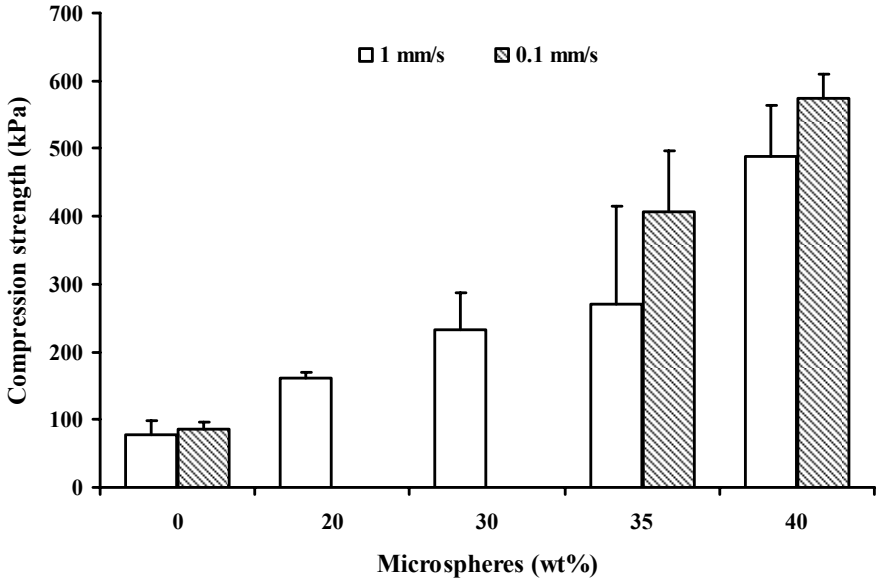

Figure 11. Compression strength of composites. Compression tests were performed on a TA-TX2i texture analyzer and the probe used has 4 mm of diameter.

extent, loosing some weight as well as breaking apart. One of the testing criteria of mechanical strength of these kind of products is friability testing. Friability is determined as the difference between the weight before and after the test and usually should not exceed 1%, which is similar to the value obtained for our microspheres which was 0.9%.

During injection, the force applied on the syringe plunger will be transferred to the microspheres, which have to resist the maximum pressure attained during extrusion (641 kPa – Figure 9). For this reason, the compression strength of the microspheres was also evaluated. If the compression strength of microspheres (force of 0.35±0.08 N) is converted into pressure, by considering a cross-section area equivalent to the equatorial area of the microspheres, the value will be 1556 kPa. Although this value may be underestimated, it is more than the double of the maximum pressure mentioned above, suggesting that the microspheres are resistant enough to withstand injection.

It is well known that autoclaving promotes polymer breakdown, changing its rheological properties, and may also impair its gel-forming ability.[20] Therefore, a decrease in alginate molecular weight, and consequently a decrease in the viscosity of the solution, were expected. Although, a decrease in Mw might present advantages, namely by facilitating *in vivo* elimination, it results in the necessity of increasing the concentration of the original solution, in order to reach the appropriated viscosity upon sterilization.

Another important parameter that has to be taken into consideration when adjusting the formulation of the vehicle is its gelation time. If the gelation time is too long (30 min, long time surgery) or too short (5 min, not enough time to prepare the mixture and inject it) the PVP procedure may be impaired and the surgery can be at risk. Taking into consideration that the time should be as short as possible, enabling a fast gelation and strengthening after injection, but long enough to prepare the mixture, fill up the syringe, and inject, we selected a Ca^{2+}/COO^{-} ratio of 0.288 in our mixtures, which gives the surgeon 10 to 15 minutes of handling time (Figure 6).

The process to extrude either a material or a mixture always depends of its physical and chemical properties, namely size, shape, surface roughness, chemical stability and chemical reaction among the different compounds. In this particular case, we are trying to extrude a gel incorporating solid particles, which brings additional difficulties. However, particles with a narrow size distribution and a uniform spherical shape can help to solve problems.

Several maximum acceptable values for extrusion force have been reported as acceptable for a product suitable for injection.[26,34,35] According to Krebs *et al.*[36], a force of 100 N is the value

accepted to inject manually, while 260 N were measured when automated injection equipment was used. In this study, we took 100 N as a reference value since our empirical data are related more with manual injections.

The extrusion rate of 0.1 mm/s is closer to the ones used during surgeries, as experienced empirically by an orthopaedic surgeon. On the other hand, extruding at 0.1 mm/s allowed a decrease of 50% of extrusion pressure when compared with extrusion rate of 1 mm/s. This behaviour was expected since lower extrusion rates corresponds to lower shear rates and higher time for accommodation of the microspheres and relaxation of polymer molecules, which is a characteristic of high fluency found in this group of materials.

The low values of injectability found for mixtures with 40% (w/w) of microspheres extruded at 1 mm/s are the result of high volume of solid phase in mixture combined with high extrusion rate and indicates that a filtering phenomenon is being experienced.[37] This means that the pressure required to filter the liquid in between the microspheres is lower than the pressure required to extrude the mixture. When that mixture was extruded at 0.1 mm/s, its injectability rose to more than 55% suggesting that filtering was eliminated. In the literature it is common to find mixtures with injectability above 70%[4,38] as acceptable to be injected, which led us to eliminate mixtures with 30% and 35% (w/w) of microspheres extruded at 1 mm/s and also the mixture with 40% either extruded at 1 or 0.1 mm/s.

Looking at the extrusion force and injectability together, the mixture with 35% (w/w) of microspheres extruded at 0.1 mm/s presented the best compromise, and was the one selected for further studies.

As discussed before, these injectable materials can be used to fill empty spaces where mechanical strength may or may not be the main property to achieve. In some cases, injectable materials are used only to fill up a cavity, preventing invasion by fibrous tissues, or to deliver drugs in order to treat some disease or to induce bone regeneration. In other situations some mechanical strength is required either to fracture stabilization or to support high loads. In order to achieve these goals, a homogeneous distribution of reinforcement phase inside a composite is an important factor to be reached, which was clearly shown by microCT scans. Moreover, large and fully interconnected spaces, between the microspheres, are established, which can be an important feature, as it may improve regeneration by facilitating vascularization and bone ingrowth.

Composites' strength is directly related to phase reinforcement strength. Since microspheres were obtained by sintering of HAp powder and its rupture force is 0.35 N, they represent a

good reinforcement element inside the alginate matrix. The maximum value of compression strength (600 kPa) obtained for these composites is lower than that of trabecular bone (3 MPa)[39], but the composites' strength is closer to trabecular bone strength than PMMA strength (115 MPa)[4] and other bone cements[40] (>70 MPa). This property allows some gains in toughness (not measured) since gels are good structures to absorb loads and avoids the initiation of cracks or microcracks that are usually induced on bone tissue around the area being treated and on adjacent vertebra.[9-11] When considering composites with 35% (w/w) of microspheres, the difference in compression strength to trabecular bone becomes eight times lower but still closer than PMMA and other bone cements. However, it is important to highlight that the mixture will be injected inside a space where some trabecular bone still exist. The new structure that will be obtained (trabecular bone plus injected composite) will present better compression strength than the composite itself since trabecular bone will work as second reinforcement phase inside of alginate matrix.

CONCLUSIONS

Since PVP is considered a minimally invasive surgery, it involves minor pre-surgery preparation of the patient and allows an immediate pain relief and a recovery in few days. Those advantages led us to prepare HAp microspheres reinforced-alginate mixtures and to test them as the injectable material. The HAp microspheres/alginate mixtures prepared were extrudable through a PVP device, using forces below 100 N. After being injected, mixtures gelified at 37 ºC and microspheres were homogeneously distributed across the composites obtaining a mechanical strength of 407 kPa for composites with 35% (w/w) of microspheres. Using this system we expect to diminish the formation of cracks that usually appear in surrounding bone after conventional PVP.

ACKNOWLEDGEMENTS

SM Oliveira is grateful to the Program for Education Development in Portugal III (PRODEP III) for supporting his salary at Escola Superior de Tecnologia de Viseu. This work was supported by Foundation for Science and Technology (FCT) under contract POCTI/FCB/41523/2001. The authors thank to Dr. Rui Pinto from Hospital de São João for all its suggestions and for supplying the injection devices.

REFERENCES

1. Ribeiro CC, Barrias CC, Barbosa MA. Calcium phosphate-alginate microspheres as enzyme delivery matrices. Biomaterials 2004;25(18):4363-73.
2. Grabowski GA, Leslie N, Wenstrup R. Enzyme therapy for Gaucher disease: the first 5 years. Blood Rev 1998;12(2):115-33.
3. Melton LJ, 3rd, Kan SH, Frye MA, Wahner HW, O'Fallon WM, Riggs BL. Epidemiology of vertebral fractures in women. Am J Epidemiol 1989;129(5):1000-11.
4. Carrodeguas RG, Lasa BV, Del Barrio JS. Injectable acrylic bone cements for vertebroplasty with improved properties. J Biomed Mater Res B Appl Biomater 2004;68(1):94-104.
5. Hee HT. Percutaneous vertebroplasty: current concepts and local experience. Neurol India 2005;53(4):475-82.
6. Hide IG, Gangi A. Percutaneous vertebroplasty: history, technique and current perspectives. Clin Radiol 2004;59(6):461-7.
7. Verlaan JJ, Oner FC, Verbout AJ, Dhert WJ. Temperature elevation after vertebroplasty with polymethyl-methacrylate in the goat spine. J Biomed Mater Res B Appl Biomater 2003;67(1):581-5.
8. Hardouin P, Grados F, Cotten A, Cortet B. Should percutaneous vertebroplasty be used to treat osteoporotic fractures? An update. Joint Bone Spine 2001;68(3):216-221.
9. Berlemann U, Ferguson SJ, Nolte LP, Heini PF. Adjacent vertebral failure after vertebroplasty. A biomechanical investigation. J Bone Joint Surg Br 2002;84(5):748-52.
10. Wilcox RK. The biomechanical effect of vertebroplasty on the adjacent vertebral body: a finite element study. Proc Inst Mech Eng [H] 2006;220(4):565-72.
11. Uppin AA, Hirsch JA, Centenera LV, Pfiefer BA, Pazianos AG, Choi IS. Occurrence of new vertebral body fracture after percutaneous vertebroplasty in patients with osteoporosis. Radiology 2003;226(1):119-24.
12. Barrias CC, Ribeiro CC, Barbosa MA. Adhesion and proliferation of human osteoblastic cells seeded on injectable hydroxyapatite microspheres. Bioceramics, Vol 16 2004;254-2:877-880.
13. Becker TA, Kipke DR, Brandon T. Calcium alginate gel: a biocompatible and mechanically stable polymer for endovascular embolization. J Biomed Mater Res 2001;54(1):76-86.
14. Alsberg E, Anderson KW, Albeiruti A, Franceschi RT, Mooney DJ. Cell-interactive alginate hydrogels for bone tissue engineering. J Dent Res 2001;80(11):2025-9.
15. Steinert A, Weber M, Dimmler A, Julius C, Schutze N, Noth U, Cramer H, Eulert J, Zimmermann U, Hendrich C. Chondrogenic differentiation of mesenchymal progenitor cells encapsulated in ultrahigh-viscosity alginate. J Orthop Res 2003;21(6):1090-7.
16. Wang L, Shelton RM, Cooper PR, Lawson M, Triffitt JT, Barralet JE. Evaluation of sodium alginate for bone marrow cell tissue engineering. Biomaterials 2003;24(20):3475-81.
17. Shapiro L, Cohen S. Novel alginate sponges for cell culture and transplantation. Biomaterials 1997;18(8):583-90.
18. Eiselt P, Yeh J, Latvala RK, Shea LD, Mooney DJ. Porous carriers for biomedical applications based on

alginate hydrogels. Biomaterials 2000;21(19):1921-7.

19. Wee S, Gombotz WR. Protein release from alginate matrices. Adv Drug Deliv Rev 1998;31(3):267-285.
20. Draget KI, Skjak-Braek G, Smidsrod O. Alginate based new materials. Int J Biol Macromol 1997;21(1-2):47-55.
21. Bajpai SK, Sharma S. Investigation of swelling/degradation behaviour of alginate beads crosslinked with Ca2+ and Ba2+ ions. Reactive & Functional Polymers 2004;59(2):129-140.
22. Ouwerx C, Velings N, Mestdagh MM, Axelos MAV. Physico-chemical properties and rheology of alginate gel beads formed with various divalent cations. Polymer Gels and Networks 1998;6(5):393-408.
23. Paul W, Sharma CP. Development of porous spherical hydroxyapatite granules: application towards protein delivery. Journal of Materials Science-Materials in Medicine 1999;10(7):383-388.
24. Jarcho M. Calcium-Phosphate Ceramics as Hard Tissue Prosthetics. Clinical Orthopaedics and Related Research 1981(157):259-278.
25. Uda H, Sugawara Y, Nakasu M. Experimental studies on hydroxyapatite powder-carboxymethyl chitin composite: injectable material for bone augmentation. J Plast Reconstr Aesthet Surg 2006;59(2):188-96.
26. Xu HH, Weir MD, Burguera EF, Fraser AM. Injectable and macroporous calcium phosphate cement scaffold. Biomaterials 2006;27(24):4279-87.
27. Weiss P, Gauthier O, Bouler JM, Grimandi G, Daculsi G. Injectable bone substitute using a hydrophilic polymer. Bone 1999;25(2 Suppl):67S-70S.
28. Iooss P, Le Ray AM, Grimandi G, Daculsi G, Merle C. A new injectable bone substitute combining poly(epsilon-caprolactone) microparticles with biphasic calcium phosphate granules. Biomaterials 2001;22(20):2785-94.
29. Gauthier O, Khairoun I, Bosco J, Obadia L, Bourges X, Rau C, Magne D, Bouler JM, Aguado E, Daculsi G and others. Noninvasive bone replacement with a new injectable calcium phosphate biomaterial. J Biomed Mater Res 2003;66A(1):47-54.
30. Kuo CK, Ma PX. Ionically crosslinked alginate hydrogels as scaffolds for tissue engineering: part 1. Structure, gelation rate and mechanical properties. Biomaterials 2001;22(6):511-21.
31. Oakenfull D, Scott A. Stabilization of gelatin by sugars and polyols. Food Hydrocolloyds 1986;1(2):163-175.
32. Poon CY. Tonicity, osmoticity, osmolality and osmolarity. Philadelphia; 2006. 250-265 p.
33. Gauthier O, Bouler JM, Weiss P, Bosco J, Aguado E, Daculsi G. Short-term effects of mineral particle sizes on cellular degradation activity after implantation of injectable calcium phosphate biomaterials and the consequences for bone substitution. Bone 1999;25(2):71S-74S.
34. Gisep A, Curtis R, Hanni M, Suhm N. Augmentation of implant purchase with bone cements: an in vitro study of injectability and dough distribution. J Biomed Mater Res B Appl Biomater 2006;77(1):114-9.
35. Ginebra MP, Rilliard A, Fernandez E, Elvira C, San Roman J, Planell JA. Mechanical and rheological improvement of a calcium phosphate cement by the addition of a polymeric drug. J Biomed Mater Res 2001;57(1):113-8.
36. Krebs J, Ferguson SJ, Bohner M, Baroud G, Steffen T, Heini PF. Clinical measurements of cement injection pressure during vertebroplasty. Spine 2005;30(5):E118-22.
37. Bohner M, Baroud G. Injectability of calcium phosphate pastes. Biomaterials 2005;26(13):1553-63.

38. Hernandez L, Gurruchaga M, Goni I. Influence of powder particle size distribution on complex viscosity and other properties of acrylic bone cement for vertebroplasty and kyphoplasty. J Biomed Mater Res B Appl Biomater 2006;77(1):98-103.
39. Yoshimine F, Latta LL, Milne EL. Sliding characteristics of compression hip screws in the intertrochanteric fracture: a clinical study. J Orthop Trauma 1993;7(4):348-53.
40. Jasper LE, Deramond H, Mathis JM, Belkoff SM. Material properties of various cements for use with vertebroplasty. Journal of Materials Science-Materials in Medicine 2002;13(1):1-5.

Chapter V

Engineering endochondral bone: *in vitro* studies

S.M. Oliveira[1,2,3,4], I.F. Amaral[2], M.A. Barbosa[2,3], C.C. Teixeira[4]

[1]ESTV – Escola Superior de Tecnologia de Viseu, Dep. de Eng. Mecânica e Gestão Industrial, Campus Politécnico de Repeses, 3504-510 Viseu, Portugal;

[2]INEB – Instituto de Engenharia Biomédica, Divisão de biomateriais, Rua do Campo Alegre 823, 4150-180 Porto, Portugal;

[3]FEUP – Faculdade de Engenharia Universidade do Porto, Dep. de Eng. Metalúrgica e de Materiais, Rua Roberto Frias, 4200-465 Porto, Portugal;

[4]NYUCD – New York University College of Dentistry, Department of Basic Science and Craniofacial Biology, 345 E. 24th Street New York, NY 10010.

ABSTRACT

Chitosan scaffolds have been shown to possess biological and mechanical properties suitable for tissue engineering and clinical applications. In the present work, chitosan sponges were evaluated regarding their ability to support cartilage cell proliferation and maturation, which are the first steps in endochondral bone formation. Chitosan sponges were seeded with chondrocytes isolated from chicken embryo sterna. Chondrocyte/chitosan constructs were cultured for 20 days, and treated with retinoic acid to induce chondrocyte maturation and matrix synthesis. At different time points, samples were collected for microscopic, histological, biochemical, and mechanical analyses. Results show chondrocyte attachment, proliferation, and abundant matrix synthesis, completely obliterating the pores of the sponges. Retinoic acid treatment caused chondrocyte hypertrophy, characterized by the presence of type X collagen in the extracellular matrix and increased alkaline phosphatase activity. In addition, hypertrophy markedly changed the mechanical properties of the chondrocyte/chitosan constructs. In conclusion, we have developed chitosan sponges with adequate pore structure and mechanical properties to serve as a support for hypertrophic chondrocytes. In parallel studies, we have evaluated the ability of this mature cartilage scaffold to induce endochondral ossification.

Keywords: Chitosan sponges, chondrocytes, maturation markers, growth cartilage, endochondral ossification, bone regeneration.

INTRODUCTION

Bone is an important component of the musculoskeletal system and often suffers injuries (caused by trauma, tumors, and others pathologies) that may result in considerable tissue loss. To address these problems, different materials, inert or bioactive, have been used for bone replacement or regeneration. Some of these materials are metals[1-3] and ceramics[4-6]. More recently, synthetic polymers[7-10] and natural polymers[11,12] have been used as templates for bone growth and regeneration.

Chitosan, the product of the partial deacetylation of the naturally occurring polysaccharide, chitin, has been shown to possess biological and mechanical properties suitable for clinical applications.[13-15] It is reported to be biocompatible and biodegradable in the presence of lysozyme, and its degradation products are non-toxic and can be incorporated into the extracellular matrix for rebuilding of normal tissues.[16,17-20] These properties, together with the ability to promote bone cell growth and differentiation have stimulated the use of chitosan as a bone regeneration template.[14,21] Moreover, its structural similarity to various glycosaminoglycans and hyaluronic acid present in articular cartilage, makes chitosan one of the most suitable materials for cartilage regeneration applications.[17,22,23] Indeed, chondrocytes have been successfully cultured on chitosan, and *in vivo* studies showed good results when this material was used as an articular cartilage implant.[22,24,25]

Although chitosan has been used as a scaffold for articular cartilage and bone formation by direct differentiation of mesenchymal cells into chondrocytes and osteoblast, respectively, to the best of our knowledge it has not been used as a template for endochondral ossification. The endochondral ossification pathway involves an intermediate cartilage stage and is responsible for the formation of long bones, vertebra, and the cranial base during development. During bone elongation, endochondral ossification mediates growth via the activity of cells in the growth plates. The growth plates are discs of transient cartilage (not permanent cartilage as in the articular surface), located at the end of long bones. Within the growth plates, chondrocytes undergo maturation/hypertrophy coordinating the replacement of the calcified cartilage matrix by new bone.

The goal of the present work was to investigate chitosan's capability to support growth

cartilage cell proliferation and maturation, as well as its potential as a template for endochondral ossification. There are numerous advantages in the use of the endochondral pathway for bone tissue engineering. Chondrocytes are resistant to low oxygen levels[26] and can induce vascular invasion and osteogenesis[27,28], therefore allowing the creation of larger osteoinductive templates. Upon implantation, this template could behave like a growth plate, remodeling into the required bone, mimicking the natural process of endochondral ossification. In fact, a major problem in engineering articular cartilage is the tendency of the cells to undergo further maturation.[29-32] We sought to take advantage of this pathway for bone regeneration.

MATERIALS AND METHODS

Preparation and characterization of chitosan powder and 3D scaffolds

Squid pen chitosan (Chitosan 123) was kindly supplied by France Chitine (Orange, France). After a purification step, chitosan with a degree of acetylation (DA) of ≅4% was prepared by heterogeneous deacetylation, according to Amaral *et al*.[33] The physicochemical properties of the resultant chitosan in terms of DA, weight average molecular weight (M_w), polydispersity index (PDI), and intrinsic viscosity ([η]), are presented in Table I. The DA was determined by Fourier transform infrared spectroscopy (FTIR) while the M_w, M_n, PDI, and [η] were determined by high performance size-exclusion chromatography.[33]

Table I. Chitosan powder properties

DA (%)	M_w ($\times 10^5$) (Da)	PDI	[η] ($dL \cdot g^{-1}$)
4.23 ± 0.46	2.1 ± 0.1	2.1 ± 0.2	8.20 ± 0.29

DA – degree of acetylation, M_w – weight average molecular weight, PDI – polydispersity index = (M_w/M_n), [η]- intrinsic viscosity.

Three-dimensional (3D) porous scaffolds were prepared from 2% (w/v) chitosan acidic solutions via thermally induced phase separation and subsequent sublimation of the ice crystals. Briefly, chitosan solution was poured onto 24-well tissue culture polystyrene plates (800 μL/well), frozen at −70ºC, and subsequently lyophilized during 48 hours. The resultant planar sponges were cut into 4×4×1 mm^3 pieces, immersed in absolute ethanol, hydrated in

serial diluted ethanol solutions, and finally equilibrated in Hank's Balanced Salt Solution (HBSS) (Gibco, Carlsbad, CA).

Scanning Electronic Microscopy (SEM)

Average pore diameter was measured on cross sections of SEM images. The maximum (l) and minimum (h) pore length were measured using a Cell Observer System (Carl Zeiss, Germany) and the average diameter determined using the following equation: $d = \sqrt{l.h}$. Results are the average (±SD) of 20 measurements.

Cell morphology, attachment and proliferation were also assessed by SEM. Briefly, the samples were collected, fixed with 2% glutaraldehyde for 5 min at 37 ºC, followed by 1 hour incubation at room temperature (RT) and overnight incubation at 4 ºC. Samples were dehydrated in serial ethanol solutions and critical-point dried. Finally, scaffolds were cut, glued on steel stubs, coated with gold-palladium and analyzed on both top and cross sectional areas by SEM.

Mechanical properties tests

Creep and load deformation tests were performed on sponges cultured with chondrocytes, sponges without cells, as well as on tibia growth plates from 6 week old chickens. For the creep test, samples were frozen in liquid nitrogen. The test was carried out on samples confined to a chamber in a bath of media, and loaded using a porous indenter (EnduraTEC-ELF 3200, Minnetonka, MM). Samples were rapidly loaded to 10 g, then the load held constant, and the change in displacement monitored for 1200 seconds. Strain versus time curves were analyzed using the biphasic theory of Mow *et al*.,[34] and the aggregate modulus and permeability computed. The load deformation test was performed on samples with 5 mm diameter, loaded with a flat, non-porous plate (EnduraTEC-ELF 3200, Minnetonka, MM). A load of 15 g was applied (47% strain produced). The stress versus strain plot was fitted with an exponential curve and the slope at 30% strain computed as the elastic modulus.

Chondrocytes culture

Cephalic (CP) and caudal (CD) chondrocytes were isolated from the upper and lower region of sternum of 14 days chicken embryos, according to the method described by Iwamoto *et al*.[35] Chondrocytes were allowed to proliferate in 100 mm dishes for 7 days at 37 ºC, 5% CO_2

in Dulbecco's modified high glucose Eagle's medium (DMEM) containing 10% NU Serum and 100 U/ml of penicillin/streptomycin (Fisher Scientic, Fairlawn, NJ). After cell expansion, 200,000 cells (15 µl of cell suspension) were seeded into the hydrated sponges previously placed in a 96-well plate. Culture medium was added 2 hours after cell seeding and changed daily for 20 days. Cultures also received 400 U/ml of hyaluronidase and ascorbic acid (10-50 µg/ml). After 10 days, cultures were treated daily (for another 10 days) with 100 nM all-trans retinoic acid (RA) to induce chondrocyte maturation and matrix synthesis. CD condrocytes do not respond to RA treatment, represent a permanent cartilage phenotype, and thus were used as control. Samples were collected every 5 days and used for different analyses. All chemical unless otherwise stated were obtained from Sigma-Aldrich, St Louis, MO.

Cell solubilization

Three sets of 2 sponges for both CP and CD chondrocytes were collected, washed with phosphate buffer saline (PBS), immersed in 150 µl of 0.1% Triton X100 (Fisher Scientific, Fairlawn, NJ), crushed manually and centrifuged at 850 *g* for 3 min. The supernatant was used for measurement of alkaline phosphatase (AP) activity, protein and DNA content.

Protein and DNA analyses

Protein content was determined using a DC protein assay (BioRad Laboratories, Hercules, CA), according to the manufacturer's protocol, and absorbance measured at 750 nm using bovine serum albumin as standard. Total DNA amount was measured according to the procedure described by Teixeira *et al.*[36] using a bisBenzididazole dye (Hoechst 33258 dye, Polyscience Inc., Northampton, UK). Fluorescence was measured at 365 nm excitation and 460 nm emission wavelengths. The results were extrapolated from a standard curve using salmon testis DNA (Sigma-Aldrich, St Louis, MO).

Alkaline Phosphatase activity

For measurement of alkaline phosphatase (AP) activity samples were mixed with a fresh solution of 1 volume of 1.5 M tris-HCl pH 9.0 containing 7.5 mM p-nitrophenylphosphate, 1 mM $ZnCl_2$, and 1 mM $MgCl_2$. Changes in absorbance were measured spectrophotometrically at 410 nm for 10 min; changes over time corresponds to the p-nitrophenylphosphate hydrolysis to p-nitrophenol. AP activity was expressed as nmol of product/min/mg of protein; 1 absorbance unit change corresponds to 64 nmol of product.

RNA isolation and real time reverse transcriptase-polymerase chain reaction (RT-PCR)

RNA was isolated before the first day of RA treatment (day 10) and 10 days after RA treatment (day 20). Total RNA was extracted with Trizol® reagent (Life Technologies, Gaitherburg, MD) according to the manufacturer's instructions with some modifications. Briefly, samples were frozen in liquid nitrogen and crushed, Trizol® reagent was added (10ml/g), the samples vortexed for 30 sec, and then kept at 4 ºC for 2 hours. Phase separation was achieved by adding chloroform (0.2 volumes) to the mixture for 15 min and then centrifuging it at 12,000 *g* for 30 min at 4 ºC. The upper aqueous phase containing the RNA was collected, mixed with 0.25 volumes of high salt precipitation solution (0.8 M sodium citrate and 1.2 M NaCl) and with 0.25 volumes of isopropanol and centrifuged at maximum speed for 30 min at 4 ºC. RNA purification was completed using RNA micro kit (Qiagen Inc, Chatsworth, CA) according to the RNeasy cleanup protocol. Real-time RT-PCR was performed using QuantiTect SYBR Green RT-PCR kit (Qiagen Inc.), a DNA Engine Optican2 system (Roche Molecular Systems, Pleasanton, CA), and primers specific for the following chick genes: *type X collagen* (forward: AGTGCTGTCATTGATCTCATTGGA, reverse: TCAGAGGAATAGAGACCATTGGATT), *alkaline phosphatase* (forward: CCTGACATCGAGGTGATCCT, reverse: GAGACCCAGCAGGAAGTCCA), *type I collagen* (forward: GCCGTGACCTCAGACTTAGC, reverse: TTTTGTCCTTGGGGTTCTTG), *runx2* (forward: CTTAGGAGAAGTGCCCGATG, reverse: CCATCCACCGTCACCTTTAT) and *VEGF* (forward: GGAAGCCCAACGAAGTTATC, reverse: AACCCGCACATCTCATCAG). *Acidic ribosomal protein (RP)* mRNA was used as a reference for quantification (forward: AACATGTTGAACATCTCCCC, reverse: ATCTGCAGACAGACGCTGGC). All primers were purchased from Qiagen Inc (Valencia, CA). Relative transcript levels were presented as ''fold change'' in gene expression and calculated using the threshold cycle (Ct) and the formula below, where ''CD'' refers to CD chondrocytes, ''CP'' refers to CP chondrocytes, and ''RP'' refers to the acidic ribosomal protein: $x=2^{\Delta\Delta Ct}$, in which $\Delta\Delta Ct=\Delta E-\Delta C$, and $\Delta E=CtCP-CtRP$, and $\Delta C=CtCD-CtRP$. A $\Delta\Delta Ct<0$ was considered a decrease while a $\Delta\Delta Ct>0$ was considered an increase in gene expression.

Histology and immunohistochemistry

Scaffolds were collected and fixed in 10% phosphate buffer formalin, dehydrated in alcohol series, embedded in paraffin, and 5 μm-thick sections cut and stained with Hematoxylin &

Eosin (H&E). For immunohistochemistry sections were deparafinized, rehydrated, and immunostaining performed using antibodies specific for chick type X collagen with the Vectastain ABC kit (Vector Laboratories, Burlingame, CA) according to the manufacturer's instructions. Sections were counter stained with 1% alcian blue and Light Green. The stained sections were mounted under glass coverslips, and scanned on Scan Scope GL series optical microscope (Aperio, Bristol, UK) at 20X magnification.

Statistical analysis

All experiments were repeated 3 to 4 times and the mean and standard error of the mean were determined. Significant differences were assessed by ANOVA. A p-value refers to a comparison of a measured parameter in the experimental group with that of the appropriate control; significance was set at $p<0.05$.

RESULTS

Characterization of chitosan scaffolds

Images obtained by SEM (Figure 1) of cross-sections of sponges show a homogeneous pore size and distribution.

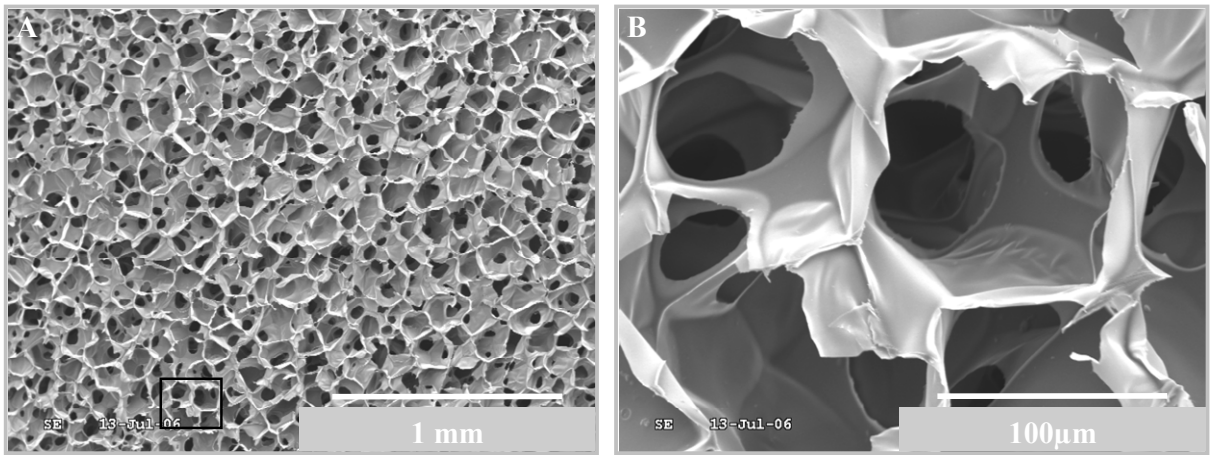

Figure 1. Homogeneous distribution of pores in chitosan sponges. SEM photomicrographs of cross sections of dehydrated chitosan sponges. Image A (lower magnification) shows high homogeneity in the size and distribution of pores and image B (higher magnification) shows the pores interconnectivity.

At higher magnification (500X) the interconnectivity can be observed among pores with an average pore size of 92±12 µm (Figure 1B). This pore dimension is considered to be within

the desired range for tissue engineering applications.[37,38]

Mechanical properties

The compression strength, elastic modulus, aggregate modulus and permeability of chitosan scaffolds while altered in the presence of cells did not approach the properties of chick growth plates (Table 2). Both chondrocytes/chitosan constructs and chitosan sponges alone had similar compression strength and permeability, while growth plate cartilage had significantly lower permeability.

Chitosan sponges without cells had the lowest elastic modulus values (7.4±2.0 kPa), and values for chondrocytes/chitosan constructs were different from the growth plates (2239±761 kPa). Interestingly, CD chondrocytes/chitosan constructs had an elastic modulus similar to the sponge itself while in the CP chondrocytes/chitosan constructs the elastic modulus increased approximately 2.5 fold (from 9.4 to 22 kPa). The aggregate modulus paralleled the elastic modulus.

Table II. Scaffolds properties

	D (μm)	σ (kPa)	E (kPa)	G (kPa)	P (m^4/Ns)
Chitosan	92 ± 12	5.0±0.6	7.4±2.0	83±21	27.4±21.5
CD + Chitosan	-	6.4±1.0	9.4±1.7	71±23	30.0±22.9
CP + Chitosan	-	7.3±2.4*	22.0±9.3**	143±6**	57.6±39.4
Growth Plate	-	-	2239±761	1249±1045	1.5±0.7

Chitosan – chitosan sponges kept in medium for 20 days at 37 ºC; CD + Chitosan - chitosan sponges in culture with caudal cells for 20 days; CD + Chitosan - chitosan sponges in culture with cephalic cells for 20 days; Growth plate – growth plate of a 6 weeks chicken tibia; D – Pore diameter; σ – Compression strength; E – Elastic Modulus at 30% strain; G – Aggregate Modulus; P – Permeability.

*Significantly different from Chitosan sample ($p < 0.05$); **significantly different from CD + chitosan and Chitosan samples ($p < 0.05$).

Chondrocyte behavior on chitosan sponges

To evaluate the chondrocytes behavior on chitosan sponges, we conducted different microscopic, histological and biochemical analyses.

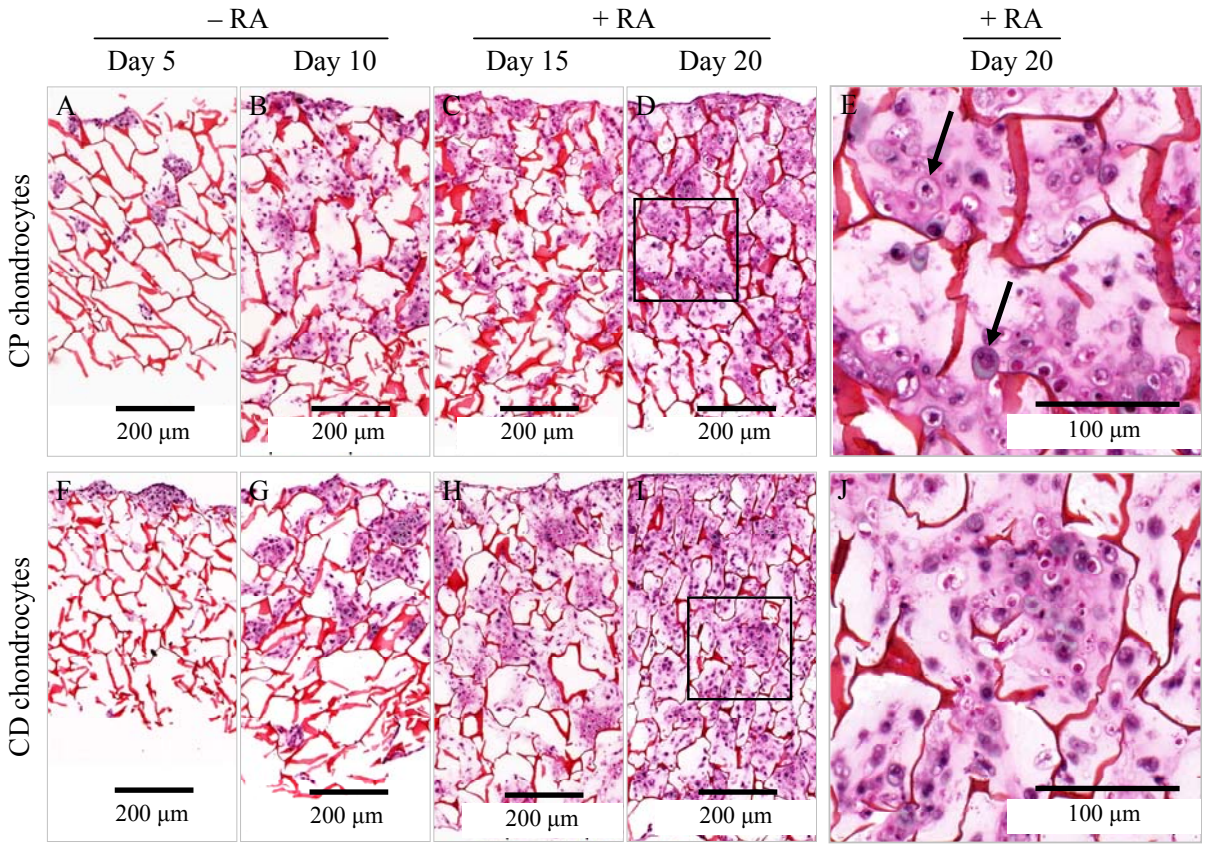

Figure 2. Chondrocytes completely fill chitosan sponges during the culture period. Photomicrographs of H&E staining of chitosan/chondrocytes constructs cultured for 20 days. A, B, C and D correspond to cross-sections of chitosan sponges culture with CP chondrocytes for 5, 10, 15 and 20 days respectively. A complete cross-section of each sponge is represented in the images. Photomicrographs F, G, H and I correspond to sponges cultured with CD chondrocytes for same time points. E and J are higher magnification images of the areas inside the square in D and I, respectively. Arrows in image E point to hypertrophic chondrocytes. At day 5, sponges appear thinner because during processing they did not maintain the original thickness in absence of cells/matrix.

Histological analyses clearly show attachment, proliferation and extracellular matrix synthesis by chondrocytes seeded in the chitosan sponges (Figure 2). At day 5, cells (purple color) migrating through connecting pores can be observed for both CP and CD chondrocytes. At day 10, chondrocytes have migrated well into the depth of chitosan sponges though they do not completely fill the pores. After 15 days in culture (5 days of treatment with RA), deposition of matrix can be observed (pink material between cells). After 20 days in culture (10 days of treatment with RA), both CP and CD chondrocytes deposited an abundant extracellular matrix filling the pores of sponges. At higher magnification hypertrophic CP chondrocytes (arrows in Figure 2E) can be observed while CD chondrocytes (Figure 2J) appear smaller.

Scanning electron photomicrographs (Figure 3) confirmed the observations from histological sections. Indeed at day 20, CP chondrocytes (Figures 3A and 3B) are totally embedded in a rich extracellular matrix completely changing the appearance of the scaffold (compare Figure 3 with Figure 1). The CD chondrocytes (Figures 3C and 3D) also filled the pores of the chitosan sponges with a compact matrix and no major differences can be observed between CP and CD scaffolds in these photomicrographs.

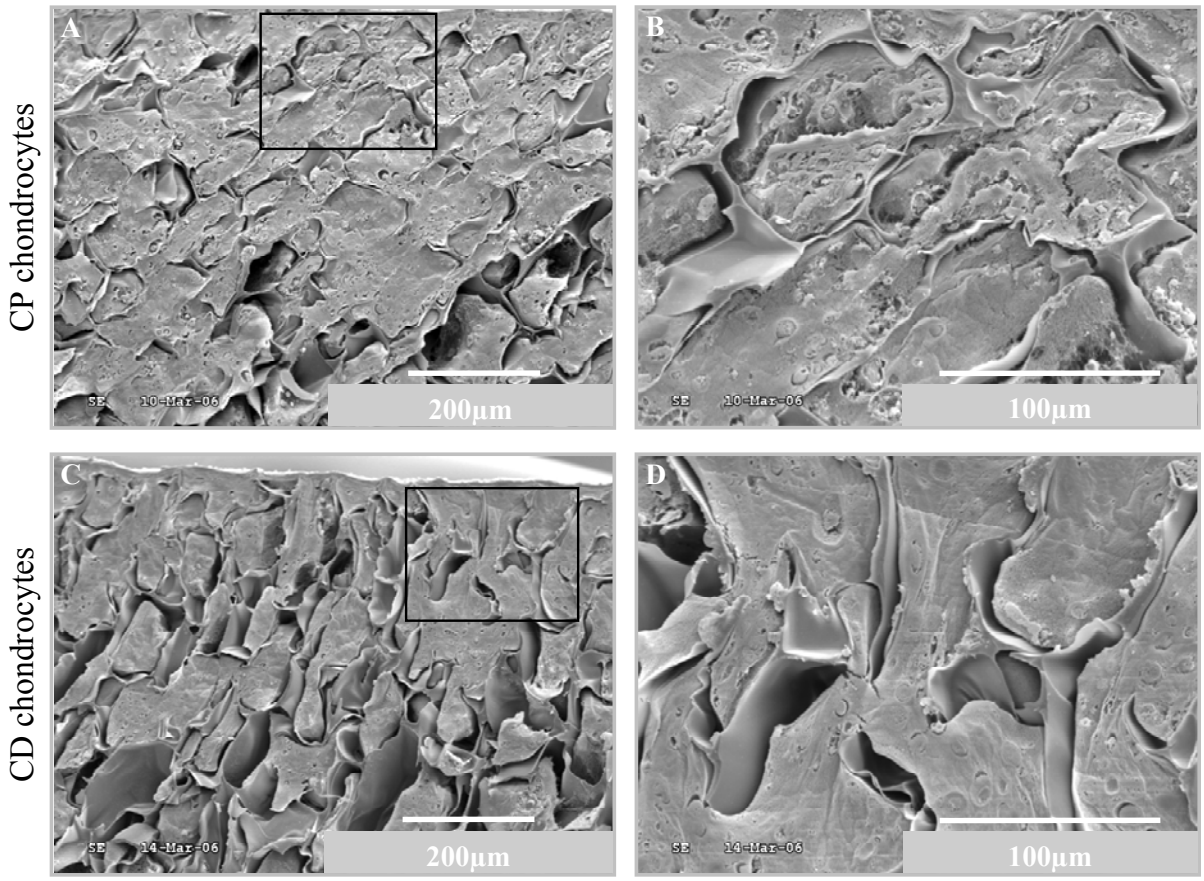

Figure 3. An abundant matrix fills the pores of chitosan sponges. SEM analyses of cross-sections of chitosan/chondrocytes constructs. At the end of the culture period, CP (A and B) and CD (C and D) chondrocytes migrated to the bottom of scaffolds and completely filled chitosan pores with a dense extra cellular matrix.

DNA measurements confirmed the increase in chondrocyte number over the culture period for both CP and CD cells. The average number of CD chondrocytes was higher than CP chondrocytes at every time point, although not statistically significant (Figure 4). With retinoic acid treatment, the proliferation rate of CP chondrocytes decreased. At the end of the culture period, the number of CD chondrocytes was slightly higher since they maintained or

even increased the proliferation rate in the presence of the retinoid.

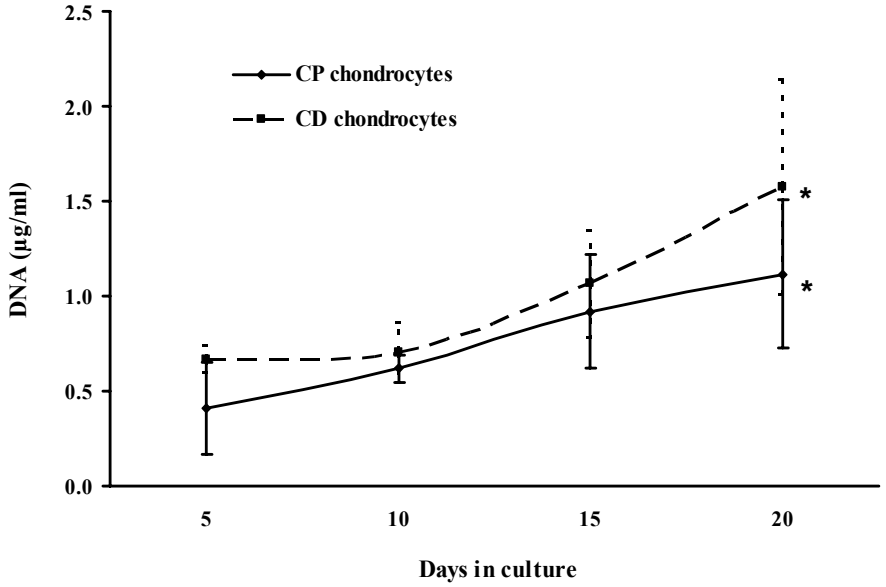

Figure 4. Increase in DNA content of cartilage/chitosan constructs during the culture period. DNA quantification was performed in samples collected after 5, 10, 15 and 20 days in culture. Note that an increase in DNA content corresponds to an increase in chondrocytes number over the culture period for both CP and CD cells. *Significantly different from respective sample at day 5 ($p< 0.05$).

To investigate chondrocyte maturation during the culture period we studied two markers of hypertrophy: alkaline phosphatase and type X collagen. In response to 10 days of RA treatment there was a significant increase in AP activity levels in both CP and CD chondrocytes (Figure 5). However, the levels of enzymatic activity were significantly higher in CP chondrocytes when compared to CD chondrocytes. Due to the long culture period, CD chondrocytes also responded to the retinoid, however their AP levels after 10 days of RA exposure (7±3 nmol/min/mg) were still 42 fold lower than AP activity levels in CP chondrocytes exposed to RA (299±109 nmol/min/mg), highlighting the different phenotypes of these cells.

Immunohistochemical analysis was conducted to detect the presence of type X collagen in the cartilage/chitosan scaffolds. As expected, in sponges seeded with CP chondrocytes, RA caused an increase in the level of type X collagen, evidenced by the strong brown color in Figure 6D. In sponges seeded with CD chondrocytes, type X collagen was not expressed at detectable levels even after 10 days of RA treatment (Figure 6H).

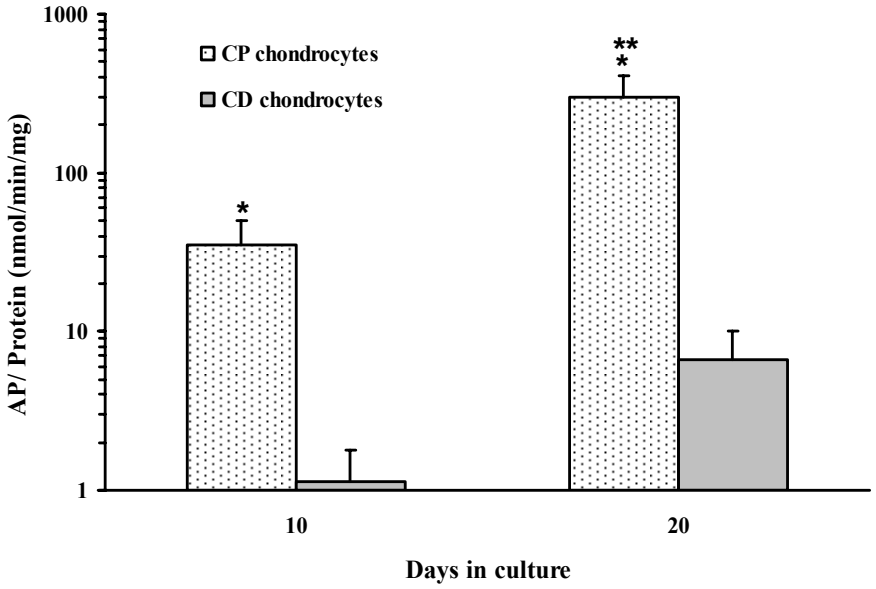

Figure 5. Retinoic acid induces alkaline phosphatase activity in CP chondrocytes. Samples were collected after 10 and 20 days in culture. Alkaline phosphatase (AP) activity was normalized to the total protein content of each sample. The AP levels increased with time, in both CP and CD chondrocytes. *Significantly different from CD chondrocytes at same time point ($p < 0.05$). **Significantly different from same sample at day 10 ($p < 0.05$).

Counter staining with alcian blue and Light Green allowed visualization of proteoglycan deposition and chitosan, respectively. Although we did not quantify the staining, an intense blue color can be observed in CP chondrocytes exposed to RA for 10 days, suggesting increased proteoglycan synthesis in these samples (compare Figure 6C with Figures 6A and 6G).

To further characterize the phenotype of chondrocytes grown on the chitosan scaffold, we conducted real time RT-PCR analyses. Results obtained are semi-quantitative and presented as a "fold change" in mRNA levels in CP chondrocytes when compared to CD cells (Figure 7). A value higher than 1, corresponds to a higher gene expression by CP chondrocytes. As expected, except for *type II collagen*, all genes studied were expressed at higher levels in CP chondrocytes than in CD chondrocytes. In response to RA treatment, *type X collagen* expression decreased (early hypertrophic marker) and *AP* gene expression increased (late hypertrophic marker). Values obtained for *runx2*, *type II collagen* and *VEGF* are around 1; no significant differences were observed between 10 and 20 days in culture.

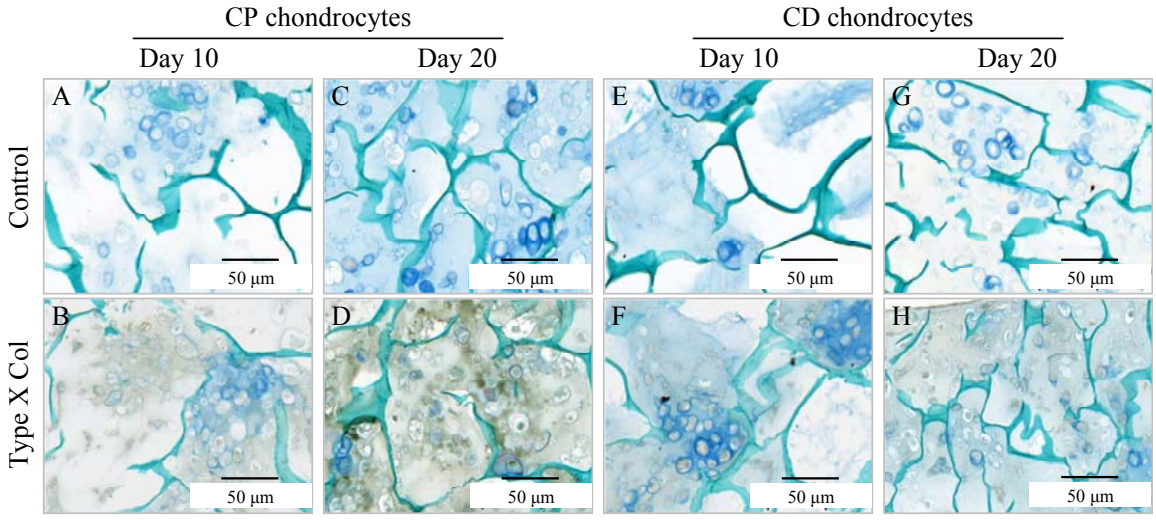

Figure 6. Retinoic acid increases type X collagen in scaffolds seeded with CP chondrocytes. Immunohistochemical analyses of type X collagen was performed on deparafinized sections of CP (A, B, C and D) and CD (E, F, G and H) chondrocytes. Sections were counterstained with alcian blue to visualize proteoglycans and Light Green to label the chitosan walls. Photomicrographs A, B, E and F correspond to 10 days in culture and pictures C, D, G and H corresponds to 20 days in culture. Upper panels show controls (incubated with pre-immune serum) of respective bottom panel. Type X collagen is evidenced by the presence of the brown color.

DISCUSSION

Chitosan has been used as biomaterial over the last decades and proved to be biocompatible and biodegradable.[39-41] Studies using low DA chitosan scaffolds showed that this material allows osteoblast[21,42] and articular chondrocyte[21,43] attachment and proliferation. The goal of the current study was to test the ability of this natural polymer to support proliferation and maturation of transient cartilage cells, the early steps in endochondral bone formation. The original chitosan powder from France Chitine had a DA of ≅30% and it was deacetylated to a DA of 4.23±0.46%, using different temperature cycles. The deacetylation of chitosan using alkali solutions is known to lead to a decrease in both average molecular weight (Mw) and intrinsic viscosity (η) as a result of the scission of glycosidic linkages and end-group peeling. Chitosan with a DA of 4% was previously reported to enable the attachment and proliferation of both osteoblasts and rat bone marrow stromal cells.[33] Therefore, chitosan with this DA was selected to produce sponges. The 3D homogeneous structures prepared presented highly interconnected pores of average size shown to allow robust chondrocyte proliferation and metabolic activity.[44] RA was used to induce chondrocyte maturation into hypertrophic cells.

RA is one of the more biologically active derivatives of retinol (vitamin A) and a well-known regulator of cartilage and skeletal formation.[45-47] We cultured both cells representative of a transient cartilage phenotype, CP chondrocytes, and cells that maintain a more stable phenotype, CD chondrocytes. Caudal cells do not readily undergo hypertrophy in response to RA and therefore, were used as a "permanent" cartilage control.

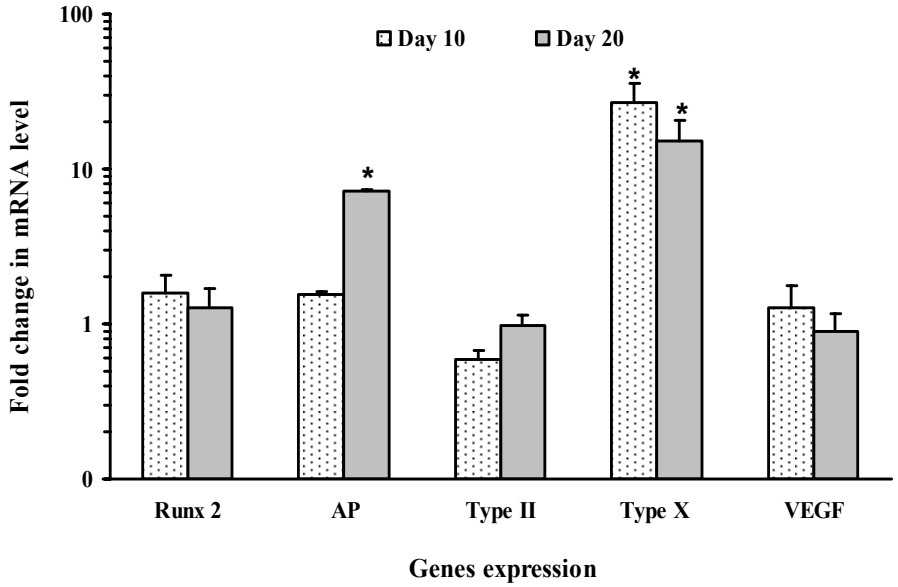

Figure 7. Gene expression profile of CP chondrocytes cultured in chitosan sponges. Real time RT-PCR semi-quantitative results are presented as fold change in mRNA levels of CP chondrocytes when compared to CD cells. Samples with CP and CD chondrocytes were both analyzed and a fold change higher than 1, corresponds to a higher gene expression by CP chondrocytes. *Significantly different from CD chondrocytes at same time point ($p < 0.05$).

In 10 days, both CP and CD chondrocytes migrated into pores deep in the chitosan sponges completely obliterating some spaces, attesting to the excellent interconnectivity between the pores. Cell proliferation continued for both CD and CP chondrocytes even during treatment with RA, though CP cells showed a slight decrease after day 15. According to Gentili *et al.*[48] chondrocytes proliferation stops only after onset of mineralization has been started. However, in our studies we did not supplement the media with β-glycerophosphate or another phosphate source. Thus our chondrocytes while expressing high AP levels, did not deposit mineral (micro computerized tomography results not shown).

Cells proliferation and matrix deposition increased in both CD and CP chondrocytes seeded scaffolds over the culture period. It was expected that such a robust synthesis of matrix would

drastically change the mechanical properties of the chitosan sponges. However, while elastic modulus, a measure of stiffness, increased 3 fold for chitosan sponges seeded with CP chondrocytes, it did not change significantly for chitosan sponges seeded CD chondrocytes. Therefore, more than the quantity, it was the quality of the matrix deposited that mostly affected stiffness of chondrocyte/chitosan constructs. Indeed, type X collagen as been reported to increase the matrix stiffness by Naumann *et al*.[49] However, the stiffness of CP chondrocytes/chitosan constructs is hundred fold lower than the stiffness of chicken growth plates. Since ceramic phases present higher compression strength than unmineralized tissues, we believe that we would observe different mechanical properties had the cultured chondrocytes been allowed to mineralize the extracellular matrix as it occurs in the native growth plate.

Although both CP and CD chondrocytes responded to RA by increasing matrix deposition, the nature of this matrix was found to be dependent on the type of cell. CP cells responded to the retinoid by expressing the hypertrophic phenotype, characterized by the presence of type X collagen in their matrix and increased AP activity. Indeed, all regulators or markers of hypertrophy studied (*runx 2*, *VEGF*, *type X collagen*, *AP*) were expressed at significantly higher levels in the CP cells when compared to the CD chondrocytes, supporting the different phenotype of these cell populations. However, overtime we observed a decrease in *type X collagen* expression and an increase in *AP* expression in CP cells. These results agree with *in vivo* data showing that *type X collagen* expression occurs in early hypertrophic chondrocytes while *AP*, a later maturation marker involved in matrix mineralization is expressed by terminally differentiated chondrocytes in the calcified region of the growth plate.[50-52]

Several studies have demonstrated that chitosan supports the articular chondrocyte phenotype and activity. The study of Lu *et al*.[23] showed that chitosan injected into the knee articular cavity of rats caused a significant increase in the density of chondrocytes in the knee articular cartilage. Also, abundant cartilage extracellular matrix protein[43] was obtained after injecting nude mice subcutaneously with an in situ-gelling chitosan solution cultured with chondrocytes. Furthermore, when pig chondrocytes were cultured on porous chitosan scaffolds they were able to proliferate and to spread into the sponges; with larger interconnected pores improving the cellularity and matrix content.[44] Another study revealed that primary chondrocytes cultured on chondroitin 4-sulfate/chitosan maintained the synthesis of cartilage-specific collagens.[17] Similar results were achieved using chitosan films seeded with both human osteoblasts and chondrocytes.[21] Osteoblasts were able to spread and to

express *type I collagen* whereas chondrocytes expressed *type II collagen*, suggesting that a chitosan scaffold is able to maintain these cells original phenotype.

Amaral *et al*.[53] investigated human osteoblast behavior in chitosan scaffolds similar to those used in the present study. They found that osteoblasts attach well and spread on chitosan sponges, displaying long cell filopodia and numerous cell-to-cell contacts. A major limitation in tissue engineering has been the availability of nutrients and oxygen once the construct reaches a critical mass. And in that aspect osteoblasts are particularly susceptible.[54-57] Cartilage (growth plate and articular cartilage) however, is characterized by large avascular regions and excellent adaptation to hypoxic conditions.[58,59] In fact, evidence supports the role of low oxygen levels in chondrocyte differentiation and endochondral bone formation.[60] These properties provide support to the bone tissue engineering approach here investigated, which explores the endochondral ossification pathway for the correction of extensive bone defects.

All the studies mentioned earlier used chitosan as a scaffold for either articular cartilage or bone. Here we reported the use of chitosan sponges as a template for transient cartilage and the creation of an improved osteoinductive scaffold for bone regeneration. Indeed, hypertrophic chondrocytes secrete factors capable of inducing osteoblast and osteoclast activity, as well as vascularization.[28,61-64] All these different cell types and their activity are necessary and responsible for endochondral bone formation. Indeed, parallel studies conducted in our laboratory show the ability of this transient cartilage/chitosan constructs to induce endochondral bone formation in the subcutaneous region of nude mice.[65]

CONCLUSIONS

The use of osteoblasts or osteoprogenitor cells to promote bone regeneration is the method most commonly exploited in current tissue engineering approaches. However, nature mostly uses the endochondral ossification pathway during bone formation, growth and healing after fracture. In addition to these considerations, there are numerous other advantages to explore the endochondral pathway for bone tissue engineering. Chondrocytes are resistant to low oxygen levels and can induce vascular invasion and osteogenesis. In this study, chitosan sponges served as excellent support for chondrocyte proliferation and intense matrix deposition. As a result of the activity of the transient cartilage cells, the mechanical properties of the chitosan scaffold changed drastically and favorably. These scaffolds can now be used

as osteoinductive grafts *in vivo*, inducing and remodeling into bone, mimicking the natural process of endochondral ossification.

ACKNOWLEDMENS

This work was supported by the Luso-American Foundation and PRODEP III from Portugal, by the American Association of Orthodontics Foundation and NIDCR grant 5K08DE017426. The authors thank Ms. Gloria Turner, Department of Pathology at New York University College of Dentistry, for her important assistance in preparation of samples for histology and immunohistochemistry. Mechanical tests were performed at the NIH sponsored Musculoskeletal Repair and Regeneration Core Center at the Hospital for Special Surgery (AR046121).

REFERENCES

1. Steinemann SG. Metal implants and surface reactions. Injury 1996;27 Suppl 3:SC16-22.
2. Disegi JA, Eschbach L. Stainless steel in bone surgery. Injury 2000;31 Suppl 4:2-6.
3. Reitman RD, Emerson R, Higgins L, Head W. Thirteen year results of total hip arthroplasty using a tapered titanium femoral component inserted without cement in patients with type C bone. Journal of Arthroplasty 2003;18(7):116-121.
4. Epinette JA, Manley MT, D'Antonio JA, Edidin AA, Capello WN. A 10-year minimum follow-up of hydroxyapatite-coated threaded cups: clinical, radiographic and survivorship analyses with comparison to the literature. J Arthroplasty 2003;18(2):140-8.
5. Xynos ID, Hukkanen MV, Batten JJ, Buttery LD, Hench LL, Polak JM. Bioglass 45S5 stimulates osteoblast turnover and enhances bone formation *In vitro*: implications and applications for bone tissue engineering. Calcif Tissue Int 2000;67(4):321-9.
6. Barrias CC, Ribeiro CC, Barbosa MA. Adhesion and proliferation of human osteoblastic cells seeded on injectable hydroxyapatite microspheres. Bioceramics, Vol 16 2004;254-2:877-880.
7. Saito N, Takaoka K. New synthetic biodegradable polymers as BMP carriers for bone tissue engineering. Biomaterials 2003;24(13):2287-2293.
8. Suzuki T, Kawamura H, Kasahara T, Nagasaka H. Resorbable poly-L-lactide plates and screws for the treatment of mandibular condylar process fractures: a clinical and radiologic follow-up study. J Oral Maxillofac Surg 2004;62(8):919-24.
9. Sittinger M, Reitzel D, Dauner M, Hierlemann H, Hammer C, Kastenbauer E, Planck H, Burmester GR, Bujia J. Resorbable polyesters in cartilage engineering: affinity and biocompatibility of polymer fiber structures to chondrocytes. J Biomed Mater Res 1996;33(2):57-63.
10. Vaccaro AR, Singh K, Haid R, Kitchel S, Wuisman P, Taylor W, Branch C, Garfin S. The use of

bioabsorbable implants in the spine. The Spine Journal 2003;3:227–237.

11. Jianqi H, Hong H, Lieping S, Genghua G. Comparison of calcium alginate film with collagen membrane for guided bone regeneration in mandibular defects in rabbits. J Oral Maxillofac Surg 2002;60(12):1449-54.
12. Chan C, Thompson I, Robinson P, Wilson J, Hench L. Evaluation of Bioglass/dextran composite as a bone graft substitute. Int J Oral Maxillofac Surg 2002;31(1):73-7.
13. Mukherjee DP, Tunkle AS, Roberts RA, Clavenna A, Rogers S, Smith D. An animal evaluation of a paste of chitosan glutamate and hydroxyapatite as a synthetic bone graft material. Journal of Biomedical Materials Research Part B-Applied Biomaterials 2003;67B(1):603-609.
14. Sashiwa H, Aiba S. Chemically modified chitin and chitosan as biomaterials. Progress in Polymer Science 2004;29(9):887-908.
15. Hoekstra A, Struszczyk H, Kivekas O. Percutaneous microcrystalline chitosan application for sealing arterial puncture sites. Biomaterials 1998;19(16):1467-71.
16. Lee KY, Ha WS, Park WH. Blood compatibility and biodegradability of partially N-acylated chitosan derivatives. Biomaterials 1995;16(16):1211-1216.
17. Suh JK, Matthew HW. Application of chitosan-based polysaccharide biomaterials in cartilage tissue engineering: a review. Biomaterials 2000;21(24):2589-98.
18. Hirano S, Tsuchida H, Nagao N. N-acetylation in chitosan and the rate of its enzymic hydrolysis. Biomaterials 1989;10(8):574-576.
19. Prashanth KVH, Tharanathan RN. Chitin/chitosan: modifications and their unlimited application potential--an overview. Trends in Food Science & Technology 2007;18(3):117-131.
20. Chellat F, Tabrizian M, Dumitriu S, Chornet E, Hilaire C, Yahia R. Study of biodegradation behavior of chitosan-xanthan microspheres in simulated physiological media. Journal of Biomedical Materials Research 2000;53(5):592-599.
21. Lahiji A, Sohrabi A, Hungerford DS, Frondoza CG. Chitosan supports the expression of extracellular matrix proteins in human osteoblasts and chondrocytes. J Biomed Mater Res 2000;51(4):586-95.
22. Nettles DL, Elder SH, Gilbert JA. Potential use of chitosan as a cell scaffold material for cartilage tissue engineering. Tissue Engineering 2002;8(6):1009-1016.
23. Lu JX, Prudhommeaux F, Meunier A, Sedel L, Guillemin G. Effects of chitosan on rat knee cartilages. Biomaterials 1999;20(20):1937-44.
24. Abe M, Takahashi M, Tokura S, Tamura H, Nagano A. Cartilage-scaffold composites produced by bioresorbable beta-chitin sponge with cultured rabbit chondrocytes. Tissue Engineering 2004;10(3-4):585-594.
25. Sechriest VF, Miao YJ, Niyibizi C, Westerhausen-Larson A, Matthew HW, Evans CH, Fu FH, Suh JK. GAG-augmented polysaccharide hydrogel: a novel biocompatible and biodegradable material to support chondrogenesis. J Biomed Mater Res 2000;49(4):534-41.
26. Rajpurohit R, Koch CJ, Tao Z, Teixeira CM, Shapiro IM. Adaptation of chondrocytes to low oxygen tension: relationship between hypoxia and cellular metabolism. J Cell Physiol 1996;168(2):424-32.
27. Maes C, Carmeliet P, Moermans K, Stockmans I, Smets N, Collen D, Bouillon R, Carmeliet G. Impaired angiogenesis and endochondral bone formation in mice lacking the vascular endothelial growth factor

isoforms VEGF164 and VEGF188. Mech Dev 2002;111(1-2):61-73.

28. Petersen W, Tsokos M, Pufe T. Expression of VEGF121 and VEGF165 in hypertrophic chondrocytes of the human growth plate and epiphyseal cartilage. J Anat 2002;201(2):153-7.
29. Pullig O, Weseloh G, Ronneberger D, Kakonen S, Swoboda B. Chondrocyte differentiation in human osteoarthritis: expression of osteocalcin in normal and osteoarthritic cartilage and bone. Calcif Tissue Int 2000;67(3):230-40.
30. Hashimoto S, Ochs RL, Rosen F, Quach J, McCabe G, Solan J, Seegmiller JE, Terkeltaub R, Lotz M. Chondrocyte-derived apoptotic bodies and calcification of articular cartilage. Proceedings of the National Academy of Sciences of the United States of America 1998;95(6):3094-3099.
31. Pullig O, Weseloh G, Gauer S, Swoboda B. Osteopontin is expressed by adult human osteoarthritic chondrocytes: protein and mRNA analysis of normal and osteoarthritic cartilage. Matrix Biol 2000;19(3):245-55.
32. Eerola I, Salminen H, Lammi P, Lammi M, von der Mark K, Vuorio E, Saamanen AM. Type X collagen, a natural component of mouse articular cartilage: association with growth, aging, and osteoarthritis. Arthritis Rheum 1998;41(7):1287-95.
33. Amaral IF, Sampaio P, Barbosa MA. Three-dimensional culture of human osteoblastic cells in chitosan sponges: the effect of the degree of acetylation. J Biomed Mater Res A 2006;76(2):335-46.
34. Mow VC, Kuei SC, Lai WM, Armstrong CG. Biphasic creep and stress relaxation of articular cartilage in compression? Theory and experiments. J Biomech Eng 1980;102(1):73-84.
35. Iwamoto M, Shapiro IM, Yagami K, Boskey AL, Leboy PS, Adams SL, Pacifici M. Retinoic acid induces rapid mineralization and expression of mineralization-related genes in chondrocytes. Exp Cell Res 1993;207(2):413-20.
36. Teixeira CC, Hatori M, Leboy PS, Pacifici M, Shapiro IM. A rapid and ultrasensitive method for measurement of DNA, calcium and protein content, and alkaline phosphatase activity of chondrocyte cultures. Calcif Tissue Int 1995;56(3):252-6.
37. Nehrer S, Breinan HA, Ramappa A, Young G, Shortkroff S, Louie LK, Sledge CB, Yannas IV, Spector M. Matrix collagen type and pore size influence behaviour of seeded canine chondrocytes. Biomaterials 1997;18(11):769-76.
38. Karande TS, Ong JL, Agrawal CM. Diffusion in musculoskeletal tissue engineering scaffolds: design issues related to porosity, permeability, architecture, and nutrient mixing. Ann Biomed Eng 2004;32(12):1728-43.
39. VandeVord PJ, Matthew HW, DeSilva SP, Mayton L, Wu B, Wooley PH. Evaluation of the biocompatibility of a chitosan scaffold in mice. J Biomed Mater Res 2002;59(3):585-90.
40. Hong Y, Song H, Gong Y, Mao Z, Gao C, Shen J. Covalently crosslinked chitosan hydrogel: Properties of *in vitro* degradation and chondrocyte encapsulation. Acta Biomaterialia 2007;3(1):23-31.
41. Ho M, Wang D, Hsieh H, Liu HC, Hsien TY, Lai JY, Hou LT. Preparation and characterization of RGD-immobilized chitosan scaffolds. Biomaterials 2005;26(16):3197-3206.
42. Amaral IF, Cordeiro AL, Sampaio P, Barbosa MA. Attachment, spreading and short-term proliferation of human osteoblastic cells cultured on chitosan films with different degrees of acetylation. J. Biomater. Sci. Polymer Edn 2007;18(4):469-485.

43. Hoemann CD, Sun J, Legare A, McKee MD, Buschmann MD. Tissue engineering of cartilage using an injectable and adhesive chitosan-based cell-delivery vehicle. Osteoarthritis Cartilage 2005;13(4):318-29.
44. Griffon DJ, Sedighi MR, Schaeffer DV, Eurell JA, Johnson AL. Chitosan scaffolds: interconnective pore size and cartilage engineering. Acta Biomater 2006;2(3):313-20.
45. Underhill TM, Weston AD. Retinoids and their receptors in skeletal development. Microscopy Research and Technique 1998;43(2):137-155.
46. Cohen AJ, Lassova L, Golden EB, Niu Z, Adams SL. Retinoids directly activate the collagen X promoter in prehypertrophic chondrocytes through a distal retinoic acid response element. J Cell Biochem 2006;99(1):269-78.
47. Pacifici M, Golden EB, Iwamoto M, Adams SL. Retinoic acid treatment induces type X collagen gene expression in cultured chick chondrocytes. Exp Cell Res 1991;195(1):38-46.
48. Gentili C, Bianco P, Neri M, Malpeli M, Campanile G, Castagnola P, Cancedda R, Cancedda FD. Cell-Proliferation, Extracellular-Matrix Mineralization, and Ovotransferrin Transient Expression during in-Vitro Differentiation of Chick Hypertrophic Chondrocytes into Osteoblast-Like Cells. Journal of Cell Biology 1993;122(3):703-712.
49. Naumann A, Dennis JE, Awadallah A, Carrino DA, Mansour JM, Kastenbauer E, Caplan AI. Immunochemical and mechanical characterization of cartilage subtypes in rabbit. J Histochem Cytochem 2002;50(8):1049-58.
50. Wang W, Kirsch T. Retinoic acid stimulates annexin-mediated growth plate chondrocyte mineralization. J Cell Biol 2002;157(6):1061-9.
51. Whyte MP. Hypophosphatasia and the role of alkaline phosphatase in skeletal mineralization. Endocr Rev 1994;15(4):439-61.
52. Lewinson D, Toister Z, Silbermann M. Quantitative and distributional changes in the activity of alkaline phosphatase during the maturation of cartilage. J. Histochem. Cytochem. 1982;30(3):261-269.
53. Amaral IF, Sampaio P, Barbosa MA. Three-dimensional culture of human osteoblastic cells in chitosan sponges: the effect of the degree of acetylation. J Biomed Mater Res A 2005;76(2):335.
54. Park JH, Park BH, Kim HK, Park TS, Baek HS. Hypoxia decreases Runx2/Cbfa1 expression in human osteoblast-like cells. Mol Cell Endocrinol 2002;192(1-2):197-203.
55. Utting JC, Robins SP, Brandao-Burch A, Orriss IR, Behar J, Arnett TR. Hypoxia inhibits the growth, differentiation and bone-forming capacity of rat osteoblasts. Exp Cell Res 2006;312(10):1693-702.
56. Warren SM, Steinbrech DS, Mehrara BJ, Saadeh PB, Greenwald JA, Spector JA, Bouletreau PJ, Longaker MT. Hypoxia regulates osteoblast gene expression. J Surg Res 2001;99(1):147-55.
57. Salim A, Nacamuli RP, Morgan EF, Giaccia AJ, Longaker MT. Transient changes in oxygen tension inhibit osteogenic differentiation and Runx2 expression in osteoblasts. J Biol Chem 2004;279(38):40007-16.
58. Vu TH, Shipley JM, Bergers G, Berger JE, Helms JA, Hanahan D, Shapiro SD, Senior RM, Werb Z. MMP-9/gelatinase B is a key regulator of growth plate angiogenesis and apoptosis of hypertrophic chondrocytes. Cell 1998;93(3):411-22.
59. Skawina A, Litwin JA, Gorczyca J, Miodonski AJ. The vascular system of human fetal long bones: a scanning electron microscope study of corrosion casts. J Anat 1994;185 (Pt 2):369-76.

60. Pfander D, Cramer T, Schipani E, Johnson RS. HIF-1alpha controls extracellular matrix synthesis by epiphyseal chondrocytes. J Cell Sci 2003;116(Pt 9):1819-26.
61. Deckers MM, Karperien M, van der Bent C, Yamashita T, Papapoulos SE, Lowik CW. Expression of vascular endothelial growth factors and their receptors during osteoblast differentiation. Endocrinology 2000;141(5):1667-74.
62. Gerber HP, Vu TH, Ryan AM, Kowalski J, Werb Z, Ferrara N. VEGF couples hypertrophic cartilage remodeling, ossification and angiogenesis during endochondral bone formation. Nat Med 1999;5(6):623-8.
63. Nakagawa M, Kaneda T, Arakawa T, Morita S, Sato T, Yomada T, Hanada K, Kumegawa M, Hakeda Y. Vascular endothelial growth factor (VEGF) directly enhances osteoclastic bone resorption and survival of mature osteoclasts. FEBS Lett 2000;473(2):161-4.
64. Pfander D, Kortje D, Zimmermann R, Weseloh G, Kirsch T, Gesslein M, Cramer T, Swoboda B. Vascular endothelial growth factor in articular cartilage of healthy and osteoarthritic human knee joints. Ann Rheum Dis 2001;60(11):1070-1073.
65. Oliveira SM, Turner G, Mijares D, Amaral IF, Barbosa MA, Teixeira CC. Engineering endochondral bone: *In vivo* studies. Tissue Engineering, Part A, In Press.

Chapter VI

Engineering endochondral bone: *in vivo* studies

S.M. Oliveira[1,2,3,4], D.Q. Mijares[4], G. Turner[4], I.F. Amaral[2], M.A. Barbosa[2,3], C.C. Teixeira[4],

[1]ESTV – Escola Superior de Tecnologia de Viseu, Dep. de Eng. Mecânica e Gestão Industrial, Campus Politécnico de Repeses, 3504-510 Viseu, Portugal;

[2]INEB – Instituto de Engenharia Biomédica, Divisão de biomateriais, Rua do Campo Alegre 823, 4150-180 Porto, Portugal;

[3]FEUP – Faculdade de Engenharia Universidade do Porto, Dep. de Eng. Metalúrgica e de Materiais, Rua Roberto Frias, 4200-465 Porto, Portugal;

[4]NYUCD – New York University College of Dentistry, Department of Basic Science and Craniofacial Biology and Department of Biomaterials and Biomimetics, 345 E. 24th Street New York, NY 10010.

ABSTRACT

The use of biomaterials to replace lost bone has been a common practice for decades. More recently, the demands for bone repair and regeneration have pushed research into the use of cultured cells and growth factors in association with these materials. In this paper we describe how a transient cartilage scaffold can induce endochondral ossification, a novel approach to engineer new bone. Chondrocytes/chitosan scaffolds (both a transient cartilage scaffold - experimental - and a permanent cartilage scaffold - control), were prepared and implanted subcutaneously in nude mice. Bone formation was evaluated over a period of 5 months. Mineralization was assessed by Faxitron, micro computed tomography, backscatter electrons, and Fourier transform infrared spectroscopy analyses. Histological analysis provided further information on tissue changes in and around the implanted scaffolds. The deposition of ectopic bone was detected in experimental implants as early as 1 month after implantation although it was only observed in few areas of the surface. After 3 months, bone trabeculae and bone marrow cavities were formed inside the scaffolds. The bone deposited was similar to the bone present in the mice vertebra. Interestingly, no bone formation was observed in control implants. In conclusion, an engineered transient cartilage template carries all the signals necessary to induce endochondral bone formation *in vivo*.

Keywords: Chitosan sponges, chondrocytes, growth cartilage, endochondral ossification, bone regeneration.

INTRODUCTION

With increasing time of life-expectation, the economic impact of musculoskeletal diseases, may now exceed 2.5% of the Gross National Product in the United States.[1] Among these diseases, problems related to bone loss are one of the major causes of disability. To replace lost bone, surgeons use autografts, considered the ideal grafting material. This approach presents disadvantages such as donor site morbidity and limited supply, which in most of cases is insufficient.[2] Due to these limitations, it is imperative to find new alternatives to autografts. Allografts and xenografs are reasonable substitutes but they also have serious limitations like the risk of rejection or disease transmission. To overcome these shortcomings several bone grafting materials have been engineered including ceramics, metals, synthetic and natural polymers. In most cases, materials are implanted into surgically created bone defects, and new bone grows on their surfaces and within their matrices. Under these conditions, it is believed that the bone is formed by osteoblasts that migrated from the adjacent, original bone and marrow cavities, a mechanism that is referred to as osteoconduction. Although this osteointegration is important and essential, there are situations (e.g. large defects) where the scaffolds, besides providing the template for tissue regeneration, need to be osteoindutive, i.e. stimulate the migration of undifferentiated cells and induce their differentiation into active osteoblasts in order to promote *de novo* bone formation. To improve the osteoinductive properties of grafting materials they have been combined with growth factors and different cells types with variable results, depending on the host regenerative capability.[3,4] Therefore, osteoinductive approaches are crucial when the bone regenerative ability is diminished or lost. Here we propose a novel approach in bone tissue engineering and the creation of an improved osteoinductive material for bone regeneration.

In the body, cartilaginous tissues can be divided into permanent and transient. While having the same embryonic origin, permanent and transient cartilage follow distinct differentiation pathways, fulfill different functions and ultimately as their names suggest have different fates. Articular, tracheal, and other related cartilage structures are classified as permanent cartilage. The chondrocytes in these structures maintain a relatively stable phenotype and persist for many years[5]. In contrast, most of the embryonic cartilaginous skeleton, the epiphyseal growth

plates of long bones, the cartilaginous callus formed at fracture sites, and the tissue created during distraction osteogenesis consist of transient cartilage.[6,7] This transient cartilage is gradually replaced by bone through a series of maturational changes during the process of endochondral bone formation. Indeed, this is the mechanism responsible for formation of most of our skeleton, and for postnatal growth.

Surprisingly, except for few reports, the bone tissue engineering field has focused on generating bone directly from osteoprogenitor cells or osteoblasts. Montufar-Solis *et al.*[8] prepared aggregates of mouse embryonic limb cells that after implantation in mice induced endochondral bone formation. Indeed, the endochondral pathway for bone formation can be activated using biomaterials carrying mesenchymal stem cells (MSCs),[9] bone morphogenetic proteins (BMPs)[10], or plasmid DNA encoding for BMP's.[11,12] To date, only Alsberg *et al.*[13] deliberately explored the endochondral pathway by implanting in mice, articular chondrocytes mixed with calvarial osteoblasts using an alginate carrier. *In vivo*, the tissue organized in a manner similar to a growth plate. This effect is not totally surprising if one considers that hypertrophic chondrocytes secrete factors capable of inducing vascularization, osteoblast and osteoclast activity.[14-17] The interplay of these different cell types is required for endochondral bone formation. Therefore, in the current work, we created a transient cartilage scaffold as a template for *in vivo* endochondral ossification. We tested the hypothesis that this transient cartilage, as an osteoinductive scaffold, carries all the signals necessary to induce new bone formation once implanted *in vivo*, even subcutaneously.

MATERIALS AND METHODS

In vitro studies

Transient cartilage scaffolds

The chondrocyte/chitosan scaffolds used in this work were characterized extensively in previous chapter.[18] Briefly, chitosan sponges were prepared from a 2% (w/v) chitosan solution by a freeze/drying process and then cut in small pieces (4x4x1 mm^3). Cephalic (CP) and caudal (CD) chondrocytes, isolated from the upper and lower regions of sternum of 14 days chicken embryos were allowed to proliferate in 100 mm dishes for 7 days in Dulbecco's modified high glucose Eagle's medium (DMEM) containing 10% NU Serum and 100 U/ml of penicillin/streptomycin (Fisher Scientic, Fairlawn, NJ), before being seeded into the chitosan sponges and cultured for 20 days at 37 ºC and 5% CO_2 in the same conditions. During the last

10 days, cultures were treated with 100 nM all-trans retinoic acid (RA) in order to induce chondrocyte maturation and matrix deposition. Prior to implantation, at day 20, alkaline phosphatase (AP) activity and protein content were measured following the protocols described in previous chapter, to confirm maturation.

***In vivo* studies**

Surgical Procedures

Adult male athymic NCr-nu/nu mice (Charles River Laboratories, NY, US) were used as surgical recipients. The animal experiments were conducted according to the guidelines of the Institutional Animal Care and Use Committee (IACUC) of New York University. Briefly, mice were received one week before scheduled surgery and feed a regular diet and sterile water, ad libidum. After surgery and for one week, trimethropim and sulfamethoxazole (20 mg/l and 100 mg/l, respectively) were added to sterile drinking water. Surgeries were performed under strict aseptic and warm conditions, with general anaesthesia produced by intraperitoneal injection of ketamine (80 mg/kg) and xylazine (10 mg/kg). Lateral longitudinal skin incisions were made in both sides of the mice dorsum and a subcutaneous pocket (1 to 1.5 cm) was created for implantation of the chondrocytes/chitosan scaffolds. On the right side, we implanted the scaffolds seeded with cephalic chondrocytes (experimental implant) whereas the left side received the scaffolds seeded with caudal chondrocytes (control). Incisions were closed with surgical staples. Two or three sponges were implanted on each side. Results shown represent three independent experiments, different surgeries, using three independent groups of implants (i.e. sponges hydrated in different periods, primary cells harvested from different chicken embryos, and mice received at different times). In the first experiment 11 mice received implants, in the second and third experiments 14 and 22 mice were implanted respectively. All animals, except 3 mice that did not recover from anesthesia, survived the surgical procedures.

Euthanasia and samples collection

The mice were sacrificed at 1, 2, 3, 4 and 5 months postoperatively and implants and surrounding tissues harvested. Briefly, animals were exposed to a gas mixture of 30% of CO_2 and 70% of O_2 for 1 min followed by CO_2 100% during 4 minutes until no signal of breathing was detected. Tissue/samples were collected and immediately immersed in 10% phosphate buffer formalin for future analyses.

Faxitron and micro computed tomography (microCT)

All fixed tissues were radiographed in a high-resolution X-ray machine (Faxitron Series 43805N – Hewlett Packard, McMinnville, OR) set at 25 kVp, and 2.5 mA for 15 s, using a KODAK dental film (Kodak, Rochester, NY, USA). Films were developed and scanned on a Gendex GXP dental X-ray processor, (Gendex, Lake Zurich, IL) and on a Minolta Dimage Scan Dual II, (Konica, Ney York, NY) respectively. The same samples were scanned by microCT (μCT40 – Scanco Medical, Basserdorf, Switzerland). Wet fixed tissues were placed in the microCT specimen holder, and sealed to prevent tissues from drying. Scans were performed using high-resolution (10 μm nominal resolution) to assess the new mineralized structure formed. Data were collected at 55 kVp and 145 μA, and reconstructed applying the cone-beam algorithm supplied by Scanco. For visualization and 3D evaluation, images were filtered using a constrained three-dimensional Gaussian filter to partially suppress noise in the volumes (σ=1.2 and support=1), and binarized using a threshold in the range 255 to 1000. The minimum threshold value was calculated comparing the 2D reconstructed images from our scans to images obtained from μCT Evaluation Program V5.0. In addition, we performed CT-based morphometrics analyses of bone volume/total volume (BV/TV).

Scanning electronic microscopy (SEM)

For SEM analysis, fixed samples were dehydrated in an ethanol series and critical-point dried. Samples were then cut, glued on steel stubs, coated with carbon and analyzed on cross sectional areas using SEM. Images of mineral phases were obtained from backscatter electrons (BSE) and its chemical composition was determined by energy-dispersive X-ray microanalysis (EDAX).

Fourier Transform Infrared spectroscopy (FTIR)

For FTIR, samples were reduced to powder and analyzed as KBr pellets using a Nicolet-Magna 550 FTIR Series-II spectrometer (GMI, Ramsey, MN). Analyses were performed in implanted materials as well as in mouse original bone (vertebras) for comparison. Before preparation of pellets, implants were dried in an oven over night.

Histology evaluation

Implants were collected and fixed in 10% phosphate buffer formalin, demineralized for 15 days, dehydrated in alcohol series, embedded in paraffin, and 5 μm-thick sections cut using a

microtome. Sections were mounted on glass slides, stained with Hematoxylin & Eosin (H&E), and scanned on Scan Scope GL series optical microscope (Aperio, Bristol, UK).

Statistical analysis

All experiments were repeated 3 to 4 times and the mean and standard error of the mean were determined. Significant differences were assessed by ANOVA. A p-value refers to a comparison of a measured parameter in the experimental group with that of the appropriate control; significance was set at $p<0.05$

RESULTS

Overview of experimental procedure

Figure 1 shows a schematic of the experimental approach in this study.

Images (SEM) of chitosan sponges, a mouse and an X-ray image of the implanted area three months after implantation are displayed.

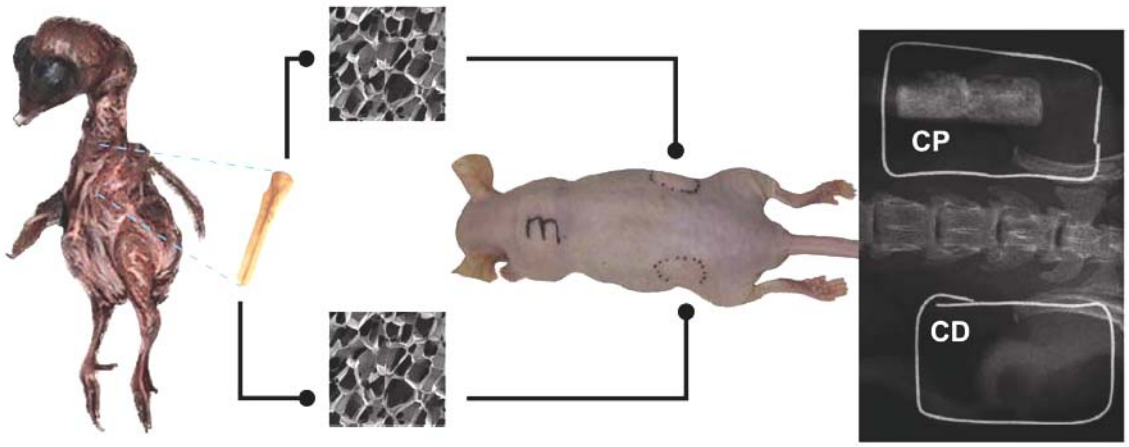

Figure 1. Schematic of experimental design. Cephalic (CP) and caudal (CD) chondrocytes were removed from the sterna of chick embryos and seeded into chitosan sponges. After treatment with retinoic acid to induce chondrocyte maturation, chondrocyte/chitosan scaffolds were implanted into subcutaneous pouches on each side of the vertebral column of nude mice. Mice were euthanized (at least 5 mice each month for five months after implantation) and different analyses performed to evaluate bone formation. The whole mouse radiographic image shows mineralization only on CP chondrocyte/chitosan sponges, implanted on the right side of the mouse. No significant increase in radiographic density was observed in CD chondrocyte/chitosan scaffolds implanted in the mouse left flank at that time.

The implant on the right side (CP chondrocytes) reveals the ability of those cells to mineralize, and the similarity between its density and the mouse bone density can be observed. In contrast, the implant on the left side did not mineralize therefore, no radiopaque area can be observed.

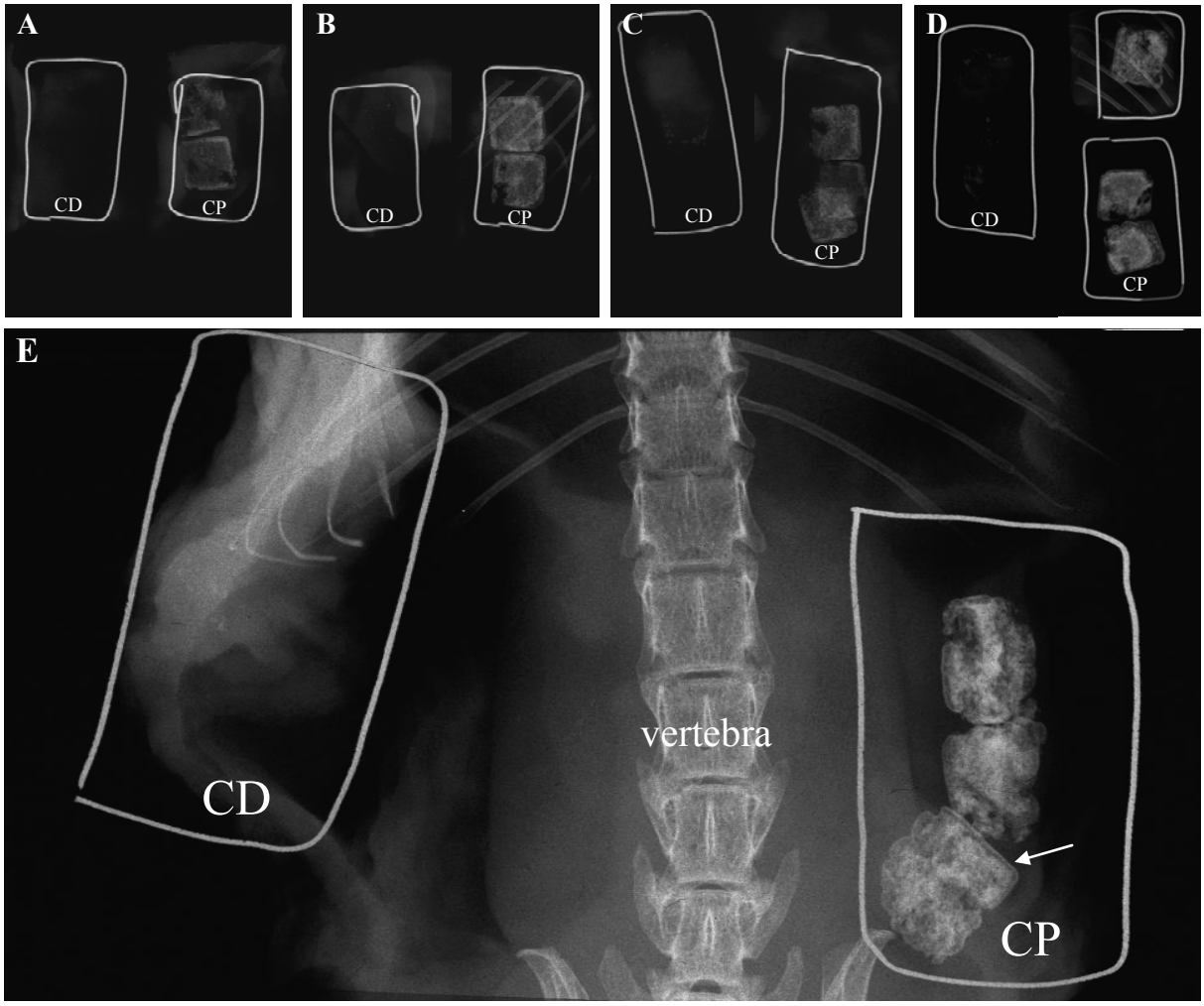

Figure 2: High resolution radiography shows an increase in mineralization during the implantation period. Samples were collected every month for 5 months after implantation, and radiographed by Faxitron (25 kV/15s). Radiographic images A to E correspond to scaffolds implanted from 1 to 5 months, respectively (A=1 month, B=2 months, C=3 months, D=4 months, E=5 months). On the left side of each photomicrograph, inside wire "boxes", are scaffolds cultured with CD chondrocytes, and on the right side scaffolds cultured with CP chondrocytes (same mouse). Wires were used to help localize the scaffolds, especially in the absence of mineralization. Image E shows mouse vertebral bodies and ribs as well as a thin mineralized layer (arrow/CP sample) similar to cortical bone.

Characterization of mineral distribution in implants

In vivo studies were conducted for 5 months and mice were collected for analyses every

month. Mineralization of experimental implants (scaffolds seeded with CP chondrocytes) was achieved in all scaffolds as confirmed by fine focus radiographs. As early as 1 month after implantation, an increase in density was observed on the periphery of the experimental implants (Figure 2A-CP) which is attributable to the presence of mineral. From the 2nd to the 5th month post-implantation (Figure 2B-CP to 2E-CP respectively) the amount of mineral increased gradually. In Figure 2B and 2D implants can be observed in the vicinity of the mouse ribs showing similar radiopacity to the mouse bones. In the 5th month after implantation (Figure 2E-CP), radiographs of implants and the mouse skeleton allow comparison between the vertebra and the scaffolds indicating considerable bone/mineral deposition in response to CP chondrocyte signaling. In addition, a thin "cortical layer" is observed (Figure 2E-white arrow) on the periphery of the implants. For all the time points studied, no comparable radiopacity was observed on control implants (pictures marked with CD); the density of these implants is similar to the soft tissue in the absence of mineralization.

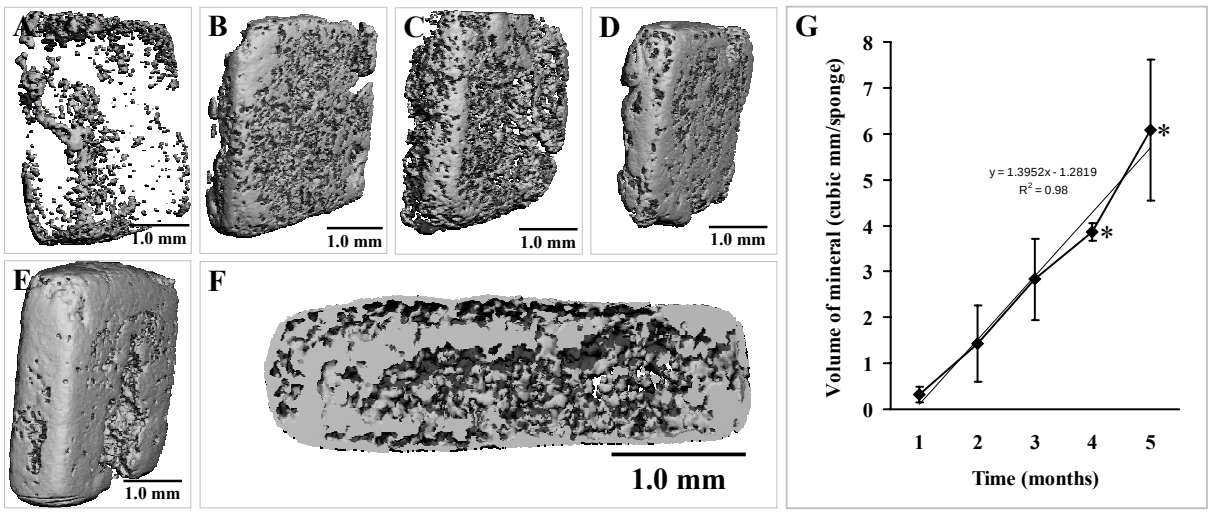

Figure 3. Accumulation of mineral in experimental scaffolds during the implantation period. Images obtained from microCT scans (3D) show gradual accumulation of mineral in the experimental scaffolds (CP chondrocytes) during the 5 months of implantation. Images A to E correspond to samples collected from month 1 to month 5 respectively and image F is the cross-sections of E (month 5). An increase of dense material is observed over time. After 5 months of implantation mineralization is observed across the chondrocyte/chitosan scaffold (F). At the threshold used to collect these data, no mineral was observed in the control implants (caudal chondrocytes, not shown). Volume of mineral was calculated from microCT scans and graphed as mean ± SD (panel G). At least 5 sponges were used to calculate the volume of mineral for each time point. * Significantly different from previous months ($p < 0.05$).

Mineral distribution across the experimental implants was assessed by microCT scans as shown in Figure 3. MicroCT results confirm that one month after implantation, mineralization has occurred only in limited areas at the surface (Figure 3A) of the experimental implants. Two months after implantation (Figure 3B) mineral can be found in almost all areas of the implant with a homogeneous distribution. On the third (Figure 3C) and fourth (Figure 3D) months after implantation, the mineral becomes denser and only few areas remain unmineralized. In the fifth month post-implantation (Figure 3E), the mineral density is significantly increased on the surface as well as inside of the implant, as observed in the cross section image (Figure 3F). As in the faxitron images, a layer of mineral can be observed on all the surface of the scaffold, suggesting the formation of a cortical bone like structure. Deeper into the scaffold, mineral is observed both in cartilage as well as in areas of bone formation (compare with histology images). Mineral quantification using microCT scans (Figure 3G) confirms a time dependent increase (more than 10 fold) in mineral volume during the implantation period studied. Control implants (CD chondrocytes) were also analyzed by microCT, however, at the threshold used for data processing, only a few speckles of mineral were observed (data not shown).

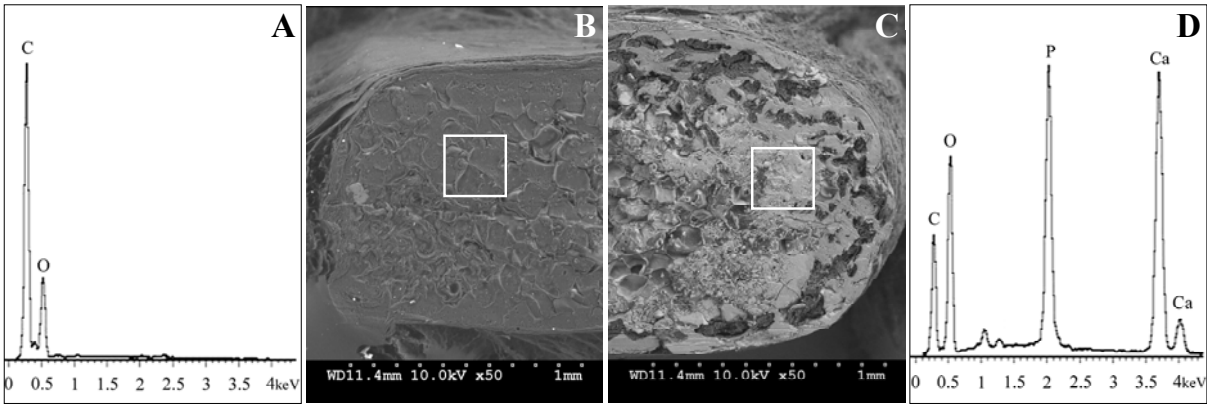

Figure 4. Backscattering scanning electron microscopy and chemical composition after 5 months of implantation. Photomicrographs were obtained from backscatter electrons (BSE) in a scanning electron microscope and they show cross-sections of control implant (B) and the experimental implant (C). White areas represent the mineralized regions and gray areas correspond to soft tissue. Qualitative analysis was determined using SEM/Energy Dispersive X-ray Analysis (EDAX) (A and D). In the middle of experimental implant we observed an area rich in "Ca" and "P", while in control implant only "C" and "O" can be detected. Note the presence of bone like layer similar to cortical bone on the surface of experimental implant (C), and the larger thickness of the experimental implant suggesting growth.

Characterization of the composition and structure of the mineral

The BSE results identified a thin layer of mineral on the surface of the experimental implants (Figure 4C) and also show that the mineralization occurred across the implant. On control implants (Figure 4B), minimal mineralization has occurred. The quantitative analyses performed using EDAX allowed us to identify "Ca" and "P" (Figure 4D) as the main elements present in the mineralized regions (white areas) of the experimental implants whereas in control (Figure 4A) only "C" and "O" elements were detected.

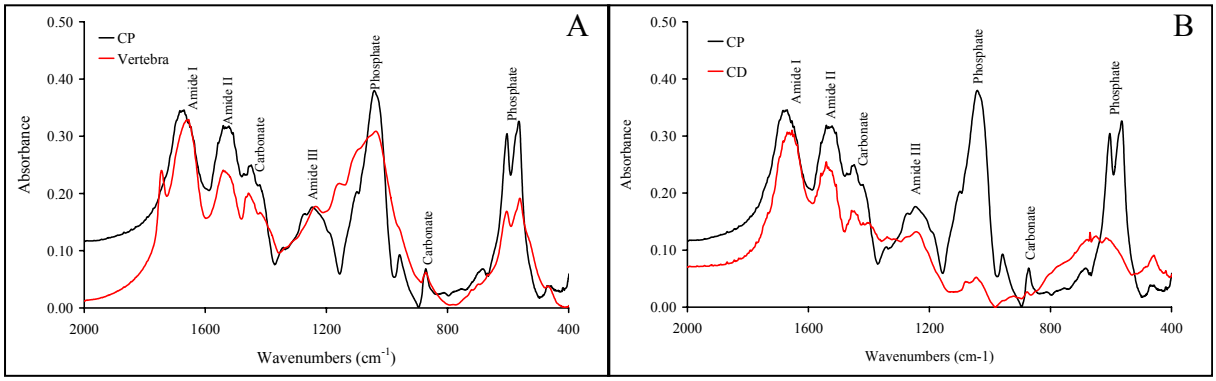

Figure 5. FTIR analyses of mouse vertebra, experimental and control scaffolds. Samples were dissected at the end of 5 months implantation, dried and mixed with KBr to prepare pellets for FTIR analyses. (A) Spectra of mouse vertebral bone and experimental **(**CP chondrocytes) scaffold both showing the presence of absorbance bands for phosphate and carbonate groups. (B) In the control (CD chondrocytes) scaffold the absorbance bands for phosphate and carbonate groups are much lower that in experimental scaffold.

In Figure 5 we compared the FTIR spectra of bone from vertebra of the mouse, with the experimental and control implants. FTIR spectrum of material collected from vertebra revealed the characteristic peaks corresponding to the mineral phase of the bone as well as peaks corresponding to the organic phase. In the mineral phase, peaks represent carbonate (CO_3) and phosphate (PO_4) groups. The experimental implants showed a very similar spectrum. In the control implants, these peaks were not observed.

Histology

Histological sections stained with H&E (Figure 6) reveal the tissue changes that occurred during the implantation period. Figures 6A to 6D show details of the experimental samples during the first four months of implantation. A bone like layer (arrows) formed at the surface of the scaffold as early as 1 month after implantation, while 3 and 4 months after implantation we can observe the formation of bone marrow like structures (Figures 6C and 6D). The

Figure 6. Histological analysis of chondrocyte/chitosan scaffolds implanted in the subcutaneous region of nude mice. Axial paraffin sections were cut through the body of the mouse (I) to include the experimental and control scaffolds. Sections were stained with hematoxylin & eosin and photographed. Details of bone forming in experimental scaffolds during the first 4 months of implantation are shown in images A through D. Images E, F, G and H correspond to high magnifications of A, B, C and D respectively showing the beginning of vascular invasion (arrows head). The control scaffolds do not undergo visible changes during the first 5 months of implantation, and therefore only the 5th month is included in this figure. A complete section is shown after 5 months of implantation (image I). Control scaffold is on the left and experimental is seen on the right side of the image. Details of control scaffold (J), vertebral body (K) and experimental scaffold (L) can be observed. Higher magnifications of control (M and P), mouse vertebra (N and Q) and experimental scaffold (O and R) show tissues details. Deep in the control sample (M), only cartilage tissue can be observed. Vascular invasion of cartilage (O – arrow head) and bone deposition (O – arrow) can be observed in the experimental sample. Detail of vertebra (N and Q) shows the presence of bone (arrow) and blood vessels (arrow head). Note bone formation deep in the experimental scaffold as well as the presence of blood vessels (R).

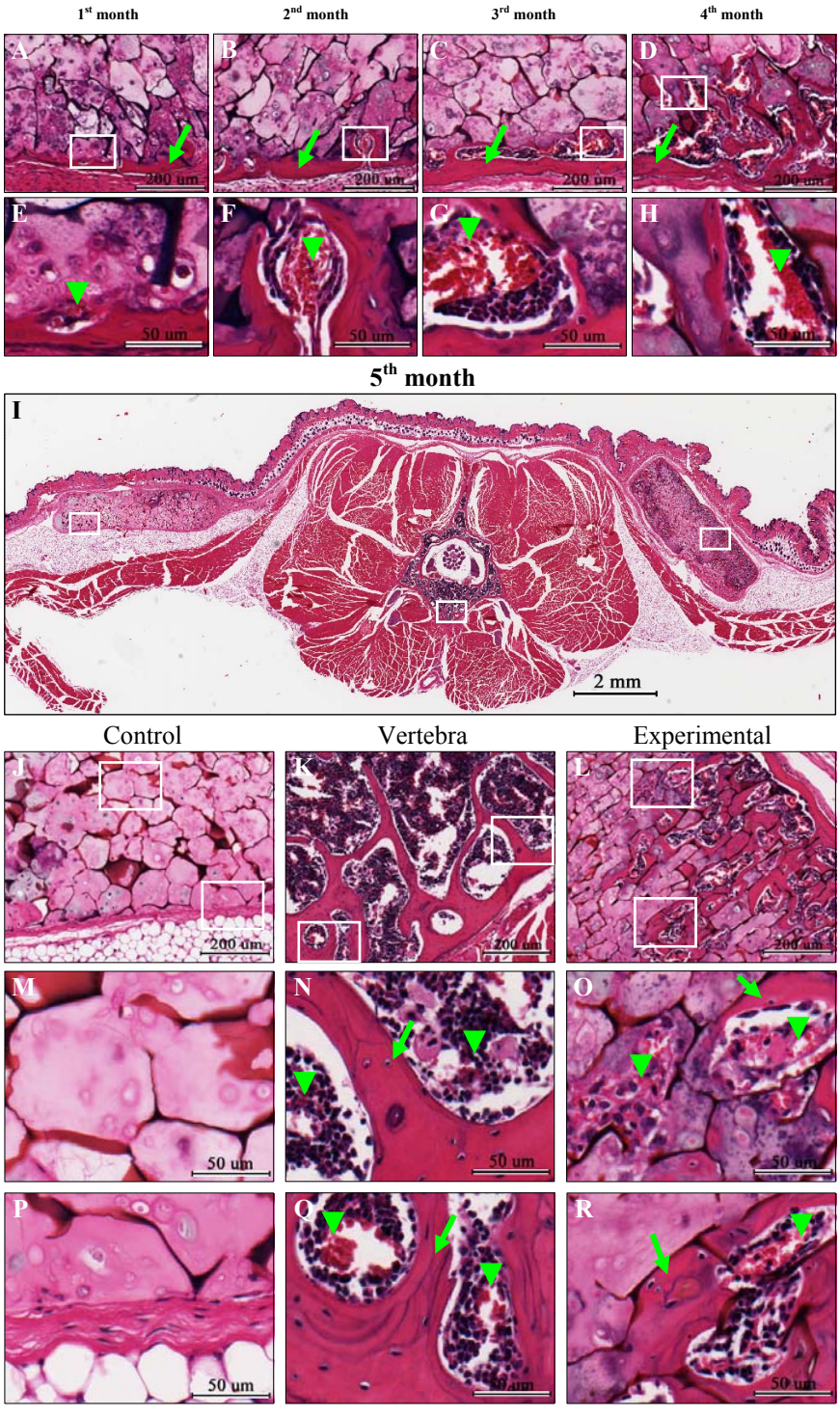

vascular invasion of the cartilage matrix is also observed as earlier as one month (arrow head in Figure 6E). In the following months (Figures 6F to 6H) vascular invasion continues deep into the sponges, and bone is deposited around these channels. In Figure 6I (a complete section through the mouse body) we can observe the implants as well as the vertebral bone. In the control implant (left side), only cartilage tissue can be seen. In the experimental implant (right side), a cortical layer of bone has formed, strikingly very similar in thickness to the cortical bone in the vertebral bodies (compare Figure 6K with 6L). Further, bone is forming across the experimental implant, along with bone marrow cavities, while in the control (Figures 6J, 6M and 6P) mostly chondrocytes and fibrous tissue can be seen invading the scaffold. At high magnification and deep into the sponges (Figure 6O – arrow heads), we can observe both vascular invasion of chondrocytes and bone deposition, consistent with changes observed at the chondroosseous junction in growth plates.

DISCUSSION

Our *in vitro* studies demonstrated that a 3D chitosan sponge can support chondrocyte proliferation and hypertrophy, characterized by expression of type X collagen and high alkaline phosphatase activity.[18] To test the hypothesis that such a transient cartilage template carries all the signals necessary to induce new bone formation, we implanted these cartilage/chitosan scaffolds into the subcutaneous region of nude mice and evaluated mineralization and new bone formation over a period of five months. As control, we used sponges seeded with CD sternal chondrocytes, shown to maintain a permanent cartilage phenotype after treatment with RA.

A plethora of studies have successfully induced new bone formation after implantation of different materials in areas adjacent to or in holes drilled into bone structures of animals.[3,4,19-21] Others have implanted materials subcutaneously or intramuscularly, and used stem cells, bone differentiation factors or gene therapy to enhance new bone formation at these ectopic areas.[22,23] In addition, it was shown that combining human bone marrow stromal cells, fibroblasts and primary articular chondrocytes could result in ectopic bone formation.[12,24-26] On the other hand, most of the studies using chondrocytes focus on articular cartilage reconstruction[27-31] or implanted the cartilage in bone forming areas.[8,32] However, in our investigation we choose to implant the cartilage/chitosan scaffolds into a non bone forming area (subcutaneous regions) to investigate the osteoinductive potential of hypertrophic

chondrocytes without the use of any bone differentiation factor or gene therapy. Indeed, as soon as 1 month after implantation mineral deposition was observed by microCT and faxitron analyses. These scaffolds were not mineralized *in vitro*, for a variety of reasons discussed in previous chapter. However, *in vivo*, and as expected hypertrophic chondrocytes with high AP activity in a matrix rich in type X collagen, rapidly triggered the mineralization phenomenon throughout the scaffold.[33-36] The main peaks in the EDAX spectrum showed the presence of "Ca" and "P" in these scaffolds, major components of mineral both in bone and growth cartilage.[37,38] The FTIR spectrum of the mineral formed in the CP constructs is identical to that obtained from the mouse vertebra, and the spectra described in the literature for bone.[39,40]

Interestingly, microCT, BSE, and histological analyses revealed the formation of a cortical layer of bone on the surface of the experimental scaffolds[20,32] as soon as one month after implantation. The presence of osteocytes like cells in that layer was confirmed in the H&E stained sections. Other studies have shown that the bone structure formed in response to signals generated by the hypertrophic chondrocytes resemble the metaphyseal cortical bone[41] formed during endochondral ossification. Indeed, in our experimental scaffolds we observed phenotypical changes and tissue transformations that closely recapitulate the activity of the cells in the growth plate and at the chondroosseous junction during endochondral bone formation. Chondrocyte hypertrophy was induced *in vitro*,[18] while mineralization of the cartilage matrix occurred after implantation, *in vivo.* The experimental scaffolds also induced abundant vascularization and extensive bone deposition, even in areas located deep into the scaffold. Further, the bone deposited in our experimental scaffolds show striking similarities (in the thickness of the cortical plate, the size of the marrow cavities and trabeculae forming deep into the scaffold) to the endochondral bone of the mouse vertebra.

Interestingly, over the period of 5 months, the experimental cartilage/chitosan scaffold and the bone forming in and around it, increased in size as can clearly be observed when comparing control and experimental BSE images. This is not totally unexpected, since during endochondral ossification there is interstitial growth resulting from proliferation, hypertrophy and *de novo* bone deposition. All those processes are at play in our attempt to engineer endochondral bone. While the scaffolds in the current implantation sites were not subject to compressive forces (possibly stretching through the skin) evidence suggest that introducing mechanical stimuli in future approaches will allow us to direct the bone growth process.[42,43,44]

Another interesting question warrants a detailed investigation. Since the instructions for bone formation by our mammalian host originated from avian chondrocytes, we are curious about

the nature of the bone tissue deposited in these scaffolds. Does the bone formed resemble mammalian or avian bone? In addition, and as some researchers proposed,[33] can chick chondrocytes transdifferentiate into "bone like cells" depositing the first layers of bone? Another question relates to the stability of the bone formed. Will endochondral ossification proceed beyond 5-6 months of implantation and will we observe further increase in the size of the original scaffold? Current and future studies in our laboratory will attempt to address these issues.

CONCLUSIONS

We have presented evidence that a transient cartilage scaffold (CP chondrocytes) created *in vitro* carries all the signals necessary to induce ectopic new bone formation *in vivo*, while a permanent cartilage scaffold failed to do so (CD chondrocytes). We extended our study beyond the 2 months of observation that characterize most bone tissue engineering approaches,[20,23,32,45] to study the stability of the bone formed and its potential to grow. We are very excited to report that endochondral ossification (subcutaneously) proceeded in a manner strikingly similar to the endochondral ossification occurring in the vertebra of the host, the mice. The nature of the bone formed in response to the chick cartilage signals, the amount, and the increase in bone tissue over the first year of implantation, are currently under investigation in our laboratory. We believe that this represents an optimized approach to bone grafting of large defects and in growing patients. The source of chondrocytes for such a clinical application would be autologous cartilage from the host (nasal, ear, costochondral) or chondrocytes obtained from different of stem cell sources, that could be induced to hypertrophy *in vitro* before implantation. A very promising approach is the use of autologous chondrocytes obtained from a bioreactor created in the space under the periosteum of the host.[46] Given that chitosan in different formulations and for multiple applications (health and food industry) is currently FDA approved,[47] we do not anticipate major obstacles to its use in humans for the novel bone regeneration approach we propose in these studies.

ACKNOWLEDMENTS

This work was supported by the Luso-American Development Foundation (Portugal), the Calouste Gulbenkian Foundation (Portugal), PRODEP (Portugal), the American Association

of Orthodontics Foundation and NIDCR grant 5K08DE017426. The authors would like to thank Mr. Nuno Pontes for the illustration work.

REFERENCES

1. Yelin E, Callahan LF. The economic cost and social and psychological impact of musculoskeletal conditions. National Arthritis Data Work Groups. Arthritis Rheum 1995;38(10):1351-62.
2. Service RF. Tissue engineers build new bone. Science 2000;289(5484):1498-500.
3. Dupraz A, Delecrin J, Moreau A, Pilet P, Passuti N. Long-term bone response to particulate injectable ceramic. J Biomed Mater Res 1998;42(3):368-375.
4. Gauthier O, Khairoun I, Bosco J, Obadia L, Bourges X, Rau C, Magne D, Bouler JM, Aguado E, Daculsi G and others. Noninvasive bone replacement with a new injectable calcium phosphate biomaterial. J Biomed Mater Res 2003;66A(1):47-54.
5. Maroudas A, Bayliss MT, Uchitel-Kaushansky N, Schneiderman R, Gilav E. Aggrecan Turnover in Human Articular Cartilage: Use of Aspartic Acid Racemization as a Marker of Molecular Age. Archives of Biochemistry and Biophysics 1998;350(1):61-71.
6. Ferguson C, Alpern E, Miclau T, Helms JA. Does adult fracture repair recapitulate embryonic skeletal formation? Mech Dev 1999;87(1-2):57-66.
7. Iwamoto M, Higuchi Y, Enomoto-Iwamoto M, Kurisu K, Koyama E, Yeh H, Rosenbloom J, Pacifici M. The role of ERG (ets related gene) in cartilage development. Osteoarthritis Cartilage 2001;9 Suppl A:S41-7.
8. Montufar-Solis D, Nguyen HC, Nguyen HD, Horn WN, Cody DD, Duke PJ. Using cartilage to repair bone: An alternative approach in tissue engineering. Annals of Biomedical Engineering 2004;32(3):504-509.
9. Pountos I, Jones E, Tzioupis C, McGonagle D, Giannoudis PV. Growing bone and cartilage. The role of mesenchymal stem cells. J Bone Joint Surg Br 2006;88(4):421-6.
10. Valimaki VV, Yrjans JJ, Vuorio EI, Aro HT. Molecular biological evaluation of bioactive glass microspheres and adjunct bone morphogenetic protein 2 gene transfer in the enhancement of new bone formation. Tissue Eng 2005;11(3-4):387-94.
11. Huang YC, Simmons C, Kaigler D, Rice KG, Mooney DJ. Bone regeneration in a rat cranial defect with delivery of PEI-condensed plasmid DNA encoding for bone morphogenetic protein-4 (BMP-4). Gene Ther 2005;12(5):418-26.
12. Bikram M, Fouletier-Dilling C, Hipp JA, Gannon F, Davis AR, Olmsted-Davis EA, West JL. Endochondral bone formation from hydrogel carriers loaded with BMP2-transduced cells. Annals of Biomedical Engineering 2007;35(5):796-807.
13. Alsberg E, Anderson KW, Albeiruti A, Rowley JA, Mooney DJ. Engineering growing tissues. Proc Natl Acad Sci U S A 2002;99(19):12025-30.
14. Deckers MM, Karperien M, van der Bent C, Yamashita T, Papapoulos SE, Lowik CW. Expression of vascular endothelial growth factors and their receptors during osteoblast differentiation. Endocrinology

2000;141(5):1667-74.

15. Petersen W, Tsokos M, Pufe T. Expression of VEGF121 and VEGF165 in hypertrophic chondrocytes of the human growth plate and epiphyseal cartilage. J Anat 2002;201(2):153-7.
16. Nakagawa M, Kaneda T, Arakawa T, Morita S, Sato T, Yomada T, Hanada K, Kumegawa M, Hakeda Y. Vascular endothelial growth factor (VEGF) directly enhances osteoclastic bone resorption and survival of mature osteoclasts. FEBS Lett 2000;473(2):161-4.
17. Gerber HP, Vu TH, Ryan AM, Kowalski J, Werb Z, Ferrara N. VEGF couples hypertrophic cartilage remodeling, ossification and angiogenesis during endochondral bone formation. Nat Med 1999;5(6):623-8.
18. Oliveira SM, Amaral IF, Barbosa MA, Teixeira CC. Engineering endochondral bone: *In vitro* studies. Tissue Engineering, Part A, In Press.
19. Hasegawa S, Ishii S, Tamura J, Furukawa T, Neo M, Matsusue Y, Shikinami Y, Okuno M, Nakamura T. A 5-7 year *in vivo* study of high-strength hydroxyapatite/poly(L-lactide) composite rods for the internal fixation of bone fractures. Biomaterials 2006;27(8):1327-1332.
20. Gauthier O, Muller R, von Stechow D, Lamy B, Weiss P, Bouler JM, Aguado E, Daculsi G. *In vivo* bone regeneration with injectable calcium phosphate biomaterial: A three-dimensional micro-computed tomographic, biomechanical and SEM study. Biomaterials 2005;26(27):5444-5453.
21. Chan C, Thompson I, Robinson P, Wilson J, Hench L. Evaluation of Bioglass/dextran composite as a bone graft substitute. Int J Oral Maxillofac Surg 2002;31(1):73-7.
22. Trojani C, Boukhechba F, Scimeca JC, Vandenbos F, Michiels JF, Daculsi G, Boileau P, Weiss P, Carle GF, Rochet N. Ectopic bone formation using an injectable biphasic calcium phosphate/Si-HPMC hydrogel composite loaded with undifferentiated bone marrow stromal cells. Biomaterials 2006;27(17):3256-3264.
23. van Gaalen SM, Dhert WJA, van den Muysenberg A, Oner FC, van Blitterswijk C, Verbout AJ, de Bruijn JD. Bone tissue engineering for spine fusion: An experimental study on ectopic and orthotopic implants in rats. Tissue Engineering 2004;10(1-2):231-239.
24. Kim H, Suh H, Jo SA, Kim HW, Lee JM, Kim EH, Reinwald Y, Park SH, Min BH, Jo I. *In vivo* bone formation by human marrow stromal cells in biodegradable scaffolds that release dexamethasone and ascorbate-2-phosphate. Biochem Bioph Res Co 2005;332(4):1053-1060.
25. Krebsbach PH, Kuznetsov SA, Satomura K, Emmons RVB, Rowe DW, Robey PG. Bone formation *in vivo*: Comparison of osteogenesis by transplanted mouse and human marrow stromal fibroblasts. Transplantation 1997;63(8):1059-1069.
26. Musgrave DS, Bosch P, Lee JY, Pelinkovic D, Ghivizzani SC, Whalen J, Niyibizi C, Huard J. Ex vivo gene therapy to produce bone using different cell types. Clin Orthop Relat Res 2000;378:290-305.
27. Kojima K, Bonassar LJ, Ignotz RA, Syed K, Cortiella J, Vacanti CA. Comparison of tracheal and nasal chondrocytes for tissue engineering of the trachea. Annals of Thoracic Surgery 2003;76(6):1884-1888.
28. Van Susante JL, Buma P, Homminga GN, Van den Berg WB, Veth RP. Chondrocyte-seeded hydroxyapatite for repair of large articular cartilage defects. A pilot study in the goat. Biomaterials 1998;19(24):2367-74.
29. Lu JX, Prudhommeaux F, Meunier A, Sedel L, Guillemin G. Effects of chitosan on rat knee cartilages. Biomaterials 1999;20(20):1937-44.

30. Dorotka R, Windberger U, Macfelda K, Bindreiter U, Toma C, Nehrer S. Repair of articular cartilage defects treated by microfracture and a three-dimensional collagen matrix. Biomaterials 2005;26(17):3617-3629.
31. Marijnissen WJCM, van Osch GJVM, Aigner J, Verwoerd-Verhoef HL, Verhaar JAN. Tissue-engineered cartilage using serially passaged articular chondrocytes. Chondrocytes in alginate, combined *in vivo* with a synthetic (E210) or biologic biodegradable carrier (DBM). Biomaterials 2000;21(6):571-580.
32. Case ND, Duty AO, Ratcliffe A, Muller R, Guldberg RE. Bone formation on tissue-engineered cartilage constructs *in vivo*: Effects of chondrocyte viability and mechanical loading. Tissue Engineering 2003;9(4):587-596.
33. Cancedda R, Cancedda FD, Castagnola P. Chondrocyte differentiation. Int Rev Citol 1995;159:265-358.
34. Hunziker EB. Mechanism of Longitudinal Bone-Growth and Its Regulation by Growth-Plate Chondrocytes. Microscopy Research and Technique 1994;28(6):505-519.
35. Kirsch T, Nah HD, Shapiro IM, Pacifici M. Regulated production of mineralization-competent matrix vesicles in hypertrophic chondrocytes. Journal of Cell Biology 1997;137(5):1149-1160.
36. Anderson HC. Molecular-Biology of Matrix Vesicles. Clin Orthop Relat Res 1995;314:266-280.
37. Yaylaoglu MB, Yildiz C, Korkusuz F, Hasirci V. A novel osteochondral implant. Biomaterials 1999;20(16):1513-1520.
38. Garimella R, Bi XH, Camacho N, Sipe JB, Anderson HC. Primary culture of rat growth plate chondrocytes: an *in vitro* model of growth plate histotype, matrix vesicle biogenesis and mineralization. Bone 2004;34(6):961-970.
39. Boskey A, Camacho NP. FT-IR imaging of native and tissue-engineered bone and cartilage. Biomaterials 2007;28(15):2465-2478.
40. Jikko A, Aoba T, Murakami H, Takano Y, Iwamoto M, Kato Y. Characterization of the Mineralization Process in Cultures of Rabbit Growth Plate Chondrocytes. Developmental Biology 1993;156(2):372-380.
41. Cadet ER, Gafni RI, McCarthy EF, McCray DR, Bacher JD, Barnes KM, Baron J. Mechanisms responsible for longitudinal growth of the cortex: Coalescence of trabecular bone into cortical bone. J Bone Joint Surg Am 2003;85A(9):1739-1748.
42. Lee C, Grad S, Wimmer M, Alini M. The Influence of Mechanical Stimuli on Articular Cartilage Tissue Engineering. Cartilage TE 2006;1:1-32.
43. Trepczik B, Lienau J, Schell H, Epari DR, Thompson MS, Hoffmann JE, Kadow-Romacker A, Mundlos S, Duda GN. Endochondral ossification *in vitro* is influenced by mechanical bending. Bone 2007;40(3):597-603.
44. Tanck E, Hannink G, Ruimerman R, Buma P, Burger EH, Huiskes R. Cortical bone development under the growth plate is regulated by mechanical load transfer. J Anatomy 2006;208(1):73-79.
45. Dong J, Uemura T, Kojima H, Kikuchi M, Tanaka J, Tateishi T. Application of low-pressure system to sustain *in vivo* bone formation in osteoblast/porous hydroxyapatite composite. Mat Sci Eng C-Bio S 2001;17(1-2):37-43.
46. Stevens MM, Marini RP, Schaefer D, Aronson J, Langer R, Shastri VP. *In vivo* engineering of organs: The bone bioreactor. Proceedings of the National Academy of Sciences 2005;102(32):11450-11455.

47. Rinaudo M. Chitin and chitosan: Properties and applications. Progress in Polymer Science 2006;31(7):603-632.

Chapter VII

Concluding remarks and future directions

CONCLUDING REMARKS

The development of a bioactive and osteoinductor injectable system was the goal of this work. Initially, the injectable system was studied in terms of its rheological properties. The system used hydroxyapatite (HAp) microspheres as reinforcement phase and polymeric solutions as the vehicle to carry the microspheres through an orthopedic injecting device. In addition, a novel osteoinductor system using a cartilage template was developed. After implantation *in vivo* extensive ectopic bone was formed.

Hydroxyapatite is a bioactive ceramic presenting high compression strength. Thus, HAp particles with different size distribution were used to prepare microspheres. "Captal s" (Cs) particles enabled the preparation of microspheres with pores smaller than those formed in microspheres prepared using either "Captal 20" (C20) or "Captal 30" (C30) particles. Additionally, the surface roughness of the first type of microspheres was the smoothest. At sintering temperatures below 1300 ºC, microspheres prepared using either C20 or C30 particles were not strong enough to enable compression strength measurements, whereas Cs microspheres supported 0.35±0.08 N, after sintering at 1200 ºC for 1 hour. As expected, the diameter of all microspheres decreased as the sintering temperature increased though C30 microspheres always presented larger diameter. After sintering at 1200 ºC for 1 hour, the diameter of Cs microspheres was 535±38 μm. Thus, Cs microspheres sintered at 1200 ºC for 1 hour were selected as the solid phase to reinforce the polymeric solution (vehicle).

Polymeric solutions of Hydroxypropylmethylcellulose (HPMC), sodium carboxymethylcellulose (NaCMC) and Alginate (ALG) were prepared at different concentrations and tested in terms of their rheological properties and injectability. In terms of rheology, viscosity was measured as a function of both shear rate and concentration of

solutions, in order to predict injectability. The use of sterile materials is a demand in the biomedical field, thus sterilization was done in an autoclave at 121 ºC for 15 minutes. Stability tests were performed in order to evaluate changes in rheological properties after solution preparation and storage.

Viscosity tests showed that either HPMC or NaCMC viscosities greatly changed with both polymeric concentration and shear rate presenting shear thinning behavior. Furthermore, NaCMC solutions presented thixotropy at high concentrations. Contrarily, small variation of viscosity versus shear rate was observed on ALG solutions though its viscosity increases slightly with concentration. Considering the above observations and taking in account that ALG is widely applied as a biomedical material and its crosslinking by ionic interactions allows a gelation at physiological pH and temperature, alginate was selected to be used as the polymer to prepare the vehicle.

Among the alginate solutions tested, non-sterile ALG 6% (w/w) (NS-ALG 6%) and sterile ALG 7.25% (w/w) (S-ALG 7.25%) presented similar properties in terms of viscosity and injectability. Both solutions were extruded using forces below 40 N. Additionally, in preliminary tests, microspheres were added to the NS-ALG 6% solutions and extruded at forces below 100 N (an accepted force for injectability).[1]

Sterile materials are a requirement for biological purposes, thus S-ALG 7.25% was chosen as the suitable vehicle and its physical stability was evaluated after storage for 3 months at 40 ºC, 25 ºC and 4 ºC. Results showed that rheological properties were maintained after storage at 4 ºC and only minor changes occurred when stored at 25 ºC. In contrast, rheological properties completely changed for solutions stored at 40 ºC.

Gelation, injectability, osmolality of mixtures (vehicle/microspheres), as well as mechanical properties of composites obtained after injection and gelation, were then investigated. Injectability tests were performed using an orthopaedic device applied in vertebroplasty surgeries and the resulting composites were tested in compression to characterize their strength.

Sterile ALG 7.25% gelation was based in $CaCO_3$ and D-glucono-δ-lactone (GDL). The concentrations were optimized to induce gelation in about 15 minutes, which seems to be the most appropriated time to perform (simulate) an injection during vertebroplasty. In these conditions, S-ALG 7.25% can work as a vehicle able to gelify *in situ* at 37 ºC. A ratio Ca^{2+}/COO^{-}=0.288 was found as the most suitable to allow gelation of S-ALG

7.25% in a period of time closest to the one specified above and was used as the ratio to prepare the injectable mixtures. Mixtures of the vehicle with different concentrations of microspheres (20, 30, 35 and 40% (w/w)) were prepared and extruded through an orthopedic device to evaluate injectability. Extruded mixtures were collected and allowed to gelify at 37 ºC for 24 hours before compression tests were performed. In those conditions only the mixture containing 40% of microspheres was difficult to inject. Mixtures prepared using 20, 30 and 35% of microspheres were easily injected at forces below 100 N. In terms of mechanical strength, mixtures prepared with higher concentrations of microspheres lead to higher strength, which is favorable in a clinical application. Among those mixtures, the ones using 35% of microspheres enabled the strongest composites and their compression strength was closer to the trabecular bone strength than most of the materials currently used in vertebroplasty.[2-4]

In the last part of this project a new approach to the development of an osteoinductive material was investigated. Bone can form either by intramembranous or endochondral mechanism. Interestingly, most bones are the result of endochondral ossification. This mechanism is based on orchestrated events occurring in a cartilage template, the growth plate. To overcome the osteoinduction limitations of the injectable system studied, we mimicked nature by developing a cartilage template able to induce endochondral ossification. Chondrocytes have the advantage to resist low oxygen concentrations and to deliver factors to induce vascular invasion and osteogenesis.[5-7] Therefore, we prepared cartilage templates using 3D chitosan sponges and chondrocytes collected from the sterna of 14 days chick embryos. In the sterna, cephalic (CP) chondrocytes differentiate and induce bone formation whereas caudal (CD) chondrocytes maintain a stable cartilage phenotype and do not induce bone formation.

Sponges were prepared by a freeze/dry process using a solution of 2% of chitosan (4% acetylated) and were characterized in terms of compression strength, permeability and pores size. Both elastic modulus and permeability were also measured on sponges cultured with chondrocytes and on tibia growth plates from 6 weeks old chicken. Those sponges proved suitable for *in vitro* cultures since they allowed proliferation and differentiation of osteoblasts.[8] After collection, chondrocytes were allowed to proliferate in culture dishes for one week before they were seeded in chitosan sponges, and cultured for 20 days using regular

medium. During the last 10 days the medium was supplemented daily with retinoic acid (RA) to induce chondrocytes maturation.[9-11] Scaffolds seeded with CD chondrocytes were used as control while scaffolds loaded with CP chondrocytes were the experimental samples. The proliferation of cells into the sponges was characterized by DNA measurements, scanning electronic microscopy (SEM) and hematoxylin & eosin (H&E) staining. Maturation was evaluated measuring alkaline phosphatase (AP) activity and gene expression by real time RT-PCR. Addicionally, immunohistochemistry using specific antibody against type X collagen was also used to evaluate chondrocytes maturation in cross-sections. Both AP and type X collagen are markers of chondrocytes undergoing hypertrophy/maturation.[12,13]

Mechanical properties were evaluated before and after culturing the scaffolds with cells and the results showed that those cultured with CP chondrocytes were the strongest. Elastic modulus of experimental samples (22.0±9.3 kPa) was enhanced while sponges without cells presented the lowest value (7.4±2.0 kPa), though similar to the elastic modulus of the control scaffolds (9.4±1.7 kPa). However, the growth plate of 6 weeks old chicken was hundred folds stiffer than experimental samples, most likely due to the presence of mineral. In terms of permeability, values were similar among scaffolds either seeded or not with cells but it decreased more that 30 folds on growth plate, in opposition to elastic modulus.

As expected, DNA increased on both control and experimental samples during 20 days in culture, showing chondrocytes proliferation even after RA treatment. Those results were confirmed by SEM and H&E images since pores were completely filled by cells and matrix.

Immunohistochemistry tests showed the deposition of type X collagen in experimental samples. Besides type X collagen synthesis, CP chondrocytes also expressed the gene for type X collagen 10 fold more than CD chondrocytes. Additionally, both AP activity and AP gene expression were increased in the matured CP chondrocytes.

The *in vitro* studies opened good perspectives in terms of the potential of the mature cartilage to induce bone formation *in vivo*. Therefore, it was planed to implant both control and experimental samples subcutaneously in the back of nude mice after *in vitro* culture for 20 days. The implantation of both control and experimental samples in the same animal and subcutaneously (area where bone is not formed naturally) were performed to clarify if the

implants are indeed the source of signals for ectopic bone formation. Animals were sacrificed monthly for five months. It was expected to observe the events leading to endochondral ossification (mineralization, vascularization and bone deposition) in experimental samples. Faxitron, micro computed tomography (microCT) and SEM using backscattered electrons were used to identify mineralization. Energy dispersive X-ray microanalysis was used to analyze the mineral phase composition and Fourier transformed infrared spectroscopy allowed the identification of the functional groups presented in explants. The structural changes, namely vascularization and ossification, were detected by histology and H&E staining.

In experimental samples, both Faxitron and microCT showed the presence of areas of high opacity as earlier as one month after implantation that increased with the implantation time. Furthermore, microCT quantification showed a linear increase in mineral content over time. The mineral formed in experimental samples was rich in Ca and P and its structures were composed by carbonate and phosphate functional groups, suggesting the formation of apatite. Additionally, those functional groups matched the same groups in the mice own bone.

Histology analyses demonstrated that blood vessels invaded scaffolds and a bone like structure was deposited. In those areas, osteocyte-like cells and bone surrounded by marrow cavities were clearly identified.

Formed bone was organized in cortical-like layer structure on the surface, while in the interior it was organized in trabecular-like structure which was similar to the structure of the mice vertebra. In control implants, neither mineralization nor bone formation were identified. Besides, a structure similar to permanent cartilage remained, although some areas were invaded by fibroblast-like cells.

FUTURE DIRECTIONS

The research projects described in this thesis provides evidence for the potential of an injectable system to fill and correct skeletal defects. The optimized rhelogical properties and the gelation timing can serve as reference to prepare other injectable systems, either using the same vehicle or a different one. Likewise, the growth cartilage scaffolds created to mimick endochondral ossification, revealed high potential for bone regeneration even in ectopic areas. While we are very excited about these different approaches to skeletal tissue regeneration, questions remain unanswered and some topics await further investigation. Therefore, in the following paragraphs we discuss some of these future directions.

Injectable System

Optimization of the opacity of the vehicle – During the injection of a material into a bone defect some issues become important, such as position of the material inside the injecting device, as well as the distribution of the material in the defect. Mechanisms need to be devised to monitor the injected material. Materials should present opacity in order to be distinguished from host tissues. In our injectable system, the HAp microspheres are opaque to X-ray but the vehicle (alginate solution) is not. Thus, studies optimizing vehicle observation, either adding X-ray opaque products to the vehicle or using a different technique (computerized tomography), to follow the material's flow, should be considered in future studies.

Unwanted side effects – On the other hand, high amount of injected material, low viscosity of material or high pressure in the defect may induce invasion of the surrounding tissue namely the vascular system which should be avoid preventing thrombus formation. Therefore, occurrence of these and other side effects need to be evaluated and techniques and properties adjusted to avoid such problems.

Partial versus complete defect filling – The extent of the injection of a material into a specific defect is an important question to be addressed. A completely filled defect enhances the possibility of osteoconduction and osteointegration of material with host bone tissue. In addition, a partially filled defect may compromise the strength. In this context is important to investigate to what extent the defect needs to be filled and how much pressure should be used

to accomplish optimal tissue response, integration and mechanical properties.

In vivo studies – The injectable system we described was able to gelify at 37 ºC. Also, both materials used to prepare the system are considered biocompatible and have been tested *in vivo*; however, when changes are implemented in materials or new surgeries techniques are used, new *in vivo* testes are required. Furthermore, to evaluate the ability of these changes to improve mechanical strength, either immediately after injection or at later stages, new *in vivo* implantation studies will be necessary. We believe that the injection of these materials into osteoporotic vertebras is a very good and simple model to test and to clarify these issues.

Cells viability after injection – The use of this injectable system as a drug delivery system or as an osteoinductor system carrying cells or growth factors (bone morphogenic proteins) are other possible applications. To address these new applications it is necessary to evaluate the system in terms of its capacity to adsorve and to deliver drugs, and the viability of cells in the mixture. In terms of drug and growth factors delivery, studies have been performed using microspheres prepared from alginate and HAp particles[15]. However, the use of sintered HAp' microspheres being carried by an alginate vehicle was not tested for this purpose yet. It is also important to test if cells viability is maintained under injection conditions and in the alginate (vehicle) environment. We believe that the use of chondrocytes will offer no major problems since they are known to resist hypoxic[6] conditions.

Endochondral ossification

In vivo long term study – The *in vivo* implantation of scaffolds to induce bone regeneration is not a new concept though most of the studies are based on osteoblast cells. Even when materials induce bone formation, the bone does not grow for long periods because it begins to resorb. However, the use of chondrocytes (cartilage template) to induce bone may offer a solution to some of these setbacks. We believe that bone will continue to be formed after the five months (described in this thesis). Therefore, a long term implantation study is necessary to address the stability of the bone formed and to potential for the bone to growth as it is normally observed as the result of the activity of the growth plate cartilage.

Bone characterization – The evidence of endochondral mechanism was clear since ectopic bone has been formed. However, the type of bone formed was not characterized. The

implanted cells were harvested from chicken, whereas the host animals were mice. Therefore the bone induction signals came from chicken cells while the induced bone cells had a mice origin. The question is: what type of bone was formed, avian or mammalian? While bone from different species is made up of the same proteins and mineral, some studies demonstrate that bone from different species, present different osteocytes densities. Thus, future work should be carried out to analyze the number of osteocytes in the ectopic bone formed and it correlates with both chicken and mouse bone.

Test the cartilage template in a bone defect – The implanted materials induced bone formation in an ectopic area so the connection between the new bone and the host bone cannot be established though this is also an important issue to be addressed. Thus it is suggested that similar experimental samples should be implanted in bone defects in order to analyze how bone grow and which type of network is established between both new and host bone.

Mechanical stress – Bone tissues are anisotropic materials because they are adapted to their mechanical functions. Thus, bones from different regions, even in the same animal, present different mechanical properties and dimensions. It is also well known that tissues, particularly bone, responds to the mechanical stress adapting to it. Furthermore, cells in proliferative zone of growth plate are aligned with load application. Therefore, it is important to study if mechanical stress can induce any kind of orientation, either in chondrocytes undergoing hypertrophy or in bone being formed in response to our cartilage template. During the present work it was possible to observe that bone has formed in preferential directions, though it was not possible to understand the primary reason.

REFERENCES

1. Bohner M, Baroud G. Injectability of calcium phosphate pastes. Biomaterials 2005;26(13):1553-63.
2. Krebs J, Ferguson SJ, Bohner M, Baroud G, Steffen T, Heini PF. Clinical measurements of cement injection pressure during vertebroplasty. Spine 2005;30(5):E118-22.
3. Yoshimine F, Latta LL, Milne EL. Sliding characteristics of compression hip screws in the intertrochanteric fracture: a clinical study. J Orthop Trauma 1993;7(4):348-53.
4. Carrodeguas RG, Lasa BV, Del Barrio JS. Injectable acrylic bone cements for vertebroplasty with improved properties. J Biomed Mater Res B Appl Biomater 2004;68(1):94-104.

5. Jasper LE, Deramond H, Mathis JM, Belkoff SM. Material properties of various cements for use with vertebroplasty. Journal of Materials Science-Materials in Medicine 2002;13(1):1-5.
6. Rajpurohit R, Koch CJ, Tao Z, Teixeira CM, Shapiro IM. Adaptation of chondrocytes to low oxygen tension: relationship between hypoxia and cellular metabolism. J Cell Physiol 1996;168(2):424-32.
7. Maes C, Carmeliet P, Moermans K, Stockmans I, Smets N, Collen D, Bouillon R, Carmeliet G. Impaired angiogenesis and endochondral bone formation in mice lacking the vascular endothelial growth factor isoforms VEGF164 and VEGF188. Mech Dev 2002;111(1-2):61-73.
8. Petersen W, Tsokos M, Pufe T. Expression of VEGF121 and VEGF165 in hypertrophic chondrocytes of the human growth plate and epiphyseal cartilage. J Anat 2002;201(2):153-7.
9. Amaral IF, Sampaio P, Barbosa MA. Three-dimensional culture of human osteoblastic cells in chitosan sponges: the effect of the degree of acetylation. J Biomed Mater Res A 2006;76(2):335-46.
10. Underhill TM, Weston AD. Retinoids and their receptors in skeletal development. Microscopy Research and Technique 1998;43(2):137-155.
11. Pacifici M, Golden EB, Iwamoto M, Adams SL. Retinoic acid treatment induces type X collagen gene expression in cultured chick chondrocytes. Exp Cell Res 1991;195(1):38-46.
12. Cohen AJ, Lassova L, Golden EB, Niu Z, Adams SL. Retinoids directly activate the collagen X promoter in prehypertrophic chondrocytes through a distal retinoic acid response element. J Cell Biochem 2006;99(1):269-78.
13. Whyte MP. Hypophosphatasia and the role of alkaline phosphatase in skeletal mineralization. Endocr Rev 1994;15(4):439-61.
14. Wang W, Kirsch T. Retinoic acid stimulates annexin-mediated growth plate chondrocyte mineralization. J Cell Biol 2002;157(6):1061-9.
15. Ribeiro CC, Barrias CC, Barbosa MA. Calcium phosphate-alginate microspheres as enzyme delivery matrices. Biomaterials 2004;25(18):4363-73.